

RECONSTRUCTION OF LATE-QUATERNARY CLIMATES OF THE  
CENTRAL GREAT PLAINS USING MAGNETIC AND  
NONMAGNETIC PARAMETERS

by

Kyeong Park

B.A., Seoul National University, 1985

M.A., Seoul National University, 1987

Submitted to the Department of  
Geography and the Faculty of  
the Graduate School of the University  
of Kansas in partial fulfillment of  
the requirements for the degree of Doctor  
of Philosophy

W. C. Johnson

Professor in Charge

V. J. Terwilliger

W. Dort, Jr.

Committee Members

Date Defended: \_\_\_\_\_

**Kansas Geological Survey**  
**Open-file Report 97-86**

Kansas Geological Survey  
Open-file Report

*Disclaimer*

The Kansas Geological Survey does not guarantee this document to be free from errors or inaccuracies and disclaims any responsibility or liability for interpretations based on data used in the production of this document or decisions based thereon. This report is intended to make results of research available at the earliest possible date, but is not intended to constitute final or formal publication.

© 1997

Kyeong Park

# ABSTRACT

Rock magnetism is a versatile methodology applicable to a wide range of paleo-environmental studies. The magnetic record of loess deposits may be one of the most detailed and useful records of Quaternary climate change on the continents. Stratigraphic variations of magnetic parameters define alternating zones of high and low concentrations of magnetic minerals. All the concentration-sensitive magnetic parameters, including susceptibility, ARM, and SIRM, show an increase within the interstadial Gilman Canyon Formation and a systematic decrease within the Wisconsinan Peoria loess. Magnetic parameters show a dramatic increase at about 13 ka. Long-term variations of magnetic concentration also synchronize with hemispheric environmental changes, including  $\delta^{18}\text{O}$  and dust content variations within the Greenland icecore. The higher resolution data produced in this research allowed identification of short term climate fluctuations such as multiple pedogeneses during the Last Interstadial and possible Younger Dryas.

Grain size characteristics of magnetic minerals also vary with the stratigraphic units. Soils with higher concentrations also exhibit a distinctively finer granulometric composition, whereas unweathered loesses with lower concentrations contain coarser grains.

The influence of climate change on magnetic records is confirmed by a high correlation between the rock magnetic parameters and biological proxies such as stable isotopes and opal phytoliths. Rock magnetic data appear to be better correlated with temperature-sensitive biological proxies than does a precipitation-sensitive index such as the aridity index derived from opal phytoliths. Simultaneous, higher resolution sampling of magnetic and biological proxies from the 14LV1071 (DB) site proved to be a better sampling tactic, and enhanced the feasibility of rock magnetic parameters as independent climate proxies.

## ACKNOWLEDGMENTS

This study would have been impossible without funding from National Science Foundation (SBR-9508272) and the Geological Society of America (Grant Number 5223-93).

Numerous people supported this project with their time and friendship. Naturally this project would not have been possible without the cooperation of people in the study area, who graciously allowed us to excavate on their property.

Several people helped me collect samples at the dusty fields in Nebraska and Kansas. Without the help from my fellow students at the University of Kansas, collecting samples would have been a lot more work. A variety of people who took paleomagnetism class helped me measure magnetic parameters and isotopic data. Steve Bozarth of the University of Kansas generously allow me to use his opal phytolith data on several sites. Erik Diekmeyer did a lot of tedious pipet analyses for his thesis, and this study used his particle size data and some chemical analysis data .

The distinguished members of my committee deserve to be recognized as well. Professor Wakefield Dort graciously allowed me to collect samples from the Sargent site and to use several unpublished  $^{14}\text{C}$  ages. He taught me the fundamentals of Quaternary geology in two fascinating courses. Chuck Martin of the Kansas State University gave excellent editorial support for the manuscript in spite of short period of time. With his generous help, this thesis has been improved a lot. Valery Terwilliger helped me think about the fundamentals of scientific work, which I haven' thought about for a while. She also provided invaluable assistance in my analyses of stable isotopes data. Randy Farr has taught me everything I know about the rock magnetism. He taught me how to use McIntoch computer and variety of machines, and how to explain experimental data. He also spent a lot of time measuring magnetic properties of loess, especially samples from the Eustis ash pit. A lot of figures in this study would be impossible without his vast knowledge of magnetism and effort.

I am especially indebted to William Johnson, my advisor, for his continued support for magnetic research and his willingness to include me in various research projects over the many years that I have been in the graduate program. He drove the old Dodge truck several times to Nebraska to help me collect the samples. He gave me excellent editorial supports in writing the grant proposals for non-native speaker. He has worked hard. I have been helped by him at each step. Thank you.

Professors from Seoul National University also supported me emotionally. They encouraged me to stay in school when I almost decided not to pursue an academic career. Thank you, Sirs. Finally, my greatest appreciation goes to my family. Since we met, Eunmi has been a good friend of mine. It is impossible to measure her support, she is a good wife and mother. My son, ChinKang also deserves appreciation. He has to stay with his parents without seeing any other family members for several years. My mother, sisters and brothers also supported our family financially and emotionally while we have been here in US. Eunmi's parents in Korea helped us financially to manage a living in foreign soil. Thanks God .

## Table of Contents

Abstract .....	i
Acknowledgments .....	ii
Table of Contents .....	iv
List of Figures .....	vii
List of Tables .....	ix
CHAPTER I: INTRODUCTION .....	1
CHAPTER II: LATE WISCONSINAN AND HOLOCENE ENVIRONMENTAL HISTORY .....	4
LATE WISCONSINAN STAGE .....	4
Stratigraphy and Environments .....	8
Peoria loess .....	9
Eolian sand deposits .....	16
Alluvial deposits .....	19
Climatic Proxies .....	20
Fossil pollen and botanical macrofossils .....	21
Stable carbon isotope .....	26
Opal phytoliths .....	30
Snail assemblages .....	32
Climate Modeling .....	33
PLEISTOCENE/HOLOCENE TRANSITION .....	35
Stratigraphy and Environments .....	36
Brady soil .....	36
Climatic Proxies .....	41
Fossil pollen and botanical macrofossils .....	41
Stable carbon isotope .....	42
Climatic Modeling .....	43
Younger Dryas .....	44
HOLOCENE .....	47
Stratigraphy and Environments .....	47
Bignell loess .....	47
Eolian sand deposits .....	48
Alluvial deposits .....	50
Climate Proxies .....	56
Fossil pollen .....	56
Stable carbon isotope .....	58
Tree rings .....	59
Climatic Modeling .....	61

<b>Chapter III: MAGNETIC PROPERTIES OF NATURAL MATERIAL</b>	<b>62</b>
<b>SUSCEPTIBILITY</b>	<b>66</b>
Concentration	66
Mineral Composition	66
Mixture of Minerals	70
<b>CRYSTAL SIZE AND DOMAINS</b>	<b>71</b>
Frequency Dependence of Susceptibility	74
<b>ARTIFICIALLY IMPARTED REMANENCES</b>	<b>78</b>
Saturation Isothermal Remanence Magnetization (SIRM)	78
Anhysteretic Remanence Magnetization (ARM)	80
<b>PREVIOUS MAGNETIC STUDY ON LOESS</b>	<b>80</b>
Rock Magnetism Record of Past Climate Change	82
Susceptibility and paleorainfall	83
Rock Magnetic Analysis	85
<b>CHAPTER IV: STUDY AREA, HYPOTHESES AND</b>	
<b>METHODOLOGY</b>	<b>88</b>
<b>STUDY AREA</b>	<b>88</b>
Climatic Setting	88
Physiographic Regions	92
Study Sites	95
<b>RESEARCH HYPOTHESES</b>	<b>99</b>
<b>METHODOLOGY</b>	<b>100</b>
Sampling	100
Measurements	101
Rock magnetic parameters	101
Stable Carbon Isotope	105
Opal Phytolith Analysis	106
<b>CHAPTER V: STUDY RESULTS</b>	
<b>EUSTIS ASH PIT</b>	<b>108</b>
Previous Study	108
Rock Magnetic Records	109
Magnetic concentration	109
Magnetic grain size	117
Magnetic mineralogy	120
Comparisons with Other Proxies	123
Spectral Analysis	128

SARGENT SITE .....	130
Rock magnetic Records .....	130
East exposure: Concentration .....	130
Magnetic grain size .....	135
West exposure: Concentration .....	135
Comparisons with Other Proxies .....	139
14LV1071 SITE (DB site)	
Core: Rock Magnetic Records .....	144
Magnetic grain size .....	146
Trench .....	151
BEISEL-STEINLE SITE .....	154
Rock Magnetic Records .....	158
Magnetic grain size .....	160
Magnetic mineralogy .....	160
Comparisons with Other Proxies .....	161
 CHAPTER VI: SUMMARY AND CONCLUSIONS	
REGIONAL MAGNETIC RECORDS .....	165
Long-Term Climatic Records .....	166
Shorter-Term Records .....	172
FUTURE RESEARCH .....	175
 REFERENCES .....	177

## List of Figures

Figure 2.1 Late Pleistocene Stratigraphy of Kansas .....	6
Figure 2.2 Late Pleistocene Stratigraphy of Nebraska .....	7
Figure 2.3 Stratigraphy of Wilson Ridge .....	18
Figure 2.4 Pollen site map .....	22
Figure 2.5 Loess $\delta^{13}\text{C}$ figure .....	29
Figure 2.6 A frequency distribution of over 400 radiocarbon ages from alluvium of Kansas and Nebraska .....	54
Figure 3.1 A model for interpreting enhanced magnetic susceptibility of soils .....	67
Figure 3.2 Ternary diagram for iron-titanium oxides .....	69
Figure 3.3 Domain size ranges of magnetite .....	73
Figure 3.4 Magnetic mixture $\chi_{\text{ARM}}/\text{SIRM}$ versus FD diagram .....	75
Figure 3.5 Variability of magnetic parameters for various magnetic grain-size .....	76
Figure 3.6 Magnetic hysteresis change .....	79
Figure 4.1 Isohyet map of the region .....	89
Figure 4.2 Dominant air mass types of the region .....	90
Figure 4.3 Potential vegetation map of the region .....	91
Figure 4.4 Physiographic map .....	93
Figure 4.5 Loess isopatcheous map and sampling sites .....	97
Figure 4.6 Granulometric modeling flow chart .....	104
Figure 5.1 Topographic map of the Eustis ash pit .....	109
Figure 5.2 Magnetic parameters from the Eustis ash pit .....	110
Figure 5.3 MS from Bignell--Eustis ash pit versus SPECMAP .....	111
Figure 5.4 MS, loess accumulation rate and median PS from the EAP .....	114
Figure 5.5 Biparametric plots of FD vs. MS and $\chi_{\text{ARM}}/\text{SIRM}$ vs. MS from the EAP .....	119
Figure 5.6 Thermal demagnetization curve .....	122
Figure 5.7 $\delta^{13}\text{C}$ data vs. MS from the EAP .....	124
Figure 5.8 MS, $\delta^{13}\text{C}$ , and pooid index within the GCF from the EAP .....	125
Figure 5.9 Spectral plots from the EAP .....	129
Figure 5.10 Topographic map of the Sargent site .....	130
Figure 5.11 MS-depth plots from the Sargent site .....	131
Figure 5.12 FD-depth plots from the Sargent site .....	132
Figure 5.13 Magnetic parameters from the east profile from the Sargent site .....	134
Figure 5.14 MS, FD, $\delta^{13}\text{C}$ , and phytolith index from the Sargent site .....	136
Figure 5.15 Biplots of FD vs. MS and $\chi_{\text{ARM}}/\text{SIRM}$ vs. FD from the east profile from the Sargent site .....	137
Figure 5.16 Biplots of FD vs. MS from the west profile from the Sargent site .....	138

Figure 5.17 MS variation compared with the regional climate proxy data . . . . .	143
Figure 5.18 Magnetic parameters from the east profile from the DB site . . . . .	145
Figure 5.19 Biplots of FD vs. MS and ARM/SIRM vs. FD from the DB site . . . . .	149
Figure 5.20 Biplots of $\chi_{ARM}/SIRM$ vs. FD from the DB site compared with synthetic magnetite samples of Maher (1988) . . . . .	150
Figure 5.21 MS, FD, $\delta^{13}C$ , and phytolith index from the 14LV1071 site . . . . .	152
Figure 5.22 Topographic map of the Beisel-Steinle site . . . . .	154
Figure 5.23 Magnetic parameters from the Beisel-Steinle site . . . . .	155
Figure 5.24 Biplots of FD vs. MS and ARM/SIRM vs. FD from the Beisel-Steinle site . . . . .	159
Figure 5.25 MS, FD and, $\delta^{13}C$ from the Beisel-Steinle site . . . . .	162
Figure 5.26 MS and loess accumulation rate at the Beisel-Steinle site . . . . .	163
Figure 6.1 MS-age variation from the region . . . . .	167
Figure 6.2 MS versus SPECMAP, GRIP icecore . . . . .	169
Figure 6.3 MS values variation between the stratigraphic units . . . . .	171
Figure 6.4 MS and FD from the Bignell Hill versus icecore . . . . .	173
Figure 6.4 MS and FD from the Sargent site versus icecore . . . . .	174

## List of Tables

Table 2.1. Wood and charcoal ages from the region. . . . .	12
Table 2.2. Brady soil ages. . . . .	37
Table 2.3. $\delta^{13}\text{C}$ values and radiocarbon ages from the Brady soil. . . . .	40
Table 2.4. Chronology of Younger Dryas. . . . .	46
Table 3.1. Commonly measured magnetic parameters . . . . .	65
Table 3.2. Magnetic behaviors and MS of different minerals . . . . .	70
Table 4.1. Opal phytolith morphotypes and photosynthetic pathways . . . . .	107
Table 5.1. GCF ages compared with Searles lake and Summit icecore . . . . .	113
Table 5.2. Correlation coefficient from the Eustis ash pit . . . . .	116
Table 5.3. Descriptive statistics from the Sargent site . . . . .	133
Table 5.4. Correlation coefficient from the Sargent site . . . . .	142
Table 5.5. Descriptive statistics from a core at the 14LV1071 site . . . . .	146
Table 5.6. Correlation coefficient from a core at the 14LV1071 site . . . . .	147
Table 5.7. Correlation coefficient from a trench at the 14LV1071 site . . . . .	153
Table 5.8. Descriptive statistics from the Beisel-Steinle site . . . . .	156
Table 5.9. Correlation coefficient from the Beisel-Steinle site . . . . .	157
Table 6.1. MS statistics from the region. . . . .	170
Table 6.2. FD statistics from the region. . . . .	172

# I. INTRODUCTION

Agricultural belts with marginal precipitation, such as the central Great Plains, are particularly vulnerable to changes in climate. Although the controls on climate variability in the late Quaternary may differ from those in the future, the change in climatic conditions and the response of the geosphere may be similar. Thus, an understanding of the regional geomorphic systems during the late Quaternary allows assessment of the range of future landscape responses. The consequences of short- and long-term climatic variations within the region and attendant changes in the vegetation probably had a measurable impact on much of the productive land, as evidenced by the Dust Bowl of the 1930s.

The sensitivity of grassland community composition and its boundaries to short-term climatic variation during the historical period is well documented for the central Great Plains (Tomanek and Hulett, 1970; Küchler, 1972). Similarly, long-term prairie expansion and contraction, in response to climatic variation, is documented for the prehistoric time scale (*e.g.*, Watts and Wright, 1966; Grüger, 1973; Bradbury, 1980; Webb *et al.*, 1983). Despite many studies, however, little is known about environmental conditions in the central Great Plains during the late Pleistocene and Holocene. Because the region has few bogs and natural lakes, there are few good preservation sites for pollen and botanical macrofossils. Therefore, climatic reconstruction in this region relies heavily on the synthesis of other proxies such as bones from vertebrate fauna, snail shells, and occasional botanical macrofossils. As a result, interpretations of late-Pleistocene vegetation from the scant fossil records of the region range from continuous taiga-like forest (Wells and Stewart, 1987) to grassland or steppe (Graham, 1987)

The quasi-continuously deposited loesses of the central Great Plains represent some of the thickest and most complete loess deposits in North America and provide the potential to reconstruct past climates. The ongoing research on magnetic records for

these deposits indicates that lower susceptibility is associated with times of rapid accumulation, *i.e.*, the cooler glacial intervals, and higher susceptibility is associated with the intercalated paleosols and weathering zones, which represent times of landscape stability and/or reduced accumulation rates. In addition to correlation with long-term regional cyclic climatic changes, the relatively rapid accumulation rates associated with loess deposits also permit the resolution of short-term changes in climate (*e.g.*, Zhou *et al.*, 1994; Heller *et al.*, 1993; An *et al.*, 1992).

The objective of this dissertation is to evaluate the potential of several magnetic parameters to serve as proxies for high-resolution climatic reconstruction. Specifically, the research questions include:

- (1) What controls the magnetic records of Quaternary loess? The magnetic susceptibility signal has been known, at least in part, as an indicator of weathering or pedogenesis, *i.e.*, climate. If the appropriate sampling sites can be chosen, variations in magnetic records of the region may explain climate.
- (2) How accurately do magnetic records correlate with other paleoclimatic indicators within the loess deposits, such as opal phytolith, and stable isotopes? How do they correlate with regional geomorphic records such as alluvial chronologies and sand dune movement? By comparing magnetic records with other climate-sensitive proxies, the feasibility of magnetic records for climate reconstruction is evaluated.
- (3) If magnetic records of the region explain climate, which rock magnetic parameters are most responsive to the climate conditions? Traditionally, susceptibility alone has been exploited to explain climate changes. Potential for other parameters is evaluated.

This research focuses on the late Pleistocene and Holocene, or about the last 40,000 years. This is an interval which has experienced dramatic changes in climate, *i.e.*, it includes the relatively mild climatic conditions of the middle Pleistocene interstadial, the glacial maximum of the late Pleistocene, the Pleistocene-Holocene transition, and the Holocene.

Chapter II summarizes that which is currently known about the paleoenvironmental history of the central Great Plains. Objectives are to summarize the current status of knowledge regarding environmental changes in the central Great Plains during the late-Quaternary and to briefly identify gaps that exist in the database. In chapter III, some basic concepts of rock magnetism are provided, and relevant research on loess magnetism is summarized.

In chapter IV, hypotheses are constructed, and study sites and methodology to confirm the working hypotheses are introduced. They are: 1) Concentration of magnetic mineral controls the magnetic records of Quaternary loess. 2) The magnetic grain size of soils are different from less-weathered loess. 3) Rock magnetic parameters correlate well with other paleo-climatic proxies. 4) Every concentration-sensitive magnetic parameters can provide the independent high-resolution data for climate variations during the late Quaternary

In chapters V, analytical results of rock magnetic investigations and comparisons with other climate-proxies are discussed site by site, and then a regional summary follows in chapter VI.

## **II. REGIONAL PALEOCLIMATE HISTORY DURING THE LATE-WISCONSINAN STAGE**

This chapter is intended to summarize what is currently known about the paleoenvironmental history of the central Great Plains. Objectives are to summarize the current status of knowledge regarding environmental changes in the central Great Plains during the late Quaternary and to briefly identify gaps that exist in the database.

Less is known about environmental conditions in the central Great Plains during the Late Pleistocene and Holocene than about many other regions of North America. This is probably because wide application of the more traditional investigative tools such as palynology and dendroclimatology is very difficult. Consequently, what is known has been and is being derived using some of the newer approaches to late-Quaternary environmental reconstruction such as stable isotope analysis, opal phytolith analysis, and environmental magnetism. Those sedimentological contexts being explored include loess, eolian sand sheets and dunes, alluvial fills, and to a lesser extent isolated lake and peat deposits. The loess deposits of the region, which represent some of the thickest and most complete loess accumulations in North America, hold the potential to provide a particularly promising avenue for the pursuit of the paleoenvironmental record.

### **LATE WISCONSINAN STAGE**

Due to its relative youth, the Late Wisconsinan Stage has the greatest chronostratigraphic resolution. Based on the chronology from Illinois, five substages of the Wisconsin have been traditionally recognized: the Altonian (70,000-28,000 yr B.P.), Farmdalian (28,000-22,000 yr B.P.), Woodfordian (22,000-12,500 yr B.P.), Twocreekan (12,500-11,000 yr B.P.), and Valderan (11,000-5,000 yr B.P.) (Willman and Frye, 1970;

Frye and Willman, 1973). This chronology of substages has, however, limited stratigraphic application in Nebraska, Kansas and eastern Colorado, and has therefore not been adopted literally.

In Nebraska, Reed and Dreeszen (1965) identified four Wisconsinan units: the Gilman Canyon Formation (an upland loess with soil development), Peoria Formation (fluvial sand and silt in valleys and loess on the uplands), Brady Interstadial soil, and Bignell Formation (dune sand and loess). For the Wisconsin of Kansas, Frye and Leonard (1952) recognized early Wisconsinan alluvial deposits and the Sanborn Formation. The late Wisconsinan units of the latter include the Peoria loess, Brady soil and Bignell loess (Figure 2.1 and 2.2). Since these early statements of stratigraphic succession, the Bignell loess has been assigned to the Holocene.

During the 1960s, the record of past climate was based primarily on continental deposits, but these were rarely continuous sedimentary records, and consequently the picture of past climatic variations that developed was incomplete (Bradley, 1985). In the next decade, studies of marine sediments revolutionized our understanding of climatic variations and enabled models of the causes of climatic changes to be tested. Undoubtedly, studies of marine sediments have provided data bases which continue to expand in quantity and quality (Ruddiman, 1985). However, the 1980s have seen a renewed focus on continental records of climate, which complement the perspective provided by marine sediment (COHMAP members, 1988). Continental deposits often provide more detailed information about short-term (high-frequency) changes of climate than do most marine records.

Time-stratigraphic units	Rock-stratigraphic units					
	Northeastern area		Southeastern area		Central and Western area	
Recent stage	Eolian and fluvial deposits					
Wisconsinan Stage	Bignell Formation	Fluvial deposits	Bignell Formation	Fluvial deposits	Bignell Formation	Fluvial deposits
	Brady Soil					
	Peoria Formation	Fluvial deposits	Peoria Formation	Fluvial deposits	Peoria Formation	Fluvial deposits
	G.C.F.					
Sangamonian Stage	Sangamon Soil					
Illinoian stage	Loveland Formation	Fluvial deposits	Loveland Formation	Fluvial deposits	Loveland Formation	
					Crete Formation	
	Yarmouth Soil					
Pre-Illinoian	Loess	Fluvial deposits	Fluvial deposits		Sappa Formation	
	Cedar Bluffs Till				Grand Island Formation	
	Fluvial deposits					
	Nickerson Till					
	Atchinson Formation					
	Atfon Soil					
	Loess	Fluvial deposits	Fluvial deposits		Fullerton Formation	
	Jowa point Till				Holdredge Formation	
	David City Formation					

9

Figure 2. 1. Late-Quaternary stratigraphic succession in Kansas (Bayne and O'Connor, 1968).

		Classification				Terrace Surfaces	
Time-Stratigraphic	Rock-stratigraphic						
	Eolian	Fluviatile	Glacial	Soils			
Wisconsinan	Late	Bignell Loess and Dunesand	Bignell Formation <u>Silt</u> sand-gravel	Absent		2a 2b	2
	Medial	Peoria Loess and Dunesand	Peoria Formation <u>Silt</u> Todd Valley Sand	Hartington Till	Brady	3	
	Early	Gilman Canyon Formation	Gilman Canyon Formation	Absent	Unnamed		3
Sangamonian	Late	Loveland Loess	Loveland Loess <u>Silt</u> sand-gravel	Absent	Sangamon	4	4

7

Figure 2. 2. Late-Quaternary stratigraphic succession in Nebraska (Reed and Dreeszen, 1965)

## **Stratigraphy and Environment**

Late Wisconsinan loess deposits form a mantle over much of the upland surface of the region, covering the central Great Plains and provide a terrestrial record of late Quaternary climate.

From Nebraska, loess deposits in the central Great Plains extend west across eastern Colorado and south across most of Kansas. The thickest deposits of loess are adjacent to and underlie the Nebraska Sand Hills (Kollmorgen, 1963; Ahlbrandt *et al.*, 1980). The oldest laterally extensive loess unit in the region is the Loveland loess, found as far west as the Colorado/Kansas state line. In Kansas, exposures of Loveland loess are patchy and are found mostly on ridges near drainages (Welch and Hale, 1987). The Peoria loess is the thickest and most laterally continuous loess deposit (Frye and Leonard, 1951), whereas the overlying Holocene Bignell loess is found discontinuously in the central Great Plains and is not identified east of the Missouri River.

Until recently, little age control existed for the timing of loess deposition in the central Great Plains. Age assumptions were based largely on the classical continental glaciation sequence, similar to that used for the loess stratigraphy of the Mississippi and Missouri River Valleys. However, younger loesses and associated buried soils exposed at a number of localities in Kansas and Nebraska have been systematically radiocarbon and, to a lesser extent, thermoluminescence-dated (*e.g.*, Souders and Kuzila, 1990; Johnson, 1993; Martin, 1993; May and Holen, 1993; Feng *et al.*, 1994a, b; Maat and Johnson, 1996). According to these age estimates, the Gilman Canyon Formation was deposited from at least 40 ka to about 20 ka, Peoria loess about 20 ka to 10.5 ka, and Bignell loess from about 9 ka to about 5.5 ka.

Unconformably overlying the Loveland loess and the Sangamon soil that caps it is the loess of the Gilman Canyon Formation (Reed and Dreeszen, 1965). The upper two-third of this loess is organic-rich and contains one or more cumulic A horizons that represent a period of slow accumulation and pedogenesis. Similarities in stratigraphic

position, soil development and molluscan assemblages indicate that it may be equivalent to the Farmdale interstadial soil (Johnson, 1990; 1993). Recent age estimates also support correlations with the Roxana silt of the Upper Mississippi River Valley (Leigh and Knox, 1994) and the Pisgah Formation of western Iowa (Forman *et al.*, 1992a). A transitional zone of loess, characterized by upwardly decreasing organic content and increasing color value (brightness), represents a slowly accelerating rate of loess deposition and separates the Gilman Canyon Formation from the overlying Peoria loess.

### *Peoria loess*

Late Wisconsinan loess deposits form a mantle over much of the upland surface of the region, covering the central Great Plains and provide a terrestrial record of late Quaternary climate. Thickest deposits lie adjacent to the Missouri River and its major tributaries (Ruhe, 1983).

Leverett (1899) first proposed the name Peoria for an interglacial period between the Iowan and Wisconsinan glacial stages. When Alden and Leighton (1917) demonstrated the Peoria was younger than the Iowan, usage shifted to that of a loess, rather than of a weathering interval. Within the Midcontinent, several names have been used for post-Farndalian loess. Ruhe (1983) preferred the term "late Wisconsin loess" because of the uncertainties in the stratigraphic equivalency from one region to another.

The Peoria loess is typically eolian, calcareous, massive, light yellowish-tan to buff silt that overlies the Loveland loess or an approximate equivalent of the Gilman Canyon Formation. Based on conventional and accelerator radiocarbon ages, deposition of the late-Wisconsinan Peoria loess in Kansas and Nebraska began about 19.5-21 ka. During the late Wisconsin, loess accumulated relatively fast. At the Bignell Hill type section in southwestern Nebraska, for example, the accumulation rate for the late-Wisconsinan Peoria loess averaged 5.7 mm/year. This rapid accumulation rate seems to be comparable to marine records and rapid enough to preserve high-resolution data for the late-

Wisconsinan environmental changes. The rate of accumulation for the Peoria loess was certainly variable, but apparent annual laminae are present at many localities near the Platte River valley of Nebraska, including the Bignell Hill and the Eustis ash pit sites (Johnson, 1993). Loess accumulation rates decreased as the regionally-expressed Brady soil began developing between 10.6 and 10.1 ka.

The lack of any well developed buried soils or other unconformities suggests that Peoria loess in the region represents a continuous deposit and that the faunal zonation reflects a change in the rate of deposition. Evidence that Peoria loess deposition was episodic has emerged from western Iowa (Daniels *et al.*, 1960; Ruhe *et al.*, 1971), central Kansas (Arbogast, 1995) and southwestern Illinois (McKay, 1979), where deposits exhibit dark, organic-rich bands that are thought to represent incipient soils formed during periods of slower deposition. Differential abundance and preservation of fossil mollusks in the loess have also been cited as evidence of episodic loess deposition (Frankel, 1957).

The loess thickness decreases gradually with distance to the south and southeast of the Platte River valley. Except for the loess of the Loess-Drift Hill area in southeast Nebraska, loess south of the Platte was deposited rather evenly on a nearly level surface of old alluvial sands and gravels. In the Loess-Drift Hill area of southeast Nebraska and in most of the area north of the Platte River, the loess mantles a previously dissected and hilly topography.

Little is known about the environmental conditions in the central Great Plains during Peoria loess deposition. Early studies, however, postulated that loess likely accumulated under dry conditions (*e.g.*, Schultz and Stout, 1948). Evidence from modern depositional environments suggests, however, that well-vegetated rather than barren surfaces favor loess deposition (Yaalon and Dan, 1974; Martin, 1993). Additionally, the rich landsnail fauna of Peoria loess in the Great Plains implies deposition on a vegetated surface (Leonard, 1952; Ostlie 1986; Wells and Stewart, 1987; Rousseau and Kukla, 1994).

Recent findings indicate that trees were present in the central Great Plains during Peoria loess deposition, although the distribution and density of tree cover is unknown. Wells and Stewart (1987) recovered *Picea glauca* (white spruce) cones, needles, and wood from Peoria loess at several sites in south-central Nebraska; radiocarbon ages on the wood range from 14,700 to 13,000 yr B.P. (Johnson, 1989). Wells and Stewart (1987) also report charcoal in Peoria loess at two locales in north-central Kansas, on the Courtland canal and Coon Creek. At the Coyote Canyon site in south-central Nebraska, bands of charcoal near the base of the Peoria loess afforded additional radiocarbon ages which range from 21,250 to 19,730 yr B.P. (Martin, 1993). At the nearby Sindt Point site, Johnson reports an additional age of 21,440 yr B.P. for *Picea* (spruce) charcoal (Table 2.1).

A upland pollen record from southeastern Kansas suggests that a *Populus* (aspen or cottonwood) parkland was present during the late Pleistocene (Fredlund and Jaumann, 1987). Watts and Wright (1966) conclude that *Picea* was the dominant vegetation cover in the Nebraskan Sand hills until 12,500 yr B.P., when it was gradually replaced by *Pinus* (pine) and herbaceous vegetation. Recent surveys of the Midcontinent pollen records by Webb *et al.* (1983) and Baker and Waln (1985) postulate parkland vegetation with treeless openings on the central Great Plains during the late Pleistocene.

Ruhe (1983) noted three major features of late-Wisconsinan (Peoria) loess: it thins downwind from the source area, decreases in particle size systematically away from the source area, and is strongly time transgressive at its base. The last feature is problematic and causes correlation problems. Ruhe (1969) realized a decrease in the age of the soil under the loess from 24,500 yr B.P. near the Missouri River to about 19,000 yr B.P. eastward across southwestern Iowa. A decrease from 25,000 to 21,000 yr B.P. was noted for the base of the loess along a transect in Illinois (Kleiss and Fehrenbacher, 1973). The top of the loess also seems to be time transgressive, ranging from about 12,500 yr B.P. in Illinois (McKay, 1979) to about 14,000 yr B.P. in central Iowa (Ruhe, 1969).

Table 2.1. Wood and charcoal ages from Late-Wisconsinan deposits in Kansas and Nebraska.

Location	Material	Sample	Age	Source
<i>Kansas</i>				
Mt. Hope Sand Co. Sedgewick Co.	<i>Picea</i> litter	Dic-3101	19,340 ± 200	Jaumann, 1991
GMD5 site 9 Edwards Co.	<i>Picea</i> charcoal	TX-6479	17,970 ± 330	Johnson, 1991a
Coon Creek Graham Co.	<i>Picea</i> charcoal	GX-9355G	17,930 ± 550	Wells and Stewart, 1987
Courtland Canal Jewell Co.	<i>Picea</i> charcoal	Beta-9320	14,450 ± 140	Wells and Stewart, 1987
<i>Nebraska</i>				
North Cove Harlan Co.	<i>Picea glauca</i>	Beta-12286	14,700 ± 100	Wells and Stewart, 1987
Coyote Canyon Harlan Co.	<i>Picea</i> charcoal	TX-7294	21,250 ± 530	Martin, 1993
Coyote Canyon Harlan Co.	<i>Picea</i> charcoal	TX-7295	19,730 ± 300	Martin, 1993
Sindt Point Harlan Co.	<i>Picea</i> charcoal	Tx-7711	21,440 ± 200	Johnson (unpublished data)
Bloomington Franklin Co.	<i>Picea</i> or <i>Larix</i>	Beta-42015	18,830 ± 180	May and Holen, 1993
South Loup River Buffalo and Grant Co.	<i>Abies balsamea</i> fragments	Tx-6128 Beta-27758	14,080 ± 190 13,160 ± 450	May, 1989 Swinehart, 1990

Despite the attention given to the Peoria loess in central Great Plains, the source of the silt is not completely certain. From their review of available data, Welch and Hale (1987) concluded that a single source was not likely for all loess deposits in Kansas and that the loess was derived from a combination of three sources: glacial outwash river flood plains, present sand dune areas, and fluvial and eolian erosion of the Ogallala Formation. The Platte River undoubtedly contributed massive quantities of loess during glacial stages, as presumed earlier by Swineford and Frye (1951). Loess is thickest immediately south of the Platte River Valley, which suggests that the alluvium in the valley was the source of the loess, at least for those deposits adjacent to the valley (Kollmorgen, 1963). Some local thickening of loess occurs to the southeast of the Platte River wherever streams enter from the Sand Hills to the northwest. With prevailing northwesterly winds, these locally thick deposits are probably partially derived from alluvium brought into this valley by these streams. In addition, nonglacial rivers in western Kansas and Nebraska probably contributed substantially more to the volume of loess in the area. Local loess deposits in excess of 23 m have been measured along the southeastern bluffs of the Arikaree and Republican Rivers (Swineford and Frye, 1951). Swineford and Frye (1951) concluded that the Arkansas River carried too sandy a sediment load to act as a major loess source and suggested that most of the loess deposited south of the Arkansas River in southwest Kansas was derived from northern sources.

In Nebraska and Kansas, radiocarbon and thermoluminescence dating indicates that Peoria loess in those areas correlates temporally with the Peoria loess of Iowa, Illinois, and Indiana (*e.g.*, Johnson *et al.*, 1993; May and Holen, 1993; Martin, 1993; Maat and Johnson, 1996). However, much of the loess in Kansas and Nebraska occurs upwind of or distant from late-Wisconsinan continental glacial outwash sources. In addition, some of the thickest deposits of loess in Nebraska occur upwind of the Platte River (Swinehart, 1990). Flint (1971) pointed out that the volume of loess on the Great

Plains is surprisingly high if it was all generated from glacial outwash derived from the Rocky mountains. At the present time, the source of loess in the Kansas and Nebraska portion central Great Plains is unknown, and more than one source may be involved (Welch and Hale, 1987).

Welch and Hale (1987) concluded that loess in northwest, north-central, west-central, central, southwest, and south-central Kansas was derived from regional sand-dune areas in central and western Nebraska (Sand Hills area), whereas loess in southwest Nebraska, eastern Colorado, southwest and south-central Kansas was derived from alpine glacial-outwash sediments of the flood plains of the Platte and Arkansas Rivers and from flood plain sediments of nonglacial rivers such as the Arikaree, Republican, Solomon, Saline, Smoky Hill, Pawnee, and Cimarron.

Trace element analysis (*e.g.*, cerium, strontium, yttrium, zirconium) was employed to gain insight into loess source and paleowind directions (Johnson *et al.*, 1993). Concentrations of many of the elements considered decrease south/southeastward away from the Platte River Valley and Sand Hills of Nebraska. Superimposed on the overall trend is an increase in concentrations at sites adjacent major river valleys due to a 'refreshening effect' (Johnson and Muhs, 1996).

Peoria loess deposition appears to relate to the formation of the Sand Hills of Nebraska. Kutzbach and Wright (1985) argue that the Sand Hills of Nebraska is the source for much of the Peorian loess in the region, and that formation of the huge transverse dunes within the Sand Hills must have occurred during a period of extreme aridity. Although strong circumstantial evidence links the Sand Hills to the adjacent body of Peoria loess, this hypothesis is not universally accepted (*e.g.*, Ahlbrandt *et al.*, 1983).

The question of the Sand Hills formation and Peoria loess deposition is germane to the investigation because, if the arguments of Kutzbach and Wright (1985) are correct, the Woodfordian, or at least some portion of it, was relatively xeric. This presumed Woodfordian aridity conflicts with at least some paleobotanical evidence in the region,

particularly that related to the widespread occurrence of spruce and other taiga-like plant taxa (Table 2.1). These taxa, typically associated with the modern boreal forest, do not suggest moisture stress. The Woodfordian macrofossil record from the central Great Plains includes several well documented and dated occurrences of *Picea* remains, indicating a cool, mesic environments.

Leonard (1952) subdivided the Peoria loess of Kansas into four zones on the basis of the molluskan fauna assemblages present. The *basal zone* is equivalent to a leached interval above the Gilman Canyon Formation and is void of molluskan material. The *lower molluskan zone*, or Iowan, produced an assemblage containing 14 species, 2 of which are diagnostic of the zone. A *transitional zone*, located between the upper and lower faunal zones contains elements of both assemblages and does not imply any abrupt changes in the depositional environment, although the depositional rate may have slowed somewhat. The *upper molluskan zone*, or Tazewellian, contains 26 species, 14 of which do not occur in the lower zone. Because of the relative youth of the Peoria loess, little of the upper zone has been removed from the upland.

Although readily visible stratigraphic breaks, such as the Jules soil recognized in Illinois (Frye and Willman, 1973; Ruhe, 1976; McKay, 1979) and the soil zones in Iowa (Ruhe *et al.*, 1971), have not yet been widely identified in Kansas and Nebraska, evidence of one or more stable or vegetated surfaces is common. One of the few indications of soil development recognized is that of a Bt horizon in the Medicine Creek valley (May and Holen, 1993); interestingly, the soil has a probable Paleoindian association (May, 1990; 1991). Other indications of soil development in the Peoria loess come from the magnetic data obtained at Fort Riley, Kansas (Johnson, 1996).

Many of the age determinations were made from *Picea* remains, indicating a cool, moist environment. For example, a radiocarbon age of 18,830 yr B.P. on *Picea* charcoal was obtained from the Woodfordian/Peoria-age deposits near Bloomington, Franklin County, Nebraska (May and Holen, 1993). Although radiocarbon data documents the

burial of vegetative material throughout the Woodfordian, two temporal clusters of ages appear from the limited data: 18-17 ka and 14-13 ka. The 18-17 ka time interval represents the Last Glacial Maximum, and the 14-13 ka interval represents the time of major deglaciation (Ruddiman, 1987). By interpreting ice-core data from Greenland, Paterson and Hammer (1987), and more recently Mayewski *et al.* (1993), recorded a dramatic decrease in atmospheric dust content from about 14 ka; this period of reduced atmospheric dust may relate to the time of relative surface stability and tree establishment. May (1989) identified deposition of the Todd Valley Formation in the South Loup River of central Nebraska at about 14 ka; the Todd Valley was subsequently buried by loess. Furthermore, Martin (1990) identified entrenchment in the Republican River of the south central Nebraska at about 13 ka, after which valleys were filled with late Peoria loess.

#### *Eolian sand deposits*

Many studies have been conducted about the morphology of dunes as well as history of eolian sand erosion, transport, and deposition in the central Great Plains. Prior to the 1950s, geomorphic investigations of eolian sand deposits were mostly qualitative in nature (Arbogast, 1995). In the past 30 years, palynological evidences and climate information derived from 'transfer function' have been used increasingly to determine local paleovegetation. In addition, age determination techniques, specifically  $^{14}\text{C}$ , Optical Simulated Luminescence (OSL), and Thermoluminescence (TL) have been widely used to establish chronologies of landscape stability and instability.

Perhaps the most controversial of the geologic aspects of the Sand Hills is the age of eolian activity that produced the dunes. Traditionally, they have been considered to be as old as the late Pleistocene Peoria loess. Lugin (1968), Wright *et al.* (1985) and others have hypothesized that deposition of loess and the development of large sand dunes occurred contemporaneously. Smith (1965) hypothesized two main periods of eolian activity in the late Pleistocene. The first period formed the large crescentic dunes,

and, following a period of dune stabilization, the second episode rejuvenated the earlier dunes and produced linear dunes. Recent attempts to model climatic changes of the last 18,000 years have modeled the Sand Hills as dating primarily from the late Pleistocene (COHMAP Members, 1988). However, no stratigraphic evidence has been reported that would lend support to these hypotheses. Some eolian sand was deposited during the last glacial episode, but the sand dunes of the Nebraska Sand Hills appear to have formed during the episodes of aridity and eolian activity occurring within the Holocene (Ahlbrandt and Fryberger, 1980).

Stabilized parabolic dunes and sand sheets cover much of the landscape of northeastern Colorado and adjacent parts of southwestern Nebraska in four geographically distinct dune fields. Muhs *et al.* (1996) reported that at least three episodes of eolian sand movement occurred between 27 ka and 11 ka, possibly between 11 ka and 4 ka, and within the past 1.5 ka. Thus, eolian sand deposition took place under both glacial and interglacial climatic conditions.

Landscape stability has also been episodic on the Great Bend Sand Prairie in the last 20,000 years (Arbogast, 1995; Arbogast and Johnson, 1997). During the late Wisconsin, Peoria loess accumulated periodically, and the prevailing northwest winds created lunettes on southern margins of playa-lake basins. A brief period of soil formation occurred during the Last Glacial Maximum about 18 ka (Figure 2.3). Floral material recovered from the late-Wisconsinan sediments was a fragment of *Picea* (*cf. glauca*) charcoal, dated to about 17,000 yrs B.P., suggests that the climate was more mesic than at present (Johnson, 1991b). The presence of white spruce during the late Wisconsin is consistent with other localities in the Arkansas River valley (Jaumann, 1991), Cheyenne Bottoms (Fredlund, 1995), Muscotah marsh in northeastern Kansas (Grüger, 1973), and Harlan County Lake in Nebraska (Wells and Stewart, 1987). At present, white spruce is associated with the Nearctic taiga from Alaska to Newfoundland and along the eastern flank of the Rocky Mountains to Montana (Jaumann, 1991).

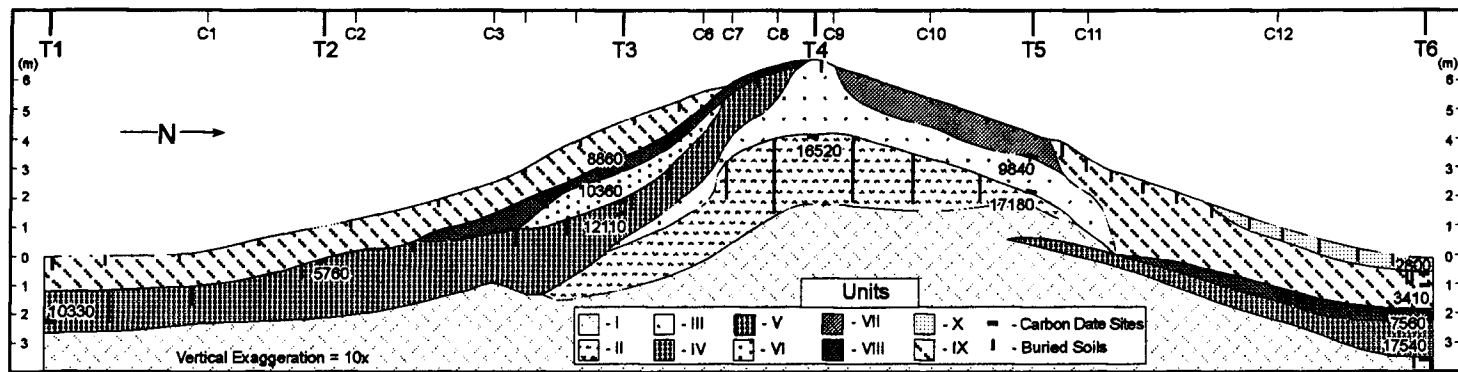


Figure 2.3. Cross sectional stratigraphy of the Wilson Ridge lunette, Kansas (after Arbogast, 1995).

In addition, gastropod species, collected from the Peorian loess, include *Discus cronkheitei*, *Helocodiscus singleyanus*, *Lymnea parva*, *Succinea avara*, and *Vertigo tridentata*. These species are presently extinct in the central Great Plains and generally found in areas of north America where more effective moisture occurs (Arbogast, 1995; Arbogast and Johnson, 1997).

#### *Alluvial deposits*

Much of the chronology of late-Wisconsinan landform evolution for the region was compiled in the 1940s and early 1950s, prior to the use of radiocarbon dating (e.g., Lugn, 1935; Schultz and Stout, 1945; Frye and Leonard, 1951), and focused to a large degree on the upland rather than valley deposits. Additionally, erosion has removed a large part of late-Quaternary record from most drainage basins in the central Great Plains (Knox, 1983). Accordingly, a comprehensive sedimentation and erosion chronology for the region during the late Wisconsin is lacking.

It is becoming increasingly apparent that entrenchment occurred in the channels of the Kansas River basin sometime during the late Wisconsin. A basal soil buried within the fill of both tributary and major stream valleys of the Kansas River basin has an age of 10,500-10,000 yr B.P. (Johnson and Martin, 1987; Johnson, 1987; Johnson and Logan, 1990), thereby providing a minimum age on the entrenchment. May (1989) has radiocarbon dated the Todd valley fluvial sand of central Nebraska to about 14,000 yr B.P., although Condra *et al.* (1950) had postulated a much earlier Wisconsinan age. Martin (1990; 1993) recognized a late-Wisconsin fill in the Republican River valley that was largely removed through entrenchment about 13,000 yr B.P. A radiocarbon age of 14,700 yr B.P. was obtained on spruce wood situated above crossbedded fluvial sand and gravel at the North Cove site located in that same reach of the Republican River valley (Wells and Stewart, 1987; Johnson, 1989). At the Prairie Dog Bay site in the Republican River valley, the stratigraphy and radiocarbon ages suggest downcutting before 11,800

yr B.P. (Martin, 1990, 1993). Speculation about the cause of this entrenchment centers on an increase in effective moisture as climatic conditions ameliorated towards the end of the Pleistocene. Spring deposits dating to this time at the North Cove site possibly formed during the increase in moisture (Johnson, 1989; Martin, 1990).

Brice (1964) studied alluvial fills and terraces in the valleys of the North Loup, Middle Loup, and South Loup rivers of central Nebraska, and identified two major terraces in the Loup valleys. The Kilgore terrace occurs as remnants 26 to 30 m above stream level along the South Loup River, the underlying fill of which Brice suggested is Peorian in age. The adjacent Elba Terrace standing 11 to 12 m above stream level, is the most prominent and extensive terrace in the main valleys and is primarily of Holocene age.

### **Climatic Proxies**

Two general quantitative methods have been applied to the reconstruction of past climates. The first is to determine past climate through the analysis of local or regional field data with the aid of transfer functions. The other method uses large-area climate modeling with the boundary conditions determined by calculation or from field data. Neither supplants the other, for the reconstructions have different spatial scales and degrees of precision. Most models of past climates also require inputs that can only be obtained from field investigations (Smiley *et al.*, 1991). Transfer functions refer to a quantitative relation between a climatic indicator, such as  $\delta^{13}\text{C}$  data from buried soils, as an independent variable, and a climatic element or complex of elements, expressed as a dependent variable. The use of analogs for estimating past climates involves considerable uncertainty, brought about both by the complex mix of factors that constitute climate and by the complex response of most proxy climatic indicators in the record. In a sense, the use of analogues involves the construction of a mental transfer function based on the assumption of appropriate modern analogue selection (Smiley *et al.*, 1991). Because each source of paleoenvironmental data records a somewhat different aspect of climate,

comparing reconstructions based on two or more environmental sensors can broaden and deepen our understanding of past climate changes.

With few suitable species and settings for dendroclimatological study and few natural wet environments to preserve fossil pollen for palynological studies, the nature and timing of late-Quaternary vegetation and climate change in the central Great Plains remain poorly understood. The region's late-Quaternary climate and vegetation conditions are inferred from the palynological records obtained from sites peripheral to the central Great Plains or from limited pollen records available at a limited number of sites in the region (Fredlund and Jaumann, 1987; Fredlund, 1995). However, some of the climatically-sensitive parameters that have recently been examined in the central Great Plains include fossil pollen, opal phytoliths, stable carbon isotopes, and rock magnetism. In addition to an expanding proxy base, recent research has indicated that the extensive loess deposits of the region contain an extractable climatic proxy record comparable to the marine isotopic record.

#### *Fossil pollen and botanical macrofossils*

Several factors in the interpretation of Great Plains fossil pollen assemblages warrant consideration. Any interpretation of pollen assemblages for vegetational reconstruction must be based on appropriate analog studies of modern vegetation and pollen (Fredlund and Jaumann, 1987). Additionally, in the central Great Plains region where ideal wet depositional sites are rare, differential pollen preservation is a problem. Modern analogs are a basis for late-Quaternary environmental reconstruction only where pollen deterioration has not significantly biased the information content of the fossil pollen assemblage (Delcourt and Delcourt, 1980). For example, differential preservation has been shown to be responsible for tremendous over representation of *Pinus* in some situations, while elsewhere rendering *Populus* invisible. Poor pollen preservation is therefore the limiting factor for many of the late-Quaternary records in the central Great

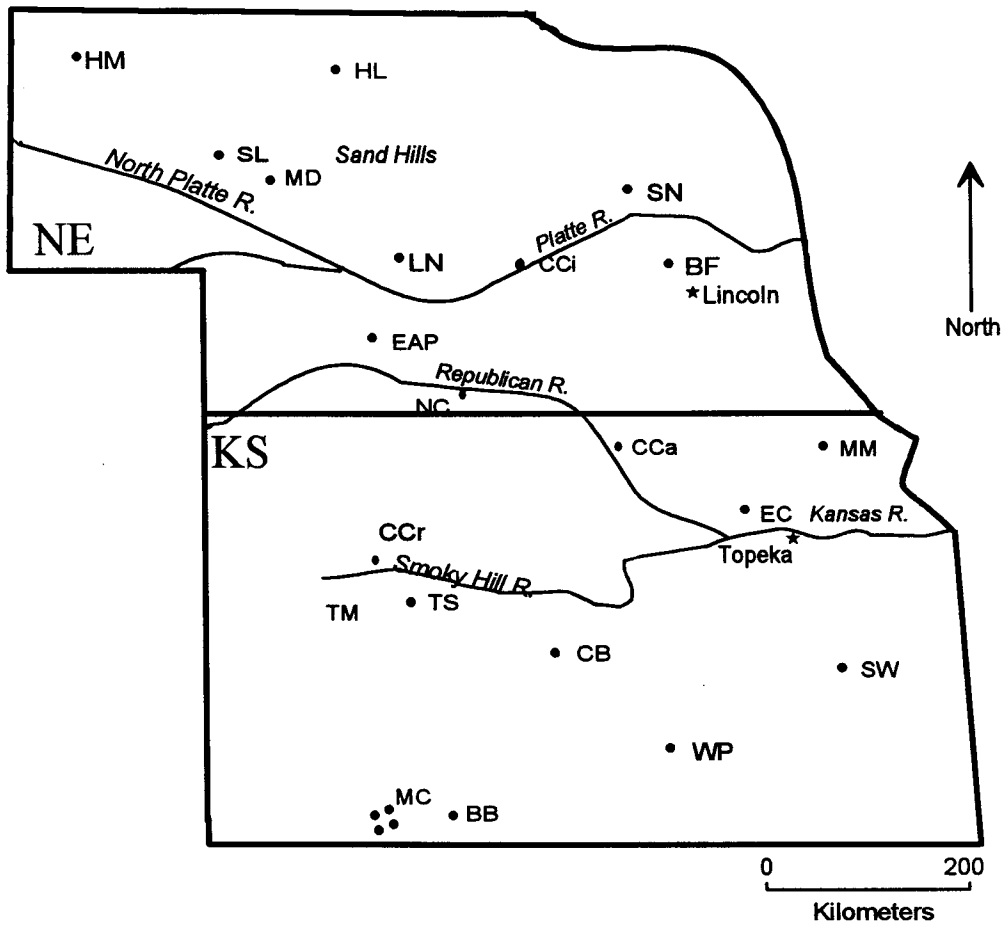


Figure 2. 4. Late-Quaternary pollen and macrobotanical sites in central Great Plains (from Fredlund and Jaumann, 1987)

Plains. Although temporally and spatially limiting, several sites in the region have produced a picture of past environments (Figure 2.4).

By the time ice lobes in Iowa and the Dakota had reached their maxima at about 14ka (Clayton and Moran, 1982), *Picea* had begun to spread its range northward into the Des Moines area (Baker and Waln, 1985). By 12ka, spruce forest was replaced along its southern margin by prairie in southern South Dakota. About 11ka, *Quercus* (oak), *Populus*, *Fraxinus* (ash), and other hardwoods, which were probably confined to the central United States in glacial time, expanded their northern ranges and mixed with *Picea* in the eastern part of the northern Great Plains and the Midwest. This admixture of trees has no close analogues in the present day, but the vegetation is presumed to have been open and dominated by spruce, with some hardwoods and no pine.

The western limit of the forest is not known. At two sites in the glaciated region of northeastern South Dakota (Pickerel Lake: Watts and Bright, 1968; Medicine Lake: Radle, 1981), deciduous trees replaced *Picea* about 11ka, and prairie developed at about 10ka. Pollen data from east-central North Dakota indicate a similar sequence. From the eastern fringe of the central Great Plains, in Iowa and Missouri, pollen and macrofossil evidence suggest that open jack-pine forest of the Farmdalian period yielded rapidly to open white-spruce forest around 22ka (Fredlund and Jaumann, 1987). A similar record of Woodfordian spruce forest comes from Muscotah Marsh in northeastern Kansas. According to Gröger (1973), a rather open vegetation with some pine, spruce, and birch as the most important tree species and local stands of alder and willow changed about 23,000 yr B.P. to a spruce forest, which prevailed in the region until at least 15,000 yr B.P. At Boney Spring, a mixed vegetation with some pine, willow, and sedge gave way to a spruce dominant forest at about 21,500 yr B.P. (King 1973). Because of a hiatus in the sedimentary record, vegetation changes resulting in the spread of a mixed deciduous forest and prairie present in the region from 11,000 to 9,000 yr B.P. remain unknown.

According to Wells and Stewart (1987), the central and northern Rocky

Mountains harbor extant populations of most of the boreal-subalpine species thus far recovered from Pleistocene sediments in the central Great Plains. Moreover, even within the Northern Plains, there are numerous refuges for Pleistocene-relict species of trees, landsnails and small mammals on forested ecological islands surrounded by steppe, an outstanding example being the Black Hills of South Dakota. Cones and needles from Harlan County, south-central Nebraska enable the positive identification of the spruce as *Picea glauca* (Johnson, 1989), the boreal white spruce of the neartic taiga that now grows from Alaska to Newfoundland and along the eastern flank of the Rocky Mountains to Montana, with outliers to the East on the Great Plains in the Cypress Hills of Saskatchewan and Black Hills of South Dakota.

The Rosebud site, near the northern edge of the Sand Hills on the Nebraska-South Dakota border, provides a pollen record of late-Pleistocene vegetation. The pollen and plant macrofossil records indicate that a boreal forest existed at that location about 12,600 yr B.P., and that soon afterward a pine forest and subsequently prairie vegetation rapidly replaced the spruce (Watts and Wright, 1966). Seeds and leaves of aquatic macrophytes at the site suggest that a fresh, open-water basin existed when spruce was prevalent, and that conditions changed to a species-poor, alkaline reed swamp with the change to prairie vegetation. This vegetation and limnologic history implies change from a cooler, probably somewhat moister climate to one of increased aridity and higher temperatures that characterizes the Sand Hills today. The pollen record of prairie vegetation at Rosebud does not significantly differ from that of modern surface samples in this area. The rapid disappearance of *Picea* pollen and its immediate replacement by *Pinus* and prairie herb pollen suggest a depositional hiatus, which makes it difficult to interpret subsequent vegetation history. It is clear is that prairie vegetation existed sometime after 12,600 yrs B.P., and that the lake subsequently dried up and either the upper pollen-bearing sediments were destroyed, or intermittent fluvial deposition with poor pollen preservation occurred.

The presence of nonarboreal taxa from sand pits near Wichita, Kansas, indicates a substantial presence of steppe or grassland taxa on the late-Pleistocene landscape of south-central Kansas (Jaumann, 1991). Not only do these taxa represent a significant portion of the pollen spectra, but they also occur in consistent numbers and presently comprise the most important herbaceous taxa of the North American grasslands. Some of these taxa include Graminaeae (grass family), Asteraceae (sunflower family), *Artemisia* (sage), *Iva* cf. *xanthifolia* (marsh elder), *Xanthium* (cocklebur), *Amorpha* cf. *canescens* (lead plant), *Phlox* cf. *pilosa* (prairie phlox), *Petalostemon* cf. *purpureus* (purple prairie clover), *Potentilla* sp. (cinquefoil), *Ambrosia* type (ragweed), *Chenopodium/Amaranthus* (goosefoot, pigweed), herbaceous Rosaceae (rose family), Fabaceae (bean family), *Epilobium* cf. *angustifolium* (willow-herb), Euphorbiaceae (spurge family), Cannabaceae (hemp family), and *Tradescantia* (spiderwort).

The closest vegetation type showing such a compositional mix can be found along the southern rim of the boreal forest on the Canadian Prairies. There, mapping of the southern limits of coniferous trees indicate that the southern natural distribution of *Picea glauca*, *Picea mariana* (black spruce), *Larix laricina* (tamarack), *Pinus banksiana* (jack pine), and *Pinus contorta* (limber pine) is confined to a narrow transitional zone between the taiga and aspen parkland (Jaumann, 1991). Mosaics of grasslands and forests characterize the aspen parkland. The fossil plant communities recorded in the Wichita sand pits and Mt. Hope Sand Company pit pollen assemblages look very much like the vegetation types in this narrow transitional zone, which prominently extend eastward into the prairie or aspen parkland.

According to Fredlund (1995), the high relative frequency of *Artemisia* pollen in the Farmdalian record from Cheyenne Bottoms in central Kansas indicates that one or more species of sage were an extremely important element in the upland grassland-steppe. This vegetation assemblage does not, however, appear to be exactly analogous to the modern sagebrush steppe of the northwestern High Plains. The pollen evidence suggests

that the regional vegetation, although dominated by grassland-steppe, was not totally treeless. Most of the arboreal elements present are boreal or taiga-like in their modern distribution. The most common trees of the Pleistocene vegetation in the region, however, were not coniferous. The low percentages of both *Picea* and *Pinus* pollen could be the result solely of long-distance transportation; this is especially likely for *Pinus* which could represent forests as far away as 400 km. In the case of *Picea*, however, it is more likely that local populations of trees were scattered along river valleys or fire-protected escarpments. It is extremely unlikely that the *Pinus* and *Picea* pollen signals from the Farmdalian portion of the record represent coniferous parklands or savannas, rather it is more likely that these low pollen percentages represent small populations of conifers limited to edaphically mesic and fire-protected situations.

#### *Stable carbon isotopes*

One recently adopted approach to quantitative reconstructions is to estimate the proportion of C<sub>3</sub> (cool-season) to C<sub>4</sub> (warm-season) plants once present at a site using carbon isotopes from the bulk carbon content in sediments, primarily in buried soils. Regionally,  $\delta^{13}\text{C}$  analyses have been applied to a variety of Quaternary soil fractions including soil organic matter, soil carbonate, and opal phytoliths (*e.g.*, Fredlund and Tieszen, 1997; Nordt *et al.*, 1994; Humphrey and Ferring, 1994; Kelly *et al.*, 1993; Fredlund, 1993).

The natural difference in the stable carbon isotopic composition of C<sub>3</sub> and C<sub>4</sub> plant species provides an opportunity to assess the long-term stability of plant communities and climate of a given region (Troughton *et al.*, 1974; Stout *et al.*, 1975). The basis of this approach is that during photosynthesis, C<sub>4</sub> plants discriminate less against isotopically heavier <sup>13</sup>CO<sub>2</sub> than do C<sub>3</sub> plants (Vogel, 1980; O'Leary, 1981). This difference in carbon isotope fractionation during photosynthesis results in a characteristic carbon isotope ratio

in plant tissue that serves as a diagnostic indicator for the occurrence of C<sub>3</sub> and C<sub>4</sub> photosynthesis. The δ<sup>13</sup>C values of C<sub>3</sub> plant species range from approximately -32 to -20‰, with a mean of -27‰, whereas δ<sup>13</sup>C values of C<sub>4</sub> species range from -17 to -9‰, with a mean of -13‰. Thus, C<sub>3</sub> and C<sub>4</sub> plant species have distinct, non-overlapping δ<sup>13</sup>C values (Nordt *et al.*, 1994).

The stable isotope ratios for <sup>12</sup>C/<sup>13</sup>C are measured by isotope ratio mass spectrometry, and the isotopic data are expressed as the difference, or delta value (δ), between the sample or standard times 1000.

$$\delta^{13}C = \frac{R_{\text{sample}} - R_{\text{standard}}}{R_{\text{standard}}} * 1000$$

$$R = {}^{13}\text{C}/{}^{12}\text{C}$$

The δ value for a carbon isotope in soil organics is defined as follows:

$$\delta^{13}C_{\text{soil}} = (\delta^{13}C_{C_3}) (x) + (\delta^{13}C_{C_4})(1 - x)$$

where δ<sup>13</sup>C<sub>C<sub>4</sub></sub> is the average of δ<sup>13</sup>C values of C<sub>4</sub> plants (-13‰); (δ<sup>13</sup>C<sub>C<sub>3</sub></sub>) is the average of δ<sup>13</sup>C values of C<sub>3</sub> plants (-27‰); and x is the proportion of carbon from C<sub>3</sub> plant sources.

The δ<sup>13</sup>C value of soil organic matter or pedogenic carbonates formed largely from respired CO<sub>2</sub> is a direct indicator of the fraction of the biomass using the C<sub>3</sub> or C<sub>4</sub> photosynthetic pathways. Humus from buried soils probably represents organic matter from the last few hundred years before burial, given the short residence times typical for humus in most modern soils (Birkeland, 1984).

The link between temperatures and grass floristics in North America is well established. Teeri and Stowe (1976) found that the percent C<sub>4</sub> in the continental United States was strongly correlated with the normal July daily minimum temperature, with a correlation coefficient of 0.97. This temperature was a better predictor of the percent C<sub>4</sub>

than either the normal July average temperature or the normal July maximum temperature. Based on their analysis, the percent of C<sub>4</sub> species in a grass flora in the continental United States is most accurately predicted by a linear combination of the normal July minimum temperature, mean annual degree-days and the log of the length of the freeze-free period. Recently, Fredlund and Tieszen (1997) reported that  $\delta^{13}\text{C}$  values correspond to mean July temperature strongly, with a correlation coefficient of 0.66.

For the Gilman Canyon Formation,  $\delta^{13}\text{C}$  values exhibit a good correlation with coincident phytolith data.  $\delta^{13}\text{C}$  data acquired in association with the correction of radiocarbon ages for the Peoria loess in Kansas and Nebraska indicate that C<sub>3</sub> plants were dominant during most of Peoria loess deposition (Figure 2.5). This reflects the cooling associated with the Last Glacial Maximum within early-middle Peoria time (ca. 18 ka). Conversely, C<sub>4</sub> plants were dominant for most of the Gilman Canyon time of pedogenesis (Figure 2.5), indicating that vegetation and thus climate during Gilman Canyon time was similar to present warm, semiarid conditions in the central Great Plains (Johnson, 1993).

Site specific factors should be borne in mind when interpreting  $\delta^{13}\text{C}$  data from soil humates. For example, the 17,000 yrs B.P. buried soil on the north flank and crest of the dune at Wilson Ridge in the Great Bend Sand Prairie (17,180  $\pm$  240, Tx-7824; 16,520  $\pm$  200, Tx-7825) yielded a  $\delta^{13}\text{C}$  value of -11.9‰. During the Last Glacial Maximum, the dune temporarily stabilized and a soil formed. A  $\delta^{13}\text{C}$  ratio of -11.9 ‰ suggests that warm-season or edaphic plants dominated, a finding contradictory with regional late-Wisconsinan mesic climatic conditions. Following landscape stability, the soil was buried by sand, presumably during another period of increased aridity and prevailing northwesterly winds (Arbogast, 1995; Arbogast and Johnson, 1997).

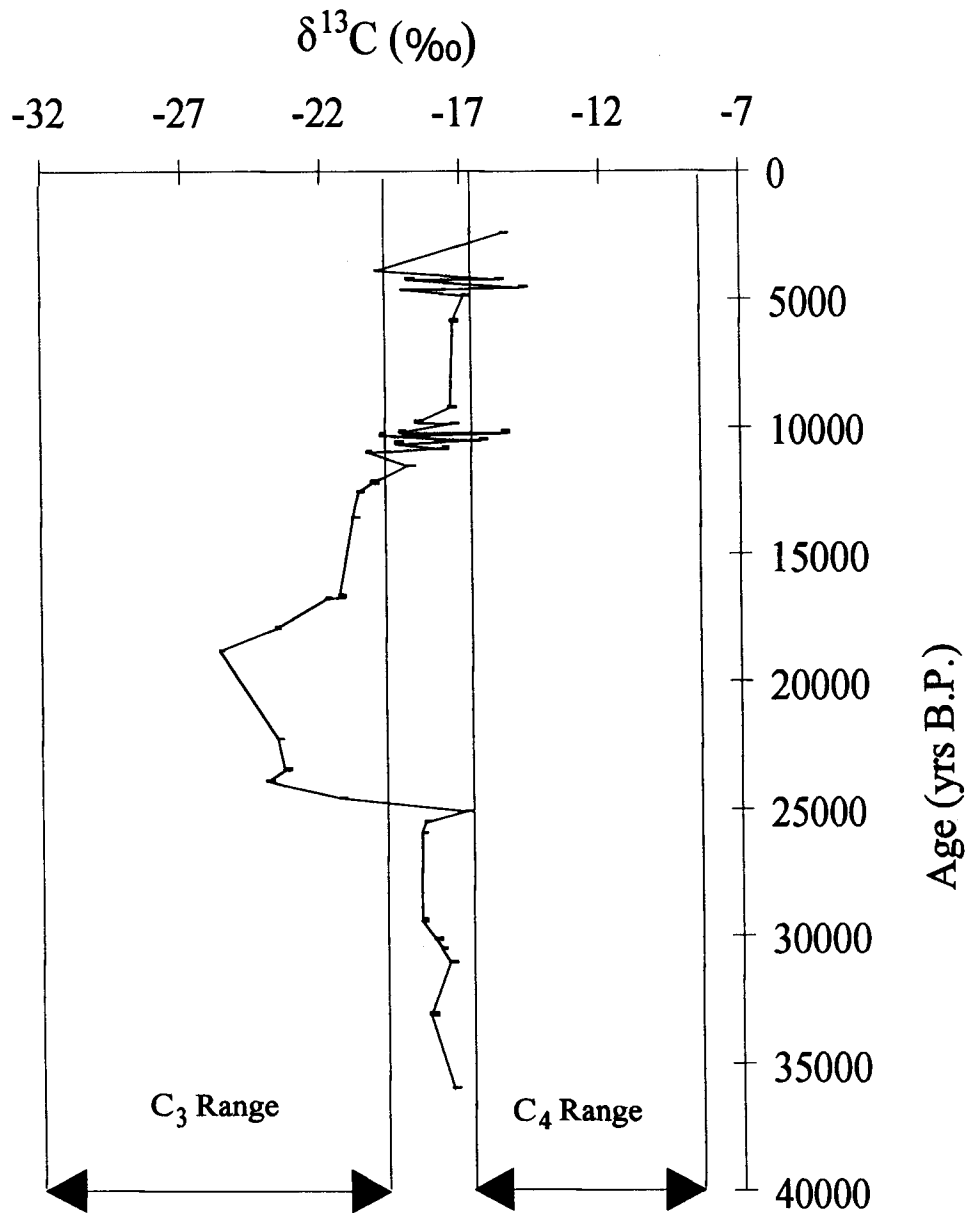


Figure 2.5.  $\delta^{13}\text{C}$  values obtained from loess deposits of Kansas and Nebraska. The ranges in C<sub>3</sub> (cool season) and C<sub>4</sub> (warm season) plants indicate mixed communities for much of the last 35,000 years (after Johnson *et al.*, 1993).

### *Opal phytoliths*

Although recent studies confirm that  $\delta^{13}\text{C}$  of soil organic matter in grassland soil samples accurately reflects the relative abundance of  $\text{C}_3$  and  $\text{C}_4$  grasses and temperature (Tieszen *et al.*, 1997),  $\delta^{13}\text{C}$  analysis cannot distinguish between the relative contribution of  $\text{C}_4$  xeric short grasses and  $\text{C}_4$  mesic tall grasses to soil organic matter (Fredlund and Tieszen, 1997). Fredlund and Tieszen (1997) and Johnson and Bozarth (1996) suggested that short-cell phytolith morphotypes can distinguish among short  $\text{C}_4$  grasses and  $\text{C}_3$  grasses.

Growing plants absorb water containing dissolved silica through their roots. Microscopic amorphous silica bodies are subsequently produced by the precipitation of hydrated silicon dioxide ( $\text{SiO}_2 \cdot n\text{H}_2\text{O}$ ) within the plant's cells, cell walls, and intercellular spaces. Silica bodies with characteristic shapes are called opal phytoliths.

On the Great Plains, two grass subfamilies commonly employ the  $\text{C}_4$  pathway: the Panicoideae and the Eragrostoideae. The panicoids include such common prairie grasses as the bluestems (*Andropogon* spp.), panicums (*Panicum* spp.), and Indian grass (*Sorghastrum nutans*), as well as domesticated grasses, *e.g.*, sorghum, and corn. The grama grasses (*Bouteloua* spp.) and buffalo-grass (*Buchloe doctyloides*), of the Chlorideae tribe of the Eragrostoideae subfamily are the two most important of these grasses in the arid southwestern region of the Great Plains. The overall pattern, where festicoids ( $\text{C}_3$ ) dominate the cool northcentral Great Plains, panicoids on the moist, warm eastern and southeastern margins, and chloridoids primarily in the western and southwestern Plains, is consistent with the pattern expected from general  $\text{C}_3$  and  $\text{C}_4$  adaptations of grasses.

It is well known that three different photosynthetic pathways exist among plant species:  $\text{C}_3$  (Calvin-Benson cycle),  $\text{C}_4$  (Hatch-Slack cycle) and CAM (Crassulacean Acid Metabolism). Twiss (1987) suggested that grass-opal phytoliths could serve as indicators of  $\text{C}_3$  and  $\text{C}_4$  pathways in grasses.

Few workers have reported opal phytolith data from sites in the central Great Plains. Among them, Fredlund *et al.* (1985) tabulated the abundance and type of phytoliths from a vertical loess section at the Eustis ash pit in south-central Nebraska. Poooid phytoliths were the most abundant forms, followed by significant vertical variation in the chloridoid and panicoid types. They concluded that increases in the chloridoid type in buried soil complexes indicated that the soil forming periods must have been warmer and drier than the periods of loess accumulation. The phytolith assemblages from the soils of the Gilman Canyon Formation are unique at the Eustis ash pit: nowhere in the entire 620,000-year record of loess accumulation at the site has anything similar been recorded. The high relative frequencies of panicoid-class phytoliths are even higher than those found in the tall-grass, panicoid-dominated prairies today. In general, the phytolith evidence of warmer soil-forming periods and cooler episodes of increased dust accumulation fits the traditionally accepted models for the loess deposition and other proxy records.

The basic taxonomic system defines those opal phytolith types common to the short C<sub>4</sub> grasses (Chloridoideae subfamily), the tall C<sub>4</sub> grasses (Panicoideae subfamily), and those produced by primarily by the cool -season C<sub>3</sub> grasses (Pooideae subfamily). Based on the classification system used by Twiss *et al.* (1969), Diester-Haass *et al.* (1973) suggested that grass opal phytoliths could serve as indicators of continental climatic change. Diester-Haass *et al.* (1976) calculated humidity-aridity tendencies using the following formula:

$$Tp = \frac{\text{chloridoid}}{\text{chloridoid} + \text{panicoid}} * 100$$

where Tp indicates the phytolith index. Since chloridoid type is characteristic for an arid grass assemblage, panicoid type for a humid assemblage, higher values indicate increased aridity, lower values indicate increased humidity. Ongoing opal phytolith analysis of the

Peoria loess is producing a climatic signal consistent with that of the carbon isotope data (Johnson *et al.*, 1993). A cool, mesic climate is apparent by the occurrence of arboreal phytolith types and C<sub>3</sub> grass types in the loess of the lower Gilman Canyon Formation and the Peoria loess.

### *Snail assemblages*

In central and western parts of Kansas where Late Pleistocene deposits are less severely affected by weathering, assemblages of fossil mollusks greatly exceed in variety of species, and in population density, the local living molluscan fauna (Leonard, 1952). During the Peoria time, approximately 30 species of landsnails were distributed on the interfluvial uplands of the Great Plains (Wells and Stewart, 1987).

Leonard (1952) recognized two main faunal zones and one transitional zone within Peoria loess of Kansas. A basal zone is devoid of fossil mollusks, but it is correlative with Gilman Canyon Formation. The basal zone silts were deposited so slowly that the substantial weathering took place. The depositional rates gradually accelerated with time until rate of accumulation outstripped rate of weathering of the basal zone.

Ecological conditions during the Peorian deposition were relatively favorable to terrestrial gastropods, since the fossil faunas were more varied than are the modern faunas in the same area. A reasonable amount of rainfall and a floral cover at least as dense as that prevailing now has been inferred to have existed over the area in Kansas in Peorian time, since terrestrial gastropod are active and can produce only during intervals when the soil and overlying organic matter are moist.

Rousseau and Kukla (1994) counted mollusk assemblages within the Eustis ash pit, where the same section and stratigraphic marker has been employed for the detailed rock magnetic measurements for this study. Based on land snail assemblages, three mollusk zones have been distinguished. The first zone ( 18 to 14 m in depth) is characterized by small number of species and the lack of *Discus* or *Columella alticola*.

This points to a moderately cool and relatively moist climate and to the presence of grassland. The second zone (14 to 10 meter) is distinguished by the presence of *Discus* and the first appearance of the Cordilleran-boreal species *Columella alticola* which indicates some arboreal vegetation was present. The third zone (10 to 1 meter) is characterized by abundance of recognized species and seems to correspond to an interval of extreme cold, with low and gradually decreasing annual precipitation concentrated in a short growing season.

### **Climatic Modeling**

Kutzbach (1987) summarized the behavior of the North American jet streams during the late Wisconsin. In July, the split flow around the North American ice sheet modeled at 18 ka persisted to 15 ka, with almost no changes having occurred. By 12 ka, two important changes appeared: first, the northern branch of the jet moved south, over and along the southern flank of the ice sheet, and merged with the southern branch over the northeastern United States. The second change was the reduced intensity of the North Atlantic extension of jets. The jet at 9 ka followed about the same track as at 12 ka, but with weakened intensity. At 6 ka and thereafter, only a single jet core was simulated over Alaska and Canada, and winds were weak compared to reconstructions of earlier periods. Specifically, the modern single jet core of July follows generally the same track as the northern branch of the split jet in July during the glacial maximum.

In January, like July, the split flow around the North American ice sheet and the intense North America/North Atlantic jet cores at 18 ka persisted to 15 ka with almost no change. At 18 ka the simulated temperatures over the continent were much lower than at present, especially over the elevated and highly reflective ice sheets (COHMAP Members, 1988). By 12 ka, the flow had adjusted to single core of high velocity winds that followed the west-coast-ridge, east-coast-trough pattern of today, and the jet maximum was almost as strong as at 18-15 ka.

The north central region, from the Rockies to the Appalachians and from immediately south of the ice sheet to 40°N, had summer temperatures of 16°C at 18-15 ka, about 7°C below present. Precipitation was less than present at 18-15 ka (colder, with the storm track shifted south of the region) and precipitation-minus-evaporation was slightly increased at 18-15 ka (evaporation decreased more than precipitation).

## PLEISTOCENE/HOLOCENE TRANSITION

The last deglaciation was a period of intense and rapid climatic changes that affected the global climate from about 20,000 to 5,000 yrs B.P. Paleoclimatologists have reconstructed global variations, including chemical composition of the atmosphere (30% increase in CO<sub>2</sub> and CH<sub>4</sub>, decrease in dust content, *etc.*), temperature of the atmosphere and surface of the ocean (mean global change of about +4°C), and major reorganization of the ocean circulation and sea-level rise of about 120 meters, followed by slow rebound of the continents below the ice caps (Bard and Broecker, 1992).

The transition between the Last Glacial Maximum and the present inter- or postglacial episode has drawn much attention from investigators for many decades. Initially, the last deglaciation was believed to have been a simple, unidirectional shift, but more recent detailed studies revealed that it was a two-step process (Duplessy *et al.*, 1981; Broecker *et al.*, 1989). During the last deglaciation, intervals of rapid warming between about 13 ka and 11 ka and at about 10 ka were separated by a distinct, brief cool climate episode occurring between about 11 ka and 10 ka.

Between about 12ka and 9ka, the climate and vegetation of central North America underwent dramatic changes (Wright, 1970; Watts, 1983; Webb *et al.*, 1983). Spruce trees had been replaced by widely distributed deciduous trees in northeastern Kansas, and deciduous trees persisted until about 9ka when grasslands expanded (Webb *et al.*, 1983). It is clear that megafaunal extinction and dissolution of disharmonious faunas began about 12ka, and that the mesic conditions under which the regionally-expressed Brady soil developed persisted until about 8ka, when the modern climate first appeared. Changes in vegetation and faunal assemblages at this time reflect a shift to warmer and drier conditions with increased seasonality (COHMAP Members, 1988) and stronger zonal air flow at the surface (Kutzbach, 1987). This was a time of major atmospheric circulation change within the central Great Plains, as well as elsewhere.

## Stratigraphy and Environments

The beginning of the Holocene, about 10 ka (Hopkins, 1975), is a time of dramatic environmental change and attendant stratigraphic discontinuities. In general, this boundary is considered only geochronometric without specific stratigraphic reference, although a stratotype in Sweden has been proposed for the boundary (Mörner, 1976); the Swedish unit has a reported age of  $10,000 \pm 250$  yrs B.P. (Fairbridge, 1983). Watson and Wright (1980) contended that a major climatic or environmental changes at 10,000 yrs B.P. were documented only locally. This contention seems faulty, however, on the regional and subcontinental scale given that research of the last several years in the central Great Plains has identified the Brady soil (Schultz and Stout, 1948) as a major pedostratigraphic marker (*e.g.*, Johnson and Martin, 1987; Johnson and Logan, 1990; Johnson and May, 1992).

### *Brady soil*

Classically, the Brady soil was associated with the upland loess deposits, but recent investigations have identified a contemporaneous soil in upland eolian sands and in alluvial valley fill (Johnson and May, 1992). It therefore appears that Brady soil development represents a time of extensive, broad-scale landscape stability. The Brady soil represents the most important break in sedimentation recorded since development of the cumulic soil of the Gilman Canyon Formation, and also marks the position of a distinct faunal discordance (Frye and Leonard, 1955). At least the early and perhaps all of the Brady soil-forming interval coincides with the Younger Dryas cold interval of the North Atlantic region.

The Brady soil was first named and described by Schultz and Stout (1948) at the Bignell Hill type locality, a loess sequence exposed along a roadcut in the south valley wall of the Platte River of western Nebraska. The soil is developed within the Peoria loess and is overlain by the Bignell loess. The name was subsequently adopted by

Table 2.2. Brady soil radiocarbon ages.

Site	Age (BP)	Lab. No.	Source
Nebraska			
Bignell Hill			
	8,080 ± 180	n.a.	Lutenegger, 1985
	9,160 ± 250	W-234	Dreeszen, 1970
	9,750 ± 300	W-1676	Dreeszen, 1970
	9,240 ± 110	Tx-7425	Johnson, 1992
	10,670 ± 130	Tx-7358	Johnson, 1992
North Cove			
west	10,550 ± 160	Tx-6319	Johnson, 1989
	10,220 ± 140	Tx-6112	Johnson, 1989
	10,270 ± 160	Tx-6320	Johnson, 1989
east	11,530 ± 150	Tx-6321	Johnson, 1989
	11,025 ± 90	PITT-824	Martin, 1993
Prairie Dog Bay			
	10,140 ± 110	DIC-3310	Cornwell, 1987
	10,360 ± 130	Tx-5909	Martin, 1993
	10,370 ± 70	PITT-824	Martin, 1993
	11,780 ± 60	PITT-0961	Martin, 1993
	9,020 ± 95	PITT-825	Martin & Johnson, 1992
Naponee			
	10,130 ± 140	Beta-33939	Souders and Kuzila, 1990
Kansas			
Speed			
	8,850 ± 140	Tx-6626	Johnson, 1990
	10,050 ± 160	Tx-6627	Johnson, 1990
Barton County			
	9,820 ± 110	Tx-7045	Feng, 1991
	10,550 ± 150	Tx-7046	Feng, 1991
Wilson Ridge			
	10,220 ± 200	Tx-8005	Arbogast, 1995
	10,180 ± 200	Tx-7826	Arbogast, 1995
	12,000 ± 220	Tx-8004	Arbogast, 1995

Ages represent the eolian phase only. An alluvial phase has been well documented throughout the Kansas River basin (Johnson *et al.*, 1997, Johnson and Martin, 1987; Johnson Logan, 1990) and adjacent river systems, such as the Loup River of central Nebraska (Brice, 1964; May, 1990) and the Pawnee River (Mandel, 1991; 1994) and Walnut River (Mandel, 1991) of the Arkansas River system.

researchers in Kansas (Frye and Fent, 1947; Frye and Leonard, 1951; Frye *et al.*, 1949). The soil is regionally extensive only in the northwestern and west central parts of Kansas, and even there it occurs discontinuously on the landscape. Frye and Leonard (1951) and Caspall (1970; 1972) recognized Brady development in northeastern and other parts of Kansas. Without the overlying Bignell loess, the Brady soil does not exist; the modern surface soil has incorporated post-Bradyan loess fall into its profile. The Brady soil is typically dark gray to gray-brown and better developed than the overlying surface soil within the Bignell loess. Strong textural B horizon development and carbonate accumulation in the C horizon are typical, although it occasionally displays evidence of having formed under poorer drainage conditions than have associated surface soils (Frye and Leonard, 1951). Feng (1991) noted that the Brady soil, as expressed in Barton County, is strongly weathered both physically and chemically.

Until recently the age of the Brady soil had been uncertain, even at the type section: Dreeszen (1970) reported two ages of 9160 and 9750 yrs B.P., both of which were believed to be too young because of contamination. Luttenegger (1985) reported an age of 8080 yrs B.P. without any stratigraphic context. Souders and Kuzila (1990) dated a core at a site in the Republican River valley and reported an age of 10,130 yrs B.P.. Johnson (1993) reported two ages of 10,670 and 9240 yrs B.P.. on the lower and upper 5 cm, respectively, of the Brady A horizon at the type section. Similar ages from the eolian phase have been obtained in south-central Nebraska and north-central and central Kansas (Table 2.2). Ages of the alluvial phase of the Brady from Nebraska and Kansas closely correspond with the ages of the eolian phase. According to age data, soil development began at about 10.5 ka and ended 9-9.5 ka, suggesting a soil forming interval of greater than 1000 years.

Arbogast (1995; 1996a) obtained several Brady era radiocarbon ages from soils buried within the eolian sand of the Great Bend Sand Prairie. Following a period of instability after a short period of stability during the Last Glacial Maximum, soil formation

occurred at the Pleistocene/ Holocene boundary, which correlates temporally with the loessal Brady soil. Two radiocarbon ages of  $10,330 \pm 100$  and  $10,360 \pm 100$  yrs B.P. were obtained at Wilson Ridge, a lunette in the Great Bend Sand Prairie.

The Brady soil is also well expressed in an alluvial facies, *i.e.*, an isochronous alluvial soil found throughout the region is temporally equivalent to the Brady soil identified within loess of the uplands. Since a large number of radiocarbon ages have been obtained from alluvial fill in the central Great Plains (Johnson *et al.*, 1996), the patterns of alluviation, erosion and particularly soil formation during the late Pleistocene through Holocene have become relatively well established.

In northwestern Nebraska, Agenbroad (1978) examined alluvial deposits at the Hudson-Meng Site (25SX115) in Whitehead Creek Valley. Four stratigraphic units were identified beneath a loess-mantled terrace. The lowermost unit, designated Unit 1, consists of alluvium and contains a bone bed and many artifacts; charcoal from the bone bed yielded a radiocarbon age of 9820 yrs B.P., and bone apatite and collagen yielded ages of 8990 and 9380 yrs B.P., respectively. Agenbroad (1978) suggested that the site was buried by alluvial sands and silts sometime after about 9,000 yrs B.P., and that a soil developed at the top of Unit I (ca. 4800 yrs B.P.) during Altithermal time.

The two ages of 8,274 yrs B.P. and 9,880 yrs B.P. determined from alluvial fill (Fill 2A) at archaeological sites Ft-50 and Ft-41 on Harry Strunk lake in southwestern Nebraska (Schultz, *et al.*, 1951; Libby, 1955) were the first radiocarbon determinations obtained on the Brady soil. At Cooper's Canyon, which is southeast of Elba, Nebraska, May (1990; 1991), in a reinvestigation of a site studied by Brice (1964), reported radiocarbon ages on humates in the silt and clay fractions of buried soils, of which two ages agree well with both those in the fill from other localities in the Loup River Basin and eolian facies. Two ages determined were 10,290 yrs B.P. from the lowest 10 cm of Cooper's Canyon gley soil, and 9250 yrs B.P. on the uppermost 10 cm of the Brady soil.

Table 2.3.  $\delta^{13}\text{C}$  values and radiocarbon ages derived from the Brady soil A horizon.\*

Location	Age range	$\delta^{13}\text{C}$ (‰)		Source
		top	bottom	
<b>Nebraska</b>				
Bignell Hill	9240-10,670	-17.40	-19.3	Johnson and May, 1992
North Cove	10,360-10,550	-16.30	-18.9	Johnson, 1989
Sargent Site	9920-10,620	-16.1	-20.1	Dort, unpublished
Elba Valley	9250-10,290	-15.4	-20.0	May, 1991
<b>Kansas</b>				
Speed roadcut	8850-10,050	-18.8	-17.5	Johnson, 1993
Barton County	9820-10,550	-18.6	-19.0	Feng, 1991

\* upper and lower 5 cm of the A horizon except in the study by Dort.

In Kansas, Holien (1982) derived a radiocarbon age of about 10.5 ka from a well-developed soil situated in the lower part of Newman Terrace fill along the lower Kansas River. Johnson (Johnson *et al.*, 1996) obtained an age of 9,820 yrs B.P. from a soil buried in alluvial fill at the Ade site within the Saline River valley near Salina, Kansas.

### **Climatic Proxies**

Evidences of climate change during late Pleistocene/Holocene are derived from the limited number of fossil pollen and macrofossils and  $\delta^{13}\text{C}$  data. Such proxies contain a climatic signal.

#### *Fossil pollen and botanical macrofossils*

The most detailed description of the nature of late Pleistocene/Holocene environmental changes in the central Great Plains comes from palynological studies undertaken along the eastern and northern periphery of the region. At Muscotah and Arlington Marshes in northeastern Kansas, Gröger (1973) documented spruce forest from 23,000 to 15,000 yrs B.P., followed by the spread of a mixed deciduous forest and prairie, which was present in the region from 11,000 to 9,000 yrs B.P. The nature and duration of the climatic changes which precipitated vegetation changes are not, however, certain because of a hiatus in sedimentation. Fredlund and Jaumann (1987) have suggested that such pollen records represent an expansion of an aspen parkland-like community across the Great Plains.

According to Wright (1989), pollen records from the Great Plains can not show the effects of minor climatic fluctuations like the Younger Dryas because climate had become too warm by 11 ka to permit reintroduction of spruce. General circulation model results also show that the temperature for winter was deeply depressed far across Eurasia, but was little changed in North America (Mathewes, 1993). The critical vegetation change identified by Shane and Anderson (1993) in east-central North America involves

the recurrence of spruce, which is limited in its southern range by summer rather than winter temperatures. The southerly position of the polar front across the North Atlantic could have resulted in a southward displacement of the jet stream and associated storm tracks, thus enhancing the cyclonic storms that could deliver cold northwesterly winds not only to the Maritime Provinces but inland to the Ohio area as well (Wright, 1989).

Another source of paleoenvironmental information comes from peat beds and logs, radiocarbon dated from 10,500 to 8,400 yrs B.P., buried in valley fills associated with the North Loup River (Bradbury, 1980). The peat is buried by alluvium which is, in turn, mantled by dune sand. The stratigraphic association of these deposits and the presence of marsh plants like *Equisetum* (horsetail) indicate that, locally, fluvial processes and riparian environments, similar to those that exist today, were followed by sand movement (Bradbury, 1980). Most recently, Ponte *et al.* (1994) dated peat recovered in a core from the central Sand Hills and radiocarbon dated it to 12,260 yrs B.P.; the peat contained 70% *Picea* pollen, indicating that the spruce forests of the late Wisconsin existed farther south into the Sand Hills than previously reported.

#### *Stable carbon isotopes*

Temporal changes in  $\delta^{13}\text{C}$  data derived from carbon contained within soil and sediment (Figure 2.5) are sufficiently large to show major shifts in vegetation during the late Wisconsin. The interval between 12,000 and 9000 yr B. P. can be interpreted as transitional between the cooler and more xeric late Pleistocene to warmer and drier Holocene. Based on a slight decrease in the  $\delta^{13}\text{C}$  values from the Brady soil at six sites in the region, the climate shifted to more xeric conditions ( $\text{C}_3$  to  $\text{C}_4$ ) from the beginning to the end of the Brady time, a period of major landscape stability and pedogenesis (Table 2.3).

The isotopic data agree with that of other climatic proxies for the region. The fossil pollen record from Muscotah Marsh in northeastern Kansas indicates that spruce

had essentially disappeared from the region by about 10,500 yrs B.P. As this decline occurred, deciduous tree species increased until about 9000 yrs B.P. From a site in central Texas, Nordt *et al.* (1994) interpreted the time between 11,000 and 8000 yrs B.P. as transitional between late-Pleistocene conditions and warmer and drier Holocene conditions based on a slight increase in the abundance of C<sub>4</sub> plant biomass using stable carbon isotopic data.

### **Climatic Modeling**

Significant deglaciation did not begin until 14 ka and ended by 6 ka. This conclusion is validated by maps of ice area, by marine  $\delta^{18}\text{O}$  records, and by terrestrial and marine records (Ruddiman, 1987; Crowley and North, 1991). With increased summer insolation during the termination, the mass imbalance of ice sheet would have increased. Ice sheet decay may also have been affected by a number of processes. For example, CO<sub>2</sub>-induced air temperature changes were large enough to cause disintegration of an extensive marine-based ice sheet on Eurasia. Broecker *et al.* (1988) suggested that changes in the coupled ocean-atmosphere circulation in the North Atlantic were responsible for the changes.

The structure of deglaciation within this 8,000-year interval is uncertain. There is evidence supporting: (1) a smooth deglaciation model with fastest ice wastage centered on 11 ka; (2) a two-step deglaciation model with rapid ice wasting from 14 to 12 ka and 10 to 7 ka, and a mid-deglacial pause with little or no ice disintegration from 12 to 10 ka; and (3) a Younger Dryas deglaciation model with two rapid deglacial steps as in (2) above, interrupted by a mid-deglacial reversal with significant ice growth from 11 to 10 ka.

The critical data supporting the smooth deglaciation model are maps of Laurentide ice area based on radiocarbon-dated glacial deposits. Although there are subtle suggestions of more rapid retreat at or near the time of the two steps mentioned above,

these curves indicate a steady progressive retreat of North American ice, with significant oscillations in retreat rate only at local spatial scales. Some marine  $\delta^{18}\text{O}$  curves also show a smooth progressive decrease toward Holocene values.

The step deglaciation model is also supported by some marine  $\delta^{18}\text{O}$  records (Mix, 1987). In addition, the distinctive patterns of change in sea-surface temperature of the North Atlantic Ocean and in Greenland ice-core  $\delta^{18}\text{O}$  values also show abrupt step-like warmings at 10 ka and approximately 13 ka; these warmings might be associated with step-like decreases in Laurentide ice volume. Regionally integrated rates of pollen change in eastern and central North America also show a rapid change centered on 13.7 and 12.3 ka. (Ruddiman, 1987).

The Younger Dryas deglaciation model is suggested by sea-surface temperature cooling between 11 and 10 ka in the North Atlantic Ocean. At least early and perhaps all of Brady pedogenesis coincides with an abrupt and brief cool interval correlative with the classic Younger Dryas cold interval of the North Atlantic region.

### *Younger Dryas*

The Younger Dryas at about 11 ka to 10 ka was the last glacial cold spell and was an abrupt, well defined event (Dansgaard *et al.*, 1989; Broecker *et al.*, 1988; Table 2.4). In this short period of time, the return to near-glacial conditions interrupted the Pleistocene/ Holocene climatic transition, during which most of the Northern Hemisphere ice sheets melted. A leading explanation for the Younger Dryas cooling depends primarily on a mechanism for cooling of North Atlantic waters, rather than on the radiation distribution or directly on the presence of the ice sheets (Wright, 1989). During deglaciation, large quantities of meltwater flowed from the melting Laurentide Ice Sheet. Appreciable evidence exists to suggest that the Younger Dryas coincided with changes in the routing of meltwater between the Mississippi and St. Lawrence drainage basins (Broecker *et al.*, 1988; Broecker *et al.*, 1989; Lehman and Keigwin, 1992; Taylor *et al.*,

1993). The influx of fresh water to high latitudes of the North Atlantic has been suggested as inhibiting the generation of dense, saline North Atlantic deep water, which, in turn, led to a reduction in heat transport to the North Atlantic (Broecker *et al.*, 1988). For this reason, the Younger Dryas was recorded much more distinctly in Europe and Greenland than in North America, and is thought to be confined to amphi-Atlantic region. General circulation model results also support that conclusion, *i.e.*, they show that temperatures for winter were deeply depressed far across Eurasia but were little changed in North America (Rind *et al.*, 1986).

Many recent studies, however, demonstrate that the varied climatic deterioration was, in fact, felt well beyond the North Atlantic (*e.g.*, An *et al.*, 1993; Mathewes *et al.*, 1993; Kudrass *et al.*, 1991; Engstrom *et al.*, 1990; Wright, 1989). In their study of pollen and chemical stratigraphy in southeastern Alaska, Engstrom *et al.* (1990) suggested that a significant climatic reversal occurred in this region between about 10,800 and 9,800 yrs B.P. The temporary return of tundra after full development of lodgepole pine parkland is regarded as a clear response to climatic reversal, even though it is not contemporaneous with any known readvance of glaciers in the area or elsewhere in the Pacific Northwest. More recently, Mathewes *et al.* (1993), in their study of the British Columbia coast, also reported a shift from forest to open, herb-rich vegetation after 11,000 yrs B.P., in response to colder and wetter conditions identified by a pollen-climate function. Shane and Anderson (1993) argued that the recurrence of spruce between about 11,000 and 10,400 yrs B.P. supports the interpretation of regional temperature decrease on the Till Plains region of Ohio, Indiana, Michigan and Illinois.

Table 2.4. Chronology of Younger Dryas.

Beginning	End	Area	Source
	10,720 $\pm$ 150	Greenland Icecore	Dansgaard <i>et al.</i> , 1989
11000	10000	Sulu Sea, SE Asia	Kudrass <i>et al.</i> , 1991
11000	10300	Ohio	Shane, 1987
11000	10000	EN32-PC4, Orca Basin	Broecker <i>et al.</i> , 1988
10800	10000	Alaska	Engstrom <i>et al.</i> , 1990
11290	10170	British Columbia	Mathewes <i>et al.</i> , 1993
11000	10000	Atlantic Canada	Mott <i>et al.</i> , 1986
11200	10500	North Atlantic	Lehman and Keigwin, 1992
	10,580-10,950	China	An <i>et al.</i> , 1993
11,010 $\pm$ 170	10,390 $\pm$ 130	South Portugal	Bard <i>et al.</i> , 1987

## HOLOCENE

The driving mechanism behind the region's environmental change was disintegration of the Laurentide ice sheet (Andrews, 1987), which promoted more arid, zonal atmospheric flow (Knox, 1983). At Muscotah Marsh, the combined effects of increased solar radiation (Kutzbach, 1985, 1987) and increased zonal flow resulted in the complete displacement of forest by grassland till 9000 yrs B.P. (Grüger, 1973).

As the Laurentide ice sheet continued to waste during the early Holocene, the steep north-south temperature gradient which had been present during the late-Wisconsin continue to weaken, promoting further zonal flow. These factors triggered the generally warm and dry conditions of the Altithermal that prevailed in the central North America from about 8000 to 5000 yrs B.P. (Knox, 1988; COHMAP Members, 1988).

### **Stratigraphy and Environments**

The Bignell loess appears to be no older than about 8000 yrs B.P. from the <sup>14</sup>C ages for the type section in Nebraska and for the Speed roadcut (Johnson, 1993). Feng (1991) speculated that the Bignell loess is relatively well weathered because it was derived from the pre-weathered Brady soil surface, perhaps eolian and alluvial phase alike.

### *Bignell loess*

The Bignell loess was first described and named at the same type locality as the Brady soil (Schultz and Stout, 1945). It is typically a gray or yellow-tan massive, calcareous silt, seldom more than 1.5 m thick. Although Bignell loess is often less compact and friable than the underlying Peoria loess, no certain identification can be made without the presence of the Brady soil (Caspall, 1970). The Bignell loess does not form a continuous mantle, but is most prevalent and thickest adjacent to river valleys, particularly the south side, and often occurs in depressions on the Peoria surface. Of the

loesses comprising the late-Quaternary stratigraphy of the central Great Plains, the Bignell is the only one that appears to have been deposited during a warm, nonglacial climate.

### *Eolian sand deposits*

Holocene history documented for the sand sheets of Nebraska, Colorado and Kansas has indicated significant eolian activity. Global climate change, resulting in shifting temperature and precipitation patterns, has been the focus of many of the studies of the sand sheets of the central Great Plains (*e.g.*, Forman *et al.*, 1992b; Yuhas, 1993; Arbogast, 1995). For example, numerous years of drought during the spring growing season reduces vegetative cover, causing dune destabilization. During historical droughts, the coverage of native short-grass vegetation was reduced, and soils were extensively eroded by eolian activity (Tomanek and Hulett, 1970).

A record of late Holocene dune activity comes from the Nebraska Sand Hills through the research of Ahlbrandt and Fryberger (1980) and Ahlbrandt *et al.* (1983). The latter work, producing the first stratigraphically controlled radiocarbon ages from this large sand sea, reported that the most recent period of dune activity was not during the Wisconsin glacial, but rather during the late Holocene (ca. 3,000-1,500 yrs B.P.). Their conclusions were based on data from seven stratigraphically controlled sites: three with maximum-limiting radiocarbon ages of about 3,000 yrs B.P. and four with maximum-limiting ages of about 10,000-5,000 yrs B.P. Based on archaeological and pollen evidence they correlate their age estimates for stabilization of the dunes at 1,500 yrs B.P. with the interstage between the Triple Lakes and Audubon glacial advances in the Colorado front Range reported by Benedict (1973). Further evidence for a Holocene age of dune development offered by Swinehart (1990) was a radiocarbon age of 13,160 yrs B.P. obtained in alluvium 3-4.5m below a 52-85m-high barchan dune in the central Sand Hills. Vibracores from fens of Cherry County in the central Sand Hills collected by Ponte *et al.* (1994) indicated multiple peat layers. Radiocarbon ages outlined two major periods of

eolian activity during the middle Holocene and two subsequent periods at about 3,500-2,800 yrs B.P. and after 1,000 yrs B.P.

The Great Plains region of northeastern Colorado is also an area of extensive sand dunes. Parabolic dunes in the region provide primary paleoclimatic information: dunes are elongate parallel to prevailing winds, causing the limbs of parabolas, anchored by vegetation, to point up wind. The dominant northwest-to-southeast orientation indicates that winds from the northwest shaped the landforms. Such strong prevailing winds on the High Plains are associated with air masses originating from the North Pacific or Canadian Arctic, and they preclude significant influence of tropical or subtropical air masses (Borchert, 1971). These dunes exhibit evidence for a late-Holocene dry period (Muhs, 1985), *i.e.*, soils developed on these dunes have morphological and textural properties similar to soils on stabilized dunes in the Nebraska Sand Hills with maximum limiting radiocarbon ages of about 3,000 yrs B.P. Forman and Maat (1990), using thermoluminescence and radiocarbon dating, obtained ages of 7-9ka on soils buried in dunes near Hudson, Colorado. Forman *et al.* (1992b) documented a succession of paleosols buried by eolian sand during the Holocene, indicating that there were four possible periods of eolian sand deposition in the Holocene: ca. 9500 to 5500 yrs B.P., 5500 to >4800 yrs B.P., 4800 to >1000 yrs B.P., and after 1000 yrs B.P., separated by relatively short intervals. Using radiocarbon dating, archaeological data and other information, Madole (1994) observed that the sand sheet of northeastern Colorado was mobilized within the last 1,000 years. Stratigraphic evidence from Nebraska and northeastern Colorado indicates extensive sand sheet reactivation and dune formation during the late Holocene, with significant mobilization during the last 1000 years in Colorado. Global climate change, resulting in different temperature and precipitation patterns, has been the focus of these studies of sand sheet activity in the central Great Plains (*e.g.*, Forman *et al.*, 1992b; Yuhas 1993; Arbogast, 1995).

Johnson (1991a) and Arbogast (1995) documented periods of dune activity in the Great Bend Sand Prairie of Kansas. The most intensive period of dune formation in the region apparently occurred between 9 and 6 ka, an interval of sand mobility widely recognized on the Great Plains. In the late Holocene, loess accumulated episodically on relatively flat landscapes, while sand sheets and dunes were mobilized from about 5,700 - 4,800, 2,300 - 1,700, 1,600 - 800, and 200 yrs B.P. The orientation of parabolic and barchan dunes indicates that prevailing winds during the Holocene have been generally southwesterly.

Recent geomorphic research in the Great Plains (Holliday, 1987; Forman and Maat, 1990; Swinehart, 1990) has indicated that the middle Holocene, or Altithermal (Antevs, 1955), was an episode of decreased precipitation and increased erosion. A number of studies suggest an Altithermal age for dune sand on the Great Plains. On the southern Plains, Holliday (1985, 1989) identified two periods of dune sand movement at about 6,500-5,500 and 5,000-4,500 yrs B.P. These latter episodes of dune sand movement have been correlated with similar-aged dune deposits in Bailey County, Texas (Gile, 1979).

It is also proposed that the Altithermal was the most likely time during which the large dunes of the Sand Hills formed (Swinehart, 1990). Following about 2,000 years of stabilization, the climate became dry enough to allow reactivation of much of the sand in the eastern part of the Sand Hills.

#### *Alluvial deposits*

During the last decade, a great deal of attention has been focused on the development of alluvial chronologies in the central Great Plains, typically in connection with geoarchaeological investigations. As a consequence, this research has resulted in a number of studies and a sizable radiocarbon data base; well over 400 radiocarbon ages

have been obtained from alluvium in Kansas and Nebraska (Johnson *et al.*, 1996). Only a sampling of the many studies is presented below.

Much of the research in Nebraska has focused on the Loup River basin. Brice (1964) recognized two major terrace systems in the basin and obtained early Holocene radiocarbon ages of 10,500, 9,000, and 8,500 yrs B.P. on fill beneath the lower of these terraces, the Elba. In a recent re-examination of the Elba terrace, May (1990; 1991) secured radiocarbon ages ranging from nearly 11,000 to 4,670 yrs B.P. from the Cooper's Canyon area. On the South Loup River, May recognized four alluvial fills, with the oldest one dating between about 10,200 and 4,700 yrs B.P., thereby correlating temporally with the Elba terrace of the North Loup. Elsewhere in the basin, Ahlbrandt *et al.* (1983) dated organic accumulations in alluvial sands at 8,410 yrs B.P. from a site on the Dismal River.

In the Kansas River basin, alluvial geomorphic studies have a relatively long history, beginning in the 1950s. The first dating of alluvial stratigraphy on the Kansas River proper was done by Holien (1982), who obtained an age of 10,450 yrs B.P. on a soil buried within lower Newman terrace fill at the Bonner Spring site. Subsequent radiocarbon dating of Newman fill at this locality (Johnson and Martin, 1987) and others (Bowman 1985; Johnson and Logan, 1990) produced more early Holocene ages. The lower Holliday terrace has dated about 4,300 yrs B.P. and younger (Johnson and Logan, 1990).

Many studies have been conducted elsewhere in the Kansas River basin on the many tributaries. Some of the first radiocarbon dating was carried out on samples collected from the Republican River basin; from various locations investigators secured early to middle Holocene ages from buried soils. Research in the basin conducted by Martin (1990; 1992) concluded that the majority of the fill which is exposed was deposited less than about 4,600 yrs B.P.

Several geoarchaeological studies were done in conjunction with cultural resource management projects focusing on federal impoundments within the Kansas River basin. Mandel (1987), in a study of the lower Wakarusa River, recognized two terraces, the lower of which produced radiocarbon ages of about 2,900 yrs B.P. and less. A study of the alluvial history of the Smoky Hill River in the vicinity of Kanopolis Lake (Mandel 1988, 1992) revealed a striking absence of early and middle Holocene fill in small valleys, and of middle Holocene fill in the main valleys and in alluvial fans.

In their study of Wolf Creek basin, Kansas, Arbogast and Johnson (1994) observed that alluviation of early-Holocene flood plains in this small basin was episodic, with at least one period of flood plain stability and soil formation about 6,800 yrs B.P. During the middle Holocene (ca. 6,500-5,300 yrs B.P.), lateral erosion and entrenchment flushed most early-Holocene fill from the main valley of Wolf Creek and the lower reaches of its larger tributaries. Following the interval of mid-Holocene erosion, sediment accumulated on flood plains between 5,300 and 3,000 yrs B.P. Late Holocene alluviation was episodic, with intervening periods of flood plain stability and soil formation about 1,800, 1,500, and 1,200 yrs B.P.

A number of studies have been conducted in the Arkansas River basin area of south-central and southeastern Kansas. Mandel examined terraces and associated fills in the Neosho (Mandel, 1989; 1992; 1993) and Verdigris Rivers (Mandel, 1993), obtaining radiocarbon ages on fill to about 4,200 yrs B.P. The most intensive study in the Arkansas River basin was that of the Pawnee River basin by Mandel (1988; 1991; 1994). Two terraces were recognized in the higher order tributaries, with fill of the high terrace dating between about 10,000 to 5,000 yrs B.P., and that of the low terrace to 3,000 yrs B.P. and younger. Of the three terraces present in the lower part of the system, the lowermost one has Holocene fill and the others are Pleistocene. Holocene valley fills in the Pawnee Basin appear to lack soil development from about 7,000 to 5,000 yrs B.P.

The alluvial record is temporally and spatially fragmented, *i.e.*, the history of valley and stream evolution stored in alluvium is scattered and wrought with gaps. So, it is only by assembling this fragmentary information that one obtains a unified perspective on the record of stream evolution. Out of the many studies conducted in recent years, a pattern of change is emerging. Large stream valleys appear to contain, more or less, alluvial fill dating throughout the Holocene, whereas small stream valleys typically contain only fill dating in the late Holocene. This model has an intuitive basis in that the probability of survival of early and middle Holocene fill in smaller streams is greatly diminished by the limited storage capacity for alluvium and the relatively high stream gradients, large area in hillslope, and associated peaked flood waves. Exceptions to this pattern do, of course, exist (*e.g.*, Lime Creek, Nebraska: May, 1996; Wolf Creek: Arbogast and Johnson, 1994), but are likely due to locally unusual valley width and other discernable factors.

A first approximation of this alluvial model was presented by Johnson and Martin (1987) in an examination of radiocarbon ages obtained from alluvial fill in the central Great Plains. In recent years, the model has evolved with a vastly expanded data base and has been articulated recently by Mandel (1995). He noted that fill in small valleys appears to be less than 4,000 years old, and that the missing early and middle-Holocene record is frequently preserved at the lower end of small stream valleys as terrace fill or alluvial fans.

From the alluvial chronologies, it is obvious that regional synchronicity of stream behavior exists in the central Great Plains (Johnson and Martin, 1987; Johnson and Logan, 1990; Mandel, 1995). When erosion and sedimentation are considered in a stream hierarchical sense, patterns of coincidence appear, such as similar times of flood-plain stability and attendant soil formation. A frequency distribution of over 400 radiocarbon ages from alluvium of Kansas and Nebraska (Figure 2.6) provides an indication of the synchronicity. The high frequencies of the last 5,000 years reflect the age of the alluvium

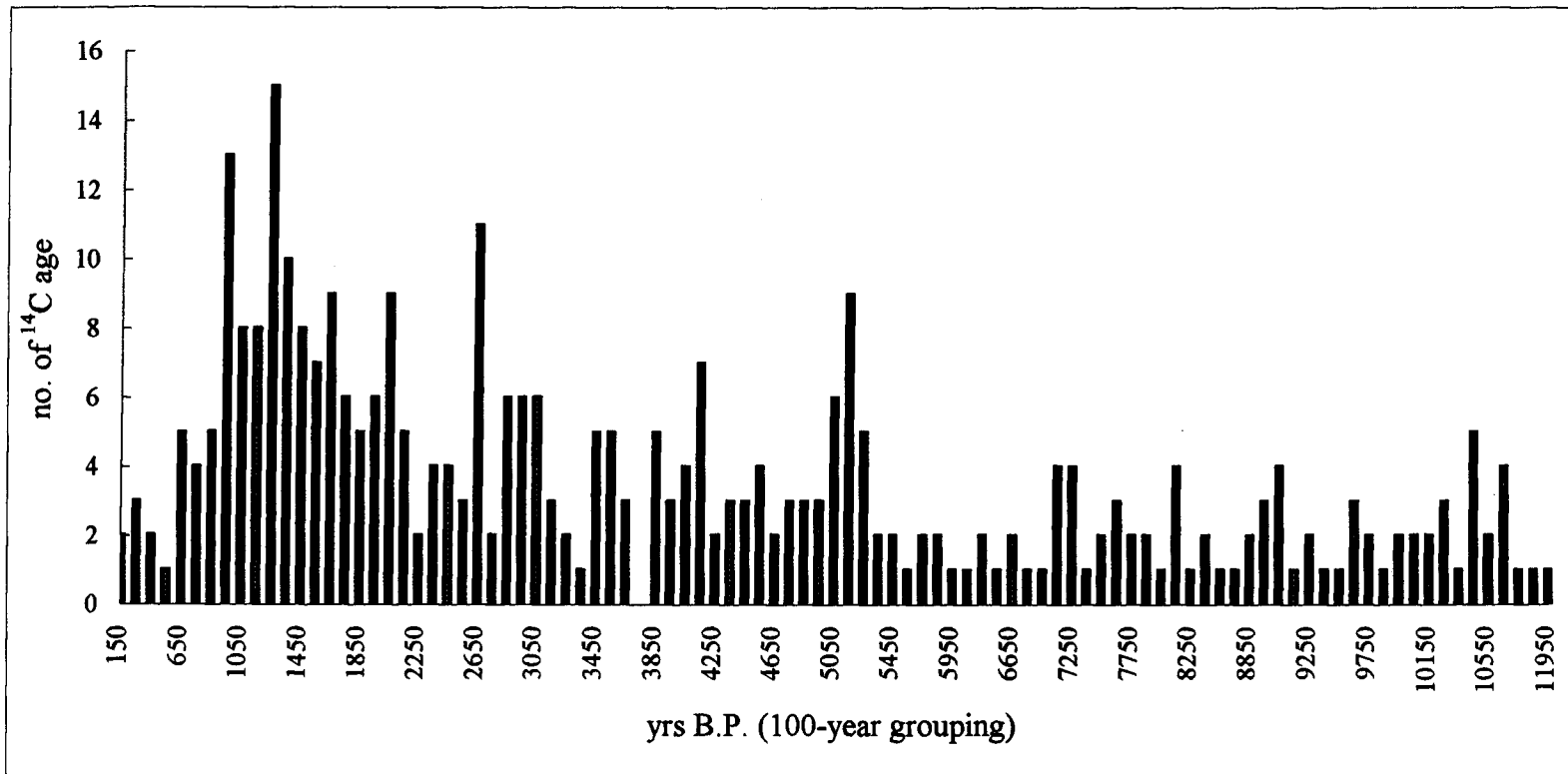


Figure 2. 6. Frequency distribution of alluvial <sup>14</sup>C ages from the Holocene obtained in Nebraska and Kansas (Johnson *et al.*, 1996).

in large and small streams, whereas those prior to about 8,000 represent the ages from the large valleys alone. Alluvial fans ages account for many ages within the 4,000 to 8,000 year range (Mandel, 1995). The greatest frequency of ages occurs about 1,200 yrs B.P., a time when pronounced low terrace stability and soil development occurred throughout the stream systems. Another notable feature of the distribution is that when the ages obtained from alluvial fans are not considered, very few alluvial ages fall within the 5,000 to 7000 yrs B.P. period. This paucity of ages suggests little flood-plain stability and/or preservation of alluvium from that interval, which coincides with the Altithermal climatic episode. Stream activity of this dry period may have been characterized by rapid sedimentation, thereby precluding soil development, in response to low-frequency, high-intensity convectional storms (Knox, 1976; 1983).

Regional synchrony in Holocene fluvial behavior suggests that climatic fluctuation is the dominant external variable in stream systems (Wendland, 1982; Knox, 1976, 1983). Changes in climate during the Holocene were frequent and episodic (*e.g.*, Wendland and Bryson, 1974; Kutzbach, 1985; COHMAP members, 1988), resulting in discrete periods of stream stability and instability (Knox, 1983).

The concept of a middle Holocene, or Altithermal (ca. 7,000-5,000 yrs B.P.) cultural hiatus on the Great Plains has become well-entrenched within the archaeological literatures. Of the various theories put forth to explain the hiatus (Reeves 1973), fluvial erosion or aggradation sufficient to dramatically alter the record for the region during the interval 7,000-5,000 yrs B.P. is most pertinent (Johnson, 1987; Mandel, 1995). Some argued that the similarity in the alluvial stratigraphic record from eastern humid portions of the region to the more arid western areas, as well as with chronologies farther afield indicates that regionally anomalous erosion and deposition do not explain the hiatus completely; rather, the increased dryness during the Altithermal was likely sufficient to reduce populations on the Plains (Wedel, 1961; Knox, 1978; Wendland, 1978). However, the rapidly expanding alluvial radiocarbon and stratigraphic data base for the region is

indicating that much of the cultural record, namely that of the Archaic period, is buried, often deeply, or lost to erosion.

### **Climatic Proxies**

Some of the climatically-sensitive parameters that have recently been examined in the central Great Plains include fossil pollen, opal phytoliths, and stable carbon isotopes. Recent archaeological investigation in DB site and Fort Riley yielded climatic proxy records including stable carbon isotopes and opal phytoliths during the Holocene (Johnson and Park, 1997b).

#### *Fossil pollen*

Palynological documentation of vegetation and climatic change within the Holocene presents some special challenges (Fredlund and Jaumann, 1987). These problems are, at least in part, the result of the taxonomic limitation of pollen analysis. Many major grassland pollen types encompass entire families of plants (Fredlund, 1991), and, consequently, large changes within grasslands can occur but not be readily apparent within the pollen record (Wright *et al.*, 1985). This taxonomic limitation explains the lack of clear palynological definition of the middle-Holocene climatic drying in the central Great Plains. Because of the limited records and inability to differentiate grass pollen, little Holocene vegetational change is apparent in the fossil pollen record (Baker and Waln, 1987).

Abundant palynological evidence exists for middle-Holocene eastward migration of the prairie/forest ecotone. Several palynological studies from areas peripheral to the central Great Plains document middle-Holocene expansion of the prairie (*e.g.*, Brush, 1967; Watts and Bright, 1968; Durkee, 1971; Van Zant, 1979). Barnosky *et al.* (1987) subsequently documented the eastward ecotonal shift between about 8,000 and 6,000 years ago through a review of data from the northern Great Plains. Using pollen/climate

transfer functions, Bartlein *et al.* (1984) estimated that precipitation in the Minnesota area was about 20% less during the middle Holocene than it is today, but that temperature was only slightly higher.

In Nebraska, a paleoecological record comes from Sears' (1961) study of Hackberry Lake in the north-central part of the Sand Hills. A radiocarbon age indicates that organic deposition began at this site about 5,040 yrs B.P., and the sediments also record a fluctuating dominance of prairie vegetation that persists to the present, but with no discernible record of the Altithermal. Since the sand dunes that enclose the Hackberry Lake basin are well-preserved barchan and barchanoid-ridge dunes that indicate prevailing wind directions to the southeast, this site appears to represent a post-Altithermal stabilization of the dunes. On the southwestern margin of the Sand Hills at Swan Lake, Wright *et al.* (1985) analyzed a core with a basal radiocarbon age of about 8,000 yrs B.P. Sedimentation in Swan Lake appeared to be continuous to the present, and pollen analysis indicated a prairie vegetation with minor fluctuations of herbs and grasses throughout this time, but with no Altithermal signal.

Two sites in Kansas provide palynological information for the Holocene: Muscotah Marsh (Grüger, 1973) and Cheyenne Bottoms (Fredlund, 1995). The Holocene portion of the record at Muscotah Marsh in north-central Kansas contains unconformities and lack close-interval radiocarbon ages, but clearly portrays middle Holocene prairie expansion and contraction. At Cheyenne Bottoms in central Kansas, the Holocene is markedly different from the late-Pleistocene Farmdalian grassland-steppe assemblage: lower *Artemisia* percentages and lower relative frequencies of arboreal pollen types characterize the Holocene. These differences suggest that the Holocene regional upland vegetation in the Holocene lacked the sage component which was so important during the Farmdalian. The Holocene vegetation also lacked diversity of tree and shrub taxa regionally present during the Farmdalian. Of all tree and shrub pollen taxa identified, only *Ulmus* (elm) and *Celtis* (hackberry) are more common during the Holocene.

Fredlund (1995) also divided the Holocene into four microzones based on changes in the local pollen signal. The latest Pleistocene-earliest Holocene zone (>9,690 yrs B.P.), through its abundance of diatoms and gastropods, suggests increasing moisture at the site. The soil developed above this zone appears to correlate temporally with the Brady soil. The high relative frequencies of *Cheno-Am* type pollen throughout the Holocene are associated with the existence of mudflats periodically exposed as fluctuations of water levels occurred within the basin. In the middle Holocene (ca. 8,500 to 3,700 yrs B.P.), frequencies of *Cheno-Am* pollen types decreased significantly, suggesting more stable, perhaps lower, water levels. The increase in *Ambrosia* (ragweed) pollen during the middle Holocene indicates less fluctuating and lower water levels. The late Holocene (> 3,700 yrs B.P.) was characterized by a return to fluctuating water levels and exposed mudflats.

The timing of the Holocene dry/warm interval appears to vary geographically. In Minnesota the maximum of Altithermal warmth and dryness occurred between about 8,000 and 4,000 yrs B.P., peaking at 7,200 yrs B.P. (Wright 1976). In the northwestern United States, most sites register greatest drought in the early Holocene, although at some sites it was delayed until the middle Holocene, concurrent with the Midwest (Barnosky *et al.*, 1987). In the Southern High Plains, widespread eolian activity began in some areas by 9,000 yrs B.P. and culminated 6,000-4,500 yrs B.P., probably because of warmer, drier conditions that reduced vegetation cover (Holliday, 1989). In the northern Great Plains, the atmospheric anomalies that produce drought today were more frequent and persistent before AD 1200 (Laird *et al.*, 1996).

#### *Stable carbon isotopes*

A gradual shift to drier and warmer conditions occurred during the late Pleistocene. Using stable oxygen and carbon isotopes from lacustrine and soil carbonates collected at Fort Hood in north-central Texas, Humphrey and Ferring (1994)

demonstrated that mesic conditions continued until 7500 yrs B.P., except for a brief drying period between about 12,000 and 11,000 yrs B.P. The slow replacement of cool-season plants by warm-season plants at Fort Hood agrees with an extended warming and drying climatic transition during the early Holocene.

By the middle Holocene, drying had reached a maximum according to most studies. Northwestern Texas was experiencing conditions of maximum temperatures, minimum precipitation, and eolian activity between 6000 and 4500 yrs B.P. (Holliday 1985, 1989; Pierce 1987).  $\delta^{13}\text{C}$  values derived from buried soils in this region revealed a shift from -23‰ in the early Holocene to -15‰ in the middle Holocene (Haas *et al.*, 1986), *i.e.*, a shift in dominance from cool-season  $\text{C}_3$  grasses to warm-season  $\text{C}_4$  grasses. Based on enriched  $\delta^{13}\text{C}$  values in soil carbonate from their Texas study, Humphrey and Ferring (1994) identified a middle-Holocene xeric episode, although the  $\delta^{18}\text{O}$  values from these same carbonates did not indicate a significant temperature change.

Limited  $\delta^{13}\text{C}$  data from the Sargent site, an upland loess exposure in southwestern Nebraska, suggest a gradual increase in dryness through the Holocene; this is interpreted as a shift in the abundance of  $\text{C}_4$  species from slightly under 50% during the late Pleistocene to 80 - 90% in the middle Holocene.  $\delta^{13}\text{C}$  data derived from the correction of radiocarbon ages obtained from soils buried in alluvial fill of the central Great Plains (Johnson *et al.*, 1996) also indicate a gradual increase in  $\text{C}_4$  plants from about 12,000 yrs B.P. through the Holocene, but these data are relatively noisy due to the edaphic conditions encountered on bottomlands.

### *Tree rings*

Variations in tree-ring widths from one year to the next have long been recognized as an important source of paleoclimatic information. The mean width of a ring in any one tree is a function of many variables, including the tree species, tree age, availability of stored food within the tree and of important nutrients in the soil, and a whole complex of

climatic factors, including sunshine, precipitation, temperature, wind speed, humidity, and their distribution through the year (Bradley, 1985). The tree is essentially a filter or transducer which, through various physiological processes, converts a given climatic input signal into certain ring-width output which is stored and can be studied in detail, even thousands of years later (*e.g.*, Yapp and Epstein, 1977; Fritts, 1983).

Unfortunately, the tree-ring record extracted from the central Great Plains covers only the last few hundred years, but does provide us with an impression of the recent variability in climate. Information on latest Holocene drought episodes comes from the ring sequences in logs buried at the Ash Hollow site in western Nebraska (Weakley, 1962). According to that record, droughts longer than 15 years occurred in 1276-1313, 1438-1455, 1512-1529, 1539-1564, 1587-1605 and 1688-1707 A.D. In the North Platte area of western Nebraska, Weakley (1943), in a study of red cedar and ponderosa pine, found 13 more or less severe droughts lasting 5 years or more during the past 400 years. Drought appeared to recur at ill-defined intervals of from 15 to 25 years.

## **Climatic Modeling**

Using a modified version of the Blytt-Sernander scheme of climatic episodes, Bryson *et al.* (1968) produced a model that subdivided the Holocene into the pre-boreal, Boreal, Atlantic, sub-Boreal, sub-Atlantic, Scandic, neo-Atlantic, and Pacific episodes. For example, during the Atlantic episode (8450-4680 yrs B.P.), the wedge of modified Pacific air that characterizes the grassland climate was expanded northeastward into central Minnesota and eastward towards the Atlantic seaboard (Bryson *et al.*, 1970).

According to recent model simulations, summer insolation had increased by around 9 ka but was still secondary in influence to the shrinking Laurentide ice sheet (COHMAP members, 1988). The glacial anticyclone persisted in eastern North America, but was much smaller than at 12 ka. With the Pacific subtropical high gaining strength adjacent to the west coast of North America, northwesterly winds replaced westerly winds along the coast in the Northwest. The Midcontinent was still cooler and more moist than at present in July. By the early Holocene (9 ka), the ice had wasted appreciably, the jet stream was no longer split, orbital parameters were favoring increased temperatures, and zonal flow was dominating (Kutzbach, 1987).

For the Altithermal, *i.e.*, 6 ka, model results produced mean summer temperatures 2° to 4°C higher than present (COHMAP members, 1988) and annual precipitation up to 25 % less than at present in the region (Kutzbach, 1987). Surface westerly winds in the midcontinent were stronger than today, with warmer and drier conditions prevailing. Since 6 ka, simulation indicates that westerly flow has weakened and summer temperatures have decreased.

### **III. MAGNETIC PROPERTIES OF NATURAL MATERIAL**

Rock magnetism, or environmental magnetism, is the term commonly applied to the study of the magnetic properties of rocks and minerals, how these properties depend on factors such as grain size and shape, temperature and pressure, and the origin and characteristics of the different types of remanent magnetizations which rocks and magnetic minerals can acquire. In contrast, paleomagnetism is a longer-term study of the strength and direction of the geomagnetic field recorded in rocks and sediments (Collinson, 1983).

Rock magnetism has been applied to recent sediments with the purpose of identifying the magnetic components and using them to trace the movement of sediment or determine the relative contributions of different components to a site (Hesse, 1997; Thompson and Oldfield, 1986). Of special interest to soil studies are two exceptional properties of iron oxides. First, the iron present within soil is very responsive to its chemical and physical environment, displaying a tendency to transform to different types of oxide and hydroxide in sympathy with edaphic conditions. Second, although the new oxide or hydroxide is often only meta-stable with respect to subsequent environmental changes, very slow reaction rates will tend to preserve the new formation even in somewhat disequilibrium conditions (Schwertmann and Taylor, 1977). Environmental magnetism also has been used in areas of lake sediments, marine sediments, and urban pollution (Dearing, 1994).

Magnetism in mineral occurs because the negative exchange energy from the interaction of the spin angular momentum of electrons dominates the magnetic ordering. All substances can be divided into three classes, according to their magnetic properties: diamagnetic, paramagnetic and ferromagnetic. Diamagnetism is a property of orbiting

electrons, and therefore all material is diamagnetic. The diamagnetic response to application of a magnetic field is acquisition of a small induced magnetization,  $J_i$ , opposite the applied field,  $H$ . The magnetization depends linearly on the applied field and is reduced to zero on removal of the field. Magnetic susceptibility is a measure of the ease with which a material can be magnetized. Magnetic susceptibility for a diamagnetic material is negative and independent of temperature. An examples of diamagnetic mineral is quartz with a typical magnetic susceptibility value of  $\sim -0.8 \times 10^{-7} \text{ m}^3/\text{kg}$ .

Paramagnetic substances contain molecules with inherent magnetic moments due to unbalanced orbital electrons. These tend to be aligned with the ambient field thereby giving material a positive susceptibility with a magnitude of about  $10^{-5} \text{ m}^3/\text{kg}$ . An example of paramagnetic mineral is biotite and dolomite.

Ferrimagnetic materials carry a remanent magnetization below a critical temperature, termed the Curie or Néel temperature, and they are paramagnetic above this temperature. The fourth, and much rarer type of substance, exhibits a different type of magnetization called ferromagnetism, because it is most common in substances containing iron. Ferromagnetic solids have atoms with magnetic moments, but unlike the paramagnetic mineral, adjacent moments interact strongly. The effect of interaction is to produce magnetizations in ferromagnetic solids that can be orders of magnitude larger than for paramagnetic solids in the same magnetizing fields.

Coupling of adjacent atomic moments in a ferromagnetic material is the results of *exchange energy* of quantum mechanical nature. Exchange energy may produce either parallel or antiparallel exchange coupling. If adjacent magnetic moments are parallel, as in iron, then the material is *ferromagnetic*. If adjacent magnetic moments are antiparallel then the material is either *antiferromagnetic* (the magnitudes of the opposing moments are equal) or *ferrimagnetic* (the magnitude of opposing moments are unequal). The most common magnetic minerals in sediments are either antiferromagnetic or ferrimagnetic.

A large effort has gone into the development of instruments and techniques that

are sensitive enough for characterizing weakly magnetic sediments without magnetic separation. First of all, magnetic susceptibility (MS) has been routinely measured to determine the concentration of ferrimagnetic minerals in sediments. MS is, however, a measurement which in isolation does not discriminate well between ferrimagnetic grain sizes nor mineral types. In soils, the total ferrimagnetic component may include primary minerals such as titanomagnetites with geological origins and secondary minerals such as magnetite and maghemite derived from chemical weathering or bacterial processes or produced during burning, and pollution dusts (Thompson and Oldfield, 1986). For these reasons, the magnetic definition of mineral type and grain size normally requires a range of magnetic parameters (Table 3.1.).

The other environmental magnetic properties of greatest use include frequency dependence of susceptibility (FD), anhysteretic remanence magnetization (ARM), and saturation isothermal remanence magnetization (SIRM). Our interest has largely focused on magnetic properties at room temperature, despite the intrinsic connection between temperature and magnetic properties. This is because in many of soil samples chemical changes readily could take place at elevated temperatures. These parameter will be discussed in detail.

Table 3.1 Rock magnetic parameters commonly measured.

Parameter	Explanations
Susceptibility	The ratio of induced magnetization to applied field, a measure of the magnetizability of a sample. Units: $\text{m}^3/\text{kg}$
Frequency Dependence	If susceptibility is measured in an alternating field with a low frequency, and then high frequency, there will be a reduction in susceptibility by superparamagnetic grains ( $< 0.03 \mu\text{m}$ in magnetite). Units: %
Anhyseretic Remanence (ARM)	If a sample is subjected to a decreasing alternating field with a small direct field super imposed, it acquires an ARM. Units: $\text{A}\cdot\text{m}^2/\text{kg}$
Anhyseretic Susceptibility ( $X_{\text{ARM}}$ )	The $X_{\text{ARM}}$ is the ARM normalized to the direct field expressed in units of $\text{m}^3/\text{kg}$ .
Saturation Isothermal Remanence (SIRM)	The highest intensity of magnetic remanence that can be induced in a sample by application of a high magnetic field (here 1.1 Tesla). Units: $\text{A}\cdot\text{m}^2/\text{kg}$
'S' Ratio	In mixed magnetite-hematite assemblages, the proportion of the magnetization acquired in high fields ( $>0.3$ Tesla) is directly related to the hematite concentration; here S is measured as $\text{IRM}_{0.3\text{T}}/\text{SIRM}$ . Units: dimensionless.

## SUSCEPTIBILITY

Susceptibility is a measure of the ease with which a material can be magnetized. In magnetic fields as weak as the earth's, the magnetization  $J_i$  induced in a material is directly proportional to the magnetic field strength  $H$ . The constant of proportionality is called magnetic susceptibility. Most environmental materials have magnetic susceptibility values controlled by ferrimagnetic minerals. The ferrimagnetic iron oxides such as magnetite, maghemite, titanomagnetite, and titanomaghemite are the dominant ferrimagnetic minerals in many soils, rocks, sediments and dusts.

### Concentration

The range of susceptibilities, where ferrimagnetic minerals are greater than  $10^{-7}$  m<sup>3</sup>/kg, covers three to four orders of magnitude ( $10^{-7}$  m<sup>3</sup>/kg to  $10^{-3}$  m<sup>3</sup>/kg; Dearing, 1994). Natural samples lying at either end of this susceptibility range vary in their concentration of ferrimagnetic minerals by a factor of about 300. Therefore, the major factor controlling the susceptibility of samples in this range will be the concentration of ferrimagnetic minerals. The concentration of magnetite in a sample can be estimated by dividing the bulk susceptibility value of the sample by the susceptibility of the assumed or known magnetite type or size (Dearing, 1994). Concentration, however, is only one of four factors controlling magnetic susceptibility. Magnetic susceptibility also depends on the mineral composition, crystal size and crystal shape (Figure 3.1).

### Mineral Composition

There are several methods used to identify and characterize ferromagnetic minerals. Most of these are nondestructive. These methods involve spectroscopy, diffractometry, thermal analysis and microscopy (Cornell and Schwertmann, 1996).

By far the most important ferrimagnetic minerals are the iron-titanium (Fe-Ti) oxides. Fe-Ti oxides are generally opaque, and petrographic examination requires

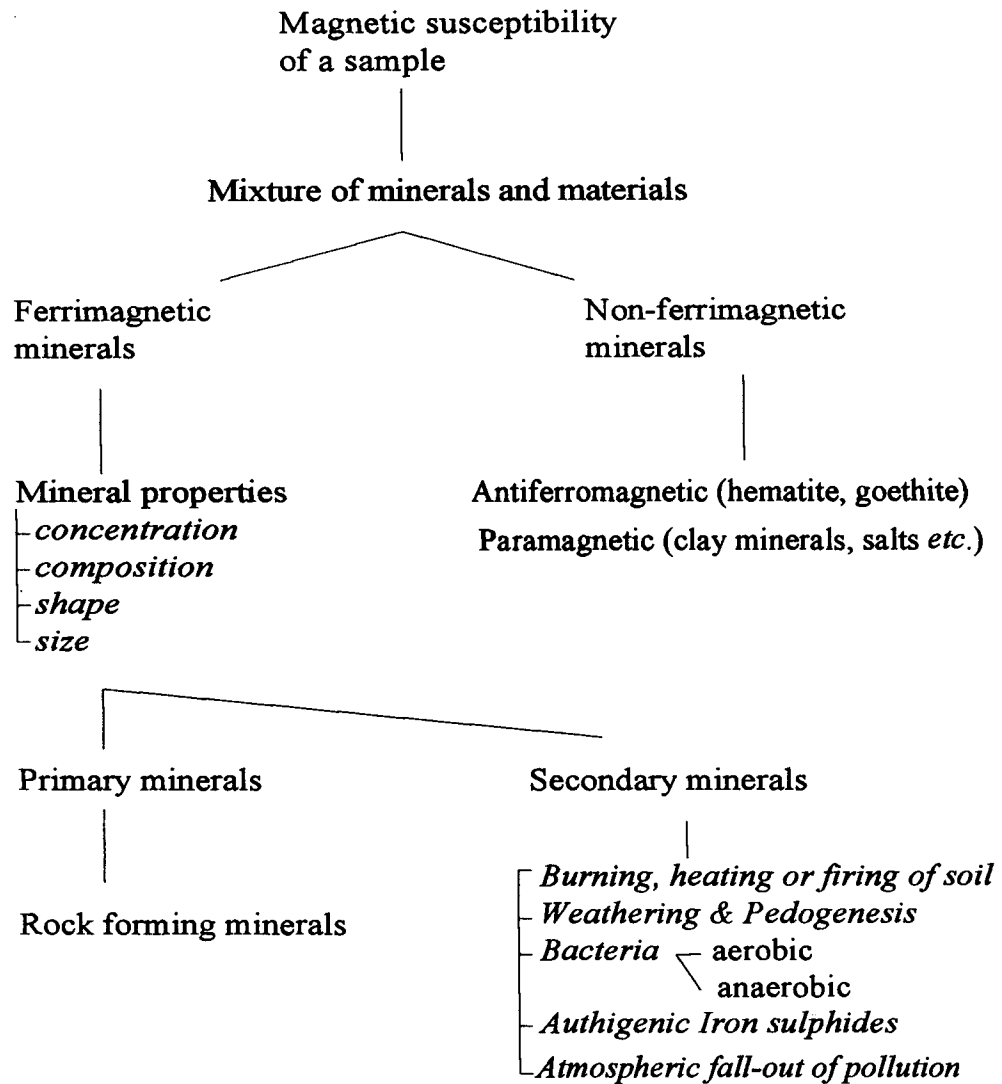


Figure 3.1. A theoretical model to interpret the enhanced magnetic susceptibility of soils (modified after Dearing, 1994).

observations of polished sections in reflected light (Butler, 1992). Composition of Fe-Ti oxides are conveniently displayed on the  $\text{TiO}_2\text{-FeO-Fe}_2\text{O}_3$  ternary diagram (Figure 3.2).

The composition of ferrimagnetic oxides varies from the 'pure' oxides of magnetite and maghemite, to 'impure' oxides such as titanomagnetite and titanomaghemite, in which the Fe atoms are partially substituted by atoms of titanium (Ti). There are continuous sequences or solid solutions of minerals between these two sets which have varying titanium contents. The titanium substitution reduces the Fe content and magnetic moment of mineral, and hence lowers the magnetic susceptibility. This is confirmed by the fact that titanomagnetite with susceptibility values are as low as 15 % of the highest values for magnetite. Where titanium substitution has progressed beyond a certain point the minerals lose ferrimagnetic status and become transformed into the paramagnetic titanium oxides ilmenite and ulvospinel.

The magnetic minerals present in the Chinese loess and paleosols have been identified using a range of analytical techniques, including rock magnetic methods (Maher and Thompson, 1992; Zhou *et al.*, 1990; Heller *et al.*, 1991), optical microscopy, and X-ray diffraction (Kukla *et al.*, 1988). Magnetite and maghemite, both strongly ferrimagnetic minerals occur as does hematite, which is much more weakly magnetic. Magnetite rather than maghemite has been identified as the dominant ferrimagnet by those studies. Maher and Thompson(1991) and Zhou *et al.* (1990) have shown that compared with the loess units, the paleosols contain a higher proportion of ultrafine-grained magnetite, of single domain and superparamagnetic dimensions.

There are five categories of magnetic behavior, shown in 3.2 ranked in decreasing order of typical magnetic susceptibility. Using this information it can be assumed that a soil sample containing predominantly ferrimagnetic minerals will have a higher susceptibility than one containing all paramagnetic minerals, and this is certainly a good guide to explaining the relative magnitude of susceptibilities in samples of pure minerals. However, it is uncommon for a natural sample to contain only one category of magnetic minerals (Jordanova *et al.*, 1997; Dearing *et al.*, 1996). It is therefore necessary to

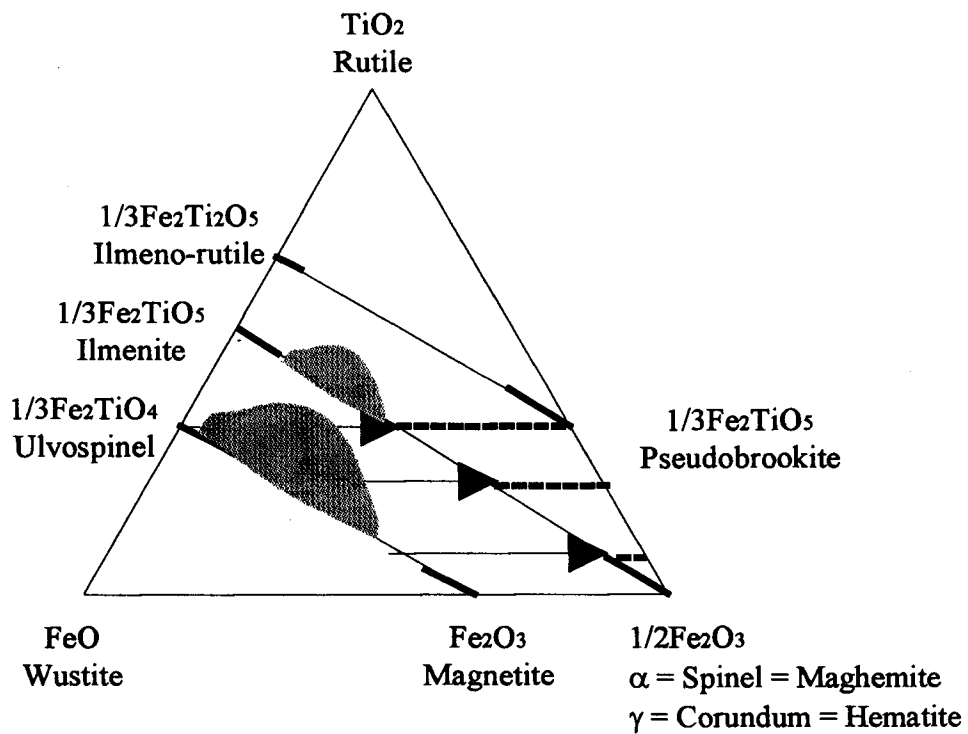


Figure 3. 2. Ternary diagram for iron-titanium oxides.

The natural solid solution compositions are shown as shaded, but these normally exsolve into the end members of the solid solutions together with other oxides. The commonly occurring minerals are shown by a solid bar. Low-temperature oxidation of the titanomagnetites causes their composition to move in the direction of the arrows, but eventually invert to ilmenohematite (after Tarling, 1983).

consider virtually all samples as a mixture of different magnetic behavior.

**Table 3.2. Magnetic behavior and magnetic susceptibility of different minerals.**

Behavior	Characteristics and minerals
ferromagnetic	strong positive susceptibility <i>e.g.</i> , pure iron, nickel, chromium
ferrimagnetic	strong positive susceptibility; some iron oxides and sulphides <i>e.g.</i> , magnetite, maghemite, pyrrhotite, greigite
canted	moderate positive susceptibility; some iron oxides
antiferromagnetic	<i>e.g.</i> , hematite, goethite
paramagnetic	weak positive susceptibility; many Fe-containing minerals and salts <i>e.g.</i> , biotite, olivine, ferrous sulphate
diamagnetic	weak negative susceptibility <i>e.g.</i> , water, organic matter, plastics, quartz, feldspars, calcium carbonate

### **Mixture of Minerals**

In theory, we can explain or predict the magnetic susceptibility of a sample in terms of the sum of the magnetic susceptibility values of individual minerals and materials. The idea of interpreting each measurement in terms of many different minerals sounds like a fairly daunting task. But in practice we can simplify matters by making some assumptions about which minerals are significant in a sample.

Samples which are not contaminated by ferrous metal do not usually contain ferromagnetic materials. However, ferromagnetic minerals are extremely rare and their contribution is very unlikely in natural loess samples. In their absence, the susceptibility of sample is most likely to be controlled by the ferrimagnetic component, and less likely

by the other categories of minerals present, shown in Table 3.2. Magnetite, for instance, is about 500-1000 times more magnetic (higher susceptibility) than the strongest canted antiferromagnetic or paramagnetic mineral, and about 10,000 times stronger than the weakest clay mineral. Ferrimagnetic iron oxides, like magnetite, are found in virtually all environments. Maghemite, also, is about 400 times stronger magnetic than hematite, and has nearly the same susceptibility as magnetite.

In igneous rocks, magnetite and maghemite may represent about 1-2 % of the minerals. But even in these relatively small proportions, their high susceptibility will often mean a greater contribution to the susceptibility of the whole sample than the combined effect of all the other minerals.

## CRYSTAL SIZE AND DOMAINS

The magnetization within a small region within a ferromagnetic grain is uniform in direction and has a preferred orientation, aligned either along specific crystallographic axes, known as magnetocrystalline easy axes or along the length of the grain (for same, elongate grains). In larger grains (*e.g.*,  $>10 \mu\text{m}$ ), however, a number of volume elements are present, each of which has its magnetization aligned along an easy axis. These volume elements are called magnetic domains. Above 10-20  $\mu\text{m}$  the crystals are divided up into different regions or cells of magnetization, known as domains, and are referred to as having multidomain behavior. In smaller crystals, normally  $<1 \mu\text{m}$ , the restricted volume allows only one domain to form, hence these show single domain behavior. In ultrafine crystals below 0.035  $\mu\text{m}$  the magnetization is strong but unstable, and thermal energy counteracts induced magnetization very quickly after a magnetic field is removed. This behavior is similar to paramagnetism, but with a much greater susceptibility. Hence, it is termed superparamagnetic behavior. Magnetic grains can be grouped into four categories of domain states: multidomain (MD), pseudo-single domain (PSD), stable single domain

(SD), and superparamagnetic (SP) (Figure 3.3).

**Multidomain:** MD grains contain greater than 10 domains, with different domains having different directions of magnetization so that the net remanence nears zero. For magnetite, MD grains are typically  $>17 \mu\text{m}$  in size. The magnetic susceptibility of coarse MD grains is slightly greater than that of smaller MD, PSD, and SD grains.

**Pseudo-single domain:** PSD grains contain 2-10 domains in each grain and are intermediate in character between the smaller SD and larger MD grains, having only incomplete canceling of domain magnetization (Banerjee and Moskowitz, 1985). For magnetite, the size range is about  $0.1-17 \mu\text{m}$ .

**Stable single domain:** SD grains contain only one magnetic domain. Therefore, magnetic remanence of SD grains is much higher and more stable than that of multidomain grain assemblages, and SD grains are also more sensitive to measurement of ARM and SIRM. For magnetite, their size range is approximately  $0.03-0.1 \mu\text{m}$ . PSD and SD grains are treated together as one group by behavior.

**Superparamagnetic:** In magnetite grains smaller than  $0.03 \mu\text{m}$  in diameter, thermal vibrations at room temperature are of the same order of magnitude as their magnetic energies. Therefore, net magnetic moments will average to zero in a zero field, so these grains are incapable of carrying a stable remanent magnetization (SP grains do not contribute to ARM or SIRM). Because magnetic domains in SP grains are thermally unstable, the grains' magnetic moment will align in the direction of the applied field. This type of behavior is termed **superparamagnetic**. The susceptibility of SP grains turns out to be much greater than that of an equivalent amount of SD or MD grains (Banerjee and Hunt, 1993; Thompson and Oldfield, 1986; Mullins, 1977).

It has been known that there are substantial differences in magnetic grain sizes between those of loesses and of paleosols, with the latter selectively enriched in the finer grains (Maher and Thompson, 1991). Maher and Thompson (1991) show that the grain size assemblages at each depth along the measured section are very sensitive to

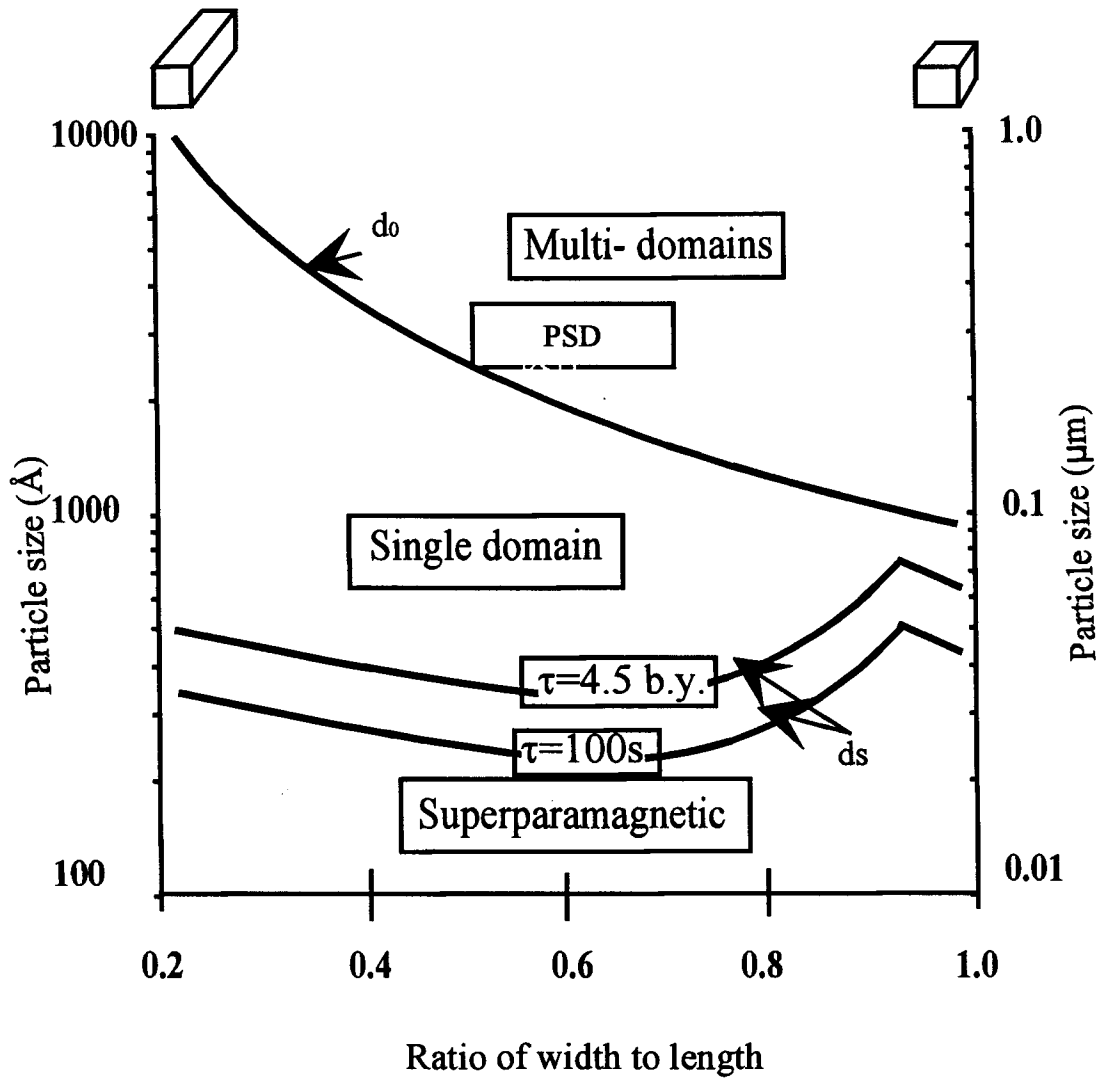


Figure 3. 3. Size and shape ranges of single-domain, superparamagnetic, and multi-domain configurations for parallelepipeds of magnetite at room temperature. Particle lengths are indicated in angstrom on the left ordinate and in microns on the right ordinate; shape is indicated by the ratio of width to length; cubic grains are at the right-hand side of diagram; progressively elongate grains are toward the left; the curve labelled  $d_0$  separates the single domain size and shape field from those of multi-domains; curves labelled  $d_s$  are distribution of grains that have  $\tau = 4.5$  billion years and 100 seconds; grains with sizes below  $d_s$  curves are superparamagnetic. (Redrawn after Butler, 1992)

stratigraphic correlations. ARM and FD are the properties most closely linked to the presence of pedogenic fine grains (approximately 0.015 - 0.1  $\mu\text{m}$ ). Comparing SIRM/ $\chi_{\text{ARM}}$  (or ARM/SIRM) ratios with FD will identify the fine grained tail from the detrital coarse mineral (Maher, 1991; Figure 3.4). These parameters will be discussed below in detail. Assembling this information on the biparametric plot provides a qualitative rather than quantitative grain size information.

Recent measurements on natural and synthetically produced magnetites have helped to define the major change in susceptibility with crystal size (Maher, 1988). It can be seen that there are two size ranges in which susceptibility reaches high values (Figure 3.5). At the coarse end of the scale, between 20 and 100  $\mu\text{m}$ , values exceed  $60,000 \times 10^{-8} \text{ m}^3/\text{kg}$ , and in crystals smaller than 0.03  $\mu\text{m}$  values exceed  $100,000 \times 10^{-8} \text{ m}^3/\text{kg}$ . These two peaks effectively divide the data into three ranges which correspond to three quite different states of ferrimagnetic behavior.

### Frequency Dependence of Susceptibility

The Bartington MS2B dual frequency sensor measures susceptibility within an AC magnetic field amplitude of 80 A  $\text{m}^{-1}$  at low frequency (470 Hz) and high frequency (4.7 kHz). Samples are measured at each frequency to obtain two values of  $\chi$  corresponding to the low ( $\chi_{\text{LF}}$ ) and high ( $\chi_{\text{HF}}$ ) frequencies. Measurements of a strong frequency-independent paramagnetic salt at both frequencies allows intercalibration of the circuits to within  $\pm 0.2\%$ . Expression of frequency dependence is as a percentage loss of susceptibility:

$$FD(\%) = 100 \frac{\chi_{\text{LF}} - \chi_{\text{HF}}}{\chi_{\text{LF}}}$$

There are a number of potential source of errors related to the sensitivity of the sensor, sample anisotropy, strong samples and contamination. First, the smallest

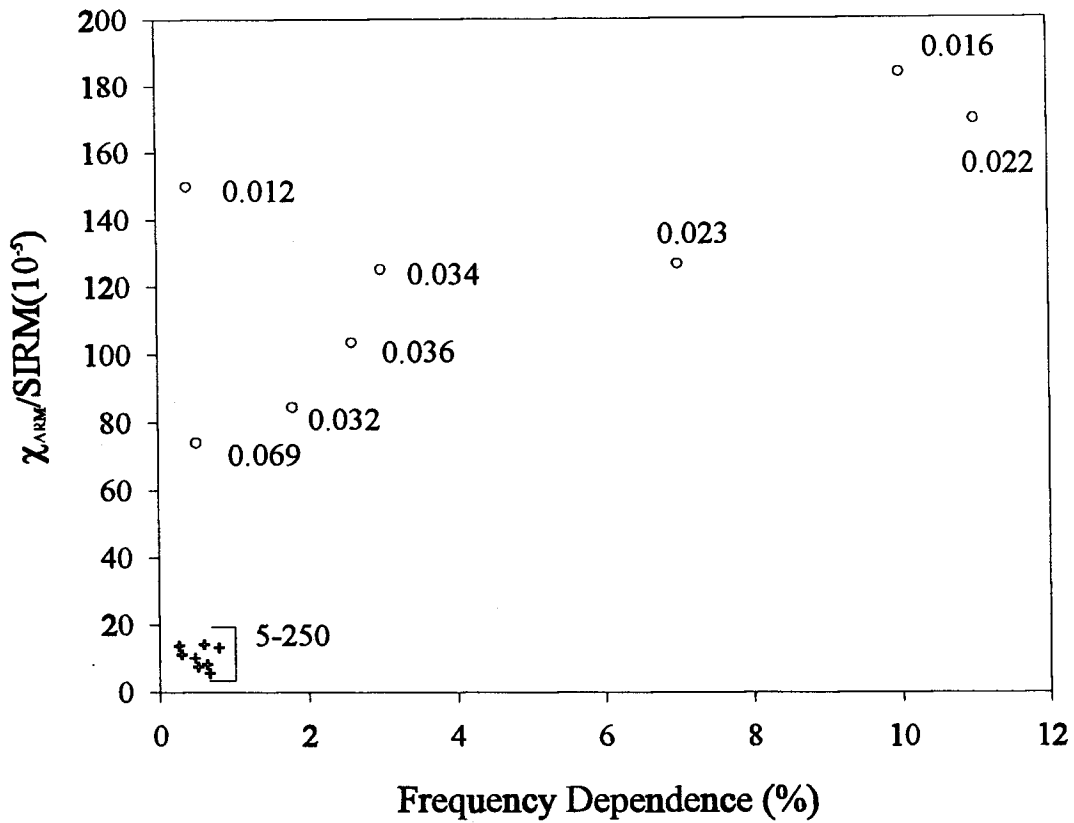


Figure 3.4. Biparametric ratio,  $\chi_{ARM}/SIRM$  versus FD (%) for synthetic magnetites of documented grain sizes. Here FD is the difference between a low frequency and a high frequency measurement of MS expressed as a percentage of the low-frequency measurement. Numbers by symbols indicate grain sizes in  $\mu\text{m}$ . (Maher, 1988; Maher and Taylor, 1988).

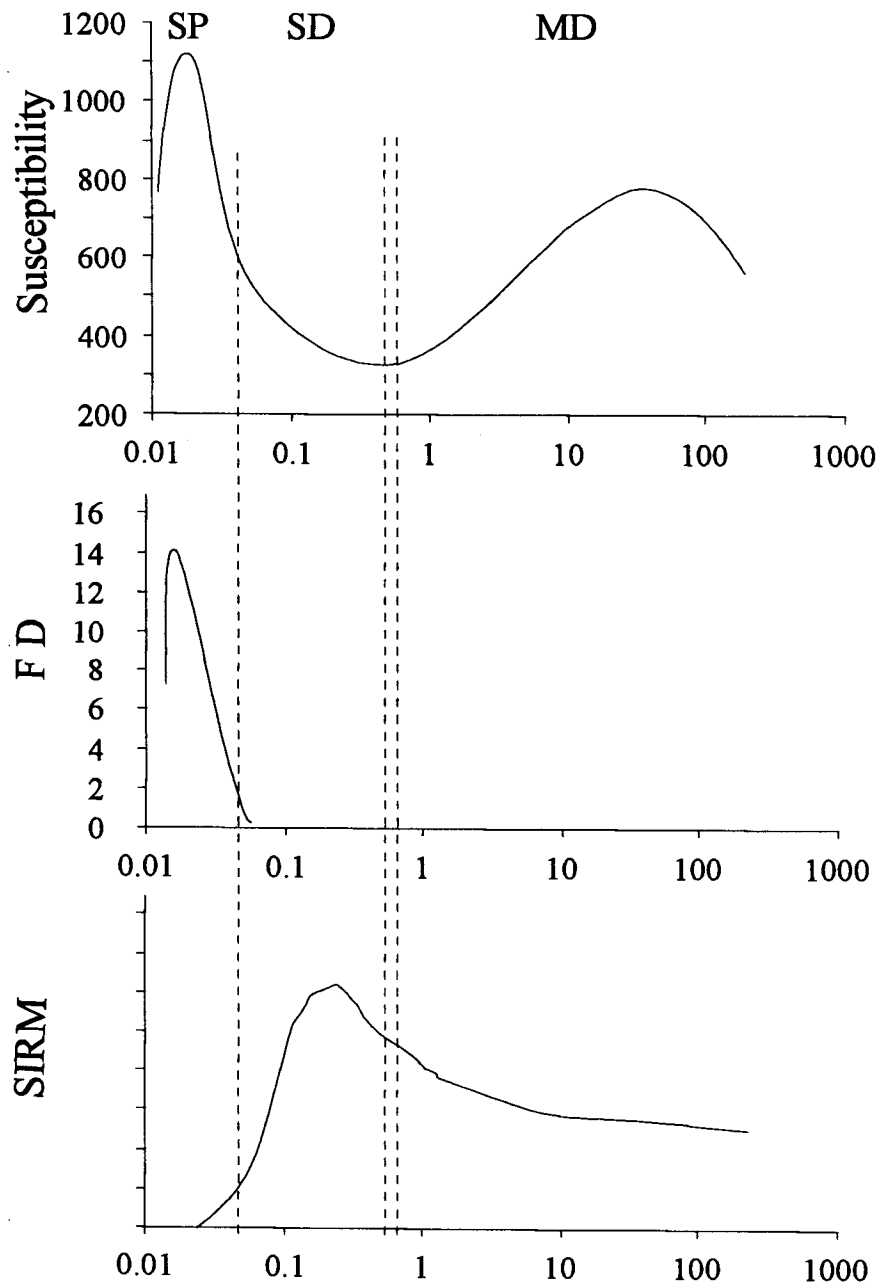


Figure 3.5. Magnetic parameter variations with magnetite grain size; a) low frequency susceptibility; b) Frequency dependence; c) saturation isothermal remanence magnetization (after Maher 1988; Dearing et al. 1985).

difference between  $\chi_{LF}$  and  $\chi_{HF}$  on the 0.1 range which is measurable and repeatable is  $\approx 0.4$  SI units on the display. Calculation of FD on samples with  $\chi_{LF}$  values  $<20.0$  are therefore subject to errors of at least  $\pm 2\%$ , which happens to be typical FD values for the unweathered loess samples of the region. Second, samples with non-randomly distributed minerals may show anisotropy with MS partly depending on sample orientation. Samples have been measured in the same orientation at both frequencies to minimize this error. Third, the presence of metallic fragments in a sample will cause artificially large differences between  $\chi_{LF}$  and  $\chi_{HF}$ .

Within the narrow range of grain volumes between SP and SD, grains are in a transitional magnetic state and exhibit a measurable time-dependent property known as magnetic viscosity. Viscosity is a measure of how fast a magnetized grain will lose magnetization over a relatively short time period, the grain relaxation time ( $\tau$ ), before reaching an equilibrium magnetization level (Figure 3.2). The measurements of FD partly exploits this time-dependency by comparing the magnetizations in an applied field created at two different frequencies. A frequency which is slower than the relaxation time allows the grain to reach equilibrium, but a higher frequency results in non-equilibrium magnetization and a lower susceptibility value.

## ARTIFICIALLY IMPARTED REMANENCES

Rocks, sediments and soils can acquire remanent magnetizations by natural processes. Such natural remanences are not as intense as those which can be artificially imparted in strong laboratory fields but they can be just as stable. Among the several different kinds of laboratory-imparted remanences, saturation isothermal remanence and anhysteretic remanence are probably the most important and widely used in rock magnetic studies (Banerjee, 1994).

### Saturation Isothermal Remanence Magnetization (SIRM)

Many of the simple magnetic parameters to characterize materials can be classified as hysteresis parameters, and interrelationships between these properties can be best understood in terms of hysteresis loops. Consider five of the most important hysteresis parameters. **Saturation magnetization**,  $M_s$ , is the magnetization induced in the presence of a large (>1 Tesla) magnetic field. Upon removal of this field the magnetization does not decrease completely to zero. The remaining magnetization is called **saturation isothermal remanent magnetization (SIRM)**. By the application of a field, in the opposite direction to that first used, the induced magnetization can be reduced to zero. **Saturation coercivity**,  $(B_0)_c$ , is the reverse field which actually makes the magnetization zero, when measurements is made in the presence of the field. An even larger field is necessary to leave no remanent magnetization after its subsequent removal. This reverse field is called the **coercivity of remanence**,  $(B_0)_{cr}$ . The gradient of the magnetization curve at the origin of Figure 3.6 is the **initial susceptibility**,  $k$  (Figure 3.6).

The most useful single artificially imparted remanence in environmental studies is probably the SIRM (Cisowski, 1980). When magnetite content falls below ten ppm, SIRM can serve as a sensitive concentration-dependent parameter (Banerjee, 1994). Although SIRM is mainly a measure of concentration of magnetite, it also depends on grain size and can be strongly influenced by other magnetic minerals such as hematite.

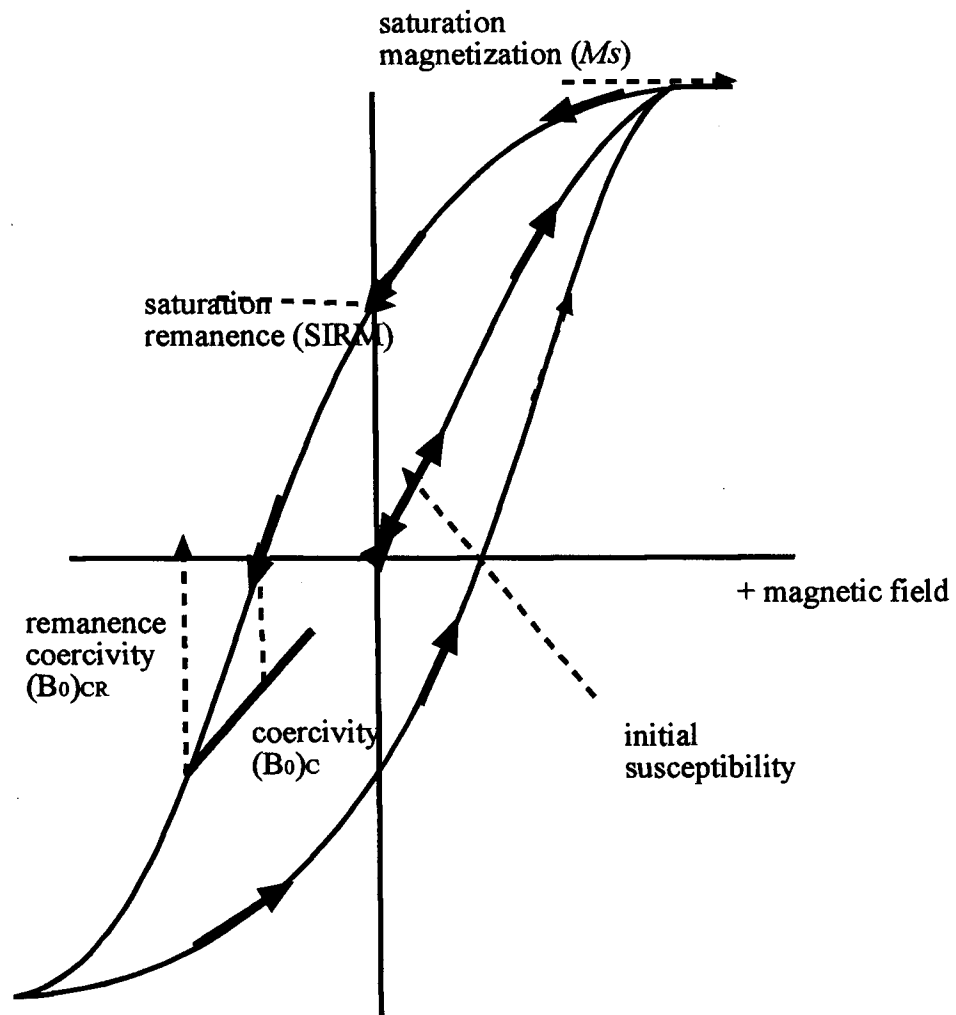


Figure 3. 6. Magnetic hysteresis loop for single domain magnetite particles performed by a specimen subjected to a forward saturating field followed by a series of increasing back fields. The changes take the form of a set of minor hysteresis loops. Five important hysteresis parameters are indicated.

Figure 3.5 illustrates the variation of SIRM with grain size for magnetite as deduced from experiments on synthetic magnetite powders. SIRM is much higher in single-domain grains of around  $0.07 \mu\text{m}$  diameter than in large multidomain grains and the range of variation through multidomain and single-domain regions is much greater for SIRM than for susceptibility. SIRM values range from virtually zero, in materials devoid of iron minerals, to over  $100 \text{ mAm}^2/\text{kg}$  in finely disseminated iron oxide ores (Thompson and Oldfield, 1986).

#### **Anhyseretic Remanence Magnetization (ARM)**

ARM is the magnetic remanence induced by subjecting a sample to a strong alternating field which is smoothly decreased to zero in the presence of a small steady field. ARMs are more sensitive to grain size than SIRM, being more efficiently acquired in SD grains than MD grains. However, the experimental and theoretical grain size dependence of this parameter is incompletely known, despite the attention devoted by magnetic workers (*e.g.*, Maher, 1988).

### **PREVIOUS MAGNETIC STUDIES OF LOESS**

The extensive sequences of loess and intercalated soils represent a detailed and quasi-continuous terrestrial record of paleoclimatic change. The evidence for these climate changes is diverse: paleontological data reveal changing mollusk assemblages (Leonard, 1952; Rousseau and Kukla, 1994), calcium carbonate is depleted and  $\text{Fe}_2\text{O}_3/\text{FeO}$  increased in paleosols (Liu *et al.*, 1985), and greater depletion of  $^{13}\text{C}$  in unweathered loess than in paleosols (Johnson, 1996). Over the last decade, investigators reported that many loess deposits around the world have preserved records of climatic and magnetic history. The magnetic properties germane to this discussion are remanence and susceptibility.

The first clear evidence that the magnetic susceptibility of land-based stratigraphic sequences provides a climate proxy that can be directly linked to Milankovitch cycle was reported by Begét and Hawkins (1989), using data from a loess exposure near Fairbanks, Alaska. Spectral analysis of the 16-m volume-susceptibility profile yielded the main Milankovitch periodicities, even though the profile probably represents no more than 250 ka. One very important difference between the Alaskan and Chinese data must be noted: whereas the paleosols in China invariably have higher susceptibility values than in the unweathered loess, the opposite relationship holds in Alaska. Begét *et al.* (1990) attributed this relationship to changes in wind intensity: it was argued that during glacial periods winds are stronger, and hence more coarse magnetite grains are entrained. When eventually deposited in loess, these grains give rise to higher susceptibility. Conversely, during interglacials (when soil forms), winds are weaker and so therefore is susceptibility.

Atmospheric activity is assumed responsible for the susceptibility variations observed in late-Wisconsin (25-14 ka) loess sequences of Indiana investigated by Hayward and Lowell (1993). Susceptibility lows characterize incipient paleosols that record periods of low loess accumulation, whereas moderate to high susceptibilities correspond to stratified or massive loess reflecting periods of intermediate to high accumulation rates. Hayward and Lowell attribute the variable detrital magnetite enrichment and loess accumulation to changing wind intensity and soil moisture based on their finding that frequency dependence of all 36 samples yielded values less than 1.5 per cent. They give preference to the influence of detrital magnetite, since no systematic variation of magnetite grain sizes between paleosols and loess was observed.

The atmospheric activity model may be applicable in Alaska and in locations near ice sheets, such as those in Indiana, but may not be appropriate for other areas. For example, large detrital magnetite grains do not seem to be important in the central Chinese Loess Plateau, where pedogenic processes control the loess magnetic properties. The susceptibility-wind relationship has been challenged in the central Great Plains (Park

*et al.*, 1993; Farr *et al.*, 1993; Rousseau and Kukla, 1994). Climate change is reflected both in the variation of concentration-sensitive rock magnetic parameters such as susceptibility, ARM and SIRM, and in the grain-size-sensitive parameters such as FD and ARM/SIRM.

The magnetic susceptibility of land-based stratigraphic sequences also provides evidence of the transition a brief climatic oscillations near the Pleistocene/Holocene transition contemporaneous with the Younger Dryas (An *et al.*, 1993).

### **Rock magnetism Record of Past Climate Change**

The source of the climatic signal of the magnetic susceptibility has been long debated. Heller and Liu's (1982) paper recognized that paleosols have susceptibility values about twice higher than those of unweathered loess. Since paleosols formed under conditions that can be generally characterized as warm and wet, whereas unmodified loess represents a dry, cold environment, magnetic susceptibility has been used a climate proxy. Furthermore, the susceptibility record is strongly correlated with the deep-sea oxygen isotope record (Heller and Liu, 1984), the concept of susceptibility as a climate proxy has begun. Indeed, earlier work in soil science had demonstrated enhanced susceptibilities in top soil compared with the underlying subsoil and parent bedrock (Le Borgne, 1955; Mullins, 1977).

All authors that have worked on Chinese loess magnetism agree on the empirical basis of the magnetic climate proxy; the remaining question is the underlying cause. Early reports (*e.g.*, Heller and Liu, 1982, 1984) appealed to the relative enrichment of magnetic particles by the leaching of carbonate from the paleosols. A second suggested cause supposes that the magnetic content is supplied as air-borne material at a constant rate from a remote source. According to this model, susceptibility variations are due to fluctuations in the relative amount of dust particles arriving from the adjacent source areas. During cold, dry intervals, large quantities of loess are blown in. When the climate is warm and

wet, vegetation cover and moisture inhibit the dust flux. Paleosols, therefore, have higher susceptibilities, whereas unmodified loess dilutes the magnetic content and leads to lower values. Kukla *et al.* (1988) first proposed this concept and went on to advance the idea of a susceptibility time scale independent of astronomic chronology by plotting the accumulation rate of the magnetic component.

As was originally pointed out by Zhou *et al.* (1990), paleosols are characterized by a higher concentration of magnetic grains than the intervening loess beds. Variations in laboratory remanences and frequency dependence of susceptibility indicated that the different magnetic components present in loess and paleosols occur in different relative proportions, a situation that cannot arise from simple concentration or dilution. Zhou *et al.* (1990) concluded that the magnetic enhancements in paleosols partly reflect *in situ* processes taking place during soil formation. It is now generally agreed that the magnetic changes due to pedogenesis are crucial to a proper understanding of magnetic climate proxy data (*e.g.*, Heller *et al.*, 1991; Liu *et al.*, 1990, 1991, Maher and Thompson, 1991)

Instead of using various magnetic parameters, the use of correct normalization of magnetic parameters has been suggested in order to reduce the number of variables in magnetic climate proxy studies. Hunt *et al.* (1995) argue that, in the Loess Plateau, the fine grained magnetic signal, often assumed to be a pedogenic signal, is measured more accurately by ferrimagnetic susceptibility normalized by saturation magnetization and by the ARM normalized by the SIRM (ARM/SIRM).

### *Susceptibility and paleo-rainfall*

If the susceptibility dust fluxes and the  $^{10}\text{Be}$  dust fluxes are proportional to one another, then one is able to separate the pedogenic and detrital susceptibility components, as shown by Beer *et al.* (1993). Having quantified the contributions to susceptibility from inherited and authigenic sources, Heller *et al.* (1993) calculated paleo-precipitation from the susceptibilities flux magnitudes. Liu *et al.* (1992) noted that the bulk susceptibilities

of specific loess and paleosol beds were directly related to present-day mean annual precipitation, with the mean susceptibilities increasing linearly from low values in the more drier western parts to higher values in the more humid central areas. Taking present-day precipitation as a calibration value for the Holocene pedogenic susceptibility, Heller *et al.* (1993) reconstructed the precipitation history for Luochuan, China.

Maier *et al.* (1994) extended the paleo-precipitation studies in space across the whole Chinese Loess Plateau using a slightly different approach. In disregarding ongoing accumulation during pedogenesis and assuming that the susceptibility as a function of rainfall reaches saturation in a relatively short interval, they derive rainfall rates from bulk susceptibility differences between paleosol and one of the most silty and unweathered loess beds. They calibrated their model with nine modern soil susceptibilities from sites across the Loess Plateau using a logarithmic relation between susceptibility and rainfall and arrive at results that are not much different from the analysis given by Heller *et al.* (1993). Maier *et al.* (1994) also identified dramatic changes in paleo-rainfall in time and space due to variations in the structure of the Asian monsoon. During interglacial periods and in the early Holocene, they saw increased rainfall throughout the central China, but particularly pronounced in the western plateau. During glacial periods, rainfall was reduced across the whole loess plateau, especially in the southwest.

Rainfall estimates of this kind represent an important step toward completing the overall paleoenvironmental picture. Although regional- to subcontinental-scale, reconstructions of rainfall variability have been generated using data from trees and historical documents, it is recognized that an understanding of the full range of paleoclimatic variability requires an even-longer perspective. The time-space patterns of these changes can be used to examine aspects of climate variability (Duplessy and Overpeck, 1994).

## Rock Magnetic Analysis

Maher and Thompson (1992) identified magnetite ( $\text{Fe}_3\text{O}_4$ ) as the main pedogenic mineral responsible for susceptibility enhancement. Their conclusion was based on isothermal and ARM acquisition, in addition to susceptibility data; their procedures employed a specific multiple regression technique to fit the experimental data from synthetic analogs. Maher and Thompson (1992) found about twice as much magnetite in soils as in loess (0.11% vs. 0.053%). Furthermore, they argued from an analysis of variance that over 90 % of the susceptibility contrast between soil and loess is due to magnetite grains lying near the superparamagnetic threshold (~30 nm). Such grains are well below the optical limit, but Maher and Thompson (1992) demonstrated their presence by using electron microscopy. Banerjee *et al.* (1993) confirmed the observation that bulk susceptibility is more frequency dependent in paleosols than in loess layers, again indicating the importance of ultrafine particles. They also explore the superparamagnetic region below ~30 nm by cooling samples down to 15° K and monitoring the loss of SIRM during rewarming to room temperature. In this way they directly demonstrate the greater importance of superparamagnetic grains in paleosol layers compared with their parent loess layers; the temperature dependence of magnetization observed also shows the sharp drop near 120° K due to Verwey transition, demonstrating that the material in question is undoubtedly  $\text{Fe}_3\text{O}_4$ .

In their early work on the Chinese loess, Heller and Liu (1984) recognized that a magnetically “hard” fraction is present with coercivities well beyond those typical of magnetite. Thermal demagnetization yields maximum blocking temperatures above 600°C, indicating that hematite is present. The analysis of Maher and Thompson (1992) also identified hematite in significant quantities but suggests little difference between loess and paleosol. Even though hematite contents exceed the corresponding values for magnetite, it must be remembered magnetite is 250 times more magnetic than hematite (Heller and Evans, 1995). The natural and laboratory remanences certainly have a

hematite contribution, but the susceptibility enhancement in paleosols is due to a magnetically “soft” mineral such as magnetite and/or maghemite ( $\gamma\text{-Fe}_2\text{O}_3$ ).

Vandenberghé *et al.* (1992) demonstrated that hematite and magnetite are the main iron-bearing minerals in a section near Jixian, but they also identified substantial amount of maghemite. Verosub *et al.* (1993) extended the idea of maghemite contribution by considering the possible significance of this mineral as the basis of the climate proxy signal, not simply as a minor constituent of unaltered parent loess. After subjecting samples to leaching with citrate-bicarbonate-dithionite (CBD), they argued that the CBD-soluble component, representing the enhanced susceptibility of a paleosol, is common to both the paleosol and underlying loess, and CBD-insoluble material is interpreted as an original airfall input. Most of the susceptibility signal in the Chinese loess paleosol sequence is from CBD-soluble material and is thus due to pedogenic processes. They explained the production of secondary ferrimagnetic minerals, especially maghemite, as either the results of pedogenesis or weathering of material in the source area of the loess or the product of *in situ* pedogenesis after deposition. The identification of the CBD-soluble material, however, remains uncertain, since both maghemite and ultrafine magnetite are removed by the procedure. CBD method is dependent on grain size as well as composition and is therefore unable to distinguish between maghemite and ultrafine magnetite grains (Maher and Thompson, 1994; Liu *et al.*, 1994).

Evans and Heller (1994) interpreted their results of acquisition of IRM in terms of two distinct ferrimagnetic components: A and B. Component A is the original air fall contribution, amounting to a mass fraction of slightly less than 1% and consisting of hematite (0.88%), maghemite (0.024%), and magnetite (0.022%). This component appears to be essentially uniform across the entire Chinese Loess Plateau and even into central Asia (Forster and Heller, 1994). Component B comprises ultrafine (below ~100 nm) magnetite particles with homogeneous characteristics but varying in amount by an order of magnitude from northwest to the southwest, a distance of 350 km. Maher (1988)

argued that a mass fraction of about 0.5% is all that is required to account for the most magnetic signal. Furthermore, the remanence properties are very similar to  $\text{Fe}_3\text{O}_4$  particles produced by magnetotactic bacteria (Penninga *et al.*, 1995; Petersen *et al.*, 1986). The uniform magnetic properties of the ultrafine magnetite fraction led Evans and Heller (1994) to argue that the magnetic enhancement resulting during the production of paleosol  $S_3$  from its parent loess is bacterial in origin and reflects the concurrent climatic shift to warmer and wetter conditions.

Direct evidence of bacterial magnetosomes has been found in the A horizon of a well developed modern soils (Fassbinder *et al.*, 1990). Although they have shown the presence of magnetic bacteria, it is not clear whether or not the magnetofossils provide the dominant source of magnetization in soils. Furthermore, direct evidence of magnetosomes has hardly been demonstrated for loess strata (Maher *et al.*, 1994).

# IV. STUDY AREA, HYPOTHESES, AND METHODOLOGY

## STUDY AREA

### **Climatic Setting**

The principal climatic features of the central Great Plains are its continentality and Rocky Mountain-induced rainshadow. The Prairie Wedge, which dominates the study region, is a consequence of the zonal westerly airflow crossing the western mountains and penetration by a modified Pacific air mass (Borchert, 1950; 1971). Isohyet patterns exhibit a longitudinal orientation, with mean annual precipitation decreasing from about 30 inches (750 mm) at the southeastern margin to less than 15 inches (380 mm) in the western and northern parts (Figure 4.1). Winters are typically cold with relatively little precipitation, mostly as snow; summers are hot with increased precipitation, chiefly associated with collision of Pacific (mP) and Arctic (cA) air masses with warm, humid (mT) air masses from the Gulf of Mexico. Since it determines the carrying capacity of the region, drought is the most significant climatic element of the Great Plains environment from the ecological, historical, and prehistoric standpoints (Weakley, 1943; Barry, 1983; Wedel, 1986). Vegetation is mostly prairie grassland, due to the subhumid-semiarid, markedly seasonal climate. The mean tropical Atlantic airflow (mT) that influences the grassland east of about the 100th meridian in normal summers has tended to give way during the summers of drought years to continental flow (Figure 4.2).

The prairie crosses the region from north to south in three broad zones (Figure 4.3). In the west, the grama-buffalograss prairie consists of short grasses, while the bluestem prairie with its tall grasses and many forbs prevails in the east. Between them lies the mixed prairie with tall, medium, and short grasses (Küchler, 1964; 1974). In the

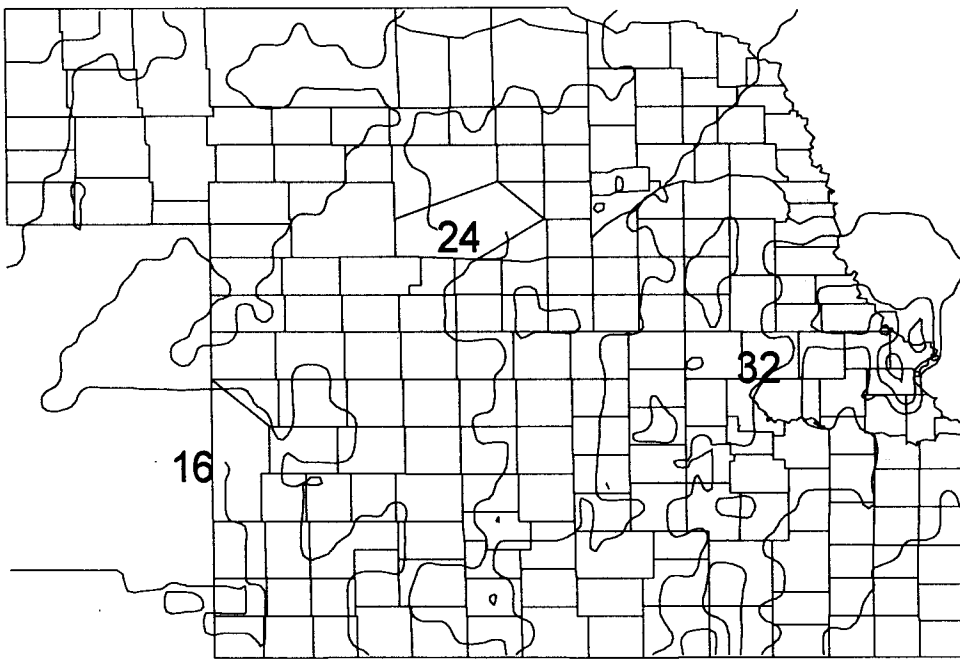


Figure 4. 1. Mean annual total precipitation (inches).



Figure 4. 2. Regions dominated by the various air mass types. The shaded regions are occupied more than 50 percent of the time by the indicated airmass.

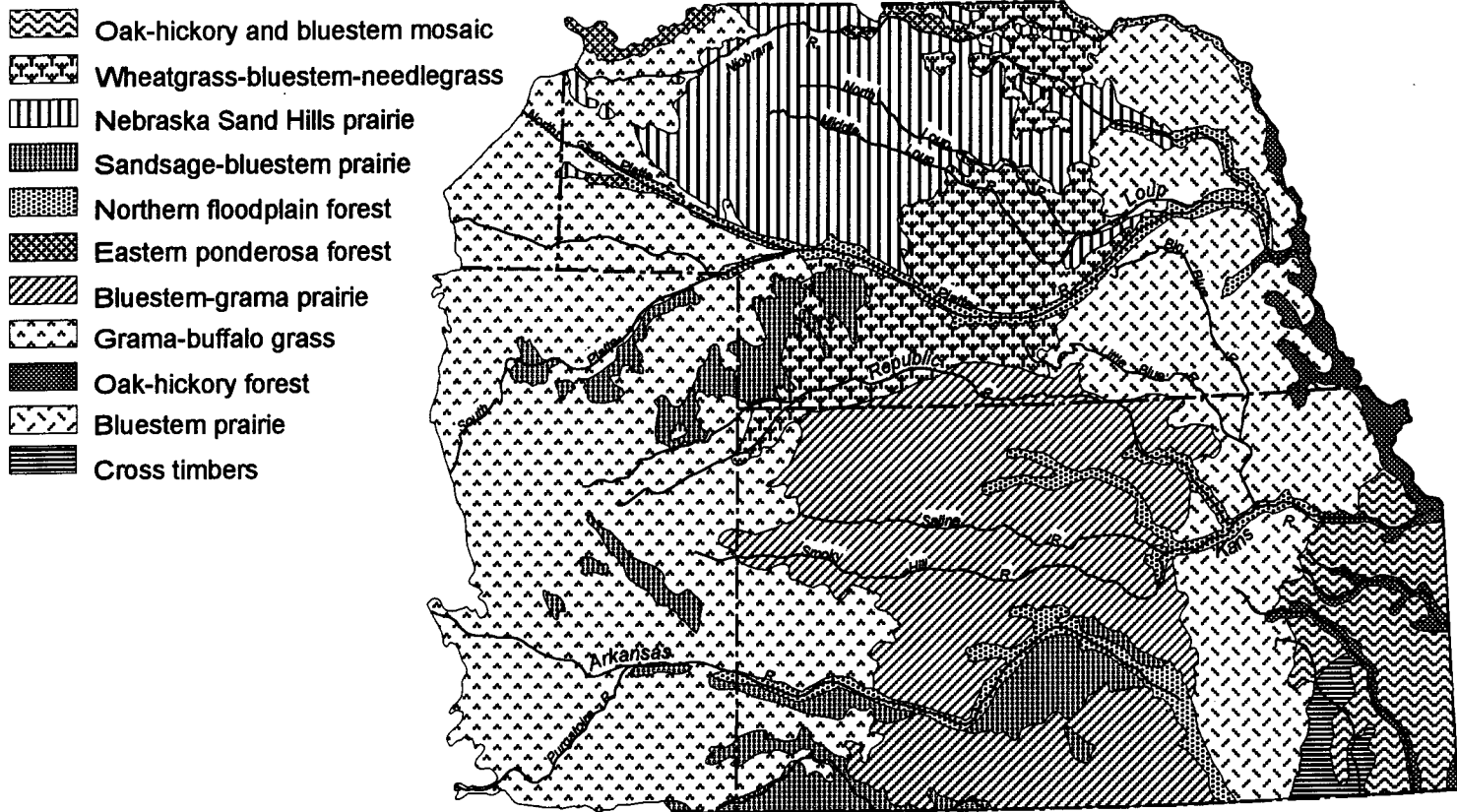


Figure 4.3. Potential vegetation map in the region (after Küchler), 1964).

sand sheets of southeastern Colorado, west-central Nebraska and central Kansas, edaphic conditions promote the existence of a sandsage-bluestem prairie. The sensitivity of prairie composition and boundaries to short-term climatic variation during the historical period is well documented for the region (Tomanek and Hulett, 1970). Similarly, long-term prairie expansion and contraction, presumably in response to climatic variation, is documented at the prehistorical time scale (*e.g.*, Watts and Wright, 1966; Gröger, 1973; Bradbury 1980). The consequence of short- and long-term climatic variations within the central Great Plains and attendant changes in the vegetation probably had measurable impact on prehistorical peoples, but the magnitude of this is certainly open to question (*cf.* Wedel, 1961; Reeves, 1973; Johnson, 1990).

According to Borchert (1950), regional distinctiveness of the grassland climate lies basically in the precipitation. Most of the annual precipitation in the region falls during the growing season from April to September. There is a greater risk of a large rainfall deficit in summer within the grassland than in the bordering regions of forests. The short-grass steppe receives markedly less rainfall than the remainder of Anglo-American east of the Rockies during the summer. The grassland is distinguished from the forest region to the north by fewer days with precipitation, less cloud cover, and lower humidity, on the average, during July and August. The grassland is characterized by large positive departures from average temperature and by frequent hot winds during summer.

### **Physiographic Regions**

The Great Plains physiographic region lies east of the Rocky Mountains and extends from southern Alberta and Saskatchewan almost to the United States-Mexico border (Figure 4.4). The central Great Plains is a large region of generally low relief sloping eastward from the Rocky Mountains toward the Missouri and Mississippi Rivers. Multiple continental glaciations, starting perhaps as early as 2.5 million years ago (Boelstorff, 1978), caused reorientation of the Missouri River system southeastward to

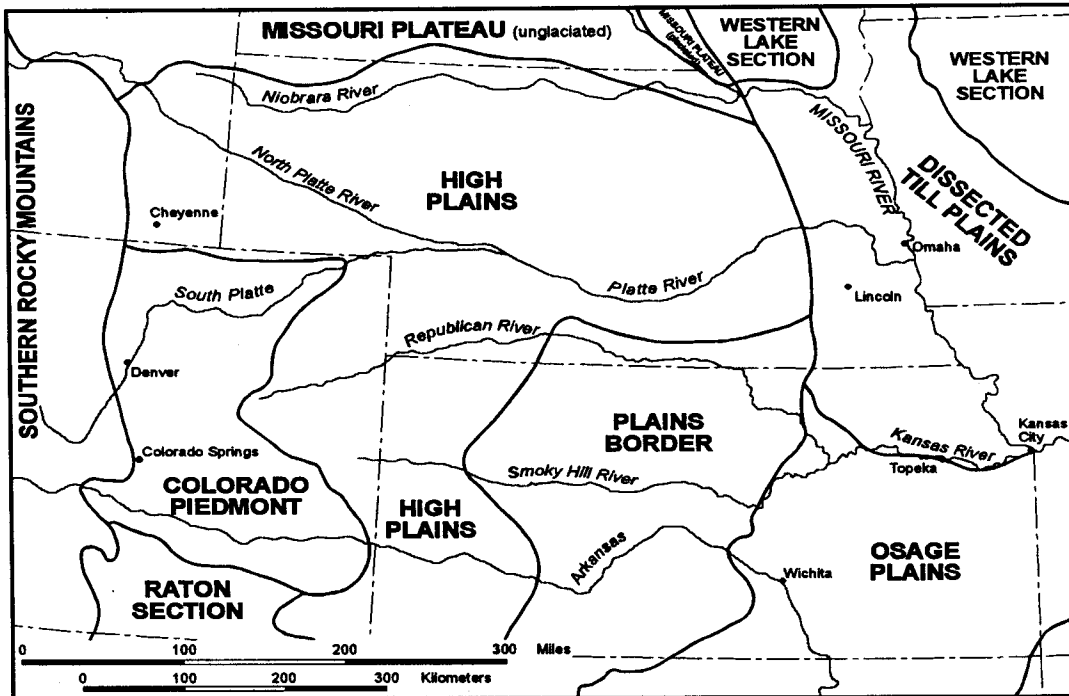


Figure 4. 4. Physiographic map of the central Great Plains.

the Mississippi River, resulting in many stream captures and other geomorphic changes (Wayne *et al.*, 1991). Each time the ice blocked eastward-flowing rivers, proglacial lakes formed, spilled across divides, and developed new courses around the glacial margin. The present course of the Missouri River through North and South Dakota is chiefly along a late Illinoian ice margin. The Platte River evolved through spasmodic uplift of the Chadron arch (Stanley and Wayne, 1972) and several early and middle Pleistocene glacial advances into eastern Nebraska and northeastern Kansas (Aber, 1991). In the middle Pleistocene, the Platte River joined with the glacially diverted Missouri River and formed a wide alluvial plain across east-central Nebraska and northeast Kansas. Quaternary erosion of the central Great Plains, which largely is drained by the Missouri River, has been mostly by fluvial processes. However, the channel network in much of the Missouri River basin was the result of drainage rearrangements by glaciation.

To the west of the Osage Cuestas is a band of grass-covered limestone hills, the Flint Hills, that constitute a preserve of the Kansas tall-grass prairie. The Flint Hills are located at the eastern edge of the huge expanse of grass-covered plains that extends continuously westward to the Front Range of the Rocky Mountains, northward into Canada, and southward into northern Texas. At their western margin, the Flint Hills dip gently under younger rocks which, in the north, slope westward under the Smoky Hills escarpment. In the south, these strata dip below the McPherson-Wellington Lowlands. Extending from north of Salina, Kansas southward to the Oklahoma border, the McPherson-Wellington Lowlands mark the outcrop belt of the thick Wellington shale.

Extensive areas of grass-covered sand dunes lying south of the Arkansas River constitute the Great Bend Sand Prairie. A similar region exists south of the Cimarron River in the southwestern corner of Kansas. During the Late-Pleistocene and Holocene, strong winds eroded fine sediments from alluvial surfaces of the Arkansas River and transported them to the dune area, which covered hundreds of square miles. North of the Great Bend Sand Prairie, Cretaceous rocks, exposed over a large portion of western Kansas, constitute the Smoky Hills, so named because of their dark shales.

From Saskatchewan to northern Texas lies the High Plains. Viewed from a broad perspective, the whole of the High Plains surface is upheld by a huge wedge-shaped, alluvial apron consisting of sediment derived from erosion of the eastern Rocky Mountains. These sediments, the Ogallala Formation, represent Miocene stream deposition similar to that presently occurring in the Arkansas River to the south. The Ogallala Formation is composed not only of river-borne sands and gravels, but also of loess, volcanic ash beds, and diatomite deposits.

The eastern part of the central Great Plains is an area of rolling hills that was invaded by one or more glacial ice masses during the Pleistocene. With the abandonment of the classic stratigraphic Nebraskan and Kansan nomenclature for glacial stages, the intrusions of ice into this region are designated as pre-Illinoian, with the exception of extreme northeastern Nebraska, which experienced glaciation during the Wisconsin Stage. The use of the traditional terms has been confused and has become ambiguous, *e.g.*, coring "Nebraskan" till yielded three separate tills separated by distinct soils (Hallberg, 1986). Despite the lack of a chronology and nomenclature, glaciers occupied the eastern fifth of Nebraska and northeastern Kansas. Glaciers apparently advanced into Kansas twice from two different directions, the second of which did so between 600 ka and 700 ka (Aber, 1991).

Central and western Nebraska is mantled by extensive deposits of Wisconsin to late-Holocene eolian sands known as the Sand Hills. The age and origin of this spectacular eolian feature are still uncertain. Ahlbrandt *et al.* (1983) suggest that the dunes are late-Holocene features, possibly derived from older, unconsolidated sediment that mantled the Great Plains. In contrast, Wells (1983) regards the Sand Hills as a coarse, upwind facies of a single late-Pleistocene sand-silt unit.

### **Study Sites**

Magnetic parameters and stable isotopic data were measured throughout the region and stable isotopic data and phytolith data are available for selected sites (Figure

4.5; Johnson, 1996; Diekmeyer, 1994; Bozarth and Dort, 1992). The study sites were selected to form a northwest-southeast oriented transect from the Platte River of Nebraska and the Arkansas River of Kansas. Low-resolution magnetic data from the sites along the transect provided a record of spatial change in magnetic parameters along the major regional environmental gradient during the late Pleistocene and Holocene. The major thrust of the dissertation research was, however, focused on the temporal change at four sites, using high-resolution data. The four sites, the Eustis ash pit, Sargent site, 14LV1071 (DB), and Beisel-Steinle site, were selected in order to provide a complete record for the last 40,000 years. Since the Eustis ash pit has a complete Pleistocene record, but no Holocene record, the latest Pleistocene and full Holocene record of the Sargent site will be used. These sites are in close proximity to each other and have nearly identical upland settings. The resulting composite section provides a complete late Pleistocene and Holocene paleoclimatic record, unique to the region. Additionally, the 14LV1071 site has a complete Pleistocene record comparable to Eustis ash pit in terms of depth and stratigraphy. The Beisel-Steinle site also has a complete record, though compressed stratigraphically.

The Eustis ash pit is an abandoned volcanic ash mine in Lincoln County, southwestern Nebraska. The site exposes the most complete late Pleistocene loess sequence in the central Great Plains. The main exposure, about 35 m high, consists of a basal layer of volcanic ash (610 ka), pre-Illinoian loesses and intercalated soils, Loveland (Illinoian) loess, Sangamon soil, Gilman Canyon Formation loess and geosol, and Peoria loess. Magnetic samples were taken from the upper 25 m to include the late Pleistocene, *i.e.*, the Gilman Canyon Formation and Peoria loess. One thing should be noted about samples collected from the site: initially, the sampling and MS measurements were done as a class project by a group of students, and R. Farr. Statistical analyses such as cross-correlation were employed to quantify the relationships among the magnetic parameters.  $\delta^{13}\text{C}$  data were derived for the Gilman Canyon Formation through Peoria loess. About thirty  $^{14}\text{C}$  ages and some thermoluminescence (TL) dating provided time-stratigraphic

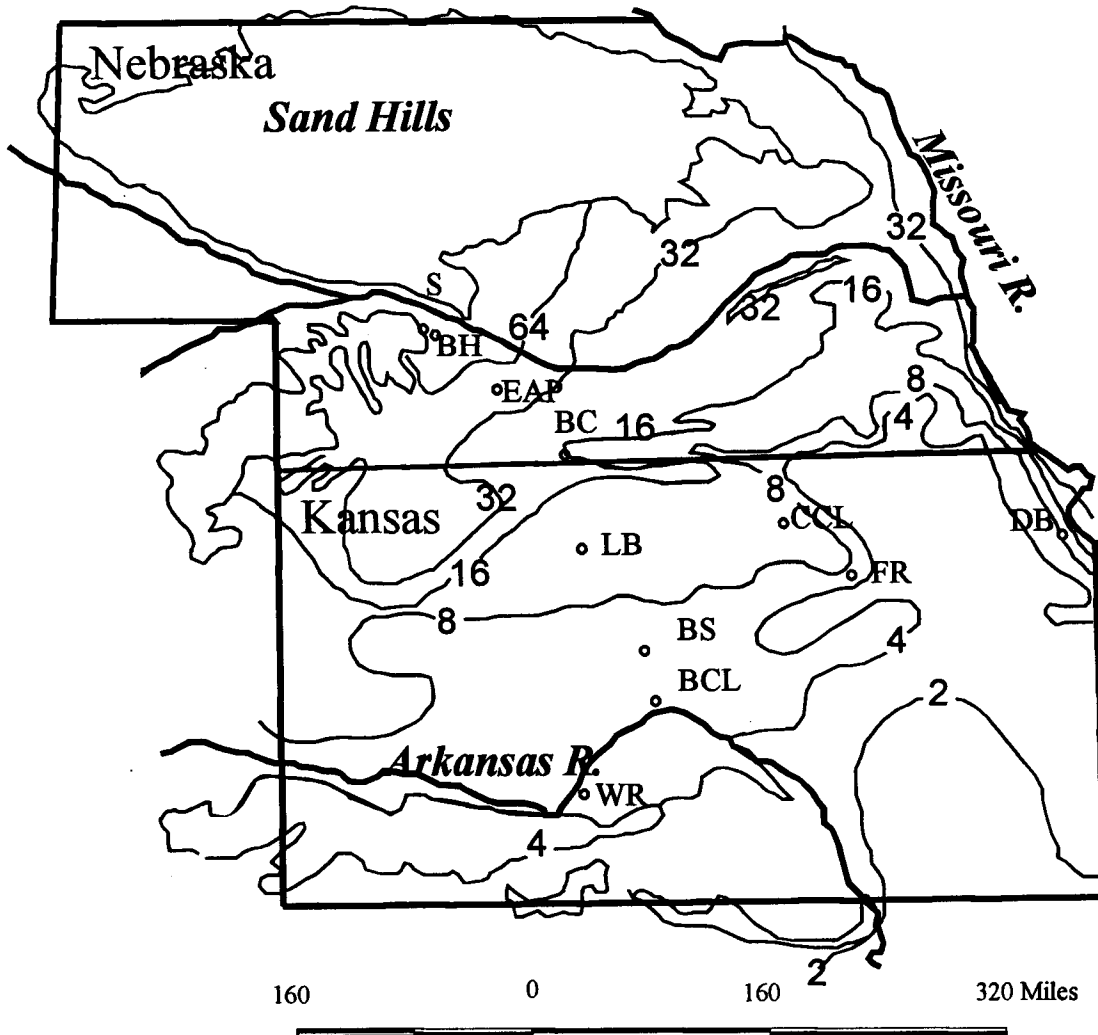


Figure 4. 5. Loess isopatcheous map and locations of magnetic sampling sites (SS=Sargent, BH=Bignell Hill, EAP=Eustis ash pit, BC=Bone Cove, LB=La-Barge ash pit, CCL=Cloud County landfill, BS=Beisel-Steinle, BCL= Barton County landfill, WR=Wilson Ridge, FR=Fort Riley, DB=Disciplinary Barracks).

control for this site. Physical and chemical data for sediment and soils are also available (Diekmeyer, 1994). Paleoenvironmental information for the Peoria loess is available in the mollusk data extracted by Rousseau and Kukla (1994). Opal phytolith analysis was completed for the Gilman Canyon Formation at this site (Bozarth and Johnson, unpublished data) expanding upon preliminary work done by Fredlund *et al.* (1985).  $\delta^{13}\text{C}$  data together with the stratigraphically-restricted opal phytolith data represent an unprecedented record of vegetation, and thereby a record of climate and its changes.

The Sargent site was brought into attention by courtesy of Dr. W. Dort in 1996. Loess appears especially thick at the Sargent site, where streams have recently incised deep canyons into upland loess deposits. Even though the Loveland loess is not exposed at the site, this site exhibit one of the best expressions of the Peoria loess (total thickness yet to be determined), the Brady soil (*ca.* 1.2 m thick), and Bignell loess (*ca.* 4.7 m) in the region. The bottom of the Brady exposure dates to 11 ka. Eleven  $^{14}\text{C}$  assays and associated  $\delta^{13}\text{C}$  data (Dort, unpublished data) in addition to high-resolution opal phytolith data (10 cm interval) are available from this site (Bozarth, unpublished data).

The 14LV1071 (DB) site, located on the western bluffs of the Missouri River, has been exposed to the indirect influences of the Pleistocene glacial periods. This site exhibit complete stratigraphy from Gilman Canyon Formation to modern soil, and therefore employed to compare magnetic records with other Nebraskan sites. In its role as a sluiceway (conduit of glacial meltwater), the Missouri River transported large quantities of fine glacial sediments from the ice fronts to the north. Persistent, high velocity winds transported these fine sediments from the Missouri River valley bottoms up onto the bluff, resulting in thick deposits of loess. The late- Quaternary stratigraphy consists of loess deposits with intercalated soils. Glacial activity began to wane after about 18 ka, following the Last Glacial Maximum, but significant loess deposition persisted until about 11 ka. Small amounts of loess accumulated during the post-glacial period (Holocene), but accumulation rates were so slow that the silt was often incorporated into the soil via pedogenesis.

The Beisel-Steinle site is exposed at a roadcut in the valley wall of the Smoky Hill River about 5.8 km southeast of Dorrance, Russell County, central Kansas. Stratigraphy at the site of interest to this study includes 1.6 m of the Gilman Canyon Formation soil, 1.1 m of Peoria loess, and 2.3 m of a Brady soil/modern soil complex. Bignell loess may also be present, however, the Gilman Canyon loess does not occur at the site. With its complete late-Quaternary stratigraphy, though compressed, this site was employed to compare with northern sites such as Eustis ash pit and Sargent site. Pleistocene-age sediments rest on the Cretaceous Dakota Formation (Johnson and Arbogast 1993), which also outcrops in the roadcut exposure.

## **RESEARCH HYPOTHESES**

As noted earlier, the goals of this study were to reconstruct the late Quaternary paleoclimate history of the central Great Plains by using magnetic and climate-sensitive biological proxies of climate and to test the feasibility of using rock magnetic parameters as a climate proxy. Several alternative hypotheses were formulated to accomplish the stated goals of the research. They include:

- H11: Concentration of magnetic mineral controls the magnetic records of Quaternary loess.
- H12: The magnetic grain size of soils are different from less-weathered loess.
- H13: Rock magnetic parameters correlate well with other paleo-climatic proxies.
- H14: Every concentration-sensitive magnetic parameters can provide the independent high-resolution data for climate variations during the late Quaternary.

## METHODOLOGY

To test the hypotheses formulated, rock magnetic parameters were measured at close interval. In order to differentiate soils from unweathered loess, rock magnetic parameters were plotted against depth and pedo-stratigraphy. Furthermore, biparametric plots were produced to compare soils with unweathered loess. Stable isotope and opal phytolith data were plotted against depth and compared with rock magnetic parameters where available. Correlation coefficients were measured to test the feasibility of the rock magnetic parameters to be an independent climate proxy.

### Sampling

Samples for magnetic analyses were collected in the field from freshly exposed or cleaned profiles (all the sites except the 14LV1071), or from cores extracted and transported to the laboratory in clear carbonate plastic liners (14LV1071). The individual magnetic samples were collected in numbered, demagnetized 8cm<sup>3</sup> plastic cubic containers with lids. The sample interval varied slightly, but averaged 40 per meter. These cubes were pressed by hand or driven with a rubber-coated, dead-blow hammer into the exposure or core to obtain the required amount of sediment. In the laboratory, the cubes were cleaned, sorted, air dried, weighed, and placed in wooden trays prior to measurement.

Samples for stable carbon isotope were collected in the field from 10-cm intervals of the cores or exposures of some of the study sites. 300 to 400-gram samples were prepared for  $\delta^{13}\text{C}$  analysis. Samples for opal phytolith analysis were done either from a core extracted with Giddings drilling machine or from exposures created by backhoe trenching. In both cases, sampling interval was 10cm.

## Measurements

Various rock magnetic parameters including susceptibility, frequency dependence, ARM, and SIRM were measured at each site. Stable isotopes data from the Fort Riley are pending except the Pump House Canyon site. Opal phytolith data are available for several sites.

### *Rock magnetic parameters*

In order to differentiate authigenic magnetic grains from exogenic detrital input of magnetic grains, it was necessary to gain as much information as possible about the abundance, mineralogy, and grain size characteristics of magnetic minerals. Susceptibility and FD measurements were obtained using a Bartington magnetic measurement system consisting of a Model MS2 susceptibility meter and a dual-frequency sensor (MS2B). ARMs and IRMs were imparted using a Schoenstedt GSD-5 model and an ASC Scientific IM10 impulse magnetizer, and obtained with a Molspin Spinner magnetometer interfaced with a McIntosh computer. Those instruments are housed in Paleomagnetic Laboratory within the department of Geology at the University of Kansas. Hysteresis properties from the selected samples were measured by R. Farr using the Quantum Design Magnetic Property Measurement System at Midwest Superconductivity Laboratory.

The abundance of magnetic minerals is indicated by parameters such as susceptibility, SIRM and ARM. The major factor controlling the susceptibility of samples in this range is the concentration of ferrimagnetic minerals, *i.e.*, the total volume of ferrimagnetic crystals (Dearing, 1994). The concentration of magnetite in a sample is estimated by dividing the bulk susceptibility value of the sample by the susceptibility of the assumed or known magnetite type or size.

There are no completely time-efficient, satisfactory methods to quantitatively discriminate ferrimagnetic minerals from other types of minerals, discern magnetite from maghemite within the same type of minerals. Banerjee *et al.* (1993) have shown that the ultrafine-grained ferrimagnetic minerals are definitely pedogenic in origin. However, it

is not yet clear whether this component is magnetite (*e.g.*, Heller and Liu, 1984; 1986) or maghemite (Verosub *et al.*, 1993). Since magnetite and maghemite, both strongly ferrimagnetic minerals, are identified as the dominant ferrimagnetic minerals by most studies both in China and North America, the type of iron oxides which occur in samples was not rigorously sought in this study. The abundance of high-coercivity minerals (predominantly hematite) was determined by the  $IRM_{0.3T}/IRM_{1.1T}$ , which is the ratio of the isothermal remanent magnetization from an applied field of 0.3 Tesla to the IRM from an applied field of 1.1 Tesla. Samples without high-coercivity material have a value of 1, while samples with hematite as the only magnetic phase should have a very low values ( $< 0.4$ ) parameter on about 50 % of the samples from several sites including Eustis ash pit, DB site, Beisel-Steinle site, and Barton County Landfill.

The SIRM demagnetization technique of Lowrie (1990) was applied on selected samples. Three different IRMs were imparted to specimens along three mutually perpendicular directions (X, Y, Z), each direction essentially corresponding to a different coercivity spectrum.

In China and some other parts of the world, it has been known that there were substantial differences in magnetic grain-sizes between the loess and paleosol samples, with the latter selectively enriched in the finest grains (Maher and Thompson, 1991). Results showed that the grain size assemblages at each depth along the measured section are very sensitive to stratigraphic correlations. ARM and FD were the properties most closely linked to the presence of pedogenic fine grains (approximately  $0.015 - 0.1 \mu\text{m}$ ). Comparing ARM/SIRM ratios with FD identified the fine grained tail from the detrital coarse mineral. Assembling this information on the cross-plot provided qualitative rather than quantitative grain size information.

Recent measurements on natural and synthetically produced magnetites have helped to define the major change in susceptibility with crystal size (Maher, 1988). It can be seen that there are two size ranges in which susceptibility reaches high values. At the

coarse end of the scale, between 20 and 100  $\mu$  m, values exceed  $60,000 \times 10^{-8} \text{ m}^3\text{kg}^{-1}$ , and in crystals smaller than 0.03  $\mu$  m, values exceed  $100,000 \times 10^{-8} \text{ m}^3\text{kg}^{-1}$ . These two peaks effectively divide the data into three ranges which correspond to three quite different states of ferrimagnetic behavior. Above 10-20  $\mu$  m the crystals are divided up into different regions or cells of magnetization, known as domains, and are referred to as having multidomain behavior. In smaller crystals, normally  $<1 \mu\text{m}$ , the restricted volume allows only one domain to form, and hence these show single domain behavior. In ultrafine crystals below 0.035  $\mu$  m, the magnetization is strong but unstable, and thermal energy counteracts induced magnetization very quickly after a magnetic field is removed. This behavior is similar to paramagnetism, but with a much greater susceptibility. Hence, it is termed superparamagnetic behavior.

For materials in which magnetite is the dominant magnetic species, magnetic methods offer the potential for rapid and non-destructive granulometry, if the grain size dependence of the measured parameters (and/or interparametric ratios) can be shown to be sufficiently size-diagnostic. Thompson and Oldfield (1986) noted that the ratio of SIRM to MS can be used as a rough estimate of magnetic grain size. However, mixtures of SP and SD grains give rise to similar SIRM/MS ratios as MD grains. An alternative method of granulometry was proposed by King *et al.* (1982), employing a comparison of  $\chi_{\text{ARM}}$ , rather than SIRM, with  $\chi$ . This method depends on  $\chi_{\text{ARM}}$  showing particular sensitivity to the SD and small PSD grain sizes, and  $\chi$  to the larger PSD and MD grains.  $\chi_{\text{ARM}}/\chi$  model is, however, complicated by the possible presence of SP magnetite grains. Firstly, a natural assemblage containing predominantly SP magnetite would be characterized by  $\chi_{\text{ARM}}/\chi$  values plotting in a similar location to those of very coarse magnetite. Secondly, if the proportion of SP to SD magnetite in a natural sample were to increase, the  $\chi_{\text{ARM}}$  vs  $\chi$  method would interpret this change as an apparent increase in grain size rather than as an actual decrease.

In view of these difficulties, a modified granulometric method of Maher (1988) was used in this study (Figure 4.6). The initial stage compared ARM not with  $\chi$  (as in

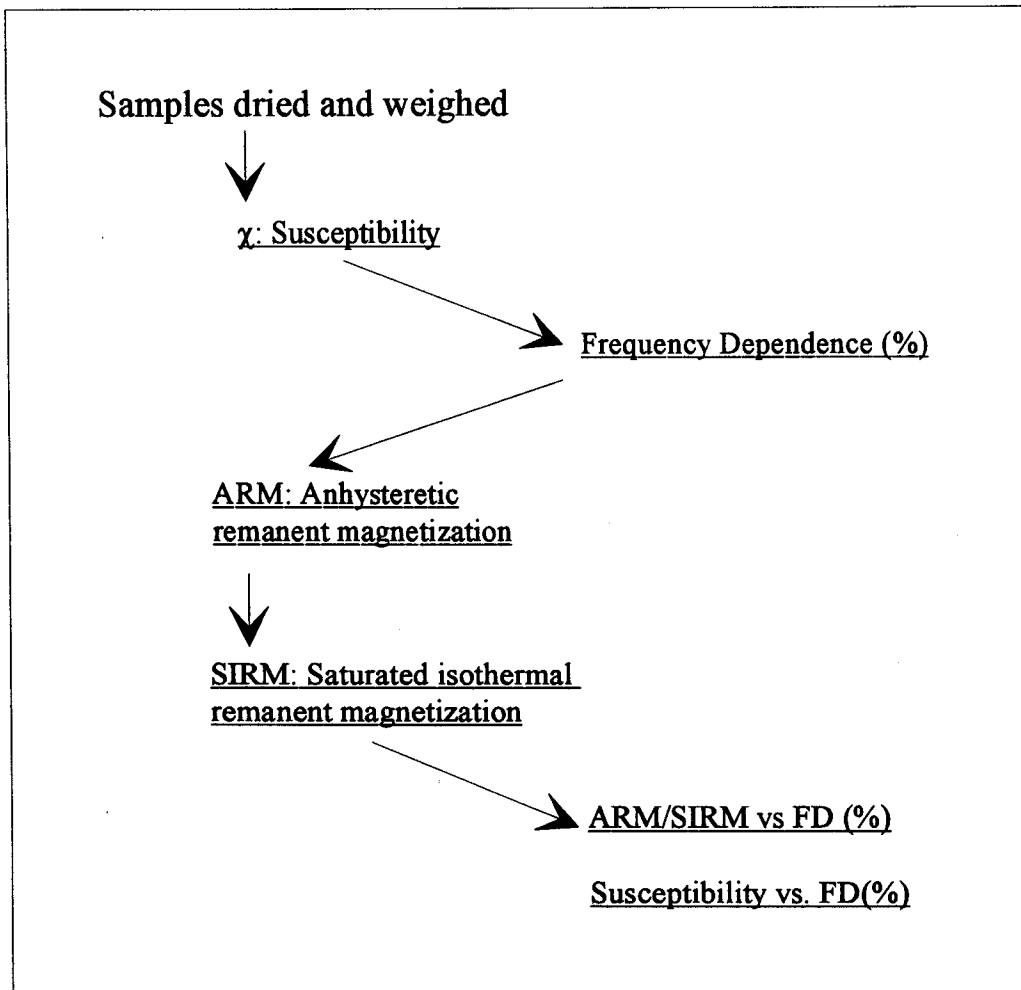


Figure 4.6. Sequence of measurements performed for magnetic grain size analysis (after Maher, 1988).

King *et al.*'s model (1983) but with SIRM. This parameter is more size-sensitive within the MD range, and both ARM and SIRM, as remanence parameters, seem to be unaffected by paramagnetic contributions. In the second stage, the ARM/SIRM was plotted against FD. The latter effectively separates the fine tail from the coarse end of the grain size-spectrum.

These relationships, however, are complicated by 1) variations in magnetic mineralogy (Verosub *et al.*, 1993) which may include SD and MD ferrimagnetic grains, and paramagnetic and canted antiferromagnetic minerals or by 2) magnetic grain interactions in SP grains which may cause groups of SP grains to show the magnetic behavior of coarser SD grains (Cisowski, 1981; Maher, 1988; Dearing *et al.*, 1996). Furthermore, ARM/SIRM is insensitive to the presence of true SP grains, because SP grains are unable to maintain remanence at room temperature due to thermal reorientation.

#### *Stable carbon isotope*

The procedure utilized was identical to that used by our laboratory for the preparation of soil and sediment samples for  $^{14}\text{C}$  humate dating, which renders the results compatible with those obtained in the course of age correction for the effects of isotopic fractionation (Johnson and Valastro, 1994). Samples were first disaggregated in 4-liter beakers filled with distilled water. They were then skimmed with a 60-mesh screen to remove floating organic debris. Next, the samples were washed through a 230-mesh screen with distilled water into a second beaker in order to remove the sand and coarse silt fractions; the fine fraction remaining is assumed to contain the adhering organic carbon. The samples were then treated with concentrated HCl in order to remove the inorganic carbon contained within the carbonate. This step is particularly important because of the significant amounts of carbonate precipitated within the loess. Following distilled water washes and oven-drying ( $100^{\circ}\text{C}$ ) in 4-liter beakers, the samples were pulverized and packaged. They were then submitted to the University of Texas

Radiocarbon Laboratory for stable carbon isotope ratio analysis.

As discussed in chapter 2, the  $\delta$  value for a carbon isotope in soil organics is defined as:

$$\delta^{13}\text{C soil} = (\delta^{13}\text{C}_{\text{C}_3}) (x) + (\delta^{13}\text{C}_{\text{C}_4})(1 - x)$$

However, soil formation and other processes may alter the isotopic signature imparted by vegetation. For example, two per mil (‰) isotopic enrichment may occur during litter decomposition (Melillo *et al.*, 1989; Wendin *et al.*, 1995). The ratio of  $\text{C}_3$  plant contribution is calculated using the modified formula considering enrichment during the pedogenesis.

$$(\delta^{13}\text{C soil}-2\text{‰}) = (\delta^{13}\text{C}_{\text{C}_3}) (x) + (\delta^{13}\text{C}_{\text{C}_4})(1 - x),$$

where  $\delta^{13}\text{C}_{\text{C}_4}$  is the average of  $\delta^{13}\text{C}$  values of  $\text{C}_4$  plants (-13‰); ( $\delta^{13}\text{C}_{\text{C}_3}$ ) is the average of  $\delta^{13}\text{C}$  values of  $\text{C}_3$  plants (-27‰); and  $x$  is the proportion of carbon from  $\text{C}_3$  plant sources. The resulting  $\text{C}_3$  plant contribution is compared with the magnetic parameters and the pooid ratio from the short cell phytolith counting where available.

#### *Opal phytolith analysis*

Phytolith analyses were done for several upland loess sites including Eustis ash pit, Sargent site, several exposures in Fort Riley, and 14LV1071 at DB site. Opal phytoliths were isolated from 5-gram subsamples using a procedure based on heavy-liquid (zinc bromide) flotation and centrifugation (Bozarth, 1991). Phytoliths were classified by Bozarth of the University of Kansas according to a convention that has been developed and used by other reports and publications (Table 4.1: Brown, 1984; Twiss, 1987). For each site analyzed, two diagrams were constructed, one for all of

the data and the other for only short-cells diagnostic of grass subfamilies and arboreal-type phytoliths. The data for short-cell morphotypes are used for this investigation since these morphotypes can distinguish among short C<sub>4</sub> grasses (Chloridoideae tribe), tall C<sub>4</sub> grasses (Panicoideae subfamily), and those produced primarily by cool-season C<sub>3</sub> grasses (Pooideae subfamily).

Pooideae morphotypes provided a basis estimating the ratio of cool-season C<sub>3</sub> plant. Phytolith index of Diester-Haass *et al.* (1973) was occasionally used to estimate humidity conditions during the sedimentation.

Table 4.1 Short-cell phytolith morphotypes and typical photosynthetic pathway represented (after Fredlund, 1997).

Phytolith morphotypes	Poaceae taxa	photosynthetic pathways
Keeled	Pooideae	C <sub>3</sub>
Rondel	Pooideae	C <sub>3</sub>
Rectangle	Pooideae	C <sub>3</sub>
Sinuate	Pooideae	C <sub>3</sub>
Saddle	Chloridoideae	C <sub>4</sub>
Simple-bilobate	Panicoideae	C <sub>4</sub>
Panicoid-type	Panicoideae	C <sub>4</sub>
Cross	Panicoideae	C <sub>4</sub>
Other lobate	Panicoideae	C <sub>4</sub>

## V. RESULTS

In many different settings, the abundance, types, and magnetic grain sizes of magnetic minerals incorporated in sediments have varied in response to climate changes. High resolution climatic proxy records could be reconstructed by using magnetic and biological records of the last 40,000 years.

Climatic proxies within the Gilman Canyon loess indicate cool, and moist conditions. Warm, dry conditions prevail during mid-Gilman Canyon time, while late Gilman Canyon time is characterized by trends toward cooler and moister conditions after formation of the Gilman Canyon soil. Climate conditions from the Peoria loess indicate cool, moist environment at the time of loess deposition. This condition continues upward through the Peoria loess profile at the Eustis ash pit and 14LV1071 site until Brady soil is encountered at about 1.5 meters below the surface. At this Brady time, Peoria loess comes under the influence of warm, dry conditions dominating the modern surface.

The relatively strong correlation between MS and other proxies from the region indicates a strong link between climate variation and those processes that generate the magnetic signal. This linkage is also supported by the synchrony of the variation in magnetic properties and northern hemisphere climate change.

### EUSTIS ASH PIT

#### **Previous Study**

This site has drawn attentions from several persons from various backgrounds. Carbon isotopic data have been derived for the Gilman Canyon Formation through the Peoria loess. About thirty  $^{14}\text{C}$  ages and some thermoluminescence (TL) dating provide time-stratigraphic control for this site. Physical and chemical data for sediment and soils are also available (Diekmeyer, 1994). Paleoenvironmental information for the Peoria loess is available in the mollusk data extracted by Rousseau and Kukla (1994). Opal

phytolith analysis has recently been completed for the Gilman Canyon Formation at this site (Bozarth and Johnson, unpublished data), expanding upon preliminary work done by Fredlund *et al.* (1985).

The stratigraphy of interest present at the site includes the Gilman Canyon loess and soil (comprising approximately 1.5 m of the section) and 16.2 m of Wisconsin-age Peoria loess (Figure 5.1.). The Bignell loess is not present at the Eustis site; the modern soil appears to be welded to the Brady soil (Souders *et al.*, 1971).

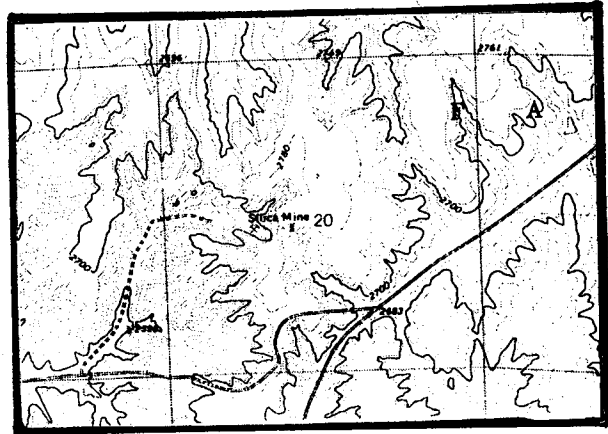


Figure 5.1. Topographic map in the vicinity of Eustis ash pit. Scale 1:24,000

Contiguous samples of 2.5 cm have been taken from the upper eighteen meters within the loess.

### Rock Magnetic Records

In order to compare measurements results with published loess studies, the MS and FD values were first measured for all samples. Selected samples were then given an ARM in a peak alternating field of 90 mT and a steady field of 0.05 mT using a modified Schonstedt alternating demagnetizer. Those samples were given IRM at 0.3 T and 1.1 T to obtain SIRM and  $IRM_{0.3T}/IRM_{1.1T}$ .

### *Magnetic concentration*

The results of MS measurements at the Eustis ash pit are summarized in Figures 5.2.a and 5.3. Broad patterns define alternating zones of relatively high and low MS in the MS-depth profile (Figure 5.2. a). These patterns are more clear in the MS-age profile (Figure 5.3) From the bottom of the profile, MS zones include: low MS, high MS, low

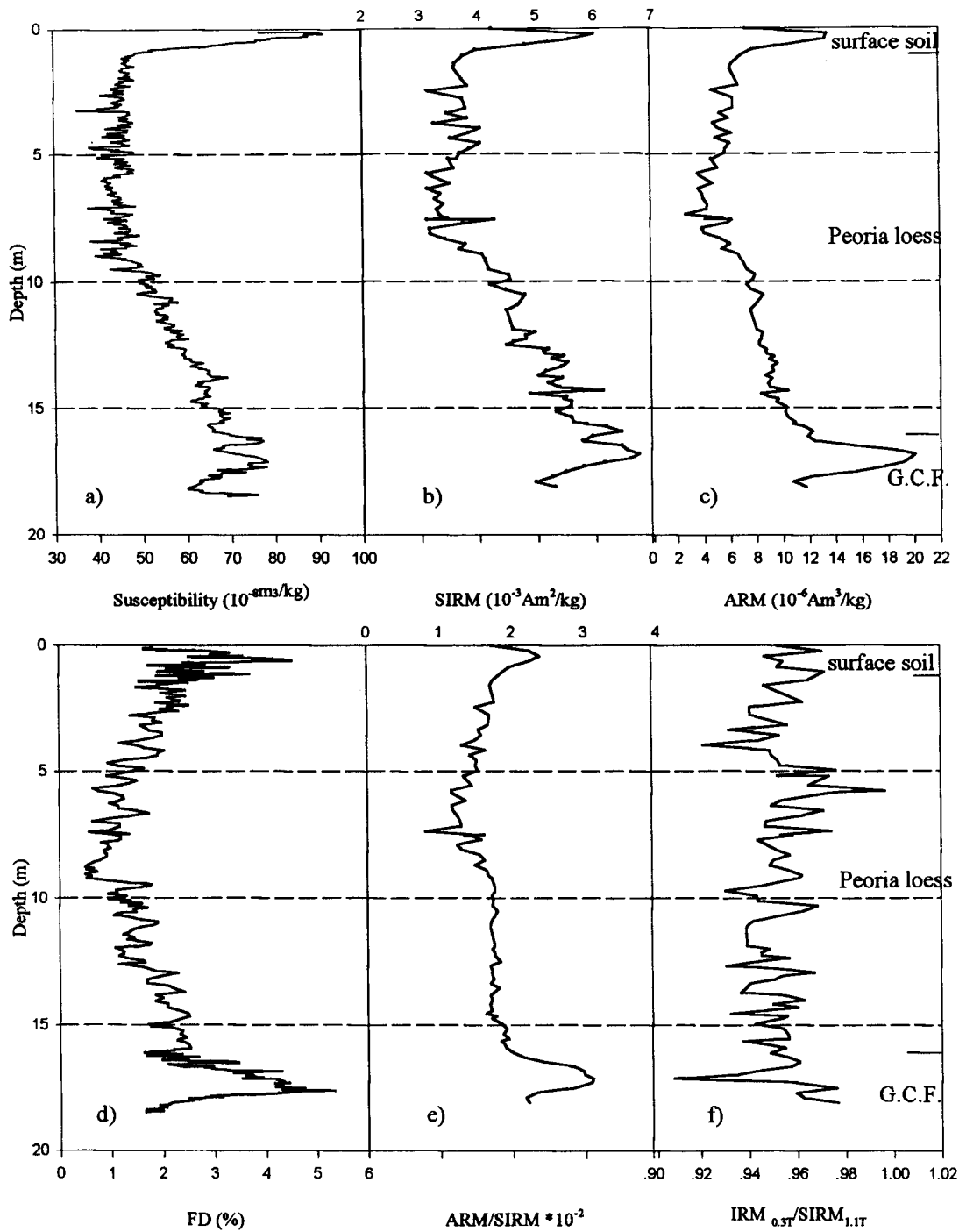


Figure 5.2. MS, SIRM, ARM, FD, ARM/SIRM, and IRM<sub>0.3T</sub>/IRM<sub>1.1T</sub> for the profile sampled at the Eustis ash pit.

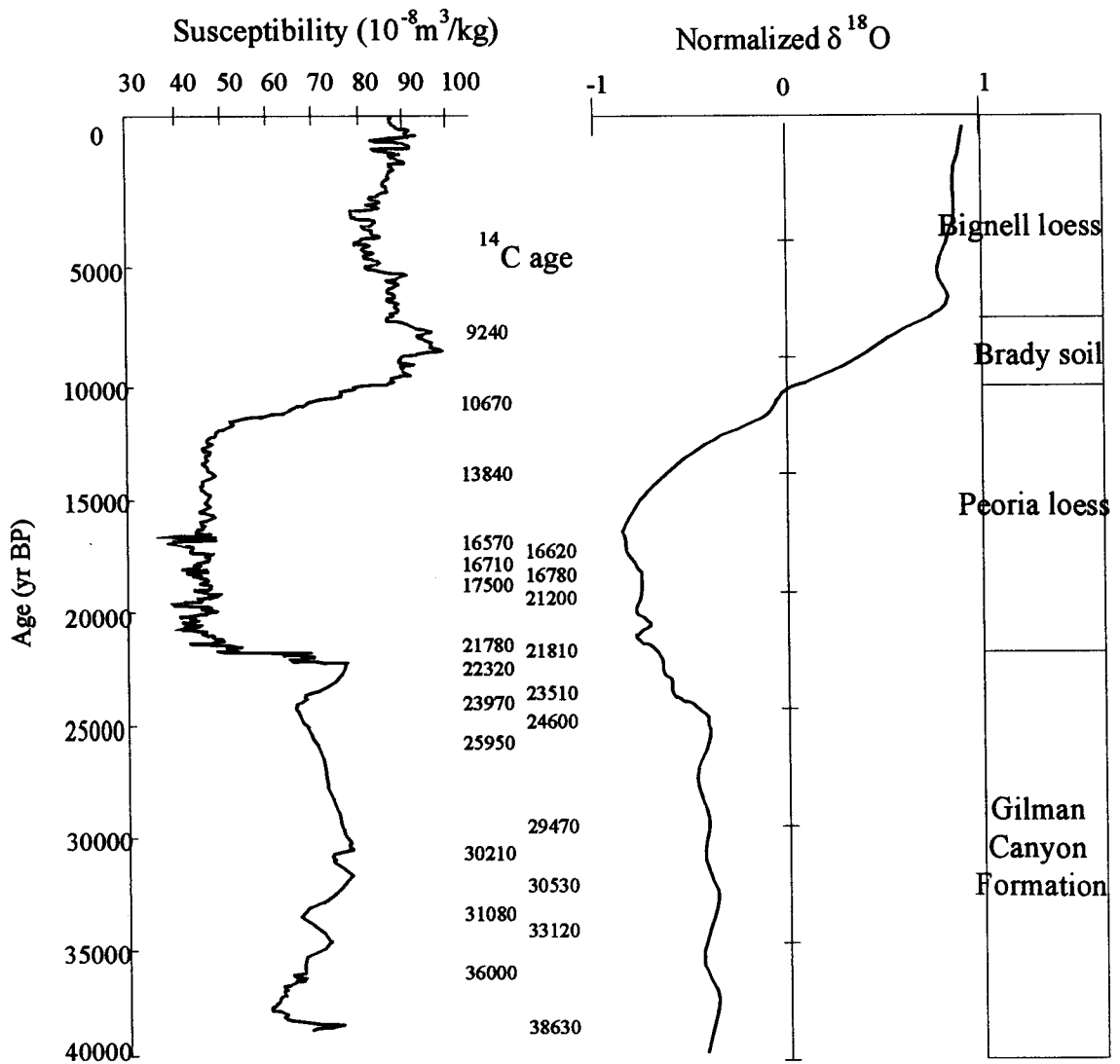


Figure 5.3. MS from the Eustis ash pit (GCF through Brady soil)-- Bignell Hill (Brady soil through modern soil) and SPECMAP oxygen isotope record (Martinson *et al.* 1987)

MS, and high MS. MS values range from *c.* 40 to 100 x 10<sup>-8</sup>m<sup>3</sup>/kg and show the systematic differences between loess and soils.

MS values of the unweathered Gilman Canyon loess (*c.* 55 x 10<sup>-8</sup>m<sup>3</sup>/kg) are lower than those of the overlying Gilman Canyon soil (*c.* 90 x 10<sup>-8</sup>m<sup>3</sup>/kg). MS intensities of the Gilman Canyon soil are nearly twice as high as those of the overlying Peoria loess. Bimodal peaks in the MS records reveal minor climate fluctuations, lending evidence for the theory of multiple periods of pedogenesis during that time (*e.g.*, Johnson, 1993). Despite the uncertainties of <sup>14</sup>C age estimates, there is a good match between the magnetic variations within the interstadial Gilman Canyon Formation and the regional climate history in terms of the general timing of episodes and the number of cycles responding to the same global climatic forcing (Table 5.1).

MS values of the overlying Peoria loess exhibit a decreasing trend until it reaches its minimum value at 9 m below the surface (Figure 5.2). An MS-age plot exhibits a more sudden decrease at about 22 ka. The weaker MS signal within the Peoria loess indicates either that the depositional rate was much faster than during the overlying Brady time and underlying Gilman Canyon time, or that pedogenesis was much slower due to cold and dry weather associated with the Last Glacial Maximum. Loess began to accumulate more than ten times faster at about 22 ka than Gilman canyon time (Figure 5.4). At the same time, the median grain size, which is a measure of the 50th percentile determined by a cumulative grain size curve, shows a sudden increase in size from 5.2  $\phi$  to 4.5  $\phi$ . At the 18-17 ka time interval representing the Last Glacial Maximum, the average MS intensities reach their minimum values (< 40 x 10<sup>-8</sup>m<sup>3</sup>/kg). Simultaneously, loess accumulation rates were higher and median particle size also exhibits an increase. Global conditions during that time are in good agreement with the findings from the site, the concentration of microparticles in Greenland ice of the Late Wisconsin being 3 to 70 times higher than in Holocene ice (Reeh, 1989). At the 14-13 ka interval, which represents the time of major deglaciation (Ruddiman, 1987), MS begins to increase rapidly.

Table 5.1. Spikes in the Gilman Canyon Formation compared with U-Th ages from Searles Lake, California (Phillips *et al.*, 1994), icecore from Summit Greenland and stacked isotopic data (Martinson *et al.*, 1987).

Searles Lake	Summit icecore		Stacked $^{18}\text{O}$	Eustis ash pit	
Mean U-Th (ka)	$^{14}\text{C}$ (ka)	Greenland Interstadial no.	$^{14}\text{C}$ (ka)	$^{14}\text{C}$ (ka)	
25.6	23.7	3	25.7	21.4	22.4
26.3	25.5	4	26.8	25.8	
28.4	28.6	5	29.3	29.8	30.5
29.8	28.8	6	30.0		31.8
31.0	29.4	7	31.3	33	34.5
34.3	32.5	8	33.9	37.6	38.5

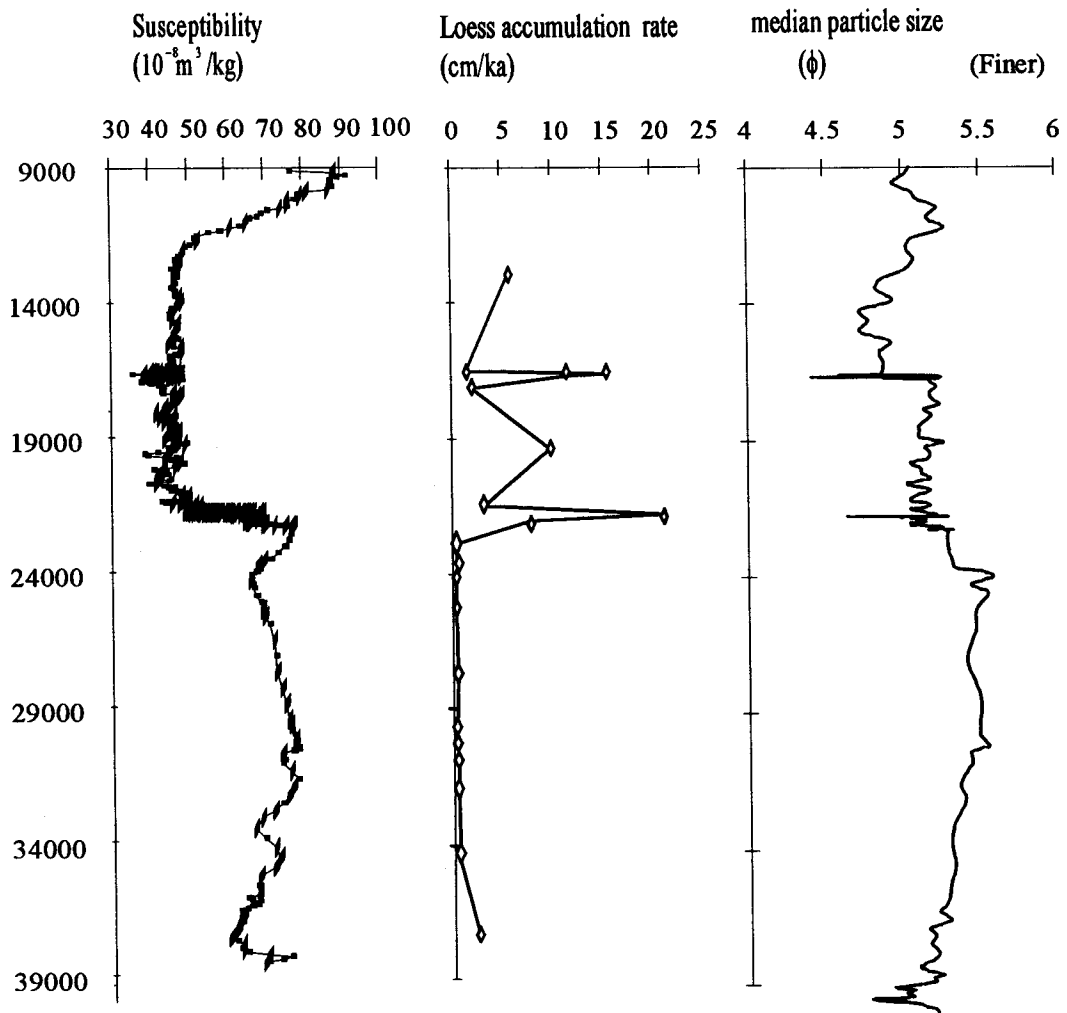


Figure 5. 4. MS, loess accumulation rate derived from RC ages, and median particle size from the Eustis ash pit.

Mass specific ARMs and SIRMs were measured for selected samples throughout the section. One thing should be noted about samples collected from the site: initially, the MS measurements were done as a class project by a group of students. The SIRM variations from the measured samples exhibit good correlations with MS variations. SIRM values vary in the range of  $SIRM = 3-7 \times 10^{-3} \text{Am}^2/\text{kg}$ . SIRMs are enriched in the Gilman Canyon soil relative to the overlying Peoria loess by a factor of three (Figure 5.2. b). SIRM variations also exhibit bimodal peaks within the Gilman Canyon Formation as discussed already in explaining MS variations.

Mass specific ARMs vary in the range of  $ARM = 2-20 \times 10^{-6} \text{Am}^2/\text{kg}$ . ARM variations again correlate well with MS and SIRM. The Gilman Canyon soil has highest ARM values and overlying Peoria loess has the lowest values. It should be noted that while the range of ARM variation seems to be much greater than those of SIRM or MS variations, the absolute values of ARMs are two orders smaller than are SIRM values, so small changes could cause seemingly greater variations. Bimodal peaks are not observed in ARM variations, which seems to be caused by the lack of close interval measurements, since bimodal peaks are observed within the Gilman Canyon Formation from the DB and Beisel Steinle sites, KS, which will be discussed later in this chapter. ARM and SIRM variations indicate a greater concentration of smaller grains with a stable single domain in the Gilman Canyon Formation than in the Peoria loess, which will be discussed in detail in the next section. The linear behavior of SIRM and ARM with MS (Table 5.2), as is indicated by very high correlation coefficient between them, suggests that MS may be controlled by ferrimagnetic concentration (Eyre and Shaw, 1994).

Table 5.2 Correlation coefficients and significance level between the magnetic parameters and  $\delta^{13}\text{C}$  data at the Eustis ash pit.

	ARM	ARM/SIRM	FD	$\delta^{13}\text{C}$	MS	SIRM
ARM	1.000					
ARM/SIRM	0.912**	1.000				
FD	0.559**	0.614**	1.000			
$\delta^{13}\text{C}$	0.448**	0.586**	0.566**			
MS	0.865**	0.639**	0.392**	0.262	1.000	
SIRM	0.894**	0.656**	0.251*	0.093	0.952**	1.000
ARM						
ARM/SIRM	0.000					
FD	0.000	0.000				
$\delta^{13}\text{C}$	0.002	0.001	0.000			
MS	0.000	0.000	0.000			
SIRM	0.000	0.000	0.028		0.000	

\*\* Correlation is significant at the 0.01 level (2-tailed).

\* Correlation is significant at 0.05 level (2-tailed).

### *Magnetic grain size*

Magnetic granulometry can be achieved with analysis of the frequency dependence of MS, hysteresis-loop parameter, and thermal demagnetization characteristics of a low-temperature saturation remanence. Such analyses on whole samples, however, can only be qualitative at most, since they give only the magnetic domain state or effective magnetic grain size of the bulk soil samples. Yet, in the absence of a massive and elaborate study of separated magnetic grains in a transmission electron microscope, such qualitative conclusions are generally representative of the samples studied (Forster *et al.*, 1994; Hunt *et al.*, 1995). For the purpose of this discussion, this study adopted the conventional grain-size assignments for magnetite: superparamagnetic,  $d < 30$  nm; single domain,  $30 \text{ nm} < d < 50$  nm; pseudo-single-domain,  $50 \text{ nm} < d < 8 \mu\text{m}$ ; and multidomain,  $d > 8 \mu\text{m}$  (Dunlop, 1973; Moskowitz and Banerjee, 1979; Dunlop, 1981).

The FD data obtained by an MS2B dual frequency bridge shows the presence of an ample amount of SP material only in the two mature soils, Gilman Canyon soil and modern/Brady soil. FD values range from 0 to 6 percent at the Eustis ash pit, which appears to be fairly low compared to Chinese loess of that age. FD values greater than 11 percent have been observed in the loess paleosol sequence at Xifeng, (Heller *et al.*, 1991), and FD values greater than 15 percent are reported from Luochuan, China (Forster *et al.*, 1994). Although the FD values variation is in qualitative agreement with previous works, recent studies suggest that the FD values can rarely be interpreted quantitatively (Forster *et al.*, 1994; Dearing *et al.*, 1996), since the FD measured using fixed low and high frequencies will discriminate only a portion of the total SP population. In the case of the Bartington susceptibility meters that we use, only the presence of grains between approximately 18 and 20 nm in diameter can be detected. Nevertheless, assuming a fairly uniform grain-size distribution of SP grains, FD should generally correlate with SP abundance, and in this study, as well as studies from Chinese loess deposits, FD values are always much higher in soils compared with less-weathered loess, reflecting abundant

pedogenic material (Thompson and Maher, 1992).

The relative variations in the amount of SD and PSD grains can be approximated by normalizing the ARM values with SIRM values to obtain ARM/SIRM. This ratio shows a sharp increase in the Gilman Canyon Formation and the modern/Brady soil, confirming a previous study (Hus and Han, 1992) which found that not only SP grains but also SD and PSD grains are relatively common in these soils. But considering that the ARM acquired per unit field is approximately five times more effective than SIRM (Hunt *et al.*, 1995), and that normalized ARM/SIRM values are only 1-2 percent, the observed two- to three-fold increase in ARM/SIRM corresponds to only a small increase in the proportion of SD and PSD grains in the soil layers.

Figure 5.5 shows the biparametric plots of FD values (percent) and ARM (normalized to SIRM) data obtained from the Eustis ash pit; also shown are published data for synthetic magnetites of controlled grain sizes (Maher(1986)'s data was obtained from a Bartington at the same frequencies). The ARM/SIRM values for the soils vary within the range occupied by those of synthetic grains of SD size or finer. Their FD values are closely correlated with synthetics in the size range ~20 nm. Hence, these data identify distinctive grain-size contrasts between the Peoria loess and soil layers. The soil horizons are characterized by the presence of ultrafine-grained magnetic minerals of SD and SP size, whereas the Peoria loess layers contain little SD and a small amount of SP minerals.

Variation in SIRM also represents changes in absolute MD content. This parameter also shows some increase in the Gilman Canyon Formation and modern/Brady soil. Similar variations in SIRM were also observed at Xifeng in the central Loess Plateau (Liu *et al.*, 1992) and at Xining, in the western Loess Plateau of China (Hunt *et al.*, 1995). It appears that paleosols formed during the warmer interglacial and interstadial periods contain not only an excess of the very small grains that dominate the FD values signal, but also the intermediate grains that carry ARM and the largest grains that carry SIRM.

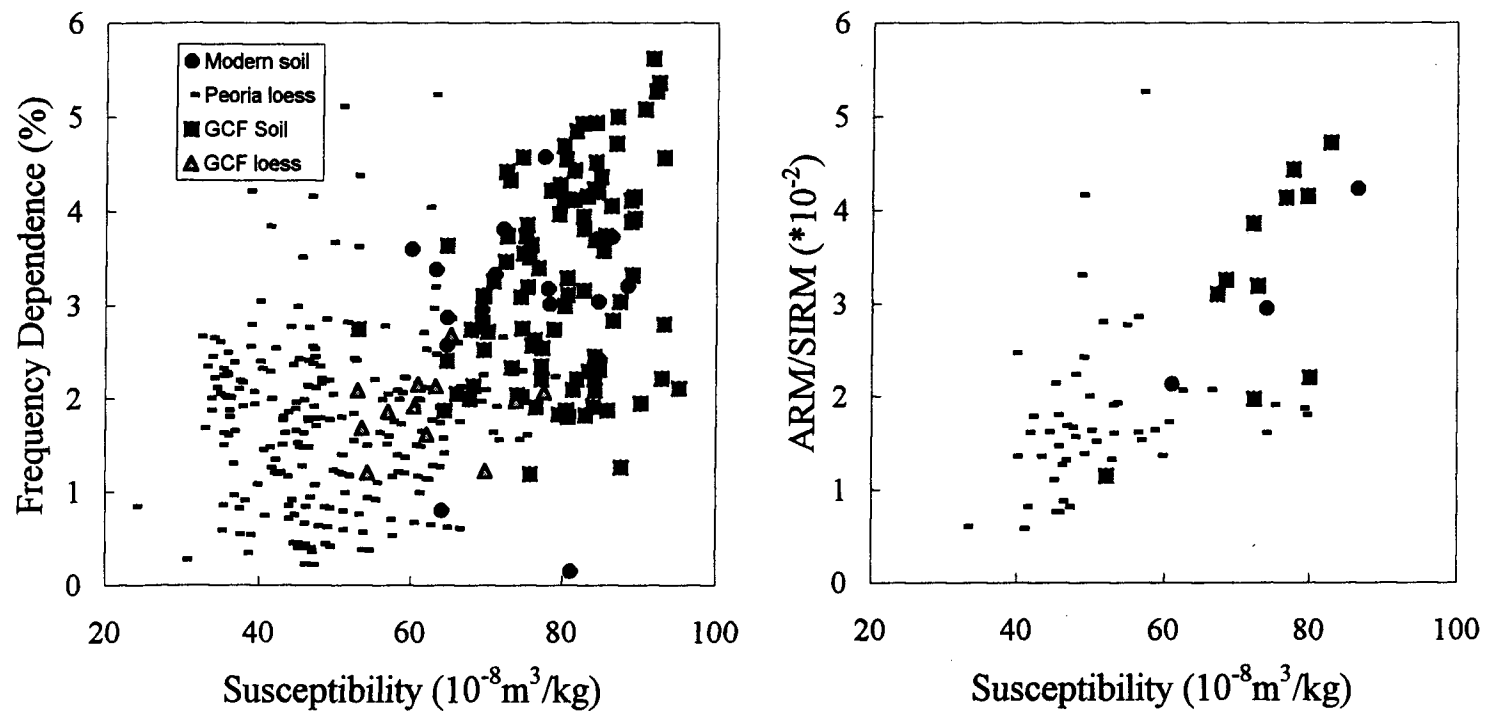


Figure 5.5. Biparametric plots of MS versus FD and MS versus the ratio ARM/SIRM for the samples from the Eustis ash pit.

Many studies have shown that variations in ferrimagnetic grain size and domain structure have an important influence on the range of the magnetic parameters that have been measured. Maher (1988) has demonstrated that two normalized properties, FD values and ARM/SIRM, are especially responsive to variations in magnetic grain size in dispersed very fine-grained synthetic magnetite samples with grain-interaction characteristics comparable to those in natural samples. Although based on simple assemblages of synthetic magnetite, her observations are consistent with a wide range of data from natural samples which include more complex mineral assemblages (Maher and Taylor, 1988).

In order to compare our results with previous studies, MS and FD values were first measured. About a quarter of all samples were then given an ARM in a peak alternating field of 90 mT and a steady field of 0.05 mT using a modified Schonstedt alternating demagnetizer. Mass specific SIRM values varied in the range of 2.0-6.0  $10^{-3}$  Am<sup>2</sup>/kg, with the lowest values in the loess layers and the highest in the Gilman Canyon and modern/Brady soil layers (Figure 5.2. b & c). ARM values varied in the range of 2-20  $10^{-6}$  Am<sup>2</sup>/kg, again with the lowest values in the Peoria loess and the highest in the soil.

If the MS signal were purely the result of dilution of a uniform source material as predicted by the magnetite-rain model (Kukla, 1987), then normalized MS should be invariant with depth. Because it is not, there is some difference in magnetic mineralogy and/or grain size between the loess and the soils.

### *Magnetic mineralogy*

Direct identification of magnetic mineralogy necessitated extraction and concentration of the magnetic phase. Magnetic mineralogy can be obtained from analysis of Mössbauer spectra, the temperature dependence of MS, and low-temperature remanence transition data. In mixed magnetite-hematite assemblages, the proportion of the magnetization acquired in high fields ( $IRM_{0.3T}/IRM_{1.1T}$ ) has been known to be

directly related to the hematite concentration.

The parameters of IRM acquisition ( $IRM_{0.3T}/IRM_{1.1T}$ ) vary little, if any, from 90 to 97 percent (Figure 5.2. f) in both the soils and the Peoria loess. Higher ratios indicate a very small proportion of antiferromagnetic hematite, which only acquire magnetic remanence at high applied fields. Therefore, this study indicates that the magnetic properties of these samples are dominated by ferrimagnetic (*e.g.*, magnetite/maghemite-type) behavior and that variations between the samples in the relative importance of imperfect anti-ferromagnets (*e.g.*, hematite) will not alone account for the large differences in rock magnetic properties encountered.

The interpretation of ferromagnetic mineralogy can be improved by stepwise thermal demagnetization of the acquired IRM (Heller, 1979). M. R. Farr used the SIRM demagnetization technique of Lowrie (1990) on selected samples (Figure 5.6). Three different IRMs are imparted to specimens along three mutually perpendicular directions, each direction essentially corresponding to a different coercivity spectrum. In both loess and soil specimens analyzed so far, thermal demagnetization of soft (<0.12T), medium (0.15-0.2 T) and hard (0.2-1 T) coercivity fractions is removed at between 550° and 600°C. The Curie temperature of pure magnetite is 575°C, and therefore these samples appear to be dominated by low-Ti magnetite (Farr *et al.*, 1993). In a few samples, the high coercivity remanence persists beyond 600°C, indicating the presence of a very minor amount of hematite. Also, in a few samples, the low and intermediate coercivity fraction curves show a downward inflection between 300° and 450°C, indicating the likely conversion of a small amount of maghemite to hematite. No samples analyzed thus far appear to contain a large concentration of maghemite (Farr, unpublished data).

Taken together, these results point to the presence of magnetite and little, if any, maghemite and hematite in the loess/soil sequence. This is in contrast to the those studies that claim to have found either only maghemite (Eyre and Shaw, 1994) or only magnetite (Evans and Heller, 1994) in the most mature soils in China.

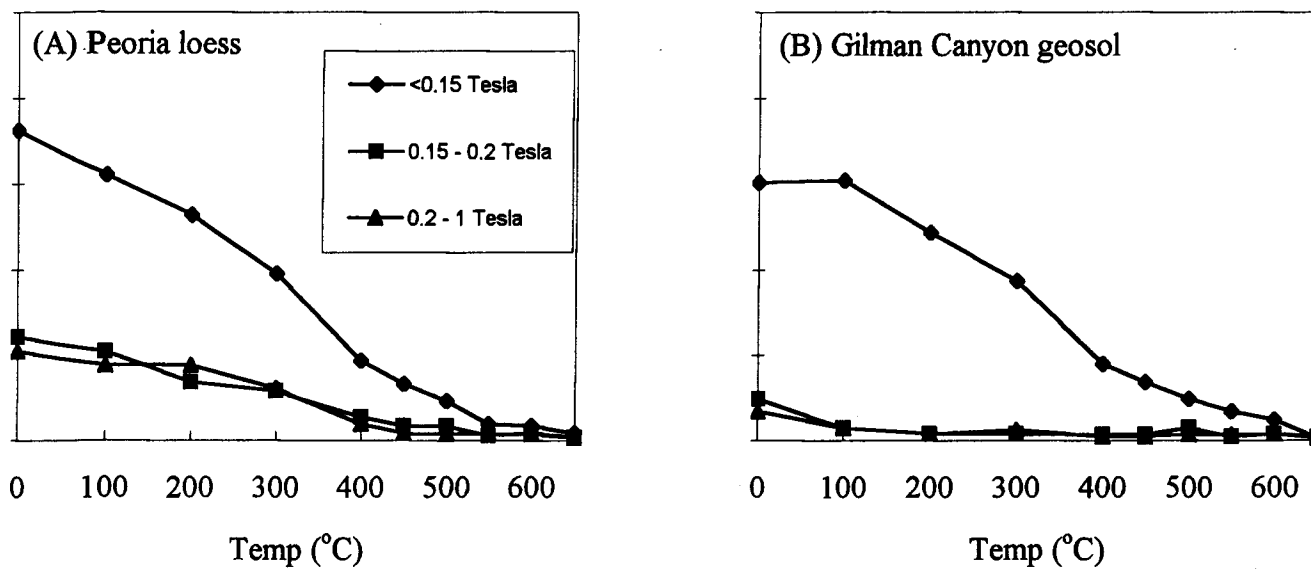


Figure 5.6. Thermal demagnetization of the soft, medium and hard coercivity fractions. (A) Data for Peoria loess sample. (B) Data for Gilman Canyon Formation soil.

### Comparisons with Other Climatic Proxies

In many different settings, the abundance, types, and magnetic grain sizes of magnetic minerals incorporated in sediments have varied in response to changes in climate. The influence of climate change on magnetic-mineral records is demonstrated by comparing magnetic parameters to geochemical and biological proxies for climate, as well as by spectral analysis of magnetic-property records that establishes a correlation with orbitally driven climate cycles (Rosenbaum *et al.*, 1996). Such comparisons between magnetic properties and more direct climate indicators are essential, because factors other than climate can strongly influence the flux of magnetic minerals into loess deposits. Examples include volcanism and changes in source area (Oldfield, 1991; Rolph *et al.*, 1993 )

$\delta^{13}\text{C}$  values from unaltered Gilman Canyon loess indicate a dominance of  $\text{C}_3$  plants, indicative of cool, moist conditions.  $\delta^{13}\text{C}$  values from the Gilman Canyon soil at the Eustis ash pit show  $\text{C}_4$  type plants (values of *c.*  $-17\text{‰}$ ) dominating at the time of the unit's formation, implying a warmer, drier climate (Figure 5.7; 5.8). This  $\text{C}_4$  landscape is comparable to the signal from the modern soil, suggesting a climate similar to that which prevails today. The  $\text{C}_4$  signal is strongest during mid-Gilman Canyon time, while late Gilman Canyon time is characterized by trends toward a  $\text{C}_3$ -dominated landscape, implying cooler, moister conditions after formation of the Gilman Canyon soil. Consistent with the findings of others (May and Souders 1988; Johnson 1993a), isotopic analysis results from Eustis also show a bimodal peak in the Gilman Canyon soil.  $\delta^{13}\text{C}$  results from the Peoria loess are in good agreement with the findings of others using  $\delta^{13}\text{C}$  for unweathered loess (Krishnamurthy *et al.* 1982; Johnson 1993a). The values tend strongly toward  $\text{C}_3$  plants ( $-25\text{‰}$ ) above the Gilman Canyon soil, indicating a moist, cool environment at the time of deposition. The  $\text{C}_3$  signal continues upward through the entire profile at the Eustis ash pit until organic matter translocated downward from the

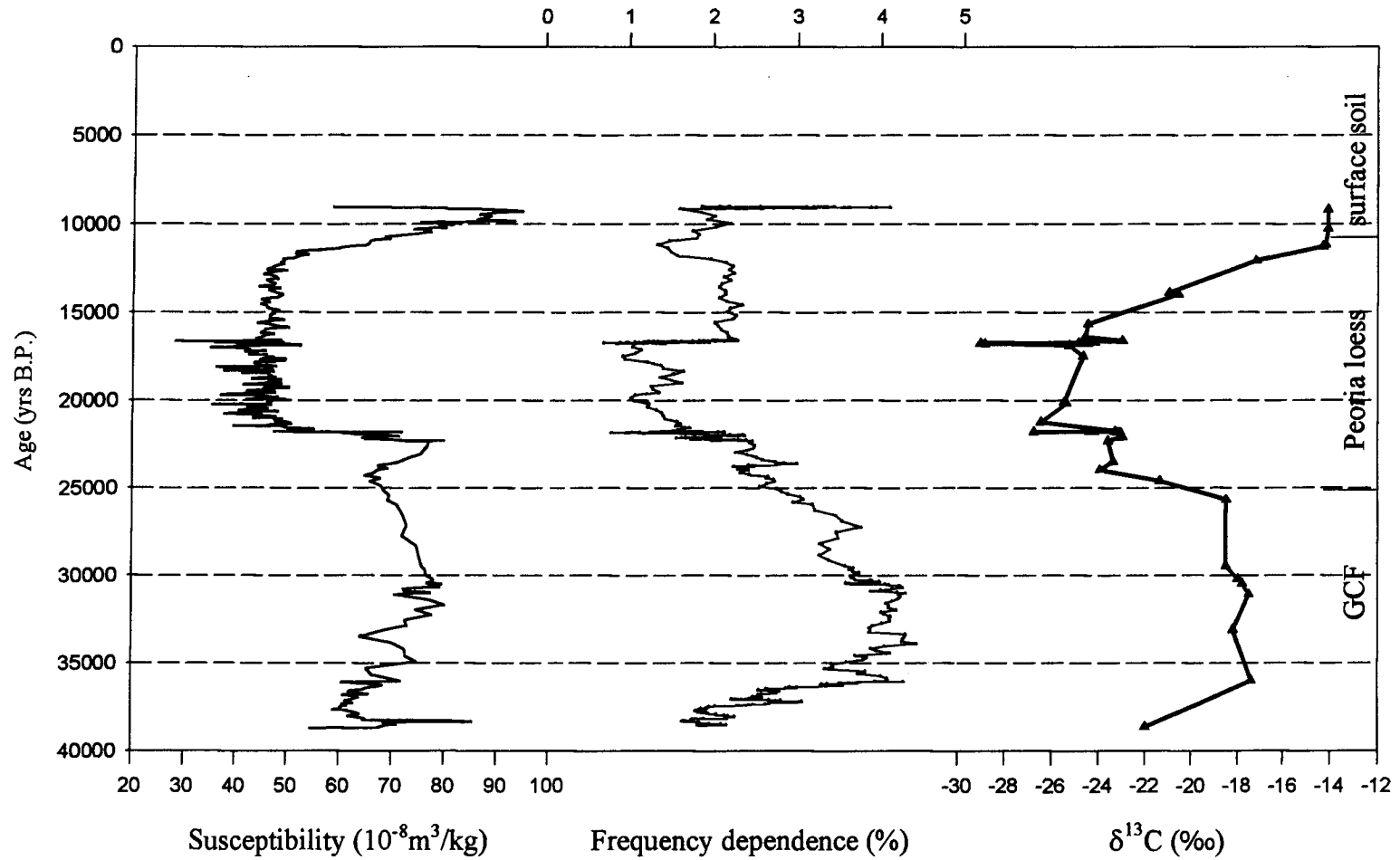


Figure 5.7. MS, FD, and  $\delta^{13}\text{C}$  data for the profile sampled at the Eustis ash pit. Ages were determined from  $^{23}\text{C}$  ages from total humates and extrapolated.

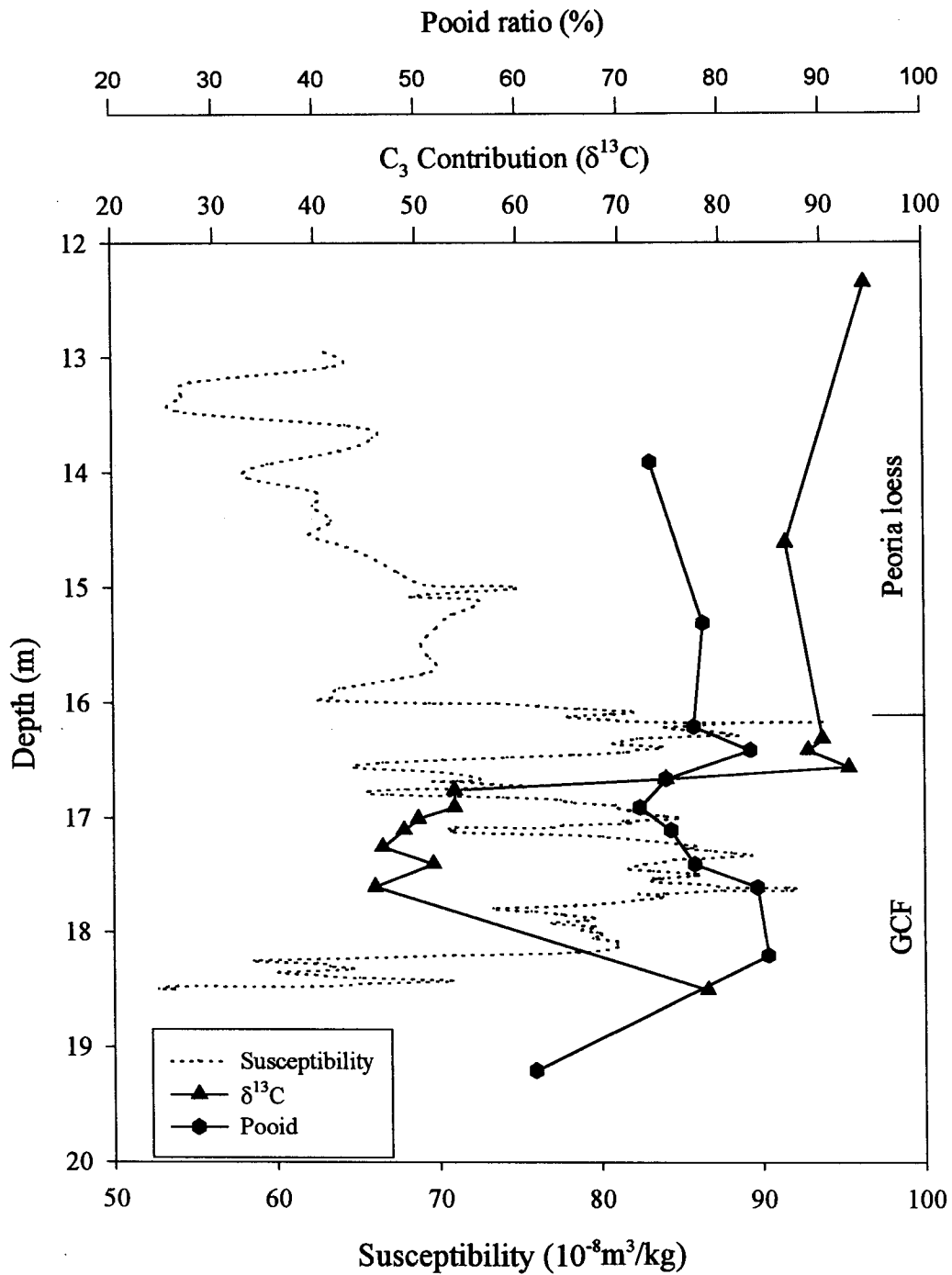


Figure 5.8. MS, δ<sup>13</sup>C data and Pooid concentration for the Gilman Canyon Formation at the Eustis ash pit.

Brady/modern soil is encountered at about 1.5 meters below the surface. At this point in the section, Peoria loess comes under the influence of C<sub>4</sub> plants dominating the modern surface.

Within the Gilman Canyon soil,  $\delta^{13}\text{C}$  data indicate that a warm and, dry climate in which short grasses dominate (Fredlund and Johnson, 1985; Figure 5.7, 5.8). C<sub>3</sub>-plant contribution obtained from the Mass balance formula during the period is about 40 per cent. Despite poor sampling resolution, phytolith data indicate higher percentage of C<sub>3</sub>-type Pooideae (*ca.* 70 per cent) compared to stable isotopic data, but lower than overlying Peoria loess.

There are two important differences between the magnetic and stable isotopic records. First, the two records are partly offset with respect to time as shown in 5.7, suggesting that pedogenesis factors and plant cover might respond to changes in climate over slightly different time frames, since both parameters have different mean residence times within the soil system. Or, offset might have resulted from measurement error between two different sampling dates. Since magnetic samples and isotopic samples are taken during different field seasons and both samples came from three composite sections rather than one large exposure, there may exist an inappropriate stratigraphic match. One recent finding from the region exhibits the synchronicity between the magnetic parameters and  $\delta^{13}\text{C}$  measurements, which favors the faulty stratigraphic match. The effects of environmental changes on the magnetic parameters have been investigated by examining the relationship between various magnetic parameters and  $\delta^{13}\text{C}$ . The correlations of ARM and  $\delta^{13}\text{C}$  at the Eustis ash pit are moderately significant. The correlations of MS and  $\delta^{13}\text{C}$  are also highly significant.

The relatively strong correlation between MS and stable carbon isotope from the site indicates a strong link between climate variation and those processes that generate the magnetic signal. This linkage is also supported by the synchrony of the variation in magnetic properties and northern hemisphere climate change as shown in Figure 5.3.

An *et al.* (1991) have suggested that, whereas MS can serve as a proxy for precipitation (summer monsoon intensity), the median grain size of loess and soils primarily reflects variations in the strength of winter winds. The median particle size variation from the Eustis ash pit was compared with MS variation and loess accumulation data calculated using the limited number of  $^{14}\text{C}$  dates from the site. The particle size data set was adopted from a previous study (Diekmeyer, 1994). First of all, a clear inverse relation was found between the variations of MS and median grain size. Weaker magnetic susceptibilities within the Peoria loess are clearly shown in Figure 5.4, which also shows that the depositional rate was much faster during that period than that of the Brady time and underlying Gilman Canyon times. Loess began to accumulate about ten times faster at 22 ka, which synchronizes with the decrease in MS and the sudden increase in median grain size. During the Last Glacial Maximum, average MS intensities reach their minimum among the lower values ( $< 40 \times 10^{-8} \text{m}^3/\text{kg}$ ). Loess accumulation rate and median particle size also exhibit a peak during that time.

A number of Chinese loess/soil studies have used the median size parameter as a proxy for wind strength. However, a bulk sample of loess or soil includes not only primary eolian dust, but is also likely to include a component of post-depositional pedogenesis (Liu *et al.*, 1992; Verosub *et al.*, 1993). Alternatively, the median diameter of chemically isolated quartz fraction has been proposed as a more reliable measure of dust flux than the bulk particle size measure (Porter and An, 1995; Xiao *et al.*, 1995).

By examining ice-core data from Greenland, Paterson and Hammer (1987) recorded a dramatic decrease in atmospheric dust content from about 13 ka. This period of reduced atmospheric dust may relate to the time of relative surface stability and tree establishment which was concurrent with the 14 ka charcoal concentration within the Peoria loess in central and western Kansas (Wells, 1983), and 13.2 ka accretionary soil formation in the sand in the Sand Hills of Nebraska (Swinehart, 1990). Regional geomorphic data also support the existence of a depositional hiatus at about 14-13 ka

(May, 1989; Martin, 1990). MS starts to bounce back from its base level at about 13-12 ka, which is comparable to regional data within error limits associated with  $^{14}\text{C}$  dating.

### **Spectral Analysis**

MS, FD, ARM, and SIRM data between 0 and 18 m were analyzed using ARAND software (Howell, 1995) to determine periodicity in the record. An age model was constructed by applying the application "Ager," which linearly interpolates ages between each  $^{14}\text{C}$  age point. Time series using a time step of 10 years were constructed using the application "Timer." These results were analyzed using the autocovariance function of the "Spectral" application. The sampling interval was set at a time step of 10 years due to the software's limit of 5000 data points. Starting frequency was 0, and 101 frequencies were calculated. Lags of 120 and a confidence interval of 80 F was used based on the total number of samples.

At the Eustis ash pit, spectral analysis of magnetic records results in a dominant period of  $\approx 197$  years (Figure 5.9). Numerous data sets demonstrate the  $\approx 200$ -year cyclicity. For example, Anderson (1992) recognized connections between solar activity (from tree ring records) and surface winds (from varve thickness in Elk lake, Minnesota) that operated on a 200-year time scale during the mid-Holocene. Leventer *et al.* (1996) also observed an approximately 200-year cycle within a multi-proxy record from a sediment core from the western side of Antarctic peninsula and suggested that a global forcing mechanism, possibly solar variability, may be related to the 200-year cyclicity noted in other paleoclimatic records around the world.

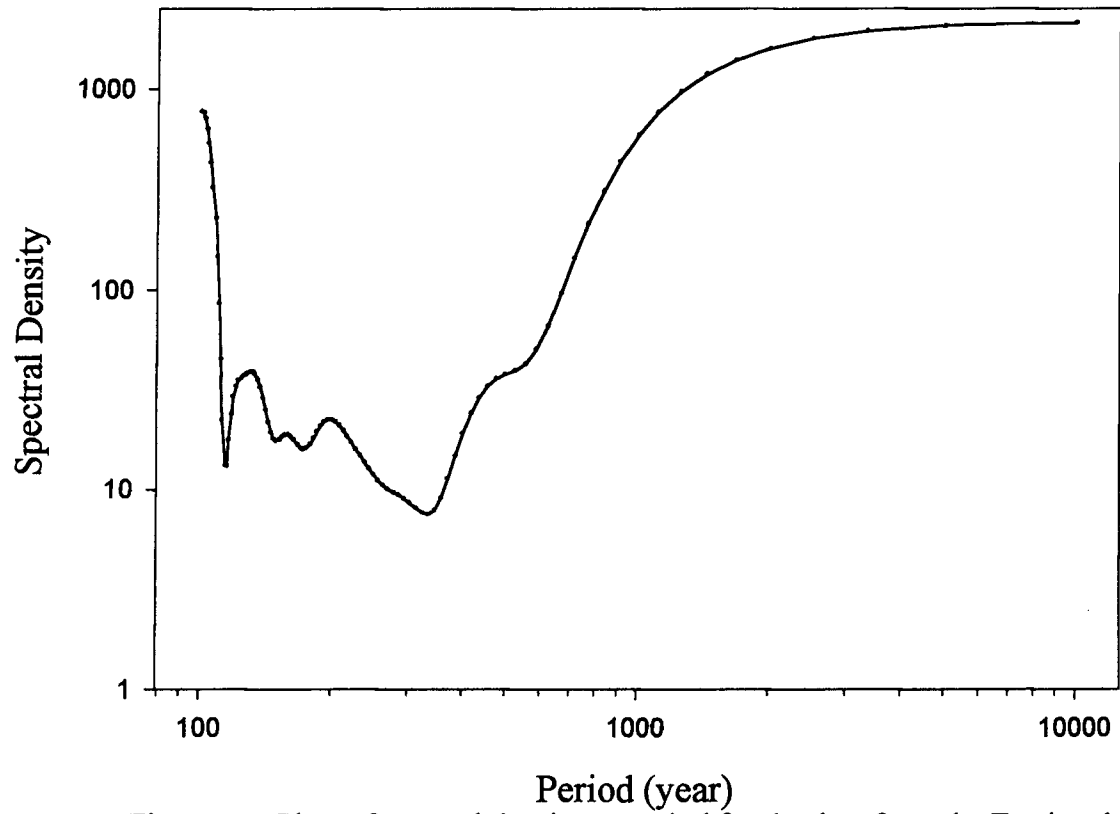


Figure 5.9. Plots of spectral density vs period for the data from the Eustis ash pit. MS, FD, ARM, and SIRM have been employed to compute the periodicity.

## SARGENT SITE

This site is one of the best expressions of the Pleistocene/Holocene boundary Brady soil (ca. 1.2 m thick) and Bignell loess (ca. 4.7 m) in the region (Figure 5.10). The Brady soil of the east exposure displays evidence of having formed under poorer drainage conditions than the associated surface soils, comparable to the Bignell Hill type locality (Frye and Leonard, 1951). The west exposure, however, displays no evidence of poor drainage. The bottom of the Brady exposure dates to 11 ka. Eleven  $^{14}\text{C}$  assays, associated  $\delta^{13}\text{C}$  data (Dort, unpublished manuscript), and high-resolution opal phytolith data (10 cm interval) are available from this site (Bozarth, unpublished manuscript).



Figure 5.10. Topographic map in the vicinity of Sargent site. Scale 1:24,000

### Rock Magnetic Records

Rock magnetic parameters were measured at two exposures from the site. The results of MS measurements at the Sargent site are presented in Figure 5.11 and FD measurements are shown in Figure 5.12.

#### *East exposure: Concentration*

The mass specific susceptibility values range from 60 to 85  $\times 10^{-8}\text{m}^3/\text{kg}$  and show the systematic differences between the Brady soil and incipient soils within the Bignell

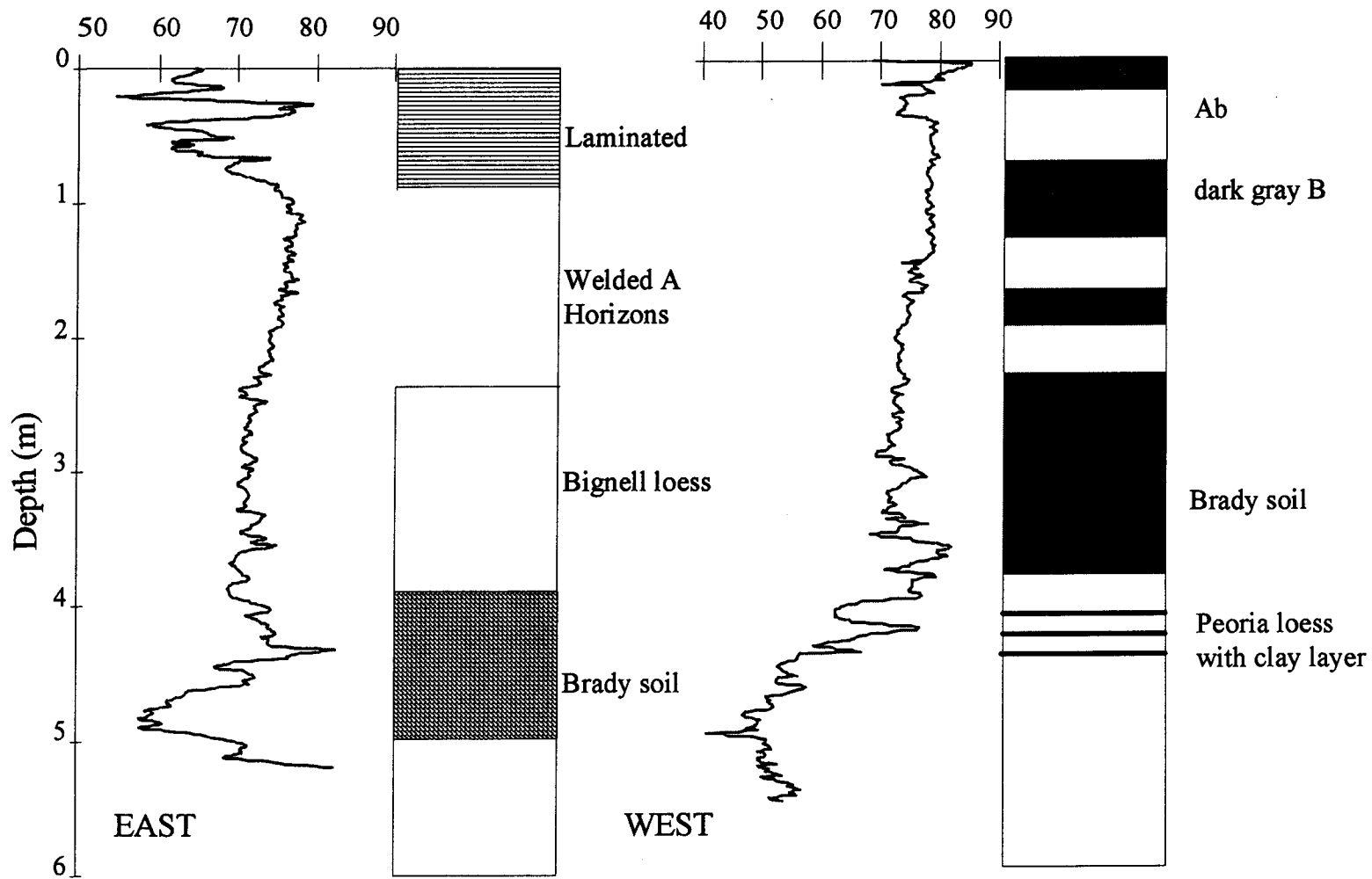


Figure 5.11. MS data and stratigraphy for the east and west profile sampled at the Sargent site.

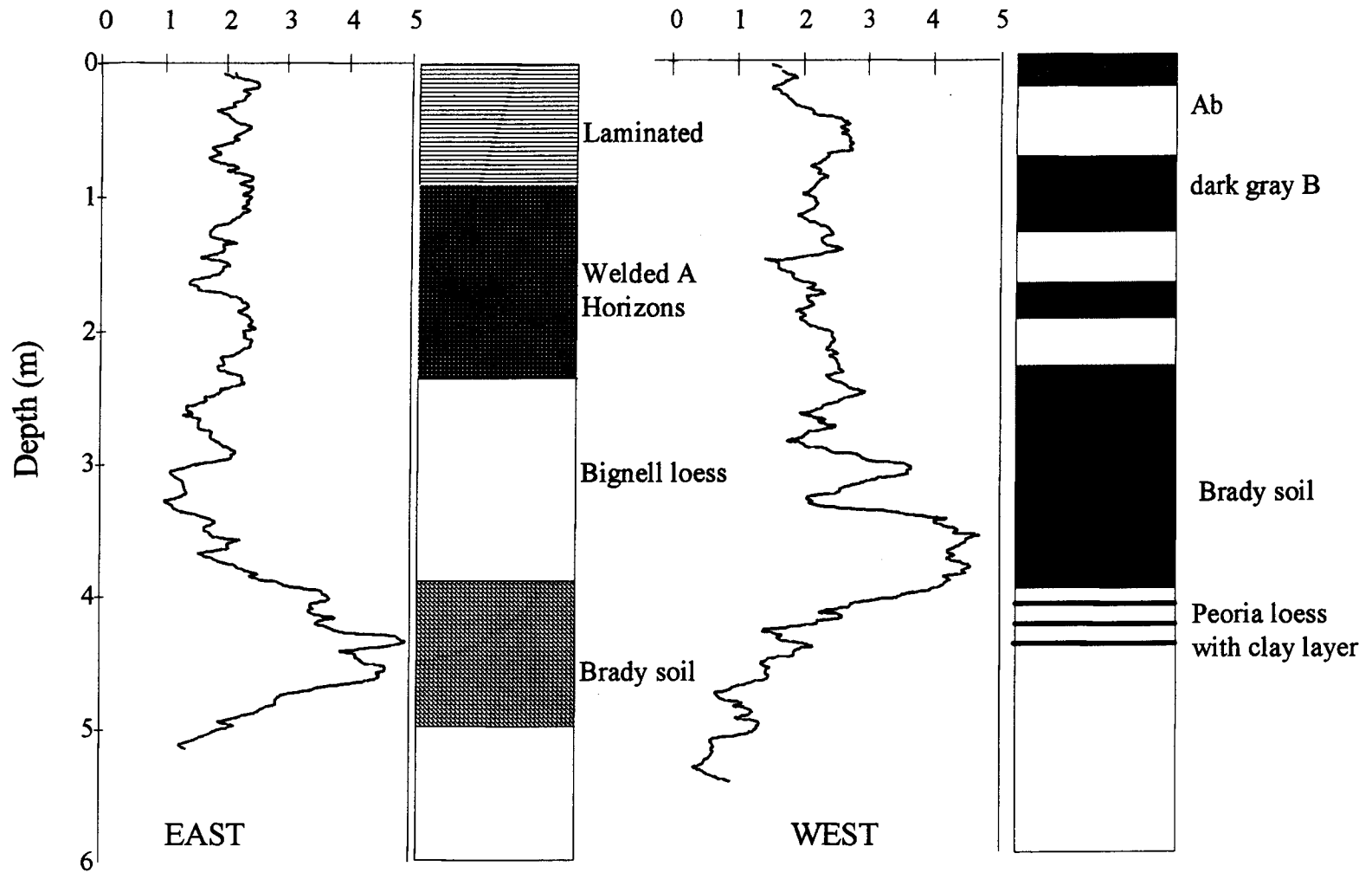


Figure 5.12. FD data and stratigraphy for the east and west profile sampled at the Sargent site.

loess (Figure 5.11). Various magnetic parameters are summarized in Table 5. 3.

Table 5.3 Descriptive statistics of magnetic parameters in the Sargent site, NE.

	No.	Minimum	Maximum	Mean	Std. dev.
ARM	114	7.21	21.82	10.68	2.33
FD	114	0.83	6.1	2.28	0.91
MS	114	58.45	82.59	71.6	4.87
SIRM	114	4.49	7.98	6.36	0.6
ARM/SIRM	114	1.08	3.41	1.7	0.41

The Peoria loess samples were taken from the very bottom of the accessible profile. At four meters below the surface, the Brady soil is distinctive in every aspect of rock magnetic parameters. MS intensity of the Brady soil is high ( $80 \times 10^{-8} \text{m}^3/\text{kg}$ ) and comparable to the modern/Brady soil from the Eustis ash pit. SIRM and ARM variations also exhibit the two- to three-fold increase within the Brady soil, which reflects the surface stability and enhanced pedogenesis during the Pleistocene/Holocene transition. Bignell loess above the Brady soil exhibits a drop in magnetic intensity, reflecting the increase of eolian activity during the Holocene. The Holocene eolian stratigraphic record in the central Great Plains occasionally contains well developed soils, and the magnetic signal from the site provides evidence of multiple buried soils (*e.g.*, Arbogast, 1995).

At one meter below the surface, MS and SIRMs exhibit a sudden drop while ARMs remain low throughout the profile (Figure 5.13.). Stratigraphically, a laminated unit is observed at this portion of the exposure. This trend is a unique one because most studies on Chinese loess report an increase in magnetic parameters within modern soil compared to loess. This may be a local phenomenon, perhaps caused by poor drainage within a closed upland basin (Schultz and Stout, 1948), or these magnetic parameters respond to regional climate variability which indicates the increased moisture at the end

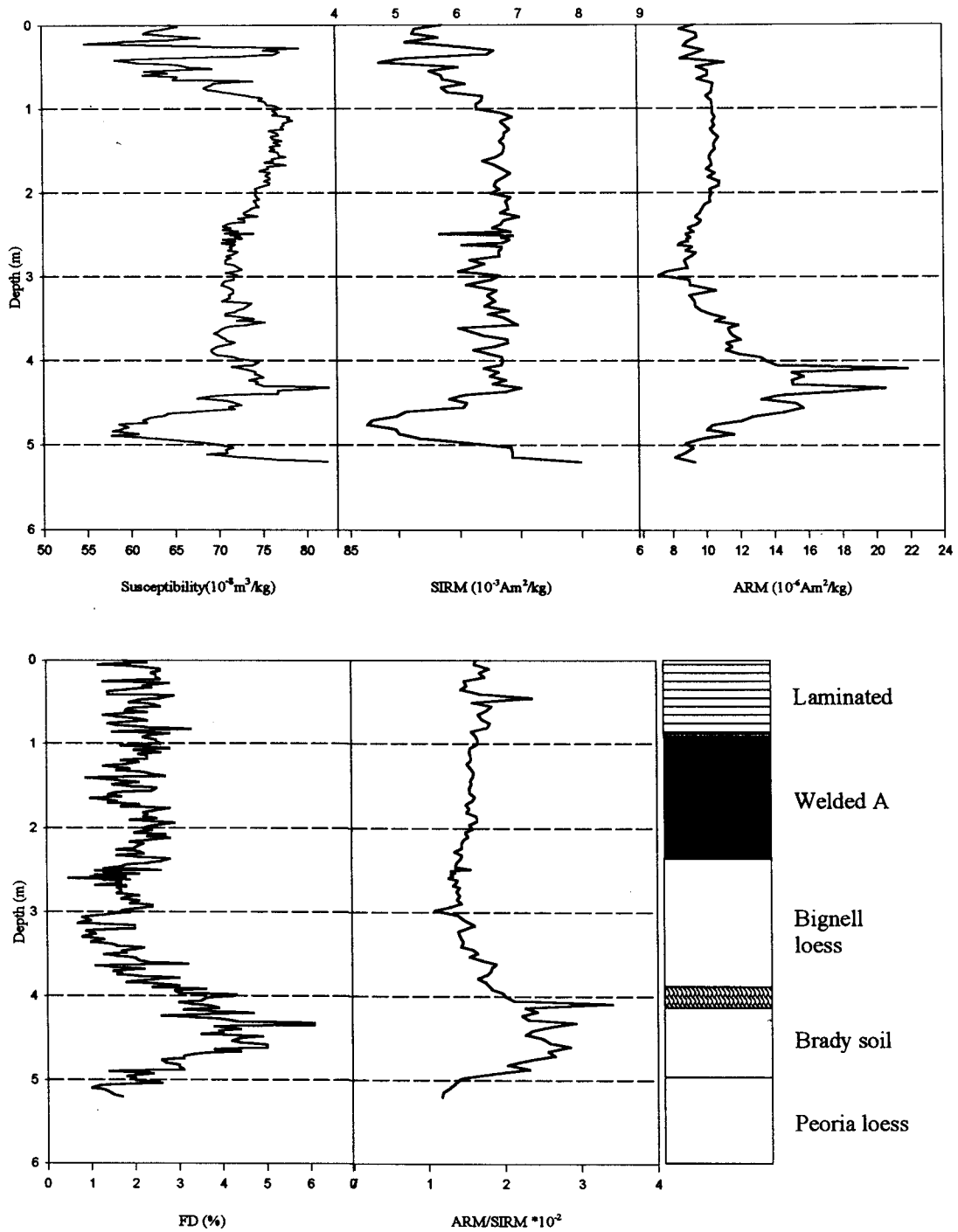


Figure 5.13. MS, SIRM, ARM, FD and ARM/SIRM data and stratigraphy for the east profile sampled at the Sargent site.

of the Holocene (Figure 5.11). Phytolith analysis in this profile also shows a drop in the phytolith index, reflecting a significant increase in Panicoids within this zone, which indicates an increase in available moisture during this depositional period (Figure 5.14: Bozarth, 1992).

#### *Magnetic grain size*

The FD data shows the presence of a significant amount of SP material only in the Brady soil. Overall, theory predicts a maximum value for the FD percentage of 14-17 percent in assemblages of spherical ferrimagnetic grains lying between 0  $\mu\text{m}$  and the SP/SD boundary (Dearing *et al.*, 1996). FD values range from 2-6 percent throughout the profile, which is very low compared to published data from China. However, considering that samples with an FD percentage >6 percent are dominated by frequency-dependent grains (Dearing *et al.*, 1996), the Brady soil at the bottom of profile is enriched with a significant amount of fine material.

Biplots of MS vs FD and  $\chi_{\text{ARM}}$ /SIRM vs FD (Figure 5.15; Maher and Taylor, 1988) also clearly differentiate three stratigraphic units. The Brady soil is enriched with higher MS, FD and  $\chi_{\text{ARM}}$ /SIRM values. Compared with the published data (Maher and Taylor, 1988) from synthetic magnetite, the Brady soil seems to have a higher proportion of single domain and pseudo single domain minerals (0.03 to 0.06  $\mu\text{m}$ ).

#### *West exposure: Concentration*

MS and FD were measured at the exposure approximately 100m west of the other exposure (Figure 5.11 and Figure 5.12). This exposure seems to have better drainage conditions than the other and does not exhibit any laminated horizons. MS and FD exhibit larger variations than in the east exposure. The lower 1.5 m of the exposure exhibits low MS (c.  $40 \times 10^{-8} \text{m}^3/\text{kg}$ ) and almost zero FD, which are characteristics of the typical Peoria loess from the region.

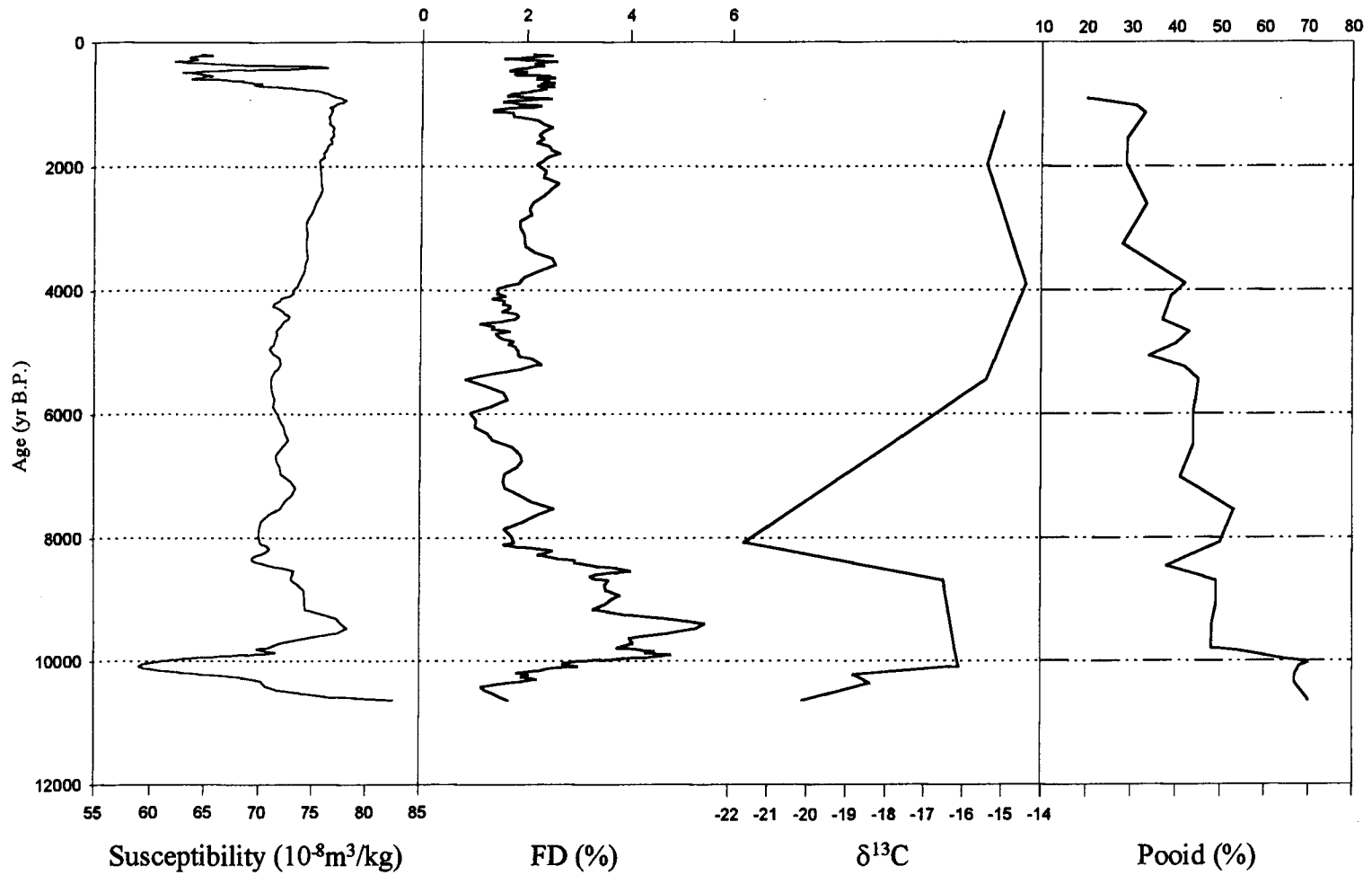


Figure 5.14. MS, FD and  $\delta^{13}\text{C}$  data (heavier to right) and Pooidae content (%) (% scale; colder to right) for the east profile sampled at the Sargent site.

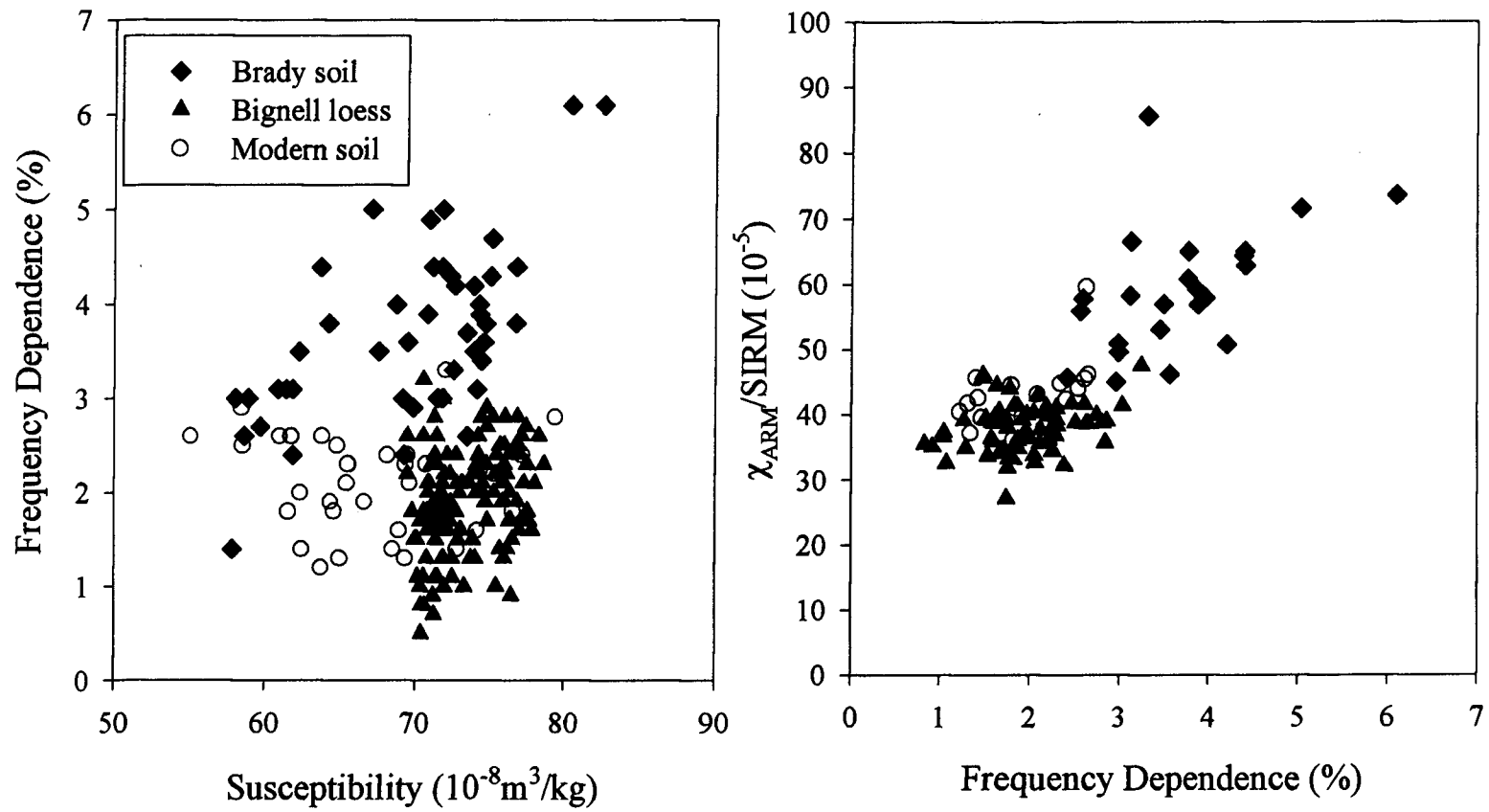


Figure 5.15. Biparametric plots of MS versus FD and the FD vs the ratio,  $\chi_{\text{ARM}}/\text{SIRM}$  for the samples from the east profile at the Sargent site.

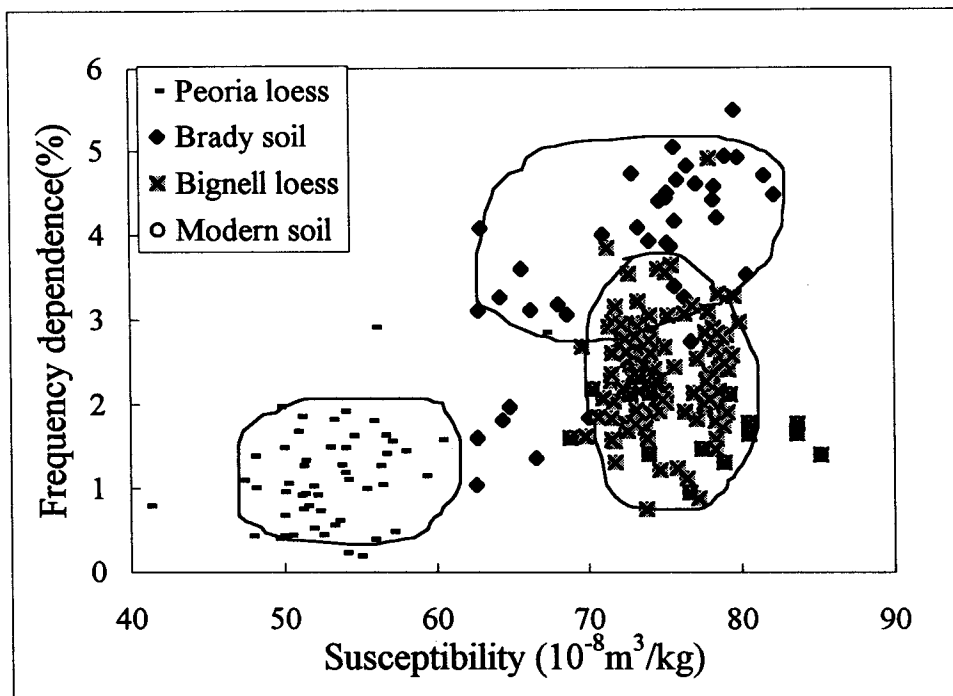


Figure 5.16. Biparametric plots of MS versus FD for the samples from the west profile at the Sargent site.

The Brady soil is revealed in both magnetic parameters; MS values range from 70-80 x 10<sup>-8</sup> m<sup>3</sup>/kg, and FD values are around 5 percent. MS and FD values are comparable to the surface soil from the Eustis ash pit and the Brady soil of the other sites from the region. The Bignell loess exhibits little variation in MS values from the Brady soil; however, FD variations are clearly different from the underlying Brady soil, as is shown in Figure 5.12. MS and FD values show little variation throughout the profile until the upper 1m exhibits a sudden drop in both parameters even though the west profile does not exhibit any apparent sign of poor drainage. As discussed earlier, both profiles exhibit a similar trend at the top of the exposures, which might indicate a change in regional climate conditions which will be discussed in detail.

The FD data shows the presence of significant amount of SP material only in the Brady soil. FD values range from 0-5 percent throughout the profile, which is very low compared to published data from China. However, considering that samples with a FD percentage >6 percent are dominated by frequency-dependent grains (Dearing *et al.*, 1996), the Brady soil at the bottom of the profile is enriched with a significant amount of fine material.

Biplots of MS vs FD also clearly differentiate three stratigraphic units (Figure 5.16). The Bignell loess and surface soil cannot be differentiated by this plot alone. Once again, the Peoria loess is depleted of finer grains. The Brady soil is enriched with higher MS and FD. According to this plot, the Brady soil seems to have a higher proportion of frequency-dependent grains.

### **Comparisons with Other Proxies**

$\delta^{13}\text{C}$  values from the Brady soil indicate a dominance of C<sub>4</sub> plants, indicative of warm, dry conditions. This C<sub>4</sub> landscape is comparable to the signal from the modern soil and Gilman Canyon Formation from the Eustis ash pit, suggesting a climate similar to that which prevails today. Unfortunately,  $\delta^{13}\text{C}$  results from the true Peoria loess are

unavailable, but the existing data indicate a trend toward an isotopically heavier environment from the top of the Peoria loess (Figure 5.14). Data from the top of the profile are also unavailable to this point, and a new field session has been planned for the summer of 1997 which could provide a more consistent and longer period of data. The one value above the Brady tends strongly toward C<sub>3</sub> plants (-22 ‰) indicating a moist, cool environment at the time of deposition. Interestingly, a phytolith index of Diester-Haass *et al.* (1973) does not exhibit any trend toward a wetter environment. Magnetic indices also do not show any abnormal values at the time of sedimentation (Figure 5.14). With the exception of one outlier, the C<sub>4</sub> signal continues upward through the entire profile at the Sargent site until the point where sampling ended.

Analysis of the fossil phytoliths indicates that a deciduous forest or open woodland was growing at the site at 11 ka (Bozarth, 1992). Vegetation appears to have shifted from deciduous forest or open woodland to parkland or savanna at about 10,400 years B.P. By 10,080 years B.P. the site was covered with a pooid dominated grassland. During the terminal Pleistocene, the climate was relatively cool and moist. At about 10 ka, there is a sudden increase in the phytolith index, reflecting an increase in Chloridoid grasses, indicating warmer and drier conditions. This appears to signal the start of the Holocene. The temperature continued to rise fairly rapidly with associated aridity until ca. 8,600 yrs B.P. Conditions continued to become warmer and more arid, but at a much slower rate, until about 3,800 yrs B.P. At this time, there appears to have been a slight increase in available moisture as evidenced by an increase in Panicoid phytoliths which continues to at least 1,000 yrs B.P. (the corresponding date of the uppermost sample collected). However, magnetic parameters exhibit a continuous increase up to 1000 yrs B.P. Again there is slight offset between the biological indices and magnetic parameters, which could be the result of either stratigraphical matching or the different response times of pedogenesis and plant cover.

One noticeable phase in the MS plot within the west profile is the decrease in MS

intensity near the top of the Holocene loess (Figure 5.11). The phytolith index also exhibits a clear trend toward a decrease (Figure 5.14). Without  $^{14}\text{C}$  age control, exact timing of this event cannot be determined at this point. However, Krishnamurty *et al.* (1995) reported a warm and dry period between 8500 and 2000 yrs B.P., followed by a cold period between 2000 and 1000 yrs B.P. from Austin Lake in Michigan. Humphrey and Ferring (1994) also observed a similar trend in north-central Texas.

There is very strong correlation between magnetic parameters, phytolith data, and stable carbon isotope from the site (Table 5.4), which again indicate a strong link between climate variation and weathering processes that generate the magnetic signal. There is also a synchrony between these parameters.

Magnetic parameter variations are also in general agreement with Pleistocene/Holocene climatic trends observed for other parts of the Great Plains (Figure 5.17). The fossil pollen record at Muscotah Marsh of in northeastern Kansas indicates that spruce had essentially disappeared from the region by about 10,500 yrs B.P. As this decline occurred, deciduous tree species increased until about 9,000 yrs B.P. Nordt *et al.* (1994) interpret the time between 11,000 and 8000 yrs B.P. as transitional between late Pleistocene conditions and the warmer, drier Holocene conditions, based on a slight increase in the abundance of  $\text{C}_4$  plant biomass in central Texas using stable carbon isotopic data.

Table 5.4 Correlation coefficients and significance level between the magnetic parameters,  $\delta^{13}\text{C}$  and phytolith index at the Sargent site.

	AI	ARM	ARM/SIRM	FD	$\delta^{13}\text{C}$	MS	Pooid	SIRM
AI	1.000	-0.373*	-0.569*	-0.549*	-0.649*	0.306	-0.494**	0.493**
ARM	-0.373*	1.000	0.886**	0.758**	-0.210	0.161	0.165	0.009
ARM/SIRM	-0.569**	0.886**	1.000	0.771**	-0.206	-0.241**	0.354*	-0.443**
FD	-0.549**	0.758**	0.771**	1.000	-0.295	-0.005	0.243	-0.185*
$\delta^{13}\text{C}$	-0.649*	0.210	0.207	0.295	1.000	-0.010	0.792**	0.163
MS	0.306	0.161	-0.241**	-0.005	0.010	1.000	-0.560**	0.851**
Pooid	-0.494**	0.165	0.354*	0.243	0.792*	-0.560**	1.000	-0.427*
SIRM	0.493**	0.009	-0.443**	-0.185*	0.163	0.851**	-0.427*	1.000
MS/SIRM	-0.601**	0.183	0.513**	0.334**	-0.279	-0.302**	0.232	-0.753**
AI								
ARM	0.030							
ARM/SIRM	0.000	0.000						
FD	0.001	0.000	0.000					
$\delta^{13}\text{C}$	0.042	0.561	0.567	0.408				
MS	0.079	0.087	0.010	0.957	0.978			
Pooid	0.003	0.350	0.040	0.166	0.006	0.001		
SIRM	0.003	0.922	0.000	0.049	0.654	0.000	0.012	

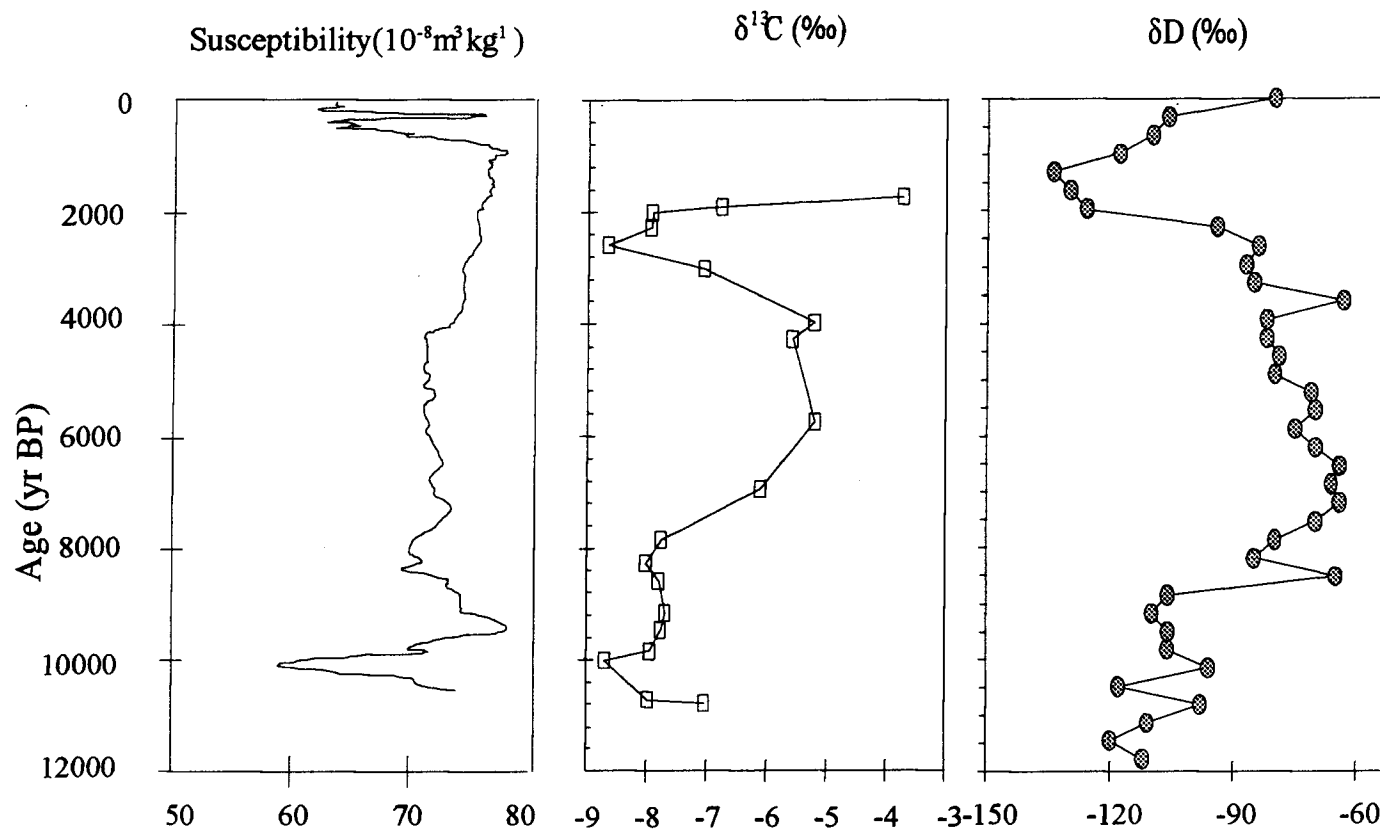


Figure 5.17. Variations in MS with ages in Sargent site compared with pedogenic carbon isotope data from north-central Texas and hydrogen isotope data from southwest Michigan (redrawn after Humphrey and Ferring, 1994 and Krishnamurthy et al., 1995).

## 14LV1071 SITE (DB site)

This site turned out to be one of the best exposure of the late-Quaternary stratigraphic record west of the Missouri River. Magnetic samples were collected from several archaeological test excavations which had been deepened by backhoe. Two profiles were selected for this study: one was taken directly from the face of test excavation 14LV1071, and another (14 m) was taken at the laboratory from the soil column taken by a Giddings drill machine. The stratigraphy of the excavation site consists of Peoria loess, Brady soil, Bignell loess, and modern soil. The core, extending to about 13 m, consists of a basal layer of Gilman Canyon Formation loess and soil, Peoria loess, Brady soil, Bignell loess and modern soil.

### **Core: Rock Magnetic Records**

There is no  $^{14}\text{C}$  age control available for the core; stratigraphic control is based solely on magnetic measurements. The results of rock magnetic measurements from the core site are summarized in Table 5.5. MS values range from 35 to  $101 \times 10^{-8}\text{m}^3/\text{kg}$  and exhibit the systematic differences between loess and soils. MS values of the supposedly Gilman Canyon soil (*c.*  $90 \times 10^{-8}\text{m}^3/\text{kg}$ ) are higher than those of the underlying unweathered Gilman Canyon loess (*c.*  $60\text{-}70 \times 10^{-8}\text{m}^3/\text{kg}$ ) and overlying Peoria loess (*c.*  $40 \times 10^{-8}\text{m}^3/\text{kg}$ ). Once again, bimodal peaks within the Gilman Canyon Formation are clearly shown in the MS-depth profile (Figure 5.18). Overlying the Gilman Canyon Formation lies the Peoria loess. MS values gradually decrease until they reach their minimum at 7 m below the surface. In the absence of  $^{14}\text{C}$  age control, it is hard to pinpoint at what point the MS values started to bounce back to the level of the Brady soil (1 m below the surface). However, comparisons to other MS profiles from the region reveal a striking resemblance.

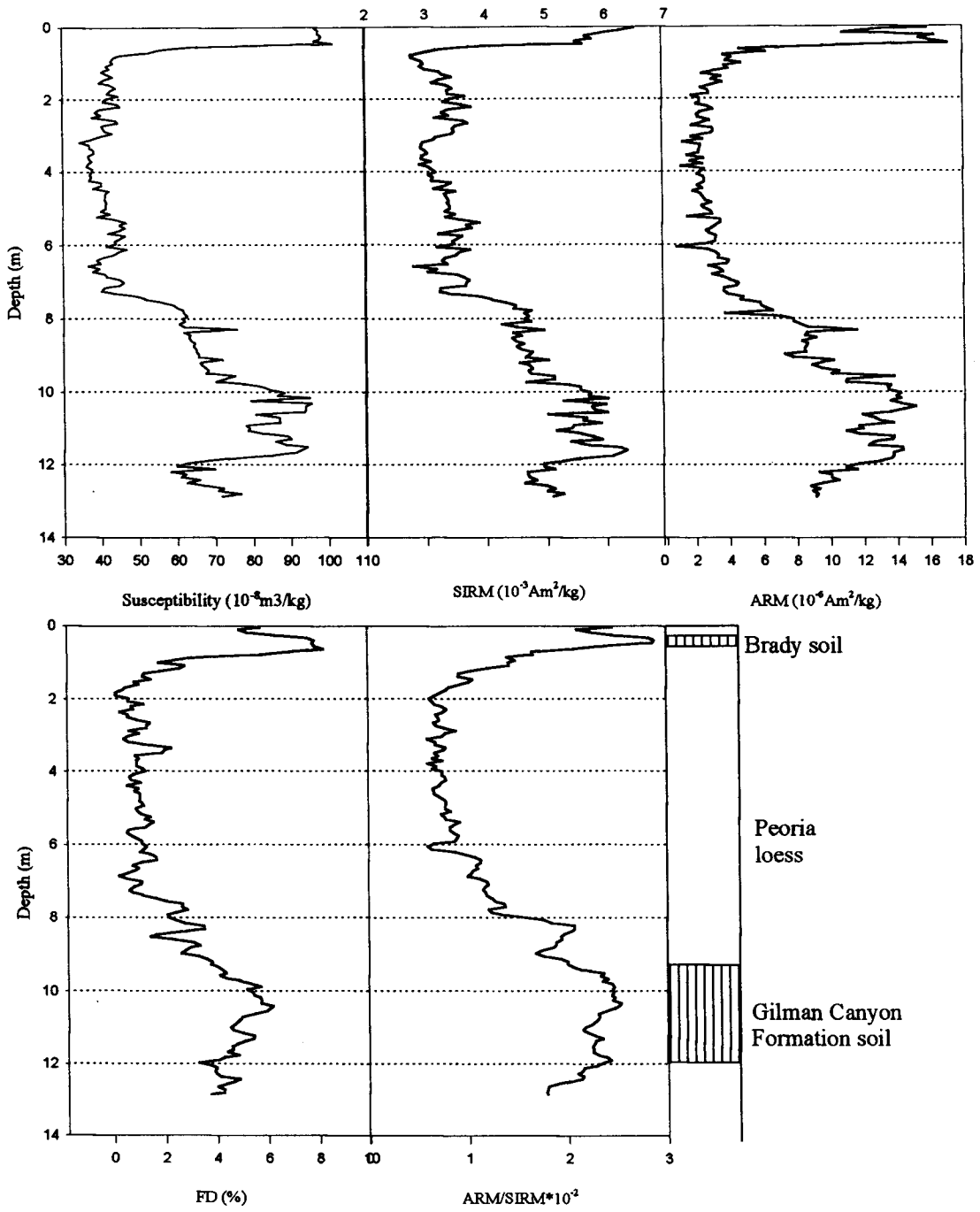


Figure 5.18. MS, SIRM, ARM, FD, and ARM/SIRM data and stratigraphy for the profile sampled at the 14LV1071 site (core).

Table 5.5. Descriptive statistics on various magnetic parameters from the DB site.

	No.	Minimum	Maximum	Mean	Std. dev.
ARM/SIRM	170	0.27	3.04	1.47	0.70
ARM	170	0.9	17.1	6.76	0.46
FD	170	0.00	8.55	2.71	2.13
MS	170	34.63	101.84	57.79	19.45
SIRM	170	2.76	6.49	4.18	1.04

ARMs and SIRMs were measured more systematically at this site than were the samples from the Eustis ash pit. SIRMs correlate well with the MS variations ( $r^2 = 0.968$ ) and are greater in the Gilman Canyon soil relative to the overlying Peoria loess by a factor of two (Figure 5.18). SIRM variations also exhibit bimodal peaks within the Gilman Canyon Formation. ARMs also correlate well with MS profiles ( $r^2 = 0.965$ ) and are more concentrated by a factor of eight compared to the overlying Peoria loess. It should be noted that ARMs are two orders smaller than SIRMs, so the absolute amounts of variation of ARMS between the stratigraphic units are quite small compared to SIRM variations. Bimodal peaks within the Gilman Canyon Formation are evident at the DB site, something not seen at the Eustis ash pit. The almost linear behavior of SIRM and ARM with MS (Table 5.6) suggests that MS may be controlled by ferrimagnetic concentration (Eyre and Shaw, 1994).

#### *Magnetic grain size*

The FD data obtained by the MS2B dual frequency bridge shows the presence of an ample amount of SP materials only in the two mature soils, Gilman Canyon soil and Brady soil. FD values range from 0 to 6 percent at the DB site. FDs from the Gilman Canyon soil (c. 6 percent) are higher than in the Peoria loess and underlying loess. These FD values seem to be quite low compared to Chinese loess, but are high enough to

Table 5.6 Correlation coefficients and significance level between the magnetic parameters at the 14LV1071 (DB) site.

	ARM/SIRM	FD	ARM	MS	SIRM
ARM/SIRM	1.000	0.858**	0.971**	0.901**	0.856**
FD	0.858**	1.000	0.841**	0.831**	0.735**
ARM	0.971**	0.841**	1.000	0.965**	0.943**
MS	0.901**	0.831**	0.965**	1.000	0.968**
SIRM	0.856**	0.735**	0.943**	0.968**	1.000
ARM/SIRM		0.000	0.000	0.000	0.000
FD	0.000		0.000	0.000	0.000
ARM	0.000	0.000		0.000	0.000
MS	0.000	0.000	0.000		0.000
SIRM	0.000	0.000	0.000	0.000	

\*\* Correlation is significant at the 0.01 level (2-tailed).

\* Correlation is significant at 0.05 level (2-tailed).

contain a significant amount of SP materials (Dearing *et al.*, 1996). FDs up to >11 percent have been observed in the loess/soil sequence at Xifeng, (Heller *et al.*, 1991), and FDs up to >15 percent are reported from Luochuan, China (Forster *et al.*, 1994).

The relative variations in the amount of SD and PSD grains can be approximated by normalizing ARM values with SIRM values to obtain ARM/SIRM. This ratio also shows a sharp increase in the Gilman Canyon Formation and Brady soil, confirming a previous study (Hus and Han, 1992) which found that not only SP grains but also SD and PSD grains are relatively common in these soils. But considering that the ARM acquired per unit field is approximately five times more effective than SIRM (Hunt *et al.*, 1995), and that normalized ARM/SIRM values are only 1-3 percent, the observed two- to three-fold increase in ARM/SIRM corresponds to only a small increase in the proportion of SD and PSD grains in the soil layers.

Figure 5.19 shows the biparametric plots of FD (percent) vs MS and ARM (normalized to SIRM) data obtained from the DB site; Figure 5.20 is published data for synthetic magnetites of controlled grain sizes (Maher, 1988). The ARM/SIRM values for the Gilman Canyon soil vary within the range occupied by those of synthetic grains of SD size or finer. Their FD values are closely correlated with synthetics in the size range ~20-30 nm. Hence, these data identify distinctive grain-size contrasts between the Peoria loess and soil layers. The soil horizons are characterized by the presence of ultrafine-grained magnetic minerals of SD and SP size, whereas the Peoria loess layers contain little SD and a small amount of SP minerals.

The variations in SIRM also represent changes in absolute MD content. This parameter again shows some increase in the Gilman Canyon Formation and modern/Brady soil. Similar variations in SIRM were also observed at Xifeng in the central Loess Plateau (Liu *et al.*, 1992) and at Xining, in the western Loess Plateau of China (Hunt *et al.*, 1995).

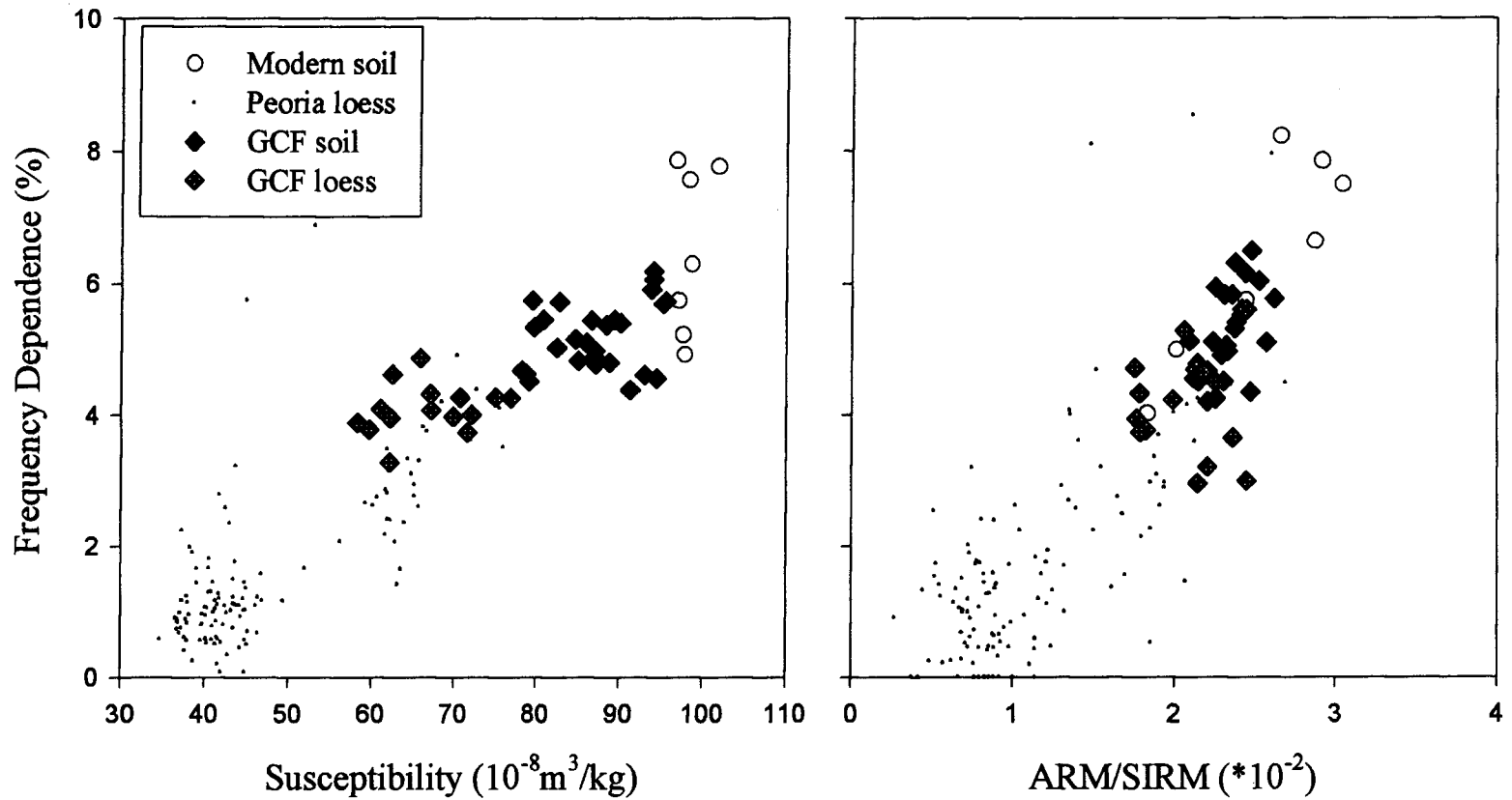


Figure 5. 19. Biparametric plots of MS versus FD and the ratio ARM/SIRM versus FD for the samples from the DB site.

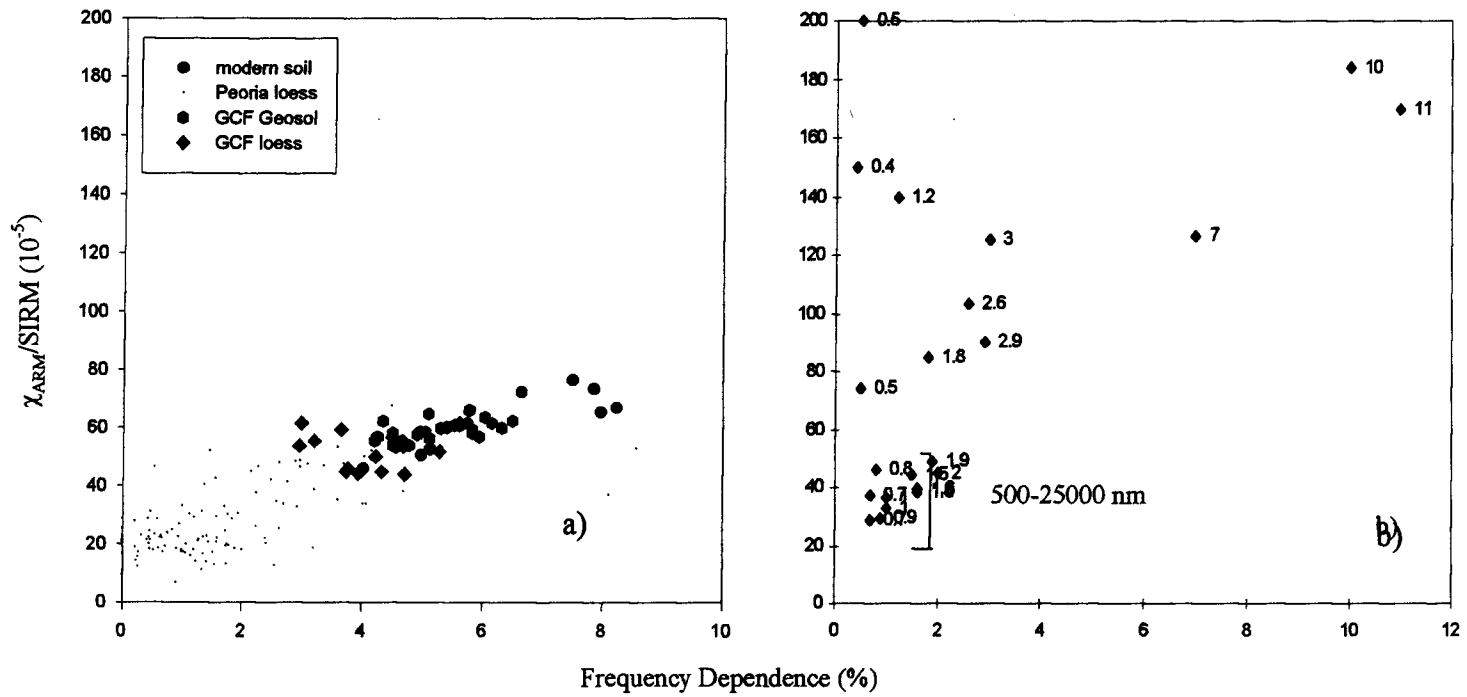


Figure 5. 20. Biprametric plots of a) frequency dependence versus  $\chi_{ARM}/SIRM$  for the samples for the DB site; b) frequency dependence versus  $\chi_{ARM}/SIRM$  for the synthetic samples (sizes in nm; Maher, 1988).

## Trench

The influence of climate change on magnetic records is demonstrated by comparing magnetic parameters to biological proxies from an archaeological excavation site (Figure 5.21). Phytolith counting data have been provided by S. Bozarth.

MS variations and FD variations are similar to core samples from the same area. MS and FD values from the Peoria loess ( $c. 40 \times 10^{-8} \text{m}^3/\text{kg}$ ;  $c. 1$  percent) are lower than in the overlying Brady soil and Bignell loess (Figure 5.21). Both parameters exhibit a sudden increase at top 1 m.  $\delta^{13}\text{C}$  values from the Peoria loess indicate a dominance of  $\text{C}_3$  plants, indicative of cool and moist conditions during the period.  $\delta^{13}\text{C}$  values are increasingly heavy toward the top of the profile, indicating the presence of more  $\text{C}_4$  plants toward the end of the Pleistocene. Both magnetic parameters and  $\delta^{13}\text{C}$  variations correlate well. MS and FD values start to exhibit the characteristic Brady signal at about 1.2 m below the surface. Simultaneously,  $\delta^{13}\text{C}$  values indicate more  $\text{C}_4$  plants at the end of the Peoria loess accumulation. Pooid ratio exceeds 80 percent within the Peoria loess but shows little change during the Brady time and Holocene. Correlation coefficients between the magnetic parameters and biological parameters are summarized in table 5.7. MS and FD values exhibit a very strong negative correlation with the pooid ratio and  $\text{C}_3$  plant ratios derived from the mass balance formula. If variations in  $\delta^{13}\text{C}$  of soil organic matter reflect the relative abundance of  $\text{C}_3$  and  $\text{C}_4$  grasses and summer temperature as recent research confirms (Fredlund and Tieszen, 1997; Tieszen *et al.*, 1997), magnetic parameters reflect temperature rather than moisture. The high percentage of panicoid indicates that moisture levels stayed relatively high. The decline in available moisture is pronounced at the top of the profile (Figure 5.21).

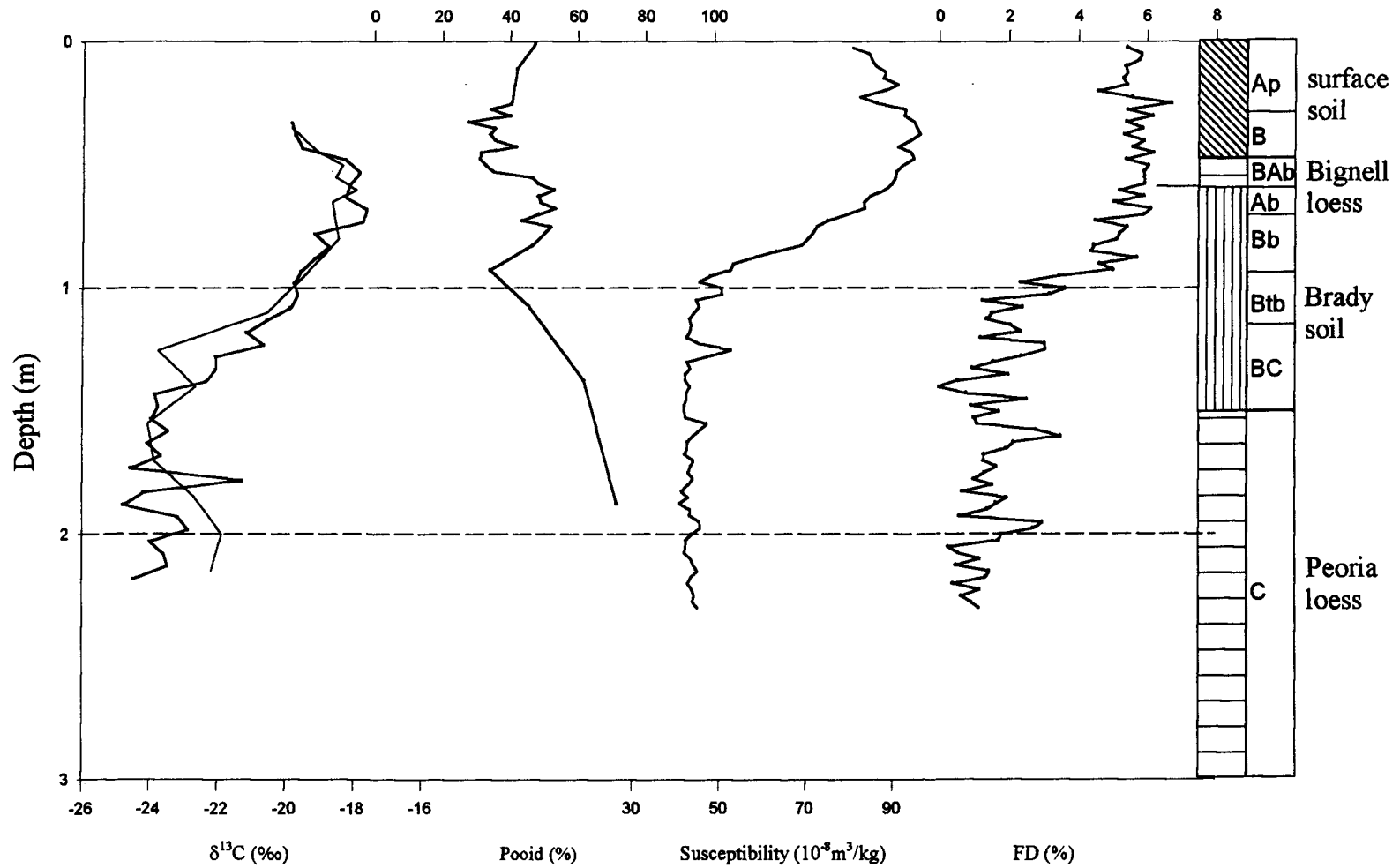


Figure 5.21.  $\delta^{13}\text{C}$  data from isotopic analysis (close interval) and  $^{14}\text{C}$  dating correction, pooid percentage, MS and FD with stratigraphy for the profile sampled at a trench in the 14LV1071 site.

Table 5.7. Correlation coefficient and significance level between the magnetic parameters and biological parameters at the 14LV1071 site.

	AI@	FD	$\delta^{13}\text{C}$	MS	Poid
AI	1.000	-0.257	0.048	-0.290	0.321
FD	-0.257	1.000	-0.846**	0.910**	-0.601**
$\delta^{13}\text{C}$	0.048	-0.846**	1.000	-0.769**	0.608*
MS	-0.290	0.910**	-0.769**	1.000	-0.647**
Poid	0.321	-0.601**	0.608*	-0.647**	1.000
AI					
FD	0.187				
$\delta^{13}\text{C}$	0.871	0.000			
MS	0.135	0.000	0.000		
Poid	0.096	0.001	0.021	0.000	

@AI = chloridoid/chloridoid+panicoid.

\*\* Correlation is significant at the 0.01 level (2-tailed).

\*. Correlation is significant at the 0.05 level (2-tailed).

## BEISEL-STEINLE SITE

Sediments and soils of late-Pleistocene and early-Holocene age are exposed in a roadcut along the valley wall of the Smoky Hill River about 5.8 km southeast of Dorrance, Russell County in central Kansas

(Figure 5.22). The upper stratigraphy at the site of interest to this study includes 1.6 m of Gilman Canyon soil, 1.1 m of Peoria loess, and 2.3 m of a Brady soil/modern soil complex. While Bignell loess may also be present, Gilman Canyon loess does not occur at the site. Pleistocene-age sediments rest on a strath terrace cut in the Cretaceous Dakota Formation (Johnson and Arbogast 1993), which also outcrops in the roadcut exposure.

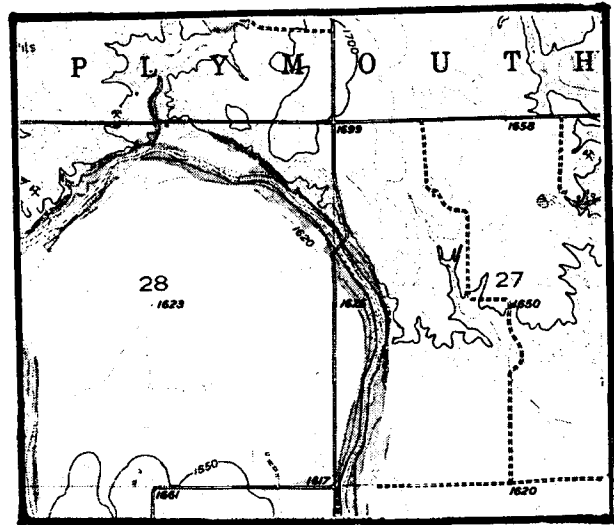


Figure 5.22. Topographic map in the vicinity of Beisel-Steinle site. Scale 1:24,000

### Rock Magnetic Records

Results of rock magnetic measurements are summarized in Table 5.8 and Figure 5.23. Broad patterns define alternating zones of relatively high and low MS in the MS-depth profile (Fig. 5.23.a). From the bottom of the profile, susceptibility zones include low MS (GCF loess), high MS (GCF soil), low MS (Peoria loess), and high MS (Brady soil and above). MS values range from 50 to  $100 \times 10^{-8} \text{m}^3/\text{kg}$  and show the systematic differences between loess and soils.

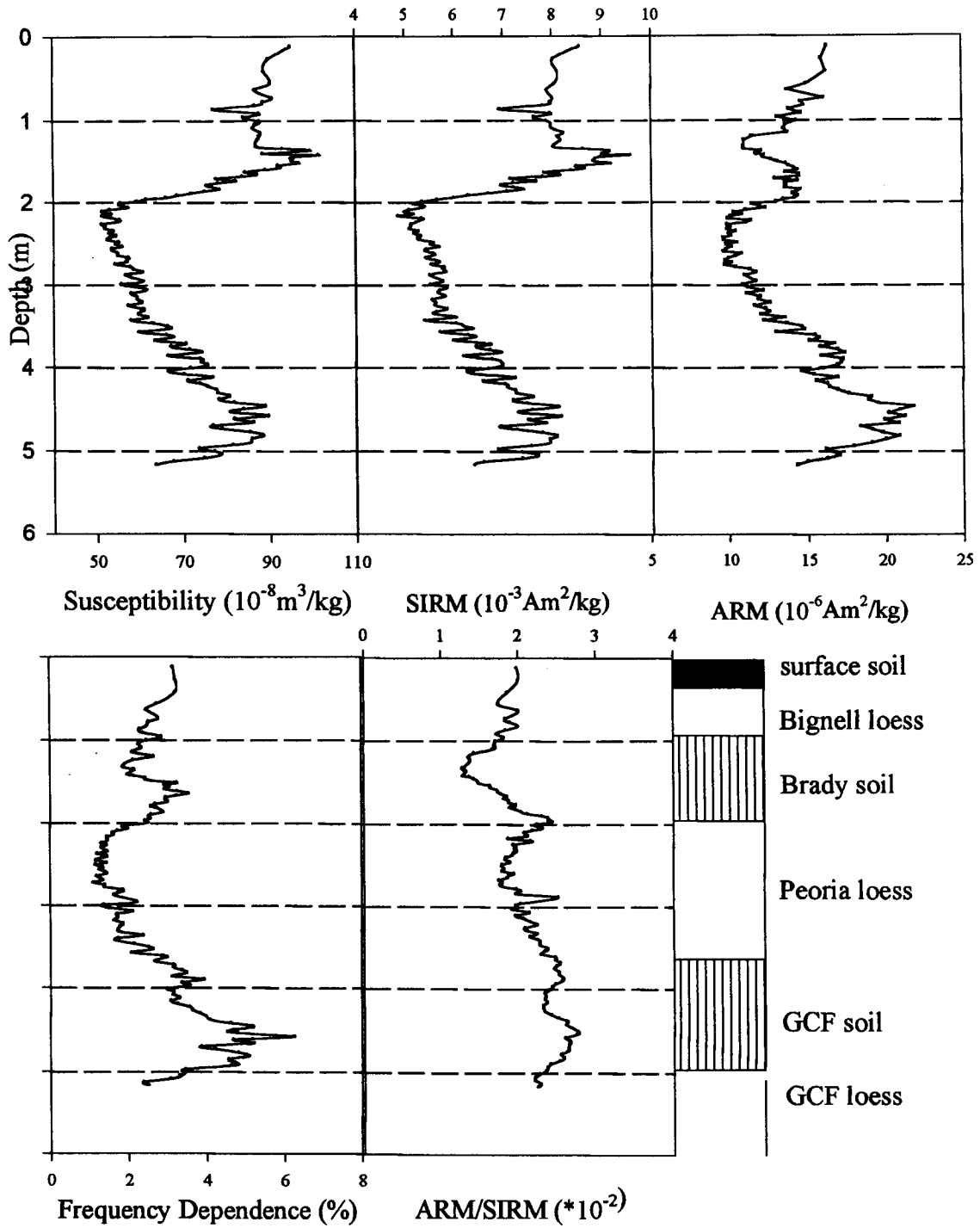


Figure 5.23. MS, SIRM, ARM, FD, and ARM/SIRM data and stratigraphy for the profile sampled at the Beisel-Steinle site.

Table 5.8. Descriptive statistics on magnetic parameters from the Beisel-Steinle site.

	No.	Minimum	Maximum	Mean	Std. dev
ARM	137	9.60	21.80	13.95	3.06
ARM/SIRM	137	1.27	2.76	2.08	0.35
FD	137	2.00	7.00	3.59	1.07
S Index	137	0.91	0.99	0.94	0.01
SIRM	137	4.85	9.59	6.75	1.19
MS	137	51.14	101.44	71.73	14.04

MS values of the unweathered Gilman Canyon loess (*c.*  $55 \times 10^{-8} \text{m}^3/\text{kg}$ ) is lower than those of the overlying Gilman Canyon soil (*c.*  $90 \times 10^{-8} \text{m}^3/\text{kg}$ ). MS intensities of the Gilman Canyon soil are nearly twice as high as those of the overlying Peoria loess. Once again, bimodal peaks in the MS records reveal minor climate fluctuations, lending evidence for the theory of multiple periods of pedogenesis during that time (*e.g.*, Johnson, 1993). Despite the uncertainties of  $^{14}\text{C}$  age estimates, there is a good match between the magnetic variations within the interstadial Gilman Canyon Formation and the regional climate history in terms of the general timing of episodes.

MS of the Peoria loess gradually decreases until it reaches its minimum value at 2 m below the surface (Figure 5.23). The MS signal within the Peoria loess is much weaker than in the underlying Gilman Canyon soil or the overlying Brady soil. However, MS minimum values ( $50 \times 10^{-8} \text{m}^3/\text{kg}$ ) are much higher than those from the sites closer to the presumed loess source area.

Mass specific ARMs and SIRMs were measured for selected samples throughout the section (Table 5.9). SIRM values are enriched in the Gilman Canyon soil relative to the overlying Peoria loess, and exhibit bimodal peaks within the Gilman Canyon Formation. SIRM values vary in the range of  $\text{SIRM} = 5\text{-}9 \times 10^{-3} \text{Am}^2/\text{kg}$  (Figure 5.23. b). Correlation coefficient between MS and SIRM variation is very high ( $r^2=0.993$ ).

Table 5.9. Correlation coefficients and significance level between the magnetic parameters,  $\delta^{13}\text{C}$  and phytolith index at the Beisel-Steinle site.

	$\delta^{13}\text{C}$	ARM/SIRM	ARM	FD	MS	SIRM
$\delta^{13}\text{C}$	1.000	0.098	0.534**	0.440*	0.594**	0.598**
ARM/SIRM	0.098	1.000	0.686**	0.842**	-0.196*	-0.253**
ARM	0.534**	0.686**	1.000	0.935**	0.569**	0.524**
FD	0.440*	0.842**	0.935**	1.000	0.304**	0.262**
MS	0.594**	-0.196*	0.569**	0.304**	1.000	0.993**
SIRM	0.598**	-0.253**	0.524**	0.262**	0.993**	1.000
$\delta^{13}\text{C}$		0.612	0.003	0.017	0.001	0.001
ARM/SIRM	0.612		0.000	0.000	0.023	0.003
ARM	0.003	0.000		0.000	0.000	0.000
FD	0.017	0.000	0.000		0.000	0.02
MS	0.001	0.023	0.000	0.000		0.000
SIRM	0.001	0.003	0.000	0.002	0.000	

\*\* Correlation is significant at the 0.01 level (2-tailed).

\* Correlation is significant at 0.05 level (2-tailed).

Mass specific ARMs vary in the range of  $ARM = 10-20 \times 10^{-6} \text{ Am}^2/\text{kg}$ . ARM variations again correlate well with MS ( $r^2 = 0.569$ ) and SIRM ( $r^2 = 0.524$ ) and are enriched in the Gilman Canyon soil, with the lowest values occurring in the overlying Peoria loess. It should be noted that, while the range of ARM variation seems to be much greater than those for SIRM or MS variations, the absolute values of ARMs are two orders smaller than SIRM values, so small changes of absolute values could cause seemingly greater variations in the diagram. Bimodal peaks are not clear in the ARM plot. ARM and SIRM variations indicate a higher concentration of smaller grains with a stable single domain in the Gilman Canyon Formation than in the Peoria loess.

#### *Magnetic grain size*

The FD data confirm the presence of an ample amount of SP material only in the Gilman Canyon soil. FD values range from 0 to 6 percent at the site. FDs from the Gilman Canyon soil (c. 6 percent) are higher than in the Peoria loess and underlying loess. These values seem to be very low but are high enough to contain a significant amount of SP materials (Dearing *et al.*, 1996). It should be noted that FD values from the Brady soil are as low as 2 percent, which indicate that almost none of the SP/SD boundary size materials are present.

Relative variations in the amounts of SD and PSD grains can also be approximated by normalizing ARM values with SIRM values to obtain ARM/SIRM. This ratio also shows a sharp increase only in the Gilman Canyon Formation, with a slight increase in the Brady soil. But considering that the ARM acquired per unit field is approximately five times more effective than SIRM (Hunt *et al.*, 1995) and that normalized ARM/SIRM values are only 1-3 percent, the observed two- to three-fold increase in ARM/SIRM corresponds to only a small increase in the proportion of SD and PSD grains in the soil.

Figure 5.24 shows the biparametric plots of MS vs FD and ARM (normalized to SIRM) data obtained from the Beisel-Steinle site. The ARM/SIRM values for the Gilman

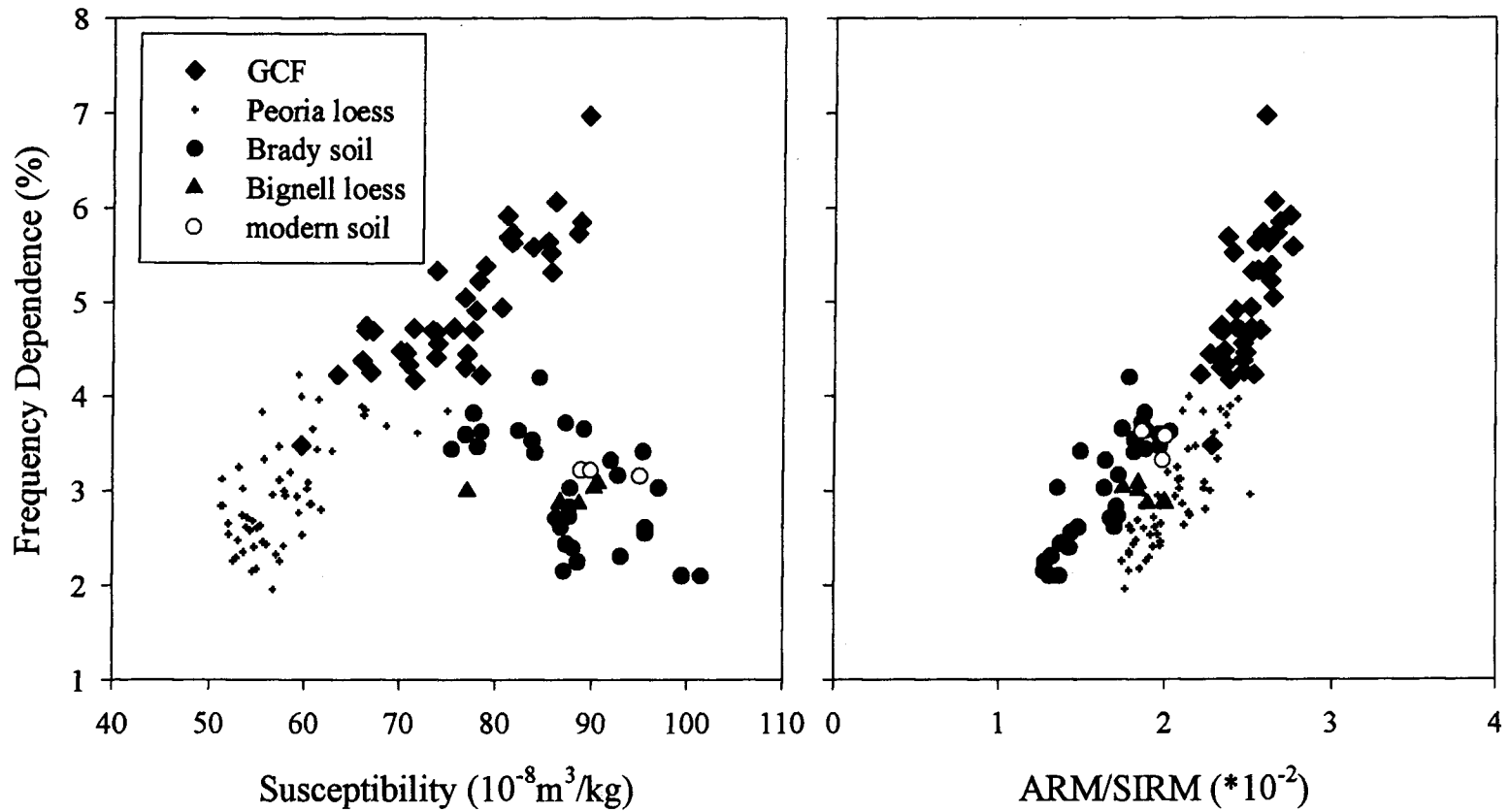


Figure 5.24. Biparametric plots of MS versus FD and the ratio, ARM/SIRM versus MS for the samples at the Beisel-Steinle site.

Canyon soil vary within the range occupied by those of synthetic grains of SD size or finer. Their FD values are closely correlated with synthetics in the size range ~20-30 nm. Hence, these data identify distinctive grain-size contrasts between the Peoria loess and the Gilman Canyon soil. The soil horizon is characterized by the presence of ultrafine-grained magnetic minerals of SD and SP size, whereas the Peoria loess layers contain little SD and small amounts of SP minerals. However, the Brady soil does not indicate any presence of finer grains despite its higher MS values, which probably reflect an over-thickened modern soil. Diekmeyer (1994) reported that none of the non-magnetic parameters such as organic matter content,  $\delta^{13}\text{C}$ , and carbonate content show any evidence of the Brady soil at this site.

It appears that soils formed during the warmer interglacial and interstadial periods contain not only an excess of the very small grains that dominate the FD signal, but also the intermediate grains that carry ARM and the largest grains that carry SIRM. If the MS signal had been purely the result of dilution of a uniform source material, as predicted by the magnetite-rain model (Kukla, 1987), then the normalized MS should be invariant with depth. Because it is not, there is some difference in magnetic mineralogy and/or grain size between the loess and the soils.

#### *Magnetic mineralogy*

The parameters of IRM acquisition ( $\text{IRM}_{0.3\text{T}}/\text{IRM}_{1.1\text{T}}$ ) vary little, if any, from 90 percent to 97 percent in both the soils and the Peoria loess. Higher ratios indicate a very small proportion of antiferromagnetic hematite, which only acquires magnetic remanence at high applied fields. Therefore, this study indicates that the magnetic properties of these samples are dominated by ferrimagnetic (*e.g.*, magnetite/maghemite-type) behavior and that variations between the samples in the relative importance of imperfect antiferromagnets (*e.g.*, hematite) will not alone account for the large differences in rock

magnetic properties encountered. These results are comparable to those from the Eustis ash pit.

### **Comparisons with Other Climatic Proxies**

The influence of climate change on magnetic-mineral records is demonstrated by comparing magnetic parameters to geochemical and biological proxies for climate. Such comparisons between magnetic properties and more direct climate indicators are essential, because factors other than climate can strongly influence the flux of magnetic minerals into loess deposits.

$\delta^{13}\text{C}$  values from unaltered Gilman Canyon loess indicate a dominance of  $\text{C}_3$  plants, indicative of cool moist conditions.  $\delta^{13}\text{C}$  values from the Gilman Canyon soil at the site show  $\text{C}_4$  type plants (values of *c.*  $-15\text{‰}$ ) dominating at the time of the unit's formation, implying a warmer, drier climate (Figure 5.25). This  $\text{C}_4$  landscape is comparable to the signal from the modern soil, suggesting a climate similar to that which prevails today. The late Gilman Canyon time is characterized by trends toward a  $\text{C}_3$ -dominated landscape, implying cooler, moister conditions after formation of the Gilman Canyon soil.  $\delta^{13}\text{C}$  results from the Peoria loess are in good agreement with the findings of others using  $\delta^{13}\text{C}$  in unweathered loess (Krishnamurthy *et al.* 1982; Johnson 1993a). The values tend strongly toward  $\text{C}_3$  plants ( $-23\text{‰}$ ) above the Gilman Canyon soil, indicating a moist, cool environment at the time of deposition. The  $\text{C}_3$  signal continues upward through the entire profile until organic matter translocated downward from the Brady soil is encountered at about 2.5 meters below the surface. At this point in the section, Peoria loess comes under the influence of  $\text{C}_4$  plants dominating the Brady soil.

The two records are, like the others, partly offset as shown in Figure 5.25, again suggesting that pedogenesis factors and plant cover might respond to changes in climate over slightly different time frames, since both parameters have different mean residence times within the soil system (An *et al.*, 1993). The effects of environmental changes on

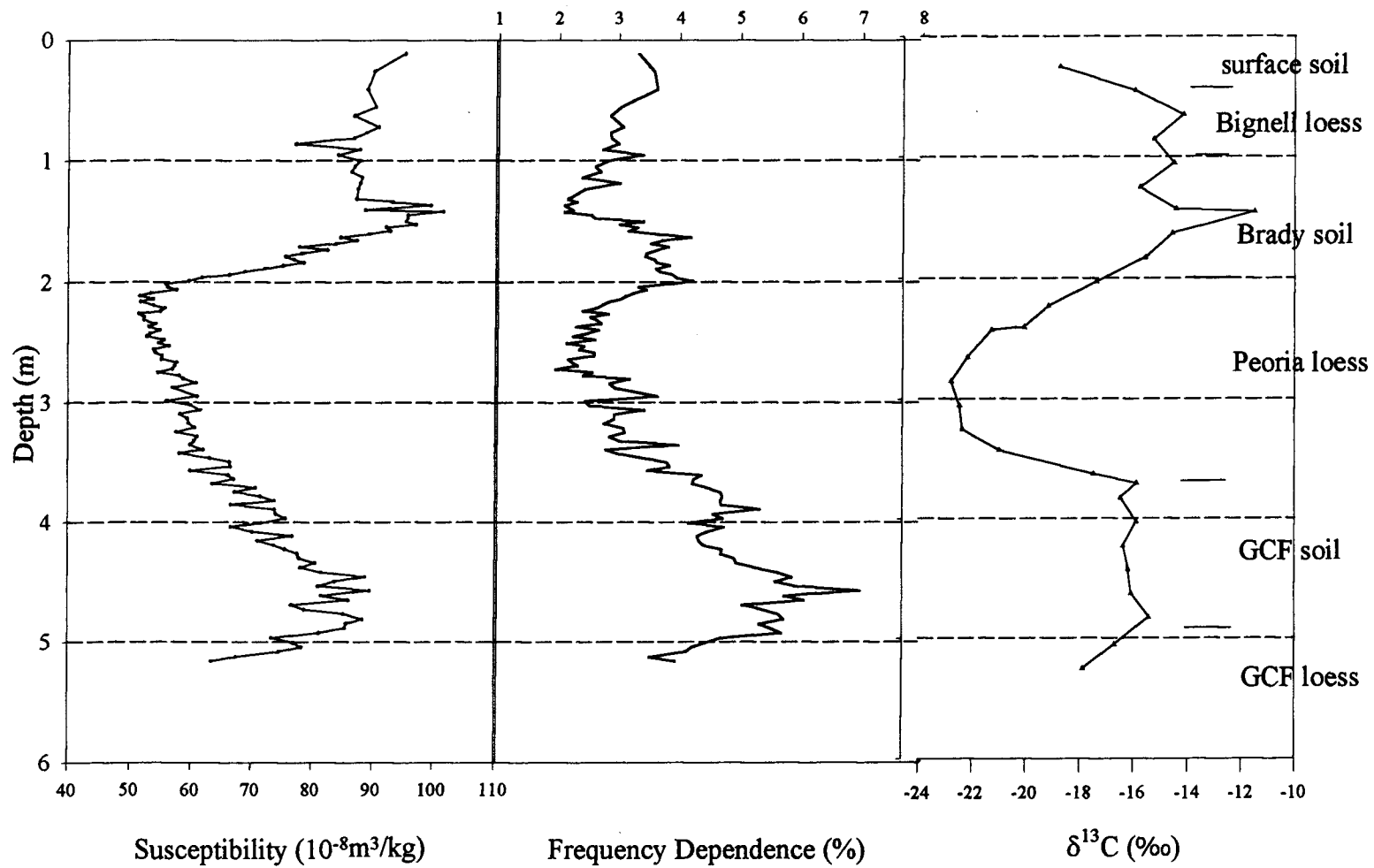


Figure 5.25. MS, FD, and  $\delta^{13}\text{C}$  data for the samples at the Beisel-Steinle site.

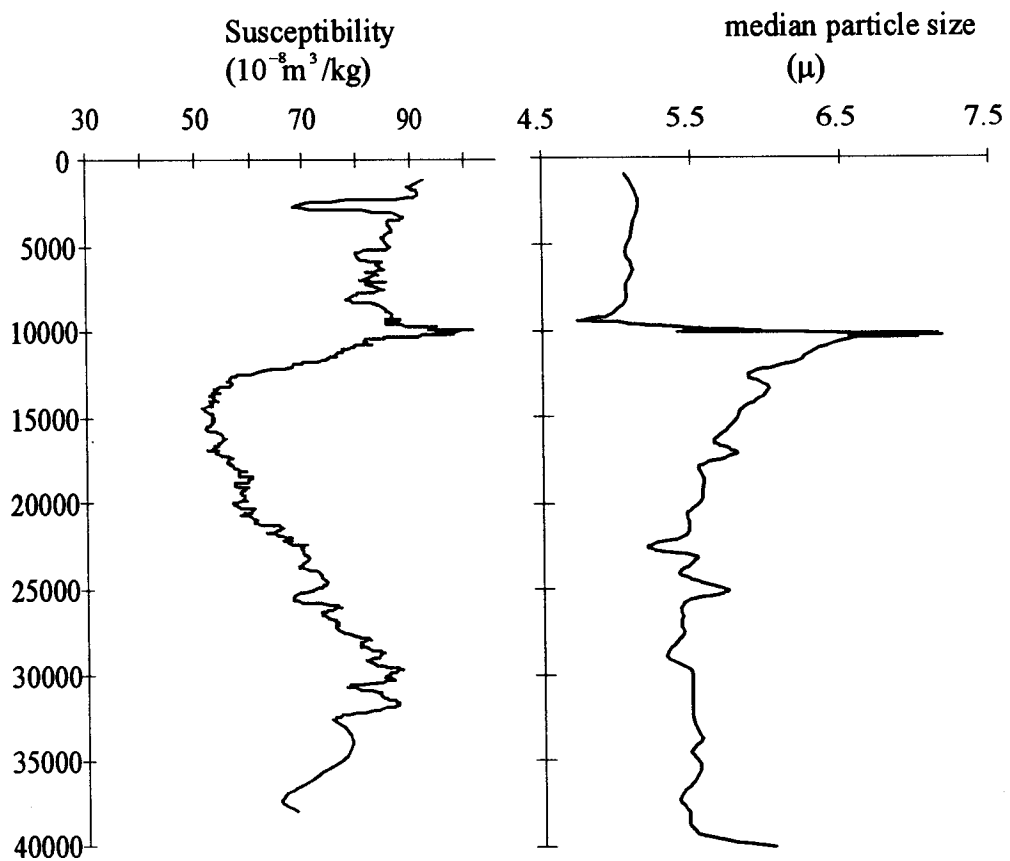


Figure 5.26. Magnetic susceptibility and median particle size from the Beisel-Steinle site.

the magnetic parameters have been investigated by examining the relationship between various magnetic parameters and  $\delta^{13}\text{C}$ . The correlation coefficients between the magnetic parameters and  $\delta^{13}\text{C}$  are listed in Table 5.9. The correlations of magnetic parameters and  $\delta^{13}\text{C}$  at the Beisel-Steinle site are moderately significant.

The relatively high correlation between magnetic parameters and stable carbon isotopes from the site indicates a strong link between climate variation and the processes which generate the magnetic signal. This linkage is also supported by the synchrony of the variation in magnetic properties and northern hemisphere climate change as shown in Figure 5.3.

An *et al.* (1991) have suggested that, whereas MS can serve as a proxy for precipitation (summer monsoon intensity), the median grain size of loess and soils primarily reflects variations in the strength of winter winds. The median particle size variation from the Beisel-Steinle site was compared with MS variation (Figure 5.26). The particle size data set is adopted from a previous study (Diekmeyer, 1994). At the site, the Peoria loess contains more than 85 percent silt, which is much finer than the 60 percent at the Eustis ash pit. Since only finer particles were wind-entrained long enough to reach central Kansas, the correlation between the particle size and MS which was found in the Eustis ash pit cannot be found except in the Brady soil unit, during which pedogenesis is presumed to have been most active to produce the finer clay minerals.

## VI. SUMMARY AND CONCLUSIONS

### REGIONAL MAGNETIC RECORDS

As was discussed in Chapter V, climatic fluctuations manifest themselves in terms of alternating loess and soils, unaltered loess corresponding to a weaker magnetic signal and soils reflecting a stronger magnetic signal. Not only concentration-dependent parameters such as MS and SIRM, but also grain size-dependent parameters including FD and ARM/SIRM correspond to the alternating stratigraphic units. Also shown was the strong correlation between the climate-sensitive proxies, including  $\delta^{13}\text{C}$  from soil humates, opal phytolith data and the magnetic parameters. By examining regional magnetic records, this study identified a regional climatic effects on magnetic records, and also discerned the influence of local climatic conditions on the degree of pedogenesis and the evolution of magnetic minerals.

The first common characteristic observed was that fairly low coercivity minerals such as magnetite are an important constituent of all the samples investigated. This was indicated by the limited number of Curie temperature data and the  $\text{IRM}_{0.3\text{T}}/\text{IRM}_{1.1\text{T}}$  data. There was also evidence of significant amounts of maghemite, indicated by CBD treatment on a limited number of samples and There may well be other magnetic phases present (such as hematite), but this study agrees with Maher and Thompson (1992) in recognizing the significance of the magnetite contribution.

Second, intersite variability in soils is smaller than what it is in Peoria loess. Intersite variability in soils from the Chinese Loess Plateau is about twice what it is in loess, suggesting that pedogenesis plays a significant role in determining magnetic characteristics (Evans and Heller, 1994). This larger variability in soils is not detected in the central Great Plains, which indicates that the climatic conditions prevailing during formation of the soils were comparable despite the hundreds of kilometers between the

sites.

Third, MS measurements available from the eleven sites studied thus far indicate a widespread MS minimum of  $30 \times 10^{-8} \text{m}^3/\text{kg}$ . There may be a MS property which supports the 'ground level' concept of Heller *et al.* (1991).

Fourth, the soil samples have ARM/SIRM ratios in the range of  $2\text{-}3 \times 10^{-2}$  and FD in the range of 4-6 %. Unaltered Peoria loess samples exhibit ARM/SIRM ratios in the range of  $< 2 \times 10^{-2}$  and FD in the range of 0-3 %, suggesting that the magnetic properties of soils are due to ultrafine magnetite grains with typical dimensions of significantly less than 100 nm (Maher, 1988).

### **Long-Term Climatic Records**

This study accepts the overwhelming evidence (*e.g.*, Zhou *et al.*, 1990; Maher and Thompson, 1991; Hus and Han, 1992; Maher and Thompson, 1992) that during the interglacials and interstadials, warmer and more humid climates were responsible for the alteration of non-magnetic (paramagnetic), iron-bearing clay minerals to strongly magnetic (ferrimagnetic), ultrafine grains of magnetite or maghemite. In all sections analyzed thus far, MS values are highest within the soils, including the Gilman Canyon geosol and Brady soil. The intervening Peoria loess has the lowest values.

A comparison among the four sites yields comparable magnetic climate proxies which provide an average picture of the climate proxy in the central Great Plains (Figure 6.1). The MS intensities of the central Great Plains loess were plotted with the regional loess/soil stratigraphy. A simple linear interpolation technique was applied between  $^{14}\text{C}$  ages, or between stratigraphic boundaries when  $^{14}\text{C}$  ages were unavailable (DB site).

The Gilman Canyon Formation is well represented in the MS-age plot. The terrestrial plant ecology of the Gilman Canyon Formation inferred from the  $\delta^{13}\text{C}$  and the limited phytolith data is characterized by primarily  $\text{C}_4$  type grasses, and a warm, possibly dry climate (Johnson, 1993b). From the MS data, it is evident that an environment

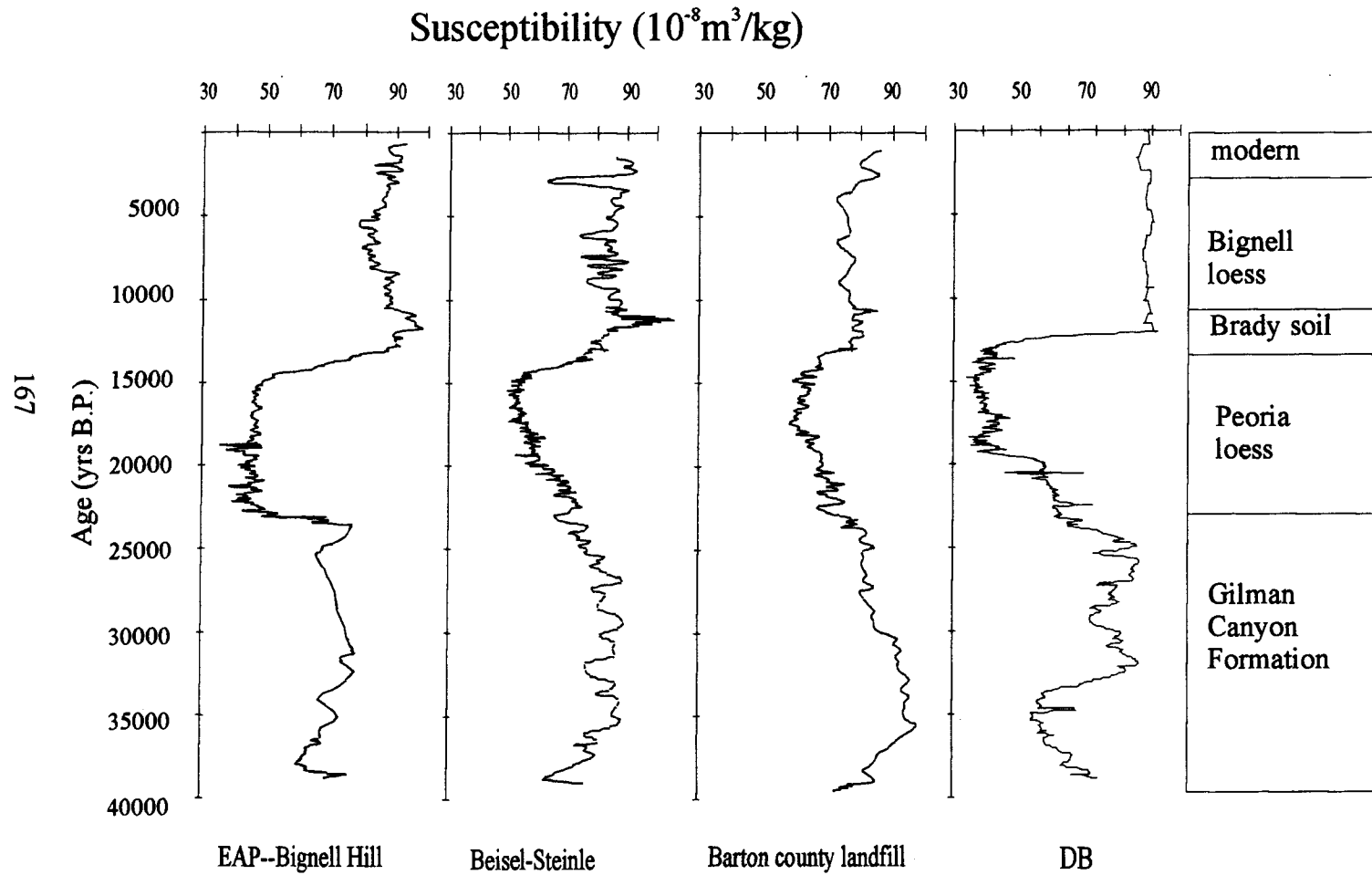


Figure 6.1. Magnetic susceptibility from sites in south-central Kansas (Barton County, Beisel-Steinle) to southwestern Nebraska (Eustis ash pit, Bignell Hill), and to northeastern Kansas (DB).

suitable for more enhanced pedogenesis existed during the Gilman Canyon period. The Gilman Canyon soil is best described as a composite geosol, in that pedogenesis was diminished somewhat during formation of the soil by an acceleration in the rate of loess fall, albeit still very low. As a result, the magnetic signal (MS and FD) typically have a bimodal peak; this bimodality is well represented at the Eustis ash pit and DB sites, but is not clear at the Beisel-Steinle or Barton County landfill sites, probably because the Gilman Canyon Formation in these sites is too compressed and/or eroded.

The MS from the composite section of Bignell Hill-Eustis ash pit can easily be correlated with oxygen isotope records from Greenland and SPECMAP (Figure 6.2). Although the patterns originate from different sedimentation processes such as eolian or chemical deposition, variable mixing and bioturbation effects, and different accumulation rates, they show coherent relative intensity changes. The last interstadial period is clearly shown in the SPECMAP, although the last interstadial is not readily evident in icecore records. However, the MS signal from the last interstadial is as strong as the signal from the Pleistocene/Holocene boundary Brady soil.

Peoria loess deposition occurred at a relatively rapid rate so as to preclude any significant pedogenesis. At more than one site, however, the increase in MS and FD within the Peoria loess suggest one or more brief periods of landscape stability. The absolute timing of this landscape stability is unknown, but is probably centered around the Last Glacial Maximum; a moderately developed glacial maximum soil has been identified elsewhere in the region (Arbogast, 1995).

It is interesting to note that one of the most recent 3-D simulation models suggests that a high glacial dust loading may have caused a significant, episodic regional warming of over 5°C downwind of major ice-margin dust sources (Overpeck *et al.*, 1996). If this model is accurate, then one or more brief soil-forming periods may have existed during the Peoria period.

At each site, MS exhibits a decreasing trend until it reaches its minimum values,

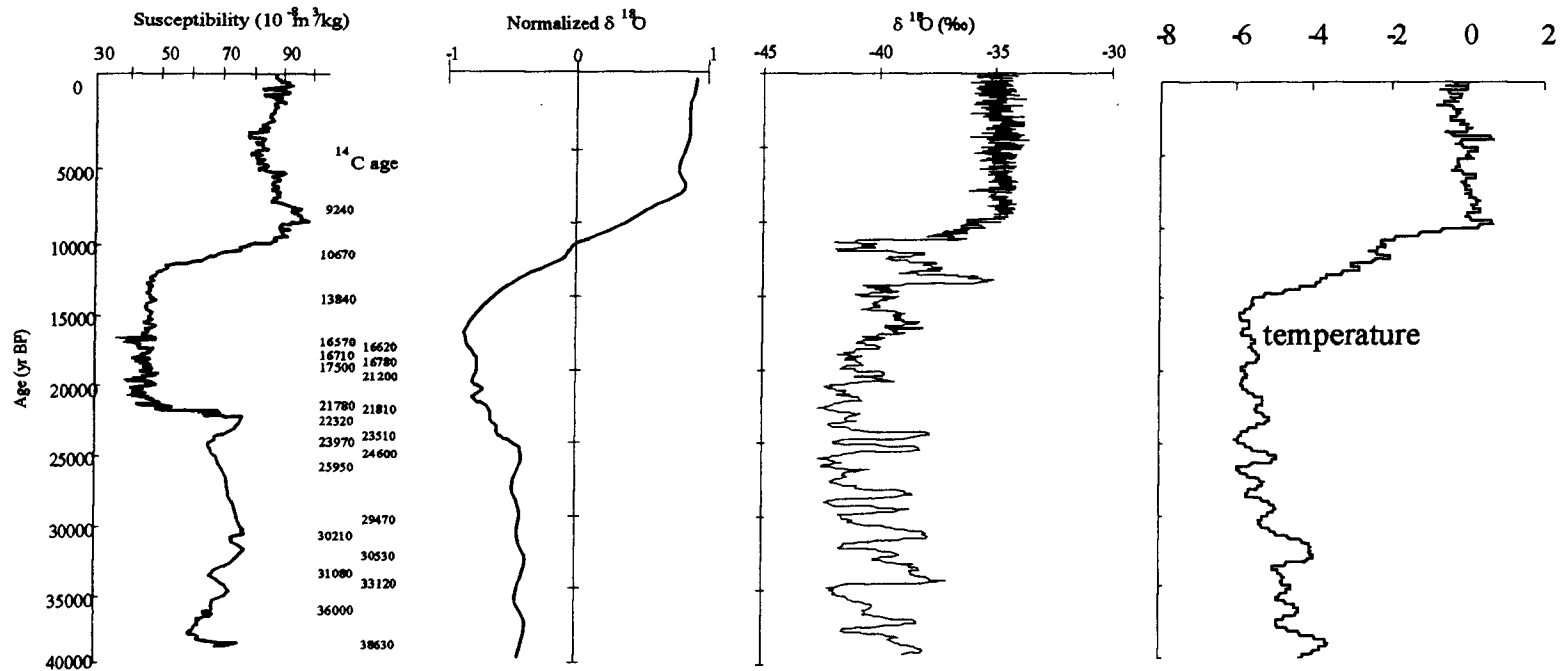


Figure 6.2. Magnetic susceptibility from the Eustis ash pit--Bignell Hill, SPECMAP oxygen isotope record (Martinson *et al.* 1987), and GRIP icecore (Johnsen *et al.*, 1992), temperature record from Greenland Berilium record (Mayewski *et al.*, 1994).

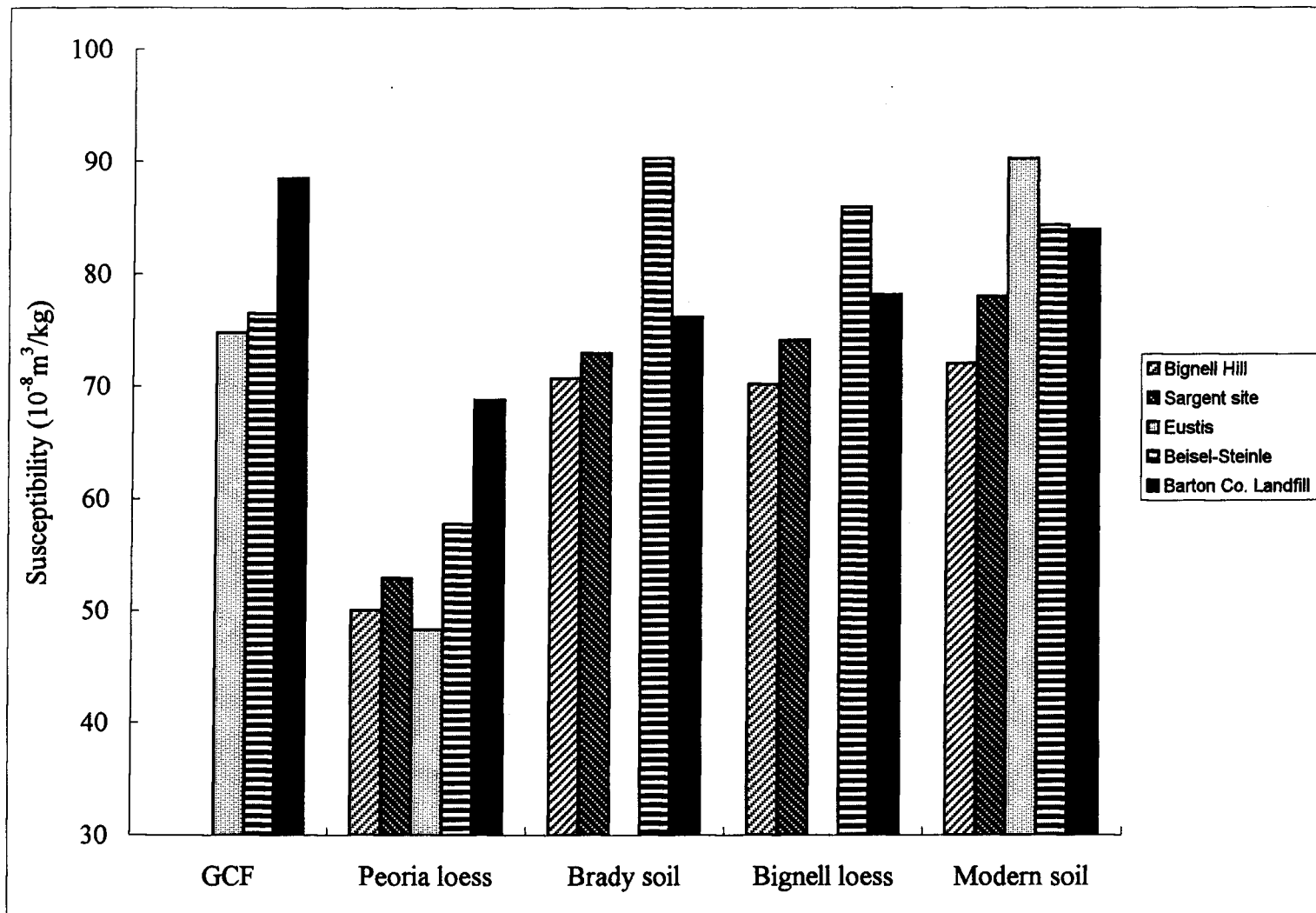
which seem to represent the Last Glacial Maximum. The weaker MS within the Peoria loess could be explained either by the difference in loess accumulation rates or by the different phase of pedogenesis among the stratigraphic units. Considering the fact that  $\delta^{13}\text{C}$  values acquired from the Peoria loess indicate the dominance of  $\text{C}_3$  plants, which demonstrates that cooling associated with the Wisconsinan glacial maximum (c. 20-18 ka) occurred in early and middle Peoria time, decreased pedogenesis/weathering during the cold interval seems the better explanation for the weaker MS signal.

Several studies in China indicate that mean MS values of loess deposits increase linearly from low values in the drier western parts of the loess plateau to higher values in the more humid central sites (Heller *et al.*, 1993). In the central Great Plains, the mean susceptibilities of Peoria loess show a systematic decrease from south to north (Fig. 6.3; Table 6.1).

Table 6.1. Magnetic MS statistics from the region (unit:  $10^{-8}\text{m}^3/\text{kg}$ ).

	Bignell Hill	Sargent	Eustis ash pit	Beisel-Steinle	Barton Co.
GCF			74.8	76.5	88.5
Peoria loess	50.03	52.90	48.3	57.7	68.8
Brady soil	70.71	72.96		90.3	76.2
Bignell loess	70.22	74.12		86	78.2
Modern soil	72.1	78.03	90.3	84.4	84

FD values provide information on grain sizes of the magnetic carriers. Apparently, much of the pedogenic magnetic material in modern soils is at or near the superparamagnetic grain sizes (SP, 30 nm to zero). Therefore, FD is considered to be a good indicator of pedogenic processes. FD, as measured conventionally using two frequencies, is only sensitive to the presence of magnetite grains between 18 and 20 nm, not to all SP (Banerjee *et al.*, 1993). At Eustis, FD correlates very well with another grain size indicator, the ARM/SIRM parameter. Correlation between these two parameters is reasonably high at every site, suggesting that there are pedogenic magnetic



grains which span the SP/SD boundary. Because a magnetic method which provides a truly quantitative measure of all SP grains produced by pedogenesis is not available, the use of FD fluctuations and ARM/SIRM could be a good measure of paleoclimate variation in the central Great Plains, at least until additional grain size-sensitive parameters are measured.

Table 6.2. FD statistics from the region (unit: %).

	Bignell Hill	Sargent	Eustis ash pit	Beisel-Steinle	Barton Co.
GCF			5	5	4.5
Peoria loess	1.5	1.1	3.3	2.8	2.8
Brady soil	3.1	3.7		3.3	5.1
Bignell loess	1.6	2.4		3.1	
Modern soil	1.8	2.2	3.3	3.2	3.4

### Shorter-Term Records

Evidence of the Altithermal, or middle Holocene dry episode appears at all sites. The depressed MS and FD values during the middle Holocene are indicative of an increased rate of deposition and decreased intensity and/or time of weathering, reflecting an interval of eolian activity widely recognized on the Great Plains.

Also, there are minor but notable decreases in the MS intensity just below the Brady soil (Figure 6.4, 6.5, and 6.6) that may indicate a climatic oscillation comparable to the Younger Dryas cold spell, lasting from about 11 ka to 10 ka (*e.g.*, Mathewes, 1993). Without accelerated mass <sup>14</sup>C ages, it is hard to confirm the presence of a short-term climatic variation like the Younger Dryas. However, a rapid rate of dust accumulation approaching 5 m/1000 year at the Bignell Hill and Sargent sites during the Peorian period has led to the preservation of a high-resolution record of climatic changes. In some Chinese loess profiles with accumulation rates of c. 1 m/1000 year, An *et al.* (1993) also report the presence of a minor climatic fluctuation, which is believed to represent the Younger Dryas in loess.

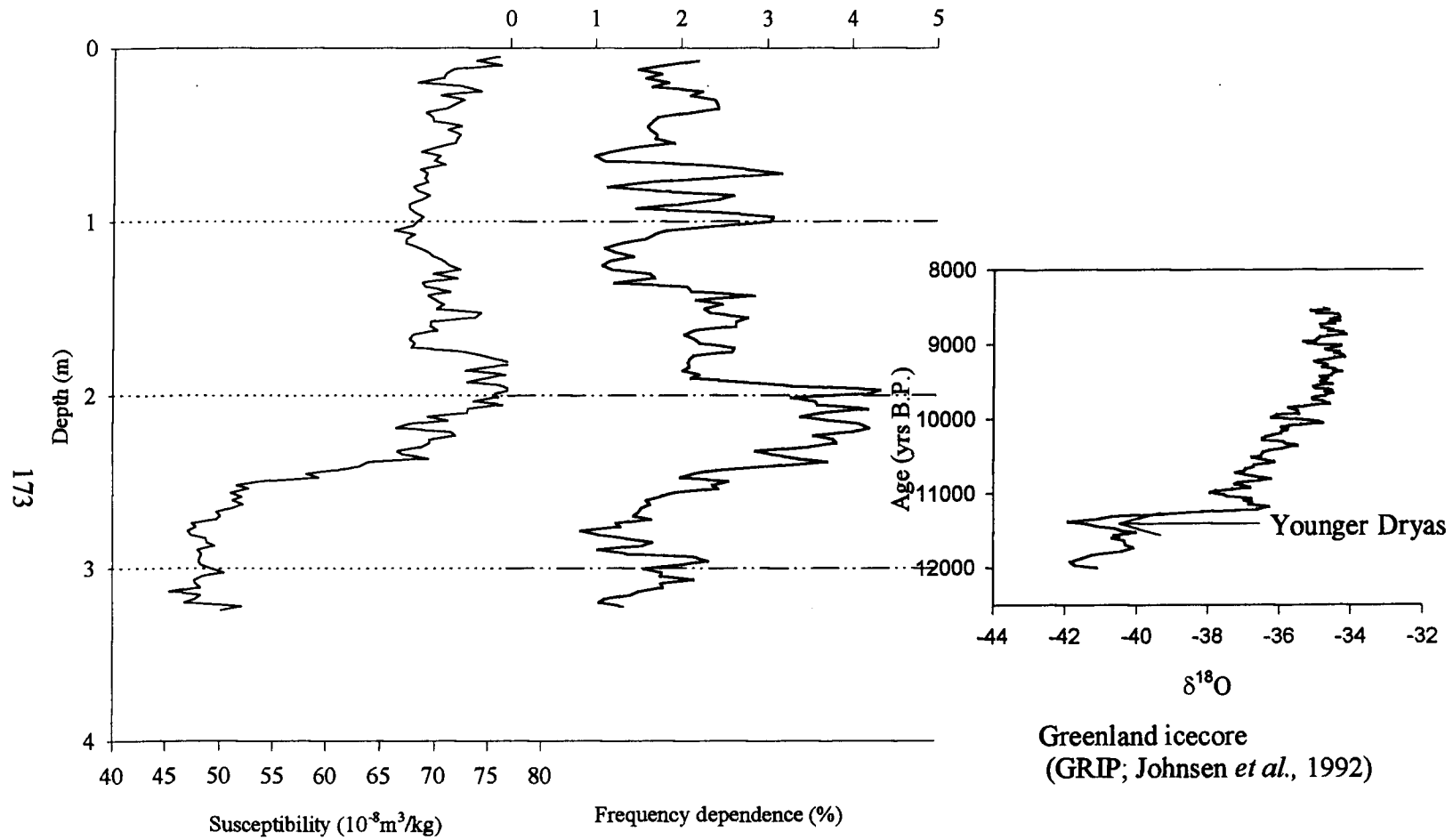


Figure 6.4. MS and FD variations from the Bignell Hill and  $\delta^{18}\text{O}$  curves from a Greenland icecore. A possible Younger Dryas climatic fluctuation is more apparent in FD plot at the Pleistocene/Holocene boundary.

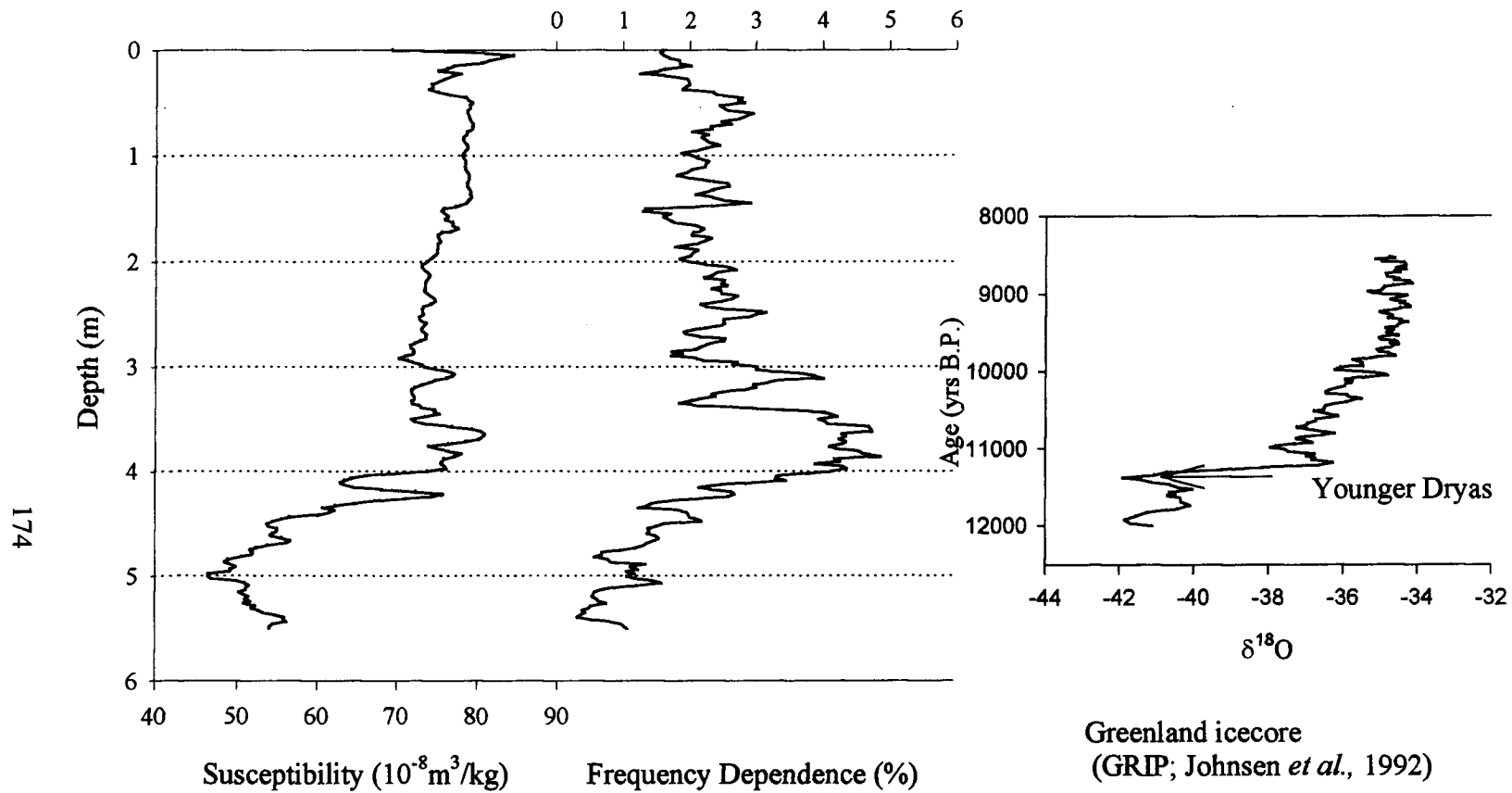


Figure 6.5. MS and FD variations from the Sargent site and  $\delta^{18}\text{O}$  curves from a Greenland icecore. A possible Younger Dryas climatic fluctuation is apparent at the Pleistocene/Holocene boundary.

## FUTURE RESEARCH

Concentration sensitive magnetic parameters including magnetic susceptibility values are highest within the interstadial and interglacial soils. The intervening unweathered loess has the lower values. Magnetic records, therefore, provide an average climate proxy in the central Great Plains. MS-age plot could identify not only longer-term climate variation but also shorter-term climate fluctuations including Younger Dryas and Altithermal period.

Magnetic parameters also exhibit good correlations with the biological proxies including  $\delta^{13}\text{C}$  values from humates and opal phytolith data from the region. However, much remains to be done in the central Great Plains before a comprehensive magnetic model for predicting climate change can emerge. Specifically, future study in the region should focus on 1) a quantitative understanding of the origin of SP grains through pedogenesis, and 2) developing a method for a truly quantitative measure of all the SP grains produced by pedogenesis.

Although close-interval magnetic analyses were conducted in this study, the precise mode of formation of these enhanced ultrafine-grained magnetic minerals remains unclear. Concentration-sensitive parameters correspond highly to the stratigraphic units, but size-sensitive parameters do as well. Although a number of biological proxies available from the region, including  $\delta^{13}\text{C}$  and phytolith analysis, and non-biological proxies such as particle size analysis confirm the possible causal relationship between climate and magnetic parameters, there is no direct transfer function comparable to the one derived from pollen analysis elsewhere. Future research should attempt to quantify the origin of ultrafine grains, and therefore an attempt should be made to derive a closer interval  $\delta^{13}\text{C}$  signal from the soil humate. An attempt to tighten the chronology of loess deposition would be useful, as regards minor climate variations.

Alternative experiments should be attempted to develop a method to measure the

amount of magnetics that is of truly pedogenic origin. MS and FD zonations can be correlated from southwestern Nebraska and beyond, while MS zones have a different character at the Bone Cove site and Sumner Hill site. MS signals in the Peoria loesses from the sites are comparable to those of well-developed soils, but FD signals do not indicate the presence of finer magnetic minerals. Differences in MS zones probably reflect the addition and mixing of sediments from different source areas. Also, archaeological remains such as hearths, produce a sharp increase in MS intensity and virtually no change in FD, complicated the investigation. A quantitative measure of truly pedogenic magnets would establish better correlation between climate and magnetic parameters.

Finally, the results of this study on loess should be integrated with other studies, such as sand dunes studies both in the Sand Hills of Nebraska and Great Bend, Kansas, and alluvial stratigraphy in the region.

## REFERENCES

- Abers, J. S., 1991, The glaciation of northeastern Kansas: *Boreas*, v. 20, p. 297-314.
- Agenbrood, L. D., 1978, The Hudson-Meng site-an Alberta bison kill in the Nebraska High Plains, Washington D. C., University Press of America, 230 p.
- Aïssaoui, D. M., McNeill, D. F., and Hurley, N. F., 1993, Applications of Paleomagnetism to Sedimentary Geology, Society for Sedimentary Geology Special Publication, n. 49, 216 p.
- Ahlbrandt, T. S., Swinehart, J. B., and Maroney, D. G. 1983, The dynamic Holocene dune fields of the Great Plains and Rocky Mountain Basins, U.S.A. *in* Brookfield M. E, and Ahlbrandt, T. S., eds., *Eolian Sediments and Processes*, Elsevier, Amsterdam, p. 379-406.
- Alam, M. S., Keppens, E., and Paepe, R., 1997, The use of oxygen and carbon isotope composition of pedogenic carbonates from Pleistocene paleosols in NW Bangladesh, as paleoclimatic indicators: *Quaternary Science Reviews*, v. 16, p. 161-168.
- Ambrose, S. H., and Sikes, N. E., 1991, Soil carbon isotope evidence for Holocene habitat change in the Kenya Rift Valley: *Science*, v. 253, p. 1402-1405.
- An, Z., Kukla, G., Porter, S. C., and Xiao, J. L., 1991, Late Quaternary dust flow on the Chinese Loess Plateau: *Catena*, v. 18, p.125-132.
- An, Z., Liu, T., Lu, Y., Porter, S. C., Kukla, G. J., Wu, X., and Hua, Y., 1990, The long-term paleomonsoon variation recorded by the loess-paleosol sequence in central China: *Quaternary International*, v. 7/8, p. 91-95.
- An, Z., Porter, W., Zhou, Y., Lu, D.J., Donahue, M. J., Heads, M. J., and Zheng H., 1993, Episodes of strengthened summer monsoon climate of Younger Dryas age on the Loess Plateau of Central China: *Quaternary Research*, v. 39, p. 45-54.
- Anderson, R. S., and Hallet, B., 1996, Simulating magnetic susceptibility profiles in loess as an aid in quantifying rates of dust deposition and pedogenic development: *Quaternary Research*, v. 45, p. 1-16.
- Anderson, R. Y., 1992, Possible connection between surface winds, solar activity and the earth's magnetic field: *Nature*, v. 358, p. 51-53.
- Anderson, W. T., Mullins, H. T., and Ito, E., 1997, Stable isotope record from Seneca Lake, New York: Evidence for a cold paleoclimate following the Younger Dryas: *Geology*, v. 25, p. 135-138.
- Andrews, J. T., 1987, The Late Wisconsin glaciation and deglaciation of the Laurentide Ice Sheet, *in* Ruddimann, W. F., and Wright, H. E., Jr., eds., *North America and adjacent oceans during the last deglaciation*. Geological Society of America, *The Geology of North America*, v. K-3, p. 13-37.
- Andrews, J. T., and Stravers, J. A., 1993, Magnetic susceptibility of Late Quaternary marine sediments Frobisher Bay, N. W. T.: an indicator of changes in provenance and processes: *Quaternary Science Reviews*, v. 12, p. 157-167.
- Arbogast, A. F., 1995, Paleoenvironments and desertification on the Great Bend Sand Prairie in Kansas. Unpublished Ph.D. Dissertation, University of Kansas, Lawrence, 371 p

- Arbogast, A. F., 1996a, Late Quaternary evolution of a lunette in the central Great Plains: Wilson Ridge, Kansas: *Physical Geography*, v. 17, p. 354-370.
- Arbogast, A. F., 1996b, Stratigraphic evidence for late-Holocene eolian sand mobilization and soil formation on the Great Bend Sand Prairie: *Journal of Arid Environments* v. 34, p. 403-414.
- Arbogast, A. F., and Johnson, W. C., 1997, Late-Quaternary landscape response to environmental change in south-central Kansas: *The Annals of Association of American Geographers* (Unpublished Manuscript).
- Aucour, A-M., Hillaire-Marcel, C., and Bonnefille, R., 1994, Late Quaternary biomass changes in a highland peatbog from equatorial Africa (Burundi): *Quaternary Research*, v. 41, p.225-233.
- Axelrod, D. I., 1985, Rise of the grassland biome, central North America: *The Botanical Review*, v. 51, p.163-201.
- Banerjee, S. K., 1994, Contributions of fine-grained magnetism to reading the global paleoclimate record: *Journal of Applied Physics*, v. 75, p. 5925-5930.
- Banerjee, S. K., 1995, Chasing the paleomonsoon over China: its magnetic proxy record: *Geology Today*, v. 5, p. 93-97.
- Banerjee, S. K, Hunt, C. P., and Liu, X. M., 1993, Separation of local signals from the regional paleomonsoon record of the Chinese Loess Plateau: a rock magnetic approach: *Geophysical Research Letters*, v. 20, p. 843-846.
- Banerjee, S. K., King, J., and Marvin, J., 1981, A rapid method for magnetic granulometry with applications to environmental studies: *Geophysical Research Letters*, v. 8, p. 333-336.
- Bard, E., Arnold, M., Fairbanks, R. G., and Hamelin, B., 1993,  $^{230}\text{Th}$ - $^{234}\text{U}$  and  $^{14}\text{C}$  ages obtained by mass spectrometry on corals: *Radiocarbon*, v. 35, p. 191-199.
- Bard, E., Arnold, M., Fairbanks, R. G., Maurice, P., Dupart, J., Moyes, J., and Duplessy, J-C, 1987, Retreat velocity of the North Atlantic polar front during the last deglaciation determined by  $^{14}\text{C}$  accelerator mass spectrometry: *Nature*, v. 328, p. 791-794.
- Barnosky, C. W., Grim, E. C., and Wright, H. E., Jr., 1987, Towards a postglacial history of the northern Great Plains: a review of the paleoecological problems: *Annals of Carnegie Museum* v., 56, p.259-273.
- Bayne, C. K., and O'Connor, H. G., 1968, Quaternary System, *in* Zeller, D. E. ed., *The stratigraphic succession in Kansas*, Kansas Geological Survey Bulletin, v. 189, p. 59-67.
- Beer, J., Shen, C., Heller, F., Liu, T-S., Bonani, G., Dittrich, B., Suter, M., and Kubik, P. W., 1993,  $^{10}\text{Be}$  and magnetic susceptibility in Chinese loess: *Geophysical Research Letter*, v. 20, p. 57-60.
- Béget, J. E., and Hawkins, D., 1989, Influence of orbital parameters on Pleistocene loess deposition in central Alaska: *Nature*, v. 337, p. 151-153.
- Béget, J. E., Stine D. B., and Hawkins D. B., 1990, Paleoclimatic forcing of magnetic susceptibility variations in Alaskan loess during the late Quaternary: *Geology*, v. 18, p. 40-43.

- Benedict, J. B., and Olson, B. L., 1978, The Mount Albion complex-a study of prehistoric man and Altithermal: Research Report of the Center for Mountain Archaeology, v.1, 213 p.
- Bettis, E. A., III, ed., 1990, Holocene alluvial stratigraphy and selected aspects of the Quaternary history of western Iowa: *Midwestern Friends of the Pleistocene*, University of Iowa, Quaternary Studies Group Contribution 36, 197 p.
- Bird, M. I., Quade, J., Chivas, A. R., Fifield, L. K., Allan, G. L., and Head, M. J., 1994, The carbon isotope composition of organic matter occluded in iron nodules: *Chemical Geology*, v. 114, p. 269-279.
- Birkeland, P. W., 1984, *Soils and Geomorphology*: Oxford University Press.
- Bloemendal, J., and deMenocal, P., 1989, Evidence for a change in the periodicity of tropical climate cycles at 2.4 Myr from whole-core magnetic susceptibility measurements: *Nature*, v. 342, p. 897-900.
- Bloemendal, J., Liu, X. M., and Rolph, T. C., 1995, Correlation of the magnetic susceptibility stratigraphy of Chinese loess and the marine oxygen isotope record: chronological and paleoclimatic implications: *Earth and Planetary Science Letters*, v. 131, p. 1-380.
- Boellstorff, 1978, chronology of some late Cenozoic deposits from the central United States and the ice ages: *Nebraska Academy of Sciences Transactions*, v. 6, p. 35-49.
- Bond, G., Heinrich, H., Broecker, W., Labeyrie, L., McManus, J., Andrews, J., Huon, S., Jantschick, R., Clasen, S., Simet, C., Tedesco, K., Klas, M, Bonani, G., and Ivy, S., 1992, Evidence for massive discharges of icebergs into the North Atlantic ocean during the last glacial period: *Nature*, v. 360, p. 245-249.
- Borchert, J. R., 1950, Climate of the central North America Grasslands: *Annals of Association of American Geographers*, v. 40, 1-39.
- Borchert, J. R., 1971, The Dust Bowl in the 1970s: *Annals of Association of American Geographers*, v. 61, 1-22.
- Bozarth, S. R., 1991, Paleoenvironmental reconstruction of the La Sena Site (25FT177) based on opal phytolith analysis, Ms. on file, Nebraska State Historical Society, 17 p.
- Bozarth, S. R., 1996, Pollen and opal phytolith evidence of prehistoric agriculture and wild plant utilization in the Lower Verde River Valley, Arizona. Unpublished Ph. D. dissertation, Univ. Of Kansas, Lawrence KS, 428 p.
- Bozarth, S., and Dort, W., 1992, Paleoenvironmental reconstruction of the Sargent site: a fossil biosilicate analysis, Ms. on file, University of Kansas, Department of Geography.
- Bradbury, J. P., 1980, Late Quaternary vegetation history of the central Great Plains and its relationship to eolian processes in the Nebraska Sand Hill: *U.S. Geological Survey Professional Paper 1120-C*, 8 p.
- Bradley, R. S., 1985, *Quaternary Paleoclimatology: Methods of Paleoclimatic Reconstruction*, Boston, Allen & Unwin.
- Broecker, W. S., 1994, Massive iceberg discharges as triggers for global climate change: *Nature*, v. 372, p. 421-424.

- Broecker, W. S., Andre, M., Wolfli, W., Oeschger, H., Bonani, G., Kennett, J., and Peteet, D., 1988, The chronology of the last deglaciation: Implications for the cause of the Younger Dryas event: *Paleoceanography*, v. 3, p. 1-19.
- Broecker, W. S., Kennett, J. P., Flower, B. P., Teller, J. T., Trumbore, S., Bonani, G., and Wolfli, W., 1989, Routing of melt water from the Laurentide Ice Sheet during the Younger Dryas cold episode: *Nature*, v. 341, p. 318-321.
- Brown, D. A., 1984, Prospects and limits of a phytolith key for grasses in the central United States: *Journal of Archaeological Science*, v. 11, p. 345-368.
- Bryson, R., 1983, Comments on the climatic environments of the Great Plains, *in* Caldwell, W. W., Schultz, C.B., and Stout, T. M., eds., *Man and the Changing Environments in the Great Plains*. Transactions of the Nebraska Academy of Sciences, v. 11, p.57-60.
- Bryson, R. A., Baerreis, D. A., and Wendland, W. M., 1970, The character of Late-Glacial and Post-Glacial climatic changes, *in* Dort, W. Jr., and Jones, J. K. Jr. eds., *Pleistocene and recent environments of the Central Great Plains*, p. 53-74., KU, Lawrence, Kansas.
- Boutton, T. W., Harrison, A. T., and Smith, B. N., 1980, Distribution of biomass of species differing in photosynthetic pathway along an altitudinal transect in southeastern Wyoming grassland: *Oecologia*, v. 45, p. 287-298.
- Burbank, D. W., and Li, J., 1985, Age and paleoclimatic significance of the loess of Lanzhou, North China: *Nature*, v. 316, p. 429-430.
- Burke, I. C., Kittel, T. G. F., Laurenroth, W. K., Snook, P., Yonker, C. M., and Parton, W. J., 1991, Regional analysis of the central Great Plains: sensitivity to climate variability: *Bioscience*, v. 41, p. 685-692.
- Butler, R. F., 1992, *Paleomagnetism: Magnetic Domains to Geologic Terranes*, Blackwell Scientific Publications, Boston, 319 p.
- Caspall, F. C., 1970, The spatial and temporal variations in loess deposition in northeastern Kansas, Ph.D. dissertation, University of Kansas, Lawrence, KS, 294 p.
- Caspall, F. C., 1972, A note on the origin of the Brady paleosol in northern Kansas: *Proceedings of the Association of American Geographers*, v. 4, p. 19-24.
- Catt, J. A., 1991, Soils as indicators of Quaternary climatic change in mid-latitude regions: *Geoderma*, v. 51, p. 167-187.
- Catt, J. A., 1995, Soils in aeolian sequences as evidence of Quaternary climatic change: problems and possible solutions: *Quaternary Proceedings*, n. 4, p. 59-68.
- Cerling, T. E., 1984, The stable isotope composition of modern soil carbonate and its relationship to climate: *Earth and Planetary Science Letters*, v. 71, p.229-240.
- Cerling, T. E., and Quade, J., 1993, Stable carbon and oxygen isotope in soil carbonate. *in* Swart, P. K., Lohmann, K. C., McKenzie, J., and Savin, S. eds., *Climate Change in Continental Isotopic Records*, American Geophysical Union, Washington, D. C., p. 217-231.
- Cerling, T. E., Quade, J., Wang, Y., and Bowman, J. R., 1989, Carbon isotope in soils and paleosols as ecology and paleoecology indicators: *Nature*, v. 341, p. 138-139.

- Chamberlin, T. C., 1897, Studies for Students: The method of multiple working hypotheses: *Journal of Geology*, v. 5, p. 837-848.
- Chang, S. R., and Kirschbank, J. K., 1985, possible biogenic magnetite fossils from the late Miocene Potamida clays of Crete, *in* Kirschbank, J. K., Jones, D. S., and MacFadden eds., *Magnetic Biomineralization and magnetoreception in Organisms*, Plenum Press, New York, p. 647-669.
- Cisowski, S., 1981, Interacting vs. non-interacting single domain behavior in natural and synthetic samples: *Physics of the earth and Planetary Interiors*, v. 26, p.56-62.
- Clapperton, C. M., Hall, M., Mothes, P., Hole, M. J., Still, J. W., Helmens, K. F., Kuhry, P., and Gemmell, A. M. D., 1997, A Younger Dryas in the equatorial Andes: *Quaternary Research*, v. 47, p. 13-28.
- Clemens, S. C., and Prell, W. L., 1992, Comments on "Paleoclimatic significance of the mineral magnetic record of Chinese loess and paleosols: *Quaternary Research*, v. 38, p. 265-267.
- COHMAP Members, 1988, Climatic changes of the Last 18,000 Years: Observations and model simulations: *Science*, v. 241, p.1043-1052.
- Collinson, D. W., 1983, *Methods in Rock Magnetism and Paleomagnetism: Techniques and instrumentation*, Chapman and Hall, London, 503 p.
- Condra, G. E., Reed, E. C., and Gordon, E. D., 1950, Correlation of the Pleistocene deposits of Nebraska: *Nebraska Geological Survey Bulletin* 15, 74 p.
- Cornell, R. M., and Schwertmann, U., 1996, *The Iron Oxide: Structure, Properties, Reactions, Occurrence, and Uses*, VCH Verlagsgesellschaft, Weinheim, Germany, 573 p.
- Crockford, R. H., and Willet, I. R., 1995, Magnetic properties of two soils during reduction, drying and re-oxidation: *Australian Journal of Soil Research*, v. 33, p. 597-609.
- Crowley, T. J., 1983, The geologic record of climatic change: *Reviews of Geophysics and Space Physics*, v. 21, p. 828-877.
- Cui, Y., Verosub, K. L., and Roberts, A. P., 1994, The effects of low-temperature oxidation on large multi-domain magnetite: *Geophysical Research Letters*, v. 21, p. 757-760.
- Curry, B. B., and Follmer, L. R., 1992, The last interglacial-glacial transition in Illinois: 123-25 ka, *in* Clark, P. U., and Lea, P. D., eds., *The Last Interglacial-Glacial Transition in North America: Boulder, Colorado*, Geological Society of America Special Paper 270, p. 71-88.
- Dalan, R. A., and Banerjee, S. K., 1996, Soil magnetism, an approach for examining archaeological landscapes: *Geophysical Research Letters*, v. 23, p. 185-188.
- Daniels, R. B., Handy, R. L., and Simonson, G. H., 1960, Dark-colored bands in the thick loess of western Iowa: *Journal of Geology*, v. 68, p. 450-458.
- Dansgaard, W., Clausen, H. B., Gundestrup, N., Johnsen, S. J., and Rygner, C., 1985, Dating and climatic interpretation of two deep Greenland ice cores: *American Geophysical Union Geophysical Monograph* 33, p. 71-76.
- Dansgaard, W., Johnsen, S. J., Clauson, H. B., Dahl-Jehnsen, D., Gundestrup, N. S., Hammer, C. U., Hvidberg, C. S., Steffenson, J. P., Steinbjornsdottir, A. E., Joujel,

- J., and Bond, G., 1993, Evidence for general instability in past climate from a 250-kyr ice-record: *Nature*, v. 364, p. 218-220.
- Dansgaard, W., White, W. C., and Johnsen, S. J., 1989, The abrupt termination of the Younger Dryas climate event: *Nature*, v. 339, p. 532-533.
- Day, R., Fuller, M. D., and Schmidt, V. A., 1976, Magnetic hysteresis properties of synthetic titanomagnetites: *Journal of Geophysical Research*, v. 81, p. 260-267.
- Dearing, J. A., 1994, *Environmental Magnetic Susceptibility*, Chi Publishing, Kenilworth, 104 p.
- Dearing, J. A., Elner, J. K., and Happey-Wood, C. M., 1981, Recent sediment flux and erosional processes in a Welsh upland lake-catchment based on magnetic susceptibility measurements: *Quaternary Research*, v. 16, p. 356-372.
- Dearing, J. A., Lee, J. A., and White, C., 1995, Mineral magnetic properties of acid gleyed soils under oak and Corsican Pine: *Geoderma*, v. 68, p. 309-319.
- Dearing, J. A., Livingstone, I., and Zhou, L., 1996, A late Quaternary magnetic record of Tunisian loess and its climatic significance: *Geophysical Research Letters*, v. 23, p. 189-192.
- Dearing, J. A., Maher, B. A., and Oldfield, F., 1985, Geomorphological linkages between soils and sediments: the role of magnetic measurements *in* Richard, K. S., Arnett, R. R., and Ellis S. eds., *Geomorphology and Soils*: George Allen and Unwin, London, p. 245-266.
- Dearing, J. A., Dann, R. J. L., Hay, K. L., Lees, J. A., Loveland, P. J., Maher, B. A., and O'Grady, K., 1996, Frequency-dependent susceptibility measurements of environmental materials: *Geophysical Journal International*, v. 124, p. 228-240.
- Dearing, J. A., Hay, K. L., Baban, S. M. J., Huddleston, A. S., Wellington, E. M. H., and Loveland, P. J., 1996, Magnetic susceptibility of soil: an evaluation of conflicting theories using a national data set: *Geophysical Journal International*, v. 127, p. 728-734.
- Dearing, J.A., Bird, P.M., Dann, R. J. L., and Benjamin, S. F., 1997, Secondary ferrimagnetic minerals in Welsh soils: a comparison of mineral magnetic detection methods and implications for mineral formation: *Geophysical Journal International*, v. 130, p. 727-736.
- Deevey, E. S., and Flint, R. F., 1957, Postglacial Hypsithermal interval: *Science*, v. 125, p.182-184.
- Deines, P., 1980, The isotopic composition of reduced organic carbon *in* Fritz, P., and Fontes, J. Ch. eds., *Handbook of Environmental Isotope Geochemistry-v.*; *The Terrestrial Environment*: Elsevier, Amsterdam, p. 329-406.
- Delaune, R. D., 1986, The use of  $^{13}\text{C}$  signature of  $\text{C}_3$  and  $\text{C}_4$  plants in determining past depositional environments in rapidly accreting marshes of the Mississippi River deltaic plain, Louisiana, USA: *Chemical Geology*, v. 59, p. 315-320.
- Denton, G. H., and Hughes, T. J., eds., 1981, *The Last Great Ice Sheets*, John Wiley & Sons, 484 p.
- Derbyshire, E., 1995, Aeolian sediments in the Quaternary record: An introduction: *Quaternary Science Reviews*, v. 14, p. 641-643.

- Derbyshire, E., Kemp, R., and Meng, X., 1995, Variation in loess and paleosol properties as indicators of paleoclimatic gradients across the loess Plateau of North China: *Quaternary Science Reviews*, v. 14, p. 681-697.
- Diekmeyer, E. C., 1994, Characterizations and paleoclimatic inferences from the post-Illinoian stratigraphic sequences at two central Great Plains sites: Unpublished M.A. Thesis, Univ. Of Kansas.
- Diester-Haass, L. D., Schrader, H. J., and Theide, J., 1973, Sedimentological and paleoclimatological investigations of two pelagic ooze cores off Cape Barbas, North-West Africa: *Meteor Forshungs Ergebnisse*, v. 16, p. 19-66.
- Ditlevsen, P. D., Svensmark, H., and Johnsen, S., 1996, Contrasting atmospheric and climate dynamics of the last-glacial and Holocene periods: *Nature*, v. 379, p. 810-812.
- Dort, W. R.,  $^{14}\text{C}$  assays and associated  $\delta^{13}\text{C}$  data from the Sargent site, Nebraska, Unpublished Manuscript.
- Dort, W. R. Jr., and Knox, J. C. Jr. (editors), 1970, *Pleistocene and Recent Environments of the Central Great Plains*, University of Kansas Press, Lawrence.
- Dreeszen, V. H., 1970, The Stratigraphic framework of Pleistocene glacial and periglacial deposits in the Central Plains, *in* Dort, W. Jr., and Knox J. C. Jr., eds., *Pleistocene and Recent environments of the Central Great Plains*, Univ. of Kansas, Lawrence, Kansas, p.9-22.
- Dudziak, A., and Halas, S., 1996, Influence of freezing and thawing on the carbon isotope composition in soil  $\text{CO}_2$ : *Geoderma*, v. 69, p. 209-216.
- Duller, G. A. T., 1996, Recent developments in luminescence dating of Quaternary sediments: *Progress in Physical Geography*, v. 20, p. 127-145.
- Dunlop, D. J., 1973, Superparamagnetic and single domain threshold sizes in magnetite: *Journal of Geophysical Research*, v. 78, p. 1780-1793.
- Dunlop, D. J., 1981, The rock magnetism of fine particles: *Physics of the Earth and Planetary Interiors*, v. 26, p. 1-26.
- Dunlop, D. J., 1990, Developments in rock magnetism: *Reports in Progress in Physics*, v. 53, p. 707-792.
- Dunlop, D. J., Argyle, K. S., and Bailey, M. E., 1990, High-temperature technique for measuring microcoercivity, crystallite size and domain state: *Geophysical Research Letters*, v. 17, p. 767-770.
- Duplessy, J-C., and Overpeck, J. eds., 1994, *PAGES/CLIVAR Intersection, Report of a Joint International Geosphere Biosphere -World Climate Research Programmes Workshop*, 44 p.
- Eick, P. M., and Schlinger, C. M., 1990, The use of magnetic susceptibility and its frequency dependence for delineation of a magnetic stratigraphy in ash-flow tuffs: *Geophysical Research Letters*, v. 17, p. 783-786.
- Ellwood, B. B., Peter, D. E., Balsam, W., and Schieber, J., 1995, Magnetic and geochemical variations as indicators of paleoclimate and archaeological evolution: Examples from 41TR68, Fort Worth, Texas: *Journal of Archaeological Science*, v. 22, p. 409-415.

- Ellwood, B. B., Petruso, K. M., Harrold, F. B., and Korkuti, M., 1996, Paleoclimate characterization and intra-site correlation using magnetic susceptibility measurements: an example from Konispol Cave, Albania: *Journal of Field Archaeology*, v. 23, p. 263-271.
- Evans, M. E., and Heller, F., 1994, Magnetic enhancement and paleoclimate: study of a loess/paleosol couplet across the Loess Plateau of China: *Geophysics Journal International*, v. 117, p. 257-264.
- Eyre, J. K., and Shaw, J., 1994, Magnetic enhancement of Chinese loess-the role of  $\gamma\text{Fe}_2\text{O}_3$ ? : *Geophysics Journal International*, v. 117, p. 265-271.
- Farr, M. R., Park, K., and Johnson, W. C., 1993, A detailed rock magnetic record from Quaternary loess and associated soils at the Eustis Ash Pit: *EOS Transactions of American Geophysical Union*, v. 74, No. 43, p. 210.
- Farr, M. R., Park, K., and Johnson, W.C., 1994, Rock magnetic properties of the Sangamon soil from southwestern Nebraska: Lack of evidence for ultrafine ferrimagnetic grains. *Geological Society of America, Abstracts with Programs*, v. 26, n. 7, A-237.
- Fassbinder, J. W. E., Stanjek, H., and Vali, H., 1990, Occurrence of magnetic bacteria in soil: *Nature*, v. 343, p. 161-163.
- Feitknecht, W., and Gallagher, K. J., 1970, Mechanism for the oxidation of  $\text{Fe}_3\text{O}_4$ : *Nature*, v. 228, p. 548-549.
- Feng, Z., and Johnson W. C., 1995, Factors affecting the magnetic susceptibility of a loess-soil sequence, Barton County, Kansas, USA: *Catena*, v. 24, p. 25-37.
- Feng, Z., Johnson W. C., Lu, Y-C, and Ward, P. A. III, 1994, Climatic signals from loess-soil sequences in the central Great Plains: *Palaeogeography, Palaeoclimatology, and Palaeoecology*, v. 110, p.345-358.
- Feng, Z., Johnson W. C., and Diffendal, R. F., 1994, Environment of eolian deposition in south-central Nebraska during the Last Glacial maximum: *Physical Geography*, v. 15, p.249-261
- Feng, Z., Johnson W. C., Sprowl, D. R., and Lu, Y-C, 1994, Temporal variations in loess depositional environment in central Kansas during the past 400,000 years: *Earth Surface Processes and Landforms*, v. 19, n. 2, p. 55-68.
- Fillippelli, G. M., 1997, Intensification of the Asian monsoon and a chemical weathering event in the late Miocene-early Pliocene: Implications for late Neogene climate change: *Geology*, v. 25, p. 27-30.
- Fine, P., Singer, M. J., 1988, Contribution of ferrimagnetic minerals to oxalate- and dithionite-extractable iron: *Soil Science Society America Journal*, v. 53, p. 191-196.
- Fine, P., Singer, M. J., La Ven, R., Verosub, K. and Southard, R. J., 1989, Role of pedogenesis in distribution of magnetic susceptibility in two California chronosequences: *Geoderma*, v. 44, p. 287-306.
- Fink, J., and Kukla G. J., 1977, Pleistocene climates in central Europe: at least 17 interglacial after the Olduvai Event: *Quaternary Research*, v. 7, p. 363-371.
- Forman, S. L., 1991, Late Pleistocene chronology of loess deposition near Luochuan, China: *Quaternary Research*, v. 36, p. 19-28.

- Forman, S. L., Bettis, E. A., Kemmis, T. L., and Miller, B. B., 1992, Chronological evidence for multiple periods of loess deposition during the late Pleistocene in Missouri and Mississippi River valleys, United States-implication for the activity of the Laurentide Ice Sheet: *Palaeogeography, Palaeoclimatology, Palaeoecology*, v 93, p. 71-83.
- Forster, T., Evans, M. E., and Heller F., 1994, The frequency dependence of low field susceptibility in loess sediments: *Geophysical Journal International*, v. 118, p. 636-642.
- Forster, T., and Heller, F., Loess deposits from the Tajik depression (Central Asia): Magnetic properties and paleoclimate: *Earth and Planetary Science Letters*, v. 128, p. 511-512.
- Frakes, L. A., and Sun, Z., 1994, A carbon isotope record of upper Chinese loess sequence: Estimates of plant types during stadials and interstadial: *Palaeogeography, Palaeoclimatology, Palaeoecology*, v. 108, p. 183-189.
- Fredlund, G. G., 1991, A comparison of Pleistocene and Holocene vegetation in the central Great Plains of North America-palynological evidence from Cheyenne Bottoms, Kansas. Ph.D. dissertation, University of Kansas, 303 p.
- Fredlund, G. G., 1993, Paleoenvironmental interpretations of stable carbon, hydrogen, and oxygen isotopes from opal phytoliths, Eustis ash pit, Nebraska. *in* Pearsall, D. M., and Piperno, D. R. eds., *Current Research in Phytolith Analysis: Applications in Archaeology and Paleoecology*, MASCA, University of Pennsylvania, Philadelphia, p.37-46.
- Fredlund, G. G., 1995, A Quaternary pollen record from the Cheyenne Bottoms, Kansas: *Quaternary Research*, v. 43, p. 67-79.
- Fredlund G. G., and Jaumann P. J., 1987, Late Quaternary palynological and paleobotanical records from the central Great Plains, *in* W. C. Johnson ed: *Quaternary Environments of Kansas*, p.167-178.
- Fredlund, G. G., and Johnson, W. C., 1985, Palynological evidence for late Pleistocene vegetation from Sanders's well locality in east-central Kansas (abs.) Institute for Tertiary-Quaternary Studies, 4th Annual Symposium, Lawrence Kansas, Programs with Abstracts, p.15.
- Fredlund, G. G., and Tieszen, L. L., 1994, Modern phytolith assemblages from the North American Great Plains: *Journal of Biogeography*, v. 21, p. 321-335.
- Fredlund, G. G., and Tieszen, L. L., 1997, Phytolith and carbon isotope evidence for late Quaternary vegetation and climate change in the southern Black Hills, South Dakota: *Quaternary Research*, v. 47, p. 206-217.
- Fredlund, G. G., Johnson, W. C., and Dort, W., Jr., 1985, A preliminary analysis of opal phytoliths from the Eustis ash pit, Frontier County, Nebraska: *TER-QUA Symposium Series*, v.1, p. 147-162. Nebraska Academy of Sciences, Institute for Tertiary-Quaternary Studies.
- Frye, J. C., and Fent, O. S., 1947, The Late Pleistocene Loesses of Central Kansas: State Geological Survey of Kansas, Bull. 70 (3), Lawrence, Kansas
- Frye, J. C., and Leonard, B. A., 1951, Stratigraphy of late Pleistocene loesses of Kansas: *Journal of Geology*, v. 59, p. 287-305.

- Frye, J. C., and Leonard, B. A., 1952, Pleistocene Geology of Kansas: State Geological Survey of Kansas, Bulletin 99.
- Frye, J. C., and Leonard, B. A., 1955, The Brady soil and subdivision of Post-Sangamonian time in the Midcontinent region. *American Journal of Science*, v. 253, p. 358-364.
- Frye, J. C., and Leonard, B. A., 1957, Ecological interpretations of Pliocene and Pleistocene stratigraphy in the Great Plains region: *American Journal of Science*, v. 255, p. 1-11.
- Frye J. C., Willman H. B., and Black R. F., 1965, Outline of Glacial Geology in Illinois and Wisconsin, *in* Wright, H. E. ed., *The Quaternary of the United States*, p. 42-61.
- Frogatt, P. C., 1988, Paleomagnetism of Last Glacial loess from two sections in New Zealand, *in* Eden, D. N., and Furkert, R. J, eds., *Loess, Its Distribution, Geology and Soils*: A.A. Balkema, Rotterdam, p. 59-68.
- Fullerton, D. S., and Richmond, G. M., 1986, Comparison of the marine oxygen isotope record, the eustatic sea level record, and the chronology of glaciation in the United States of America. *in*, Sibrava, V., Bowen, D. Q., and Richmond, G. M., eds., *Quaternary Glaciations in the Northern Hemisphere*, *Quaternary Science Reviews*, v. 5, p. 197-200.
- Gale, S. J., and Hoare, P. G., 1991, *Quaternary Sediments: Petrographic Methods for the Study of Unlithified Rocks*, Halsted Press, New York 323 p.
- Geiß, C. E., Heider, F., and Soffel, H. C., 1996, Magnetic domain observations on magnetite and titanomaghemite grains (0.5-10 $\mu$ m): *Geophysical Journal International*, v. 124, p. 75-88.
- Graham, R. W., 1987, Late Quaternary mammalian faunas and paleoenvironments of the southwestern plains of the United States. *in* Graham, R. W., Semken, H. A., Jr., Graham, M.A. eds., *Late Quaternary Biogeography and Environments of the Great Plains and Prairies*, Illinois State Museum, Springfield, p.24-86.
- GRIP Members, 1993, Climate instability during the last interglacial period recorded in the GRIP ice core: *Nature*, v. 364, p. 203-207.
- Grimley, D. A., 1996, Stratigraphy, magnetic susceptibility, and mineralogy of loess-paleosol sequences in southwestern Illinois and eastern Missouri, Unpublished Ph. D dissertation, University of Illinois, Urbana-Champaign. Illinois.
- Grimley, D. A., and Johnson, W. H., 1991, Stratigraphy and magnetic susceptibility of four Quaternary loesses and paleosols near Thebes, Illinois. *Geological Society of America Abs. Programs*, v.16, p.15-16.
- Gottula, J. J., and Souders, V. L., 1989, Radiocarbon dates in an anomalous sequence within the Gilman Canyon Formation near Ord, Nebraska (abs.): *Proceedings of the Nebraska Academy of Sciences*, p.50.
- Goudie, A., 1983, *Environmental Change*, Clarendon Press, Oxford, 258 p.
- Grüger, J., 1973, Studies on the late-Quaternary vegetation history of northeastern Kansas: *Geological Society of America Bulletin*, v. 84, p. 239-250.

- Gu, Z., Liu, R., and Liu, Y., 1991, Response of the stable isotope composition of loess-paleosol carbonate to paleoenvironmental changes. *in* Liu, T., Ding, Z., and Guo Z. eds., *Loess, environmental and global change*: Science Press, Beijing, p.82-92.
- Guillet, B., Faivre, P., Mariotti, A., and Khobzi, J., 1988, The  $^{13}\text{C}/^{12}\text{C}$  ratios of soil organic matter as a means of studying the past vegetation in intertropical regions: examples from Columbia (South America): *Palaeogeography, Palaeoclimatology, and Palaeoecology*, v. 65, p. 51-58.
- Haas, H., Holliday, V., and Stuckenrath, R., 1986, Dating of Holocene stratigraphy with soluble and insoluble organic fractions at the Lubbock Lake archaeological site, Texas: an ideal case study: *Radiocarbon*, v. 28(2A), p. 473-485.
- Hall, S. A., and Valastro, S., Jr., 1995, Grassland vegetation in the Southern Great Plains during the Last Glacial Maximum: *Quaternary Research*, v. 44, p. 237-245.
- Han, J., Hus, J. J., Paepe, R., Vandenberghe, R. E., and Liu, T., 1991, The rock magnetic properties of the Malan and Lishi formations in the Loess Plateau of China, *in* Liu T., Ding, Z., and Guo Z. eds., *Loess, environment and global change*: Science Press, Beijing, China, p. 30-47.
- Han, J., Keppens, E., Liu, T., Paepe, R., and Jiang, W., 1997, Stable isotope composition of the carbonate concretion in loess and climate change: *Quaternary International*, v. 37, p. 37-43.
- Hanna, E., 1996, The role of Antarctic sea ice in global climate change: *Progress in Physical Geography*, v. 20, p. 371-401.
- Harasko, G., Pfutzner, H., and Futschick, 1994, On the effectiveness of magnetotactic bacteria for visualizations of magnetic domains: *Journal of Magnetism and Magnetic Materials*, v. 133, p.409-412.
- Hartstra, R. L., 1982, Grain-size dependence of initial susceptibility and saturation magnetization-related parameters of four natural magnetites in the PSD-MD range: *Geophysics Journal of Royal Astronomical Society*, v. 71, p. 477-495.
- Hartstra, R. L., 1983, TRM, ARM and Isr of two natural magnetites of MD and PSD grain size: *Geophysics Journal of Royal Astronomical Society*, v. 73, p. 719-737.
- Hayward, R. K., and Lowell, T. V., 1993, Variations in loess accumulation rates in the mid-continent, United States, as reflected by magnetic susceptibility: *Geology*, v. 21, p. 821-824.
- Heinrich, H., 1988, Origin and consequences of cyclic ice rafting in the northeast North Atlantic Ocean during the past 130,000 years: *Quaternary Research*, v. 29, p. 143-152.
- Heller, F., Liu, X., Liu, T, and Xu, T. 1991, Magnetic susceptibility of loess in China: *Earth and Planetary Science Letters*. v.103, p. 301-310.
- Heller, F., and Evans, M., 1995, Loess magnetism: *Reviews of Geophysics*, v. 33, p.211-240.
- Heller, F., and Liu, T. S., 1986, Paleomagnetic and sedimentary history from magnetic susceptibility of loess in China: *Geophysical Research Letters*, v. 13, p. 1169-1172.
- Heller, F., Shen, C. D., Beer, J., Liu, X. M., Liu, T. S., Bronger, A., Suter, M., and Bonani, G., 1993, Quantitative estimates of pedogenic ferromagnetic mineral

- formation in Chinese loess and paleoclimatic implications: *Earth and Planetary Science Letters*, v. 114, p. 395-390.
- Henshaw, P. C., Jr., and Merrill, R. T., 1980, Magnetic and chemical changes in marine sediments: *Reviews of Geophysics and Space Physics*, v. 18, p. 483-504.
- Hibbard, C. W., Frye, J. C., and Leonard A. B., 1944, Reconnaissance of Pleistocene deposits in north-central Kansas: *Kansas Geological Survey Bulletin*, v. 52, p. 1-28.
- Hilton, J., 1986, Normalized magnetic parameters and their applicability to paleomagnetism and environmental magnetism: *Geology*, v. 14, p. 887-889.
- Hopkins, D. M., 1975, Time-stratigraphic nomenclature for the Holocene Epoch: *Geology*, v.3, p. 10.
- Hovan, S. A., Rea, D. K., Pisias, N. G., and Shackleton, N. J., 1989, A direct link between the China loess and marine  $\delta^{18}\text{O}$  records: Aeolian flux to the north Pacific: *Nature*, v. 340, p. 296-298.
- Howell, P., 1995, ARAND software, Providence, Rhode Island, Brown University.
- Hrouda, F., Jelinek, V., and Zapletal, K., 1997, Refined technique for susceptibility resolution into ferromagnetic and paramagnetic components based on susceptibility temperature-variation measurement: *Geophysical Journal International*, v. 129, p. 715-719.
- Humphrey, J. D., and Ferring C. R., 1994, Stable isotopic evidence for latest Pleistocene and Holocene climatic change in north-central Texas: *Quaternary Research*, v. 41, p.200-213.
- Hunt, C. P., Banerjee, S. K., Han, J., Solheid, P., Oches, E., Sun, W., and Liu, T., 1995, Rock-magnetic proxies of climate change in the loess-paleosol sequences of the western Loess Plateau of China: *Geophysical Journal International*, v. 123, p. 232-244.
- Hunt, C. P., Singer, M. J., Kletetschka, G., TenPas, J., and Verosub, K., 1995, Effects of citrate-bicarbonate-dithionite treatment on fine-grained magnetite and maghemite: *Earth and Planetary Science Letters*, v. 130, p. 87-94.
- Hus J. J., and Geeraerts, R., 1986, Paleomagnetic and rock magnetic investigation of Late Pleistocene loess deposits in Belgium: *Physics of the Earth and Planetary Interiors*, v. 44, p. 21-40.
- Hus, J. J., and Han J., 1992, The contribution loess magnetism in China to retrieval of past global changes-some problems: *Physics of the Planetary Interiors*, v. 70, p.154-168.
- Imbrie, J., and Imbrie, J. Z., 1980, Modeling the climatic response to orbital variations: *Science*, v. 207, p. 943-952.
- Imbrie, J., and 8 others, 1984, The orbital theory of Pleistocene climate; Support from a revised chronology of the marine  $\delta^{18}\text{O}$  record, *in*, Berger, A., Imbrie., J., Hays, J. Kukla, G., and Saltzman, B. eds., *Milankovitch and Climate, Part 1*: Dordrecht, Reidel, p.269-305.
- Jasper, J. P., Gargosian, R. B., 1989, Glacial-interglacial climatically forced  $^{13}\text{C}$  variations in sedimentary organic matter: *Nature*, v. 342, p.60-62.

- Jaumann, P., 1994, Century to millennium-scale Holocene climate variability at the prairie-forest border, west-central Minnesota: American Quaternary Association, Program and Abstracts, p. 220.
- Jenkins, G. M., and Watts, D. G., 1968, Spectral Analysis and Its Applications, Holden-Day, San Francisco, 525 p.
- Johnsen, S. J., Clausen, H. B., Dansgaard, W., Fuhrer, K., Gundestrup, N., Hammer, C. U., Iversen, P., Jouzel, J., Stauffer, B., and Steffenson, J. P., 1992, Irregular glacial interstadials recorded in a new Greenland ice core: *Nature*, v. 359, p. 311-313.
- Johnson W. C., 1990, Age determinations on the Gilman Canyon Formation and Brady paleosol in Kansas (abs.): American Quaternary Association, Program and Abstracts, p.21.
- Johnson, W. C., 1991 a, Buried soil surfaces beneath the Great Bend Prairie of central Kansas and archaeological implications: *Current Research in the Pleistocene*, v. 8, p. 108-110.
- Johnson, W. C., 1991 b, Late Pleistocene and Holocene eolian stratigraphy of the central Kansas and paleoenvironmental reconstructions (abs.). *Geological Society of America, Abstracts with Programs* 23: p. A284.
- Johnson, W. C. ed., 1993a, INQUA Paleopedology Commission 6 Field Guide, Kansas Geological Survey Open-File Report 93-30, 1993.
- Johnson, W. C., 1993b, Surficial geology and stratigraphy of Phillips county, Kansas, with emphasis on the Quaternary period: *Kansas Geological Survey Technical Series*, No.1.
- Johnson W. C., and Bozarth, S. R., 1996, Variation in opal phytolith assemblages as an indicator of late-Quaternary environmental change on Fort Riley, Kansas, Technical Report submitted to UASCERL.
- Johnson, W. C., and Logan, B., 1990, Geoarchaeology of the Kansas River basin, central Great Plains. *in*, Lasca, N. P., and Donahue, J. eds., *Archaeological geology of North America: Geological Society of America, Decade of North American Geology, Centennial Special Volume* 4, p.267-299.
- Johnson, W. C., and Martin, C. W., 1987, Holocene alluvial-stratigraphic studies from Kansas and adjoining states of the east-central Plains, *in* Johnson, W. C. ed., *Quaternary Environments of Kansas: Kansas geological Survey, Guidebook Series* 5, p. 109-122.
- Johnson, W. C., and May, D. W., 1992, The Brady Geosol as an indicator of the Pleistocene/Holocene boundary in the central Great Plains, Abstract with Programs AMQUA 1992.
- Johnson, W.C., and Muhs, D., 1996, Unpublished trace element data.
- Johnson, W. C., May, D. W., and Souders, V. L., 1990, Age and distribution of the Gilman Canyon Formation of Nebraska and Kansas, American quaternary Association, Programs with Abstracts.22, p. A87.
- Johnson W. C., Park, K., Diekmeyer E., and Muhs, D. R., 1993, Chronology, stratigraphy, and depositional environments of the late Wisconsin (Peoria) Loess

- of Kansas and Nebraska, Geological Society of America Abstract with Programs, A-59.
- Johnson, W. C., and Valastro, S., 1994, Laboratory preparation of soil and sediment samples for radiocarbon dating of humates (total, humic acid, and humin fractions): Kansas Geological Survey, Open File Report 94-50.
- Johnson, W. C., and Park, K., 1996, Loess-derived magnetic signatures of global warming events in the central Great Plains: Programs and Abstracts of the 14th American Quaternary Association Meeting, p. 171.
- Johnson, W. C., and Park, K., 1997 a, Late Wisconsinan and Holocene environmental history of the central Great Plains: in *Archaeology and Paleocology of the Central Great plains*, edited by J. L. Hofman, Arkansas Archaeological Survey Resources Series, p. 3-31.
- Johnson, W. C., and Park, K., 1997 b, Rock magnetic and carbon isotopic signals from the loess sequence on Fort Riley, Kansas: Abstract, Nineteenth Annual Flint Hills Archaeological Conference, Manhattan, KS.
- Johnson, W. C., Park, K., Isaacson, J. S., and Johnson, D. L., 1997, Late Pleistocene and Holocene environments on Fort Riley, Kansas: *Current Research in Pleistocene*, v. 14. (submitted).
- Johnson, W. H., Hansel, A. K., Bettis, E. A., III, Karrow, P. F., Larson, G. J., Lowell, T. V., and Schneider, A. F., 1997, Later Quaternary temporal and event classifications, Great Lakes Region, North America: *Quaternary Research*, v. 47, p. 1-12.
- Jones, R. L., and Beavers, A. H., 1964, A technique for magnetic susceptibility determination of soil materials: *Soil Science Society of America Proceedings*, v. 28, p. 47-49.
- Jordanova, D., Petrovsky, E., Jordanova, N., Evlogiev, J., and Butchvarova, V., 1997, Rock magnetic properties of recent soils from northeastern Bulgaria: *Geophysical Journal International*, v. 128, p. 474-488.
- Jouzel, J., Lorius, C., Petit, J. R., Genthon, C., Barkov, N. I., Kotlyakov, V. M., and Petrov, V. M., 1987, Vostok ice core: a continuous isotope temperature record over the last climatic cycle (160,000 years): *Nature*, v. 329, p.403-407.
- Keen, D. H., 1995, Molluscan assemblages from the loess of north central China: *Quaternary Science Reviews*, v. 14, p. 699-706.
- Kelly E. F., Amundson, R. G., Marino, B. D., and DeNiro, M. J., 1991, Stable carbon isotopic composition of carbonate in Holocene grassland soils: *Soil Science Society America Journal* v. 55, p.1651-1658.
- Kelly E. F., Amundson, R. G., Marino, B. D., and DeNiro, M. J., 1991, Stable isotope ratios of carbon in phytoliths as a quantitative method of monitoring vegetation and climate change: *Quaternary Research*, v. 35, p. 222-233.
- Kelly, E. F., Yonker, C., and Marino, B., 1993, Stable carbon isotope composition of paleosols: an application to Holocene, *in* Swart, P. K., Lohmann, K. C., McKenzie, J., and Savin, S., eds., *Climate Change in Continental Isotopic Records*, *Geophysical Monograph* v. 78, p. 233-239.

- Kemp, R. A., Derbyshire, E., Meng, X., Chen F., and Pan, B., 1995, Pedosedimentary reconstruction of a thick loess-paleosol sequence near Lanzhou in north-central China: *Quaternary Research*, v. 43, p. 30-45.
- Kent, D. V., 1982, Apparent correlations of paleomagnetic intensity and climatic records in deep-sea sediments: *Nature*, v. 299, p.538-539.
- King, J., Banerjee, S. K., Marvin, J., and Özdemir, Ö., 1982, A comparison of different magnetic methods for determining the relative grain size of magnetite in natural materials: some results from lake sediments: *Earth and Planetary Science Letters*, v. 59, p. 404-419.
- King, J., Banerjee, S. K., and Marvin, J., 1983, A new rock-magnetic approach to selecting sediments for geomagnetic paleointensity studies: application to paleointensity for the last 4000 years: *Journal of Geophysical Research*, v. 88, p. 5911-5921.
- King, J. E., 1973, Late Pleistocene palynology and biogeography of the western Missouri Ozarks: *Ecological Monographs*, v. 43, p. 539-565.
- Kletetschka, G., and Banerjee, S. K., 1995, Magnetic stratigraphy of Chinese loess as a record of natural fires: *Geophysical Research Letters*, v. 22, p. 1341-1343.
- Krishnamurthy, R. V., and Bhattacharya, S. K., Paleovegetational history in the Kashmir basin, India, derived from  $^{13}\text{C}/^{12}\text{C}$  ratio in paleosols: *Earth and Planetary Science Letters*, v. 95, p. 291-296.
- Krishnamurthy, R. V., DeNiro, M. J., and Pant, R. K., 1982, Isotope evidence for Pleistocene climatic changes in Kashmir, India: *Nature*, v. 298, p.640-641.
- Krishnamurthy, R. V., Syrup, K. A., Baskaran, M., and Long, A., 1995, Late glacial climate record of Midwestern United States from the Hydrogen isotope ratio of lake organic matter: *Science*, v. 269, p. 1565-1567.
- Küchler, A. W., 1972, The oscillation of the mixed prairies in Kansas: *Erdkunde*, v. 26, p. 120-129.
- Kukla, G. J., 1977, Pleistocene land-sea correlations I. Europe: *Earth Science Reviews*, v 13, p. 307-374.
- Kukla, G. J., 1987, Loess stratigraphy in Central China: *Quaternary Science Reviews*, v. 6, p. 191-219.
- Kukla, G. J., and An, Z., 1989, Loess stratigraphy in central China: *Palaeogeography, Palaeoclimatology, Palaeoecology*, v. 72, p. 203-225.
- Kukla, G., Heller, F., Liu, X. M., Xu, T. C., Liu, T. S., and An, Z., 1988, Pleistocene climates in China dated by magnetic susceptibility: *Geology*, v. 16, p. 811-814.
- Kunzig, R., 1996, In deep water: *Discover*, December 1996, p.86-96.
- Kurmann, M. H., 1985, An opal-phytolith and palynomorph study of extant and fossil soils in Kansas (U.S.A.): *Palaeogeography, Palaeoclimatology, Palaeoecology*, v. 49, p. 217-245.
- Kutzbach, J. E., 1981, Monsoon climate of the early Holocene-climatic experiment with the Earth's orbital parameters for 9,000 years ago: *Science*, v. 214, p. 61.
- Kutzbach, J. E., 1985, Modeling of paleoclimate: *Advances in Geophysics*, v. 28, p.159-196.

- Kutzbach, J. E., 1987, Model simulations of climatic patterns during the deglaciation of North America, *in* Ruddiman, W. F., and Wright, H. E. Jr., eds., North America and adjacent oceans during the last deglaciation, Geological Society of America, The Geology of North America, v. K-3, p. 425-446.
- Kutzbach, J. E., and Wright, H. E., 1985, Simulation of the climate of 18, 000 years BP: results for the North American/North Atlantic/European sector and comparison with the geological record of North America: *Quaternary Science Reviews*, v. 4: p. 147-187.
- Laird, K. R., Fritz, S. C., Maasch, K. A., and Cumming, B. F., 1996, Greater drought intensity and frequency before AD 1200 in the Northern Great Plains, USA: *Nature*, v. 384, p. 552-554.
- Le Borgne, E., 1955, Susceptibilité magnétique anormal de sol superficial: *Annals of Geophysics*, v. 11, p. 399-419.
- Lemke, R.W., Laird, W. M., Tipton M. J, Lindvall R. M., 1965, Quaternary geology of the Northern Great Plains: *in* The Quaternary of the United States, p. 15-27.
- Leonard, A. B., 1952, Illinoian and Wisconsinan molluscan faunas in Kansas: *University of Kansas Paleontological Contributions*, v. 4, p. 1-38.
- Leonard, A. B., 1959, Handbook of Gastropods in Kansas: *University of Kansas Museum of Natural History Publication* v. 20, p. 1-224.
- Leventer, A., Domack, E. W., Ishman, S. E., Brachfeld, S., McClennen, C. E., and Manley, P., 1996, Productivity cycle of 200-300 years in the Antarctic Peninsula region: Understanding linkages among the sun, atmosphere, oceans, sea ice, and biota: *Geological Society of America Bulletin*, v. 108, p. 1626-1644.
- Leverett, F., 1899, The Illinois glacial lobe: *U.S. Geological Survey Monograph* 38, 817 p.
- Levi, S., and Merrill, R. T., 1978, Properties of single-domain, pseudo-single-domain, and multidomain magnetite: *Journal of Geophysical Research*, v. 83, p. 309-323
- Liddicoat, J. C., and Coe, R. S., 1997, Paleomagnetic investigation of lake Lahontan sediments and its application for dating pluvial events in the northwestern Great Plains: *Quaternary Research*, v. 47, p. 45-53.
- Lin, B., Liu, R., and An Z., 1991, Preliminary research on stable isotopic compositions of Chinese loess: *in* Liu, T., ed., *Loess, Environment and Global Change*, Science Press, Beijing, China, p.124-131.
- Liu, X., Rolph, T., and Bloemendal, J., 1995, The citrate-bicarbonate-dithionite (CBD) removable magnetic component of Chinese loess: *Quaternary Proceedings*, n. 4, p. 53-58.
- Liu, X., Liu, T., Shaw, J., Heller, F., Xu, T., and Yuan B., 1991, Paleomagnetic and paleoclimatic studies of Chinese loess, *in* Liu, T., Ding, Z., and Guo, Z. eds., *Loess, Environment and Global Change*, Science Press, Beijing, China, p. 61-81.
- Liu, X., Shaw, J., Liu, T., and Heller, F., 1993, Magnetic susceptibility of the Chinese loess-paleosol sequence: environmental change and pedogenesis: *Journal of the Geological Society, London*, v. 150, p.583-588.

- Liu, X., Rolph, T., Bloemendal, J., Shaw, J., and Liu, T. S., 1994, Remanence characteristics of different magnetic grain size categories at Xifeng, central Chinese Loess Plateau: *Quaternary Research*, v. 42, p.162-165.
- Liu, X., Rolph, T., Bloemendal, J., Shaw, J., and Liu, T., 1995, Quantitative estimates of paleoprecipitation at Xifeng, in the Loess Plateau of China: *Palaeogeography, Palaeoclimatology, Palaeoecology*, v. 113, p.243-248.
- Liu, X., Shaw, J., Liu, T. S., Heller, F., and Yuan, B., 1992, Magnetic mineralogy of Chinese loess and its significance: *Geophysics Journal International*, v. 108, p.301-308.
- Livingstone, I., and Warren, A., 1996, *Aeolian Geomorphology*, Longman, Essex, England, 211 p.
- Lovley, D. R., Stoltz, J. F., Nord, G. L., Jr., and Phillips, E. J. P., 1987, Anaerobic production of magnetite by a dissimilatory iron-reducing microorganism: *Nature*, v. 330, p. 252-254.
- Lowrie, W., 1990, Identification of Ferromagnetic minerals in a rock by coercivity and unblocking temperature properties: *Geophysical Research Letters*, v. 17, p. 159-162.
- Lugn, A. L., 1934, Pleistocene geology of Nebraska: *Nebraska State Museum Bulletin* 41, v.1, pt.1.:319-356.
- Lugn, A. L., 1935, The Pleistocene geology of Nebraska: *Bulletin of Nebraska Geological Survey*, ser.2, v.10, 223 p.
- Lund, S. P., 1996, A comparison of Holocene paleomagnetic secular variation records from North America: *Journal of Geophysical Research*, v. 101, p. 8007-8024.
- Mahaney, W. C., 1995, Dating methods: review for 1993: *Progress in Physical Geography*, v. 19, p. 130-137.
- Machel, H. E., and Burton, E. A., 1992, Sediment magnetism: Comments on soil erosion, bushfire, or bacteria? *Geology*, v. 20, p. 670-671.
- Maher B. A., 1986, Characterization of soils by mineral magnetic measurements: *Physics of the Earth and Planetary Interiors*, v. 42, p. 76-92.
- Maher, B. A., 1988, Magnetic properties of some synthetic sub-micron magnetites: *Geophysical Journal*, v. 94, p. 83-96.
- Maher, B. A. and Taylor R. M., 1988, Formation of ultrafine-grained magnetite in soils: *Nature*, v. 336, p.368-370.
- Maher, B. A., and Thompson R., 1991, Mineral magnetic record of the Chinese loess and paleosols: *Geology*, v.19, p. 3-6.
- Maher, B. A., and Thompson R., 1992, Paleomagnetic significance of the mineral magnetic record of the Chinese loess and paleosols: *Quaternary Research*, v. 37, p. 155-170.
- Maher, B. A., and Thompson, R., 1994, Pedogenesis and paleoclimate: Interpretation of the magnetic susceptibility record of Chinese loess-paleosol sequences: *Comments and reply: Geology*, v.22, p.857-858.
- Maher, B. A., and Thompson, R., 1995, Paleorainfall reconstruction from pedogenic magnetic susceptibility variations in the Chinese loess and paleosols: *Quaternary Research*, v. 44, p.383-391.

- Maher, B. A., Thompson, R., and Zhou, L. P., 1994, Spatial and temporal reconstructions of changes in the Asian paleomonsoon: A new mineral magnetic approach: *Earth and Planetary Science Letters*, v. 125, p. 461-471.
- Martin, C. W., 1990, Late Quaternary landform evolution in the Republican River basin, Nebraska: Ph.D. dissertation, University of Kansas, Lawrence, 289 p.
- Martin, C. W., 1992, The response of fluvial systems to climate change: An example from the central Great Plains: *Physical Geography*, v. 13, p. 101-114.
- Martin, C. W., 1993, Radiocarbon ages on late Pleistocene loess stratigraphy of Nebraska and Kansas, central Great Plains, U.S.A.: *Quaternary Science Reviews*, v.12, p. 179-188.
- Martin C. W., and Johnson, W. C., (in review), Variation in radiocarbon ages of soil organic matter fractions from Late Quaternary buried soils. *Geology*.
- Martinson, D. G., Pisias, N. G., Hays, J. D., and Imbrie, J., 1987, Age dating and orbital theory of the ice ages: development of a high-resolution 0 to 300,000- year chronostratigraphy: *Quaternary Research*, v. 27, p. 1-29.
- Mathewes, R. W., Heuser L. E., and Patterson R. T., 1993, Evidence for a Younger Dryas-like cooling event on the British Columbia coast: *Geology*, v. 21, p. 101-104.
- Matt, P. B., and Johnson, W. C., 1996, Thermoluminescence and new  $^{14}\text{C}$  estimates for late Quaternary Loesses in southwestern Nebraska: *Geomorphology*, v. 17, p. 115-128.
- May D. W., and Holen S. R., 1993, Radiocarbon ages of soils and charcoal in Late Wisconsinan loess, south-central Nebraska: *Quaternary Research*, v.39, p.55-58.
- May, D. W., and Souders, V. L., 1988, Radiocarbon ages for the Gilman Canyon Formation in Dawson County, Nebraska, (abs.), *Nebraska Academy of Sciences: Proceedings*, p.47-48.
- Mayewski, P.A., Meeker, L. D., Whitlow, S., Twicker, M. S., Morrison, M. C., Alley, R. B., Bloomfield, P., and Taylor, K., 1993, The atmosphere during the Younger Dryas: *Science*, v.261, p. 195-197.
- Mayewski, P.A., Meeker, L. D., Whitlow, S., Twicker, M. S., Morrison, M. C., Bloomfield, P., Bond, G. C., Alley, R. B., Gow, A. J., Grootes, P. M., Meese, D. A., Ram, M., Taylor, K. C., Wumkes, W., 1994, Changes in atmospheric circulation and ocean ice cover over the North Atlantic during the last 41, 000 years: *Science*, v. 263, p. 1747-1751.
- McPherson, G. R., and Boutton, T. W., and Midwood, A. J., 1993, Stable carbon isotope analysis of soil organic matter illustrates vegetation change at the grassland/woodland boundary in southwestern Arizona, USA: *Oecologia*, v. 93, p. 95-101.
- Mehra, O. P., and Jackson, M. L., 1960, Iron oxide removal from soils and clays by dithionite-citrate system buffered with sodium bicarbonate: *Clays and Clay Minerals*, v. 5, p. 317-327.
- Mitchell, M. J., 1976, An overview of climatic variability and its casual mechanisms: *Quaternary Research*, v. 6, p. 481-493.

- Morris, A., 1996, Glossary of basic paleomagnetic and rock magnetic terms, *in* Morris, A., and Tarling, D. H., eds., *Paleomagnetism and Tectonics of the Mediterranean Region*, Geological Society Special Publication, n. 105, p. 401-415.
- Moskowitz, B. M., Frankel, R. B., and Bazylinski, D. A., 1993, Rock magnetic criteria for detection of biogenic magnetite: *Earth and Planetary Science Letters*, v. 120, p. 283-300.
- Muhs, D. R., 1985, Age and paleoclimatic significance of Holocene sand dunes in northeastern Colorado: *Annals of the Association of Geographers*, v. 75, p. 566-582.
- Muhs, D. R., Stafford, T. W., Cowherd, S. D., Mahan, S. A., Kihl, R., Maat, P. B., Bush, C. A., and Nehring, J., 1996, origin of the late Quaternary dune fields of northeastern Colorado: *Geomorphology*, v. 17, p. 129-149.
- Mullins, C. E., 1977, Magnetic susceptibility of the soil and its significance in soil science - a review: *Journal of soil Science*, v. 28, p. 223-246.
- Nadelhoffer, K. F. and Fry, B., 1988, Controls on natural nitrogen-15 and carbon-13 abundances in forest organic matter: *Soil Science Society of America Journal*, v. 52, p. 1633-1640.
- Nagata, T., 1961, *Rock Magnetism*, Maruzen Company LTD., Tokyo, 350 p.
- NOAA PAGES, 1996, *PaleoVu*, ver, 1.01., Computer Program for Windows.
- Nordt, L. C., Boutton, T. W., Hallmark, C. T., and Waters, M. R., 1994, Late Quaternary vegetation and climate changes in central Texas based on the isotopic composition of organic carbon: *Quaternary Research*, v. 41, p.109-120.
- Oches, E. A., and Banerjee, S. K., 1996, Rock-magnetic proxies of climate change from loess paleosol sediments of Czech republic: *Studia Geophysica et Geodaetica*, v. 40, p. 287-300.
- Oldfield, F., 1991, Environmental magnetism: personal perspective: *Quaternary Science Reviews*, v. 10, p. 73-81.
- Oldfield, F., 1991, Sediment magnetism: Soil erosion, bushfires, or bacteria?: *Geology*, v. 19, p. 1155-1156.
- O'Leary, M. H., 1981, Carbon isotope fractionation in plants: *Photochemistry*, v. 20, p. 553-567.
- Opdyke, N. D., and Channell, J. E. T., 1996, *Magnetic Stratigraphy*, International Geophysics Series, v. 64, Academic Press, 346 p.
- Osborn, G., Clapperton, C., Davis, P. T., Reasoner, M., Rodbell, D. T., Seltzer, G. O., and Zielinski, G., 1995, Potential glacial evidence for the Younger Dryas event in the Cordillera of North and South America: *Quaternary Science Reviews*, v. 14, p. 823-832.
- Osterkamp, W. R., Fenton, M. M., Gustavson, T. C., Hadley, R. F., Holliday, V. T., Morrison, R. B., and Toy, T. J., 1987, *Great Plains*, *in* Graf, W. L., ed., *Geomorphic Systems of North America: Geological Society of America Centennial special volume 2*. Boulder, Colorado: Geological Society of America, p.163-210.

- Overpeck, J., Rind, D., Lacy, A., and Healy, R., 1996, Possible role of dust-induced regional warming in abrupt climate change during the last glacial period: *Nature*, v. 384, p. 447-449.
- Oviatt, C. G., 1997, Lake Bonneville fluctuations and global climate change: *Geology*, v. 25, p. 155-158.
- Özdemir, Ö., and Banerjee, S. K., 1982, A preliminary magnetic study of soil samples from west-central Minnesota: *Earth and Planetary Science letters*, v. 59, p. 393-403.
- Özdemir, Ö., Dunlop, D. J., and Moskowitz, B. M., 1993, The effects of oxidation of the Verwey transition in magnetite: *Geophysics Research Letters*, v. 20, p. 1671-1674.
- Park, J., D'Hondt, S. L., King, J. W., and Gibson, C., 1993, Late Cretaceous precessional cycles in double time: A warm earth Milankovitch response: *Science*, v. 261, p. 1431-1434.
- Park, K., Farr, M. R., and Johnson, W. C., 1993, Magnetic susceptibility record of two Quaternary sections, Nebraska(abs.): *EOS Transactions, American Geophysical Union*, v. 74, p. 116.
- Park, K., 1994, Rock magnetic paleoclimatic record from Quaternary loess in the central Great Plains, *Association of American Geographers, Programs with Abstracts*, p. 289.
- Park, K., Johnson, W. C., Farr, M. R., 1995, Regional variation of rock magnetic parameters in the loess deposits of the central Great plains: Abstract with Programs, *Geological Society of America 29th Meeting*, P. 20, A. 79..
- Park, K., Johnson, W. C., and Farr, M. R., 1996, Reconstruction of Late-Quaternary climates of the central Great Plains using magnetic parameters: *Institute of Tertiary-Quaternary Studies Symposium*.
- Parkinson, W. D., 1983, *Introduction to Geomagnetism*, Elsevier, New York., 433 p.
- Pavich, M. J., Brown, L., Harden, J., Klein, J., and Middleton, R., 1986,  $^{10}\text{Be}$  distribution in soils from Merced River terraces, California: *Geochimica et Cosmochimica Acta*, v. 50, p. 1727-1735.
- Penninga, I., de Warrd, H., Moskowitz, B. M., Bazylinski, D. A., and Frankel, R. B., 1995, Remanence measurements on individual magnetotactic bacteria using a pulsed magnetic field: *Journal of Magnetism and Magnetic Materials*, v. 149, p. 279-286.
- Peteet, D., 1995, Global Younger Dryas?: *Quaternary International*, v. 28, p. 93-104.
- Peteet, D., Rind, D., and Kukla, G., 1992, Wisconsinan ice-sheet initiation: Milankovitch forcing, paleoclimatic data and global climate modeling, *in* Clark, P. U., and Lea, P. D., eds., *The Last Interglacial-Glacial Transition in North America*: Boulder, Colorado, Geological Society of America Special Paper 270, p. 53-69.
- Petersen, N. T., von Dobeneck, T., and Vali, H., 1986, Fossil bacterial magnetite in deep-sea sediments from the South Atlantic Ocean: *Nature*, v. 320, p. 611-615.
- Petit, J. R., Mounier, L., Jouzel, J., Korotkevich, Y. S., Kotlyakov, V. I. and Lorius, C., 1993, Paleoclimatological and chronological implications of the Vostok core dust record: *Nature* v. 343, p. 56-58.

- Phillips, F. M., Campbell, A. R., Smith, G. I., and Bischoff, J. L., 1994, Interstadial climatic cycles: A link between western North America and Greenland?: *Geology*, v. 22, p. 1115-1118.
- Piperno, D. R., 1988, *Phytolith Analysis-An Archaeological and Geologic Perspective*, Academic Press, New York, 280 p.
- Pisias, N. G., Martinson, D. G., Moore Jr., T. C., Shackleton, N. J., Prell, W., Hays, J., and Boden, G., 1984, High resolution stratigraphic correlation of benthic oxygen isotopic records spanning the last 300,000 years: *Marine Geology*, v. 56, p. 119-136.
- Pillans, B., and Wright, I., 1990, 500,000-year paleomagnetic record from New Zealand loess: *Quaternary Research*, v. 33, p.178-187.
- Platte, J. R., 1964, Strong Inference: certain systematic methods of scientific thinking may produce much more rapid progress than others: *Science*, v. 146, p. 347-353.
- Porter, S. C., and An, Z., 1995, Correlation between climate events in the North Atlantic and China during the last deglaciation: *Nature*, v. 375, p. 305-308.
- Potter, D. K., and Stephenson, A., 1986, The detection of fine particles of magnetite using anhysteretic and rotational remanent magnetizations: *Geophysics Journal of Royal Astronomical Society*, v. 87, p. 569-582.
- Prante, M. C., 1989, *Grain Size: A program to aid pedologic particle-size analysis*, University of Kansas, Department of Geography (unpublished).
- Prell, W. L., Imbrie, J., Martinson, D. G., Morley, J. J., Pisias, N. G., Shackleton, N. J., and Streeter, H. F., 1986, Graphic correlation of oxygen isotope stratigraphy application to the late Quaternary: *Paleoceanography*, v. 1, p. 137-162.
- Priestley, M. B., 1981, *Spectral Analysis and Time Series, Volume 1: Univariate Series*, Academic Press, London, 653 p.
- Priestley, M. B., 1981, *Spectral Analysis and Time Series, Volume 2: Multivariate Series, Prediction and Control*, Academic Press, London, 653 p.
- Pye, K., 1987, *Aeolian Dust and Dust Deposits*, Academic Press, 265 p.
- Pye, K., 1995, The nature, origin, and accumulation of loess: *Quaternary Science Reviews*, v. 14, p. 653-667.
- Reeh, N., 1989, dynamic and climatic history of the Greenland Ice Sheet, *in* Fulton, R. J., ed., *Quaternary geology of Canada and Greenland*, Geological Society of America, *The Geology of North America*, v. K-1, p. 795-822.
- Rind D., Peteet, D., Broecker, W., McIntyre, A., and Ruddiman W., 1986, The impact of cold North Atlantic sea surface temperatures on climate: implications for the Younger Dryas cooling (11 - 10 k): *Climate Dynamics*, v. 1, p. 3-33.
- Ritter, D. F., 1996, Is Quaternary geology ready for the future?: *Geomorphology*, v. 16, p. 273-276.
- Quade, J., and Cerling, T. E., 1995, Expansion of C<sub>4</sub> grasses in the late Miocene of northern Pakistan: evidence from stable isotopes in paleosols: *Palaeogeography, Palaeoclimatology, Palaeoecology*, v. 115, p. 91-116.
- Rolph, T. C., Shaw, J., Derbyshire, E., and Wang, J., 1989, A detailed geomagnetic record from Chinese loess: *Physics of the Earth and Planetary Interiors*, v. 56, p. 151-164.

- Rolph, T. C., Shaw, J., Derbyshire, E., and Wang, J., 1993, The Magnetic mineralogy of a loess section near Lanzhou, China., *in* Pye, K. ed., *The Dynamics and Environmental Context of Aeolian Sedimentary Systems*, p.311-323.
- Rosenbaum, J. G., Reynolds, R. L., Adam, D. P., Drexler, J., Sarna-Wojcicki, A. M., and Whitney, G. C., 1996, Record of middle Pleistocene climate change from Buck Lake, Cascade Range, southern Oregon-Evidence from sediment magnetism, trace-element geochemistry, and pollen: *Geological Society of America Bulletin*, v. 108, p. 1328-1341.
- Rousseau, D-D., and Kukla, G., 1994, Late Pleistocene climate record in the Eustis loess section, Nebraska, based on land snail assemblages and magnetic susceptibility: *Quaternary Research*, v. 42, p. 176-187.
- Ruddiman, W. F., and Duplessy, J. C., 1985, Conference on the Last Deglaciation: timing and mechanism: *Quaternary Research*, v. 23, p. 1-17.
- Ruhe, R. V., 1965, Identification of Paleosols in loess deposits in the United states, *in* *Loess and Related Eolian Deposits of the World*, INQUA vol. 12.
- Ruhe, R. V., 1976, Stratigraphy of midcontinental loess, U.S.A., *in*, Mahaney, W. C., ed., *Quaternary Stratigraphy of North America*: Dowden, Hutchinson, and Ross, Stroudsburg, Pennsylvania, p.197-211.
- Ruhe, R. V., 1983, Depositional environments of late Wisconsin loess in the midcontinental United States. *in* Porter, S. C. ed., *Late Quaternary environments of the United States-v.1*, *The Late Pleistocene*, University of Minnesota Press, Minneapolis, p.130-137.
- Rutter, N., 1992, Presidential Address, XIII INQUA congress 1991: Chinese loess and global Change: *Quaternary Science Review*, v. 11, p. 275-281.
- Rutter, N., Ding, Z., Evans, M. E., and Wang Y., 1990, Magnetostratigraphy of the Baoji loess-paleosol section in the north-central China Loess Plateau: *Quaternary International*, v. 7/8, p.97-102.
- Sandgren P., and Thompson, R., 1990, Mineral magnetic characteristics of podzolic soils developed on sand dunes in the Lake Gosciadz Catchment, central Poland: *Physics of the Earth and Planetary Interiors*, v. 60, p.297-313.
- Schneider, S. H., 1987, Climatic modeling: *Scientific American*, v. 256, n. 5., p. 72-78. 80.
- Schultz, C. B., 1968, The stratigraphic distribution of vertebrate fossils in the Quaternary eolian deposits in the midcontinent region of North America, *in*, Schultz, C. B., and Frye, J. C. eds., *Loess and Related Eolian Deposits of the World*, University of Nebraska Press, Lincoln, p.115-138.
- Schultz, C. B., and Stout, T. M., 1945, Pleistocene loess deposits of Nebraska: *American Journal of Science*, v. 243, p. 231-244.
- Schultz, C. B., and Stout, T. M., 1948, Pleistocene Mammals and terraces in the Great Plains: *Geological Society of America Bulletin*, v. 59, p.553-591.
- Schwartz, D., 1988, Some podzols on Bakete Sands and their origins, People's Republic of Congo: *Geoderma*, v. 43, p.229-247.

- Schwartz, D., Marriotti, Lanfranchi, R., and Guillet, B., 1986,  $^{13}\text{C}/^{12}\text{C}$  ratios of soil organic matter as indicators of vegetation changes in the Congo: *Geoderma*, v. 39, p.97-103.
- Shane, L. C. K., 1987, Late-glacial vegetational and climatic history of the Allegheny Plateau and the till plains of Ohio and Indiana: *Boreas*, v. 16, p.1-20.
- Shane, L. C. K., and Anderson, K. H., 1993, Intensity, gradients and reversals in late glacial environmental changes in east-central North America: *Quaternary Science Reviews*, v. 12, p. 307-320.
- Singer, M. J., and Fine P., 1989, Pedogenic factors affecting magnetic susceptibility of North California soils: *Soil Science Society of America Journal*, v. 53, p. 1119-1127.
- Singer, M. J., Fine P., Verosub, K. L., and Chadwick, O. A., 1992, Time dependence of magnetic susceptibility of soil chronosequences on the California coast: *Quaternary Research* v. 37, p. 323-332.
- Singer, M. J., Verosub, K. L., Fine, P., and TenPas, J., 1996, A conceptual model for the enhancement of magnetic susceptibility in soils: *Quaternary International*, v. 34-36, p. 243-248.
- Smalley, I., 1995, Making the material: the formation of silt-sized primary mineral particles for loess deposits: *Quaternary Science Reviews*, v. 14, p. 645-651.
- Smith, R. M., Twiss P. C., Krauss, R. K., and Brown, M. J., 1970, Dust deposition in relation to site, season, and climatic variables: *Soil Science Society of America Proceedings*, v. 34, p.112-117.
- Snowball, I., and Thompson, R., 1990, A mineral magnetic study of Holocene sedimentation in Lough catherine, Northern Ireland: *Boreas*, v. 19, p. 127-146.
- Soffel, H. C., and Chouker, A. C., 1992, Rock magnetism in the global paleomagnetic database (GPMDB): *Physics of the Earth and Planetary Interiors*, v. 70, p. 141-145.
- Souders, V. L., and Kuzila M. S., 1990, A report on the geology and radiocarbon ages of four superimposed horizons at a site in the Republican River Valley, Franklin County, Nebraska: *Proceedings of the Nebraska Academy of Sciences*, Nebraska Academy of Sciences, Lincoln, p. 65.
- Stephenson, A., 1971, Single domain grain distributions. 1. A method for the determination of single domain size distributions: *Physics of Earth and Planetary Interiors*, v. 4, p. 353-360.
- Stewart, J. W. B., and Cole, C. V., 1989, Influences of elemental interactions and pedogenic processes in organic matter dynamics: *Plant and Soil*, v. 115, p. 199-209.
- Stolz, J. F., Chang, S-B, R., and Kirschvink, J. L., 1986, Magnetotactic bacteria and single-domain magnetite in hemipelagic sediments: *Nature*, v. 321, p. 849-851.
- Stoner, J. S, Channel, J. E. T., and Hillaire-Marcel, C., 1995, Magnetic properties of deep-sea sediments off southwest Greenland: Evidence for major differences between the last two deglaciations: *Geology*, v. 23, p. 241-244.
- Sun, W., Banerjee, S. K., and Hunt, C. P., 1995, The role of maghemite in the enhancement of magnetic signal in the Chinese loess-paleosol sequence: An

- extensive rock magnetic study combined with citrate-bicarbonate-dithionite treatment: *Earth and Planetary Science Letters*, v. 133, p. 493-505.
- Tarduno, J. A., 1995, Superparamagnetism and reduction diagenesis in pelagic sediments: Enhancement or depletion?: *Geophysical Research Letters*, v. 22, p. 1337-1340.
- Tarling, D. H., 1983, *Paleomagnetism: Principles, and Applications in Geology, Geophysics and Archaeology*, Chapman and Hall, London, 379 p.
- Taylor, K. C., Lamorey, G. W., Doyle, G. A., Alley, R. B., Grootes, P. M., Mayewski, P. A., White, J. W. C., and Barlow, L. K., 1993, The flickering switch of late Pleistocene climate change: *Nature*, v. 361, p. 432-436.
- Taylor, R. M., Maher, B. A., and Self, P. G., 1987, Magnetite in soils: I. The synthesis of single-domain and superparamagnetic magnetite: *Clay Minerals*, v. 22, p. 411-422.
- Teeri, J. A., and Stowe L. G., 1976, Climatic patterns and the distribution of C4 grasses in North America: *Oecologia*, v. 23, p. 1-12.
- Thompson, R., and Maher, B. A., 1995, Age models, sediment fluxes and palaeoclimatic reconstructions for the Chinese loess and paleosol sequences: *Geophysical Journal International*, v. 123, p. 611-622.
- Thompson, R., and Oldfield F., 1986, *Environmental Magnetism*: Allen and Unwin, London.
- Thompson, R., Bloemendal, J., Dearing, J. A., Oldfield, F., Rummery, T. A., Stober, J. C., and Turner, G. M., 1980, Environmental applications of magnetic measurements: *Science*, v. 207, p. 481-486.
- Thompson, R., Cameron, T. D. J., Schwarz, C., Jensen, K. A., van Lemberge, V. M., and Sha, L. P., 1992, The magnetic properties of Quaternary and Tertiary sediments in the southern North Sea: *Journal of Quaternary Science*, v. 7, p. 319-334.
- Thorp, J., Johnson, W. M., and Reed E. C., 1950, Some post-Pleistocene buried soils of central United States: *Journal of Soil Sciences*, v. 2, p.1-19.
- Thouveny, N., de Beaulieu, J. L., Bonifay, E., Creer, K. M., Gulot, J., Icole, M., Johnsen, S., Jouzel, J., Reille, M., Williams, T., and Williamson, D., 1994, Climate variations in Europe over the past 140 kyr deduced from rock magnetism: *Nature*, v. 371, p. 503-507.
- Tieszen, L. L., and Boutton, T. W., 1989, Stable carbon isotopes in terrestrial ecosystem research, *in* Ehleringer, J. R., and Rundel, P. W. eds., *Stable Isotopes in Ecological Research*, p. 167-195.
- Tieszen, L. L., Reed, B. C., Bliss, N. B., Wylie, B. K., and DeJong, D. D. (in press), NDVI, C<sub>3</sub> and C<sub>4</sub> grass production and distribution in Great Plains grasslands cover: *Ecological Applications*.
- Tite, M. S., and Linington R. C., 1975, Effect of climate on the magnetic susceptibility of soil: *Nature*, v. 256, p. 565-566.
- Twiss, P. C., 1983, Dust deposition and opal phytoliths in the Great Plains, *in* Caldwell, W. H., Schultz, C.B., and Stout T. M. eds., *Man and the Changing Environments in the Great Plains*. Transactions of the Nebraska Academy of Sciences, v. 11, p.73-82.

- Twiss, P.C., 1987, Grass-opal phytoliths as climatic indicators of the Great Plains Pleistocene, *in* Johnson W. C. ed., *Kansas Quaternary Environments of Kansas*, Geological Survey, Guidebook Series 5, p. 179-188.
- Twiss, P. C., Suess, E., and Smith, R. M., 1969, Morphological classification of grass phytoliths: *Soil Science Society of America Proceedings*, v. 33, 109-115.
- Vandenberghe, J., An, Z., Nugteren, G., Lu, H., and Van Huissteden, K., 1997, New absolute scale for the Quaternary climate in the Chinese loess region by grain-size analysis: *Geology*, v. 25, p. 35-38.
- Van Velzen, A. J., and Zijderveld, D. A., 1995, Effects of weathering on single-domain magnetite in Early Pliocene marine marls: *Geophysics Journal International*, v. 121, p. 267-278.
- Verosub, K. L., 1988, Geomagnetic secular variation and the dating of Quaternary sediments: *GSA Special Paper*, v. 227, p. 123-137.
- Verosub, K. L., Fine, P., Singer, M. J., and TenPas, J., 1993, Pedogenesis and paleoclimate: Interpretation of the magnetic susceptibility record of Chinese loess-paleosol sequences: *Geology*, v. 21, p. 1011-1014.
- Vincenz, S. A., 1965, Frequency dependence of magnetic susceptibility of rocks in weak alternating fields: *Journal of Geophysical Research*, v. 70, p.1371-1377.
- Vogel, J. C., 1980, *Fractionation of the Carbon Isotopes During Photosynthesis*, Springer Verlag, Berlin.
- Wang, Y., and Zheng, S., 1989, Paleosol nodules as Pleistocene paleoclimatic indicators, Luochuan, P. R. China: *Palaeogeography, Palaeoclimatology, Palaeoecology*, v. 76, p. 39-44.
- Wang, Y., Amundson, R., and Trumbore, S., 1996, Radiocarbon dating of soil organic matter: *Quaternary Research*, v. 45, p. 282-288.
- Wang, Y., Evans, M. E., Xu, T. C., Rutter, N., Ding, Z., and Liu, X. M., 1992, Rescaled range analysis of paleoclimatic proxies: *Canadian Journal of Earth Science*, v. 29, p. 296-300.
- Wang, Y., McDonald, E., Amundson, R., McFadden, L., Chadwick, O., 1996, An isotopic study of soils in chronological sequences of alluvial deposits, Providence Mountains, California: *Geological Society of America Bulletin*, v. 108, p. 379-391.
- Watson, E. C., 1945, The discovery of X-rays: *American Journal of Physics*, v. 13, p. 281-291.
- Watson, R. A., and Wright H. E., Jr., 1980, The end of the Pleistocene: a general critique of chronostratigraphic clarification: *Boreas*, v. 9, p. 153-163.
- Webb, T., III., Cushing, E. J., and Wright, H. E., JR., 1983, Holocene changes in the vegetation of the Midwest, *in* Wright, H. E., Jr., ed., *Late Quaternary Environment of the United State*, v. 2, The Holocene, University of Minnesota Press, Minneapolis.
- Wedin, D. A., Tieszen, L. L., Dewey, B., and Pastor, J., 1995, Carbon isotope dynamics during grass decomposition and soil organic matter formation: *Ecology*, v. 76, p. 1383-1392.

- Welch, J. R., and Hale, J. M., 1987, Pleistocene loess in Kansas-status, present problems, and future considerations, *in* Johnson, W. C. ed., Quaternary Environments of Kansas, Kansas Geological Survey, Guidebook Series 5, p. 67-84.
- Wells, P. V., 1983, Late Quaternary vegetation of the Great Plains: *in* Caldwell, W. W., Schultz, C.B., and Stout, T. M., eds., Man and the Changing Environments in the Great Plains. Transactions of the Nebraska Academy of Sciences, v. 11, p. 83-89.
- Wells, P. V., and Stewart, J. D., 1987, Spruce charcoal, conifer macrofossils, and landsnail and small-vertebrate faunas in Wisconsinan sediments on the High Plains of Kansas, *in* Johnson, W. C. ed., Quaternary Environments of Kansas, Kansas Geological Survey, Guidebook Series 5, p. 129-140.
- Wendland, W. M., 1978, Holocene man in the Plains-the ecological setting and climatic background: *Plains Anthropologist*, v. 23, p. 273-287.
- White, A. F., Peterson, M. L., and Hochella, M. F., Jr., 1994, Electrochemistry and dissolution kinetics of magnetite and ilmenite: *Geochimica et Cosmochimica Acta*, v. 58, p. 1859-1875.
- Williams, R. D., and Cooper, J. R., 1990, Locating soil boundaries using magnetic susceptibility: *Soil Science*, v. 150, p. 889-895.
- Williams, T., Thouveny, N., and Creer, K. M., 1996, Paleoclimatic significance of the 300 ka mineral magnetic record from the sediments of Lac du Bouchet, France: *Quaternary Science Reviews*, v. 15, p. 223-235.
- Woodcock, D. W., and Wells, P. V., 1990, Full-glacial summer temperatures in eastern North America as inferred from Wisconsinan vegetational zonation: *Palaeogeography, Palaeoclimatology, Palaeoecology*, v. 79, p.305-312.
- Wright, H. E., Jr., 1971, Retreat of the Laurentide Ice Sheet from 14,000 to 9000 years ago. *Quaternary Research*, v. 1, p. 316-330.
- Wright, H. E., Jr., 1984, Sensitivity and response time of natural systems to climatic change in the Late Quaternary: *Quaternary Science Reviews*, v. 3, p. 91-131.
- Wright, H. E., Jr., 1989, The amphi-Atlantic distribution of the Younger Dryas paleoclimatic oscillation: *Quaternary Science Reviews*, v. 8, p. 295-306.
- Wright, H. E., Jr., 1992, Patterns of Holocene climatic change in the Midwestern United States: *Quaternary Research*, v. 38, p.129-134.
- Wright, H. E., Jr., Almendinger, J. C., and Gröger, J., 1985, Pollen diagram from the Nebraska Sandhills and the age of dunes: *Quaternary Research*, v. 24, p. 115-120.
- Xiao, J., Porter, S. C., An, Z., Kumai, H., and Yoshikawa, S., 1995, Grain size of quartz as an indicator of winter monsoon strength on the Loess Plateau of Central China during the last 130, 000 yr: *Quaternary Research*, v, 43, p. 22-29.
- Xu, T-C., and Liu, T. S., 1993, Implication of the magnetic susceptibility curve from the Chinese loess profile at Xifeng: *Quaternary Science Reviews*, v. 12, p. 249-254.
- Yapp, C. J., and Poths, H., 1996, Carbon isotopes in continental weathering environments and variations in ancient atmospheric CO<sub>2</sub> pressure: *Earth and Planetary Science Letters*, v. 137, p. 71-82.
- Zheng, H., An, Z., and Shaw, J., 1992, New contributions to Chinese Plio-Pleistocene magnetostratigraphy: *Physics of the Earth and Planetary Interiors*, v. 70, p.146-153.

- Zheng, H., Oldfield, F., Yu, L., Shaw, J., and An, Z., 1991, The magnetic properties of particle-sized samples from the Luo Chuan loess section: evidence for pedogenesis: *Physics of the Earth and Planetary Interiors*, v. 68, p. 250-258.
- Zheng, H., Rolph, T., Shaw, J., and An, Z., 1995, A detailed palaeomagnetic record for the last interglacial period: *Earth and Planetary Science Letters*, v. 133, p. 339-351.
- Zhou, L. P., Oldfield, F., Wintle, A. G., Robinson, S. G., and Wang J. T., 1990, Partly pedogenic origin of magnetic variations in Chinese loess: *Nature*, v. 346, p. 737-739.
- Zhou, W., An, Z., and Mead, M. J., 1994, Stratigraphic division of Holocene loess in China: *Radiocarbon*, v. 36, p. 37-45.
- Zielinski, G. A., and Mershon, G. R., 1997, Paleoenvironmental implications of the insoluble microparticle record in the GISP2 (Greenland) ice core during the rapidly changing climate of the Pleistocene-Holocene transition: *GSA Bulletin*, v. 109, p. 547-559.